



**CALIFORNIA  
ENERGY  
COMMISSION**

## **Durability of Catalytic Combustion Systems**

# **CONSULTANT REPORT**

MARCH 2002  
P500-02-040F



Gray Davis, Governor

# CALIFORNIA ENERGY COMMISSION

***Prepared By:***

Catalytica Energy Systems  
430 Ferguson Drive,  
Mountain View, CA 94043  
Contract No. 500-97-033,

Troy Kinney  
David Yee  
James C. Schlatter

***Prepared For:***

Avtar Bining, Ph.D.,  
***Contract Manager***

Mike Batham, P.E.,  
***Environmentally-Preferred  
Advanced Generation Team Lead***

Terry Surles,  
***Deputy Director  
Technology Systems Division***

Steve Larson,  
***Executive Director***

## **Legal Notice**

This report was prepared as a result of work sponsored by the California Energy Commission (Commission). It does not necessarily represent the views of the Commission, its employees, or the State of California. The Commission, the State of California, its employees, contractors, and subcontractors make no warranty, express or implied, and assume no legal liability for the information in this report; nor does any party represent that the use of this information will not infringe upon privately owned rights. This report has not been approved or disapproved by the Commission nor has the Commission passed upon the accuracy or adequacy of the information in this report.

## **Acknowledgments**

Catalytica Energy Systems, Inc. wishes to publicly express its appreciation for the organizations that have contributed both funding and counsel during the execution of this extensive and multi-dimensional development program. These partners include the California Energy Commission, the United States Department of Energy, the California Air Resources Board, and the Gas Research Institute. Special thanks go to Silicon Valley Power (City of Santa Clara, CA) for allowing and supporting the installation and operation of a first-of-its-kind gas turbine on their Santa Clara site.

# Table of Contents

Section	Page
Legal Notice.....	i
Acknowledgments .....	ii
Preface .....	xiii
Executive Summary.....	1
Abstract.....	9
<b>1.0 Introduction.....</b>	<b>10</b>
1.1. Project Background.....	10
1.1.1. Technology Concept.....	11
1.1.2. Project Approach .....	12
1.1.3. Problem Statement .....	13
1.1.4. Project Purpose .....	15
1.2. Project Goals .....	15
1.2.1. Technical Objectives.....	16
1.2.2. Economic Objectives .....	16
1.3. Expenditure Summary .....	18
1.4. Report Organization.....	18
<b>2.0 Approach.....</b>	<b>20</b>
2.1. RAMD Engine Testing .....	20
2.1.1. Introduction.....	20
2.1.2. Approach .....	22
2.1.3. Test Bed Selection .....	22
2.1.4. Description of Testing Procedures .....	23
2.1.4.1. Engine Monitoring .....	23
2.1.4.2. Engine Test Cycle .....	24
2.1.5. RAMD Definitions.....	25
2.1.5.1. Reliability.....	25
2.1.5.2. Availability .....	25
2.1.5.3. Maintainability.....	26
2.1.5.4. Durability.....	26
2.1.6. Test Results.....	27
2.1.6.1. RAMD Calculations .....	27
2.1.6.2. Combustor Configuration.....	27
2.1.6.3. Emissions Measurements .....	29
2.1.6.4. Phase I Emissions Results .....	29
2.1.6.5. Phase II Emissions Results .....	32

2.1.6.6.	Phase III Emissions Results.....	34
2.1.7.	Conclusions .....	36
2.2.	Control System Design.....	37
2.2.1.	Introduction.....	37
2.2.2.	Approach .....	37
2.2.3.	Concept Development .....	38
2.2.4.	Control System Design .....	39
2.2.4.1.	Simulation Studies.....	39
2.2.4.2.	Implementation on KHI Engine Control System.....	39
2.2.4.3.	Program Replan.....	39
2.2.5.	Control System Development and Testing.....	40
2.2.5.1.	Load Following.....	40
2.2.5.2.	Load Rejection.....	44
2.2.5.3.	Breaker Auto-Resynchronization.....	48
2.2.6.	Conclusions .....	48
2.3.	Axial Support Development.....	49
2.3.1.	Introduction.....	49
2.3.2.	Approach .....	49
2.3.3.	Material Property Data .....	50
2.3.3.1.	Creep Testing .....	51
2.3.3.2.	Fatigue Testing.....	52
2.3.3.3.	Elastic-Plastic Testing .....	53
2.3.3.4.	Material Constitutive Model for Structural Analysis.....	53
2.3.4.	Structural Analysis .....	54
2.3.5.	Analysis Results.....	57
2.3.5.1.	Fatigue Analysis .....	57
2.3.5.2.	Creep Analysis.....	58
2.3.6.	Conclusions .....	60
2.4.	Fuel/Air Premixer Development .....	60
2.4.1.	Introduction.....	60
2.4.2.	Approach .....	62
2.4.3.	CFD Analysis.....	63
2.4.3.1.	Lobed Mixer CFD .....	63
2.4.3.2.	Fuel Peg CFD Analysis and Design.....	66
2.4.4.	Cold Flow Testing of Premixer .....	70
2.4.4.1.	Background .....	70
2.4.4.2.	Test Results.....	71
2.4.5.	Flameholding Study.....	72
2.4.5.1.	Background .....	72
2.4.5.2.	Test Results.....	76
2.4.6.	Flameholding Study -- Simulation & Analysis.....	78
2.4.6.1.	Background .....	78
2.4.6.2.	Analysis Results.....	79
2.4.7.	Conclusions .....	82
2.5.	Catalyst Materials Development .....	83
2.5.1.	Introduction.....	83

2.5.2.	Approach .....	84
2.5.3.	New Ceramic Materials Development .....	85
2.5.3.1.	Effect of hydrolysis and precipitation processes .....	85
2.5.3.2.	Precipitation by Microfluidization.....	86
2.5.3.3.	Effect of H <sub>2</sub> O concentration and acid/base catalysis .....	86
2.5.3.4.	Effect of drying technique.....	87
2.5.4.	Thermal Stability Testing of New Catalyst Materials .....	88
2.5.4.1.	900°C HPAR results .....	90
2.5.4.2.	975°C HPAR results .....	91
2.5.5.	Catalyst Performance Testing.....	91
2.5.6.	Production of Engine Catalyst.....	95
2.5.7.	Conclusions .....	95
2.6.	Fuel Variability Study .....	96
2.6.1.	Introduction.....	96
2.6.2.	Approach .....	96
2.6.3.	Modification of CESI test facilities .....	96
2.6.4.	Natural Gas Variability Parametric Tests.....	97
2.6.4.1.	Testing Procedures.....	98
2.6.4.2.	Test Results.....	99
2.6.5.	Conclusions .....	102
<b>3.0</b>	<b>Project Outcomes.....</b>	<b>103</b>
3.1.	Technical Outcomes.....	103
3.2.	Project Economic Outcomes.....	106
3.2.1.	Commercialization Potential.....	107
3.2.1.1.	Market Background .....	107
3.2.1.2.	Current Gas Turbine Market .....	107
3.2.1.3.	Emissions as a Market Driver .....	111
3.2.1.4.	Technology Cost and Performance.....	113
3.2.1.5.	Market Penetration.....	116
3.2.1.6.	Market Requirements .....	117
3.2.2.	Conclusions .....	122
3.3.	Production Readiness.....	123
3.3.1.	Introduction.....	123
3.3.2.	Manufacturing Overview .....	124
3.3.3.	Production Capacity Constraints .....	127
3.3.4.	Identification of Hazardous or Non-recyclable Materials. ....	127
3.3.5.	Projected Product Cost.....	128
3.3.6.	Commercialization Investment .....	128
3.3.7.	Production Implementation Plan .....	128
3.4.	Benefits to California .....	129
3.4.1.	Economic and Energy Benefits .....	130
3.4.2.	Environmental Benefits.....	132
3.4.3.	State and Local Economic Impact.....	134
<b>4.0</b>	<b>Conclusions and Recommendations.....</b>	<b>135</b>

<b>5.0</b>	<b>Glossary.....</b>	<b>137</b>
<b>6.0</b>	<b>Notes and References .....</b>	<b>141</b>



## **Appendices**

Appendix A:	Cost Data for Technology Cost and Performance Data Analysis
Appendix B:	RAMD Basic Definitions
Appendix C:	RAMD Emission Results
Appendix D:	Axial Retainer Material Test Results
Appendix E:	Fuel/Air Premixer Figures
Appendix F:	Catalyst Materials Development Figures
Appendix G:	Fuel Variability Figures
Appendix I:	Market Requirements Development
Appendix II:	RAMD Testing and Control System Development
Appendix III:	Combustion Catalyst Axial Support Mechanical Durability
Appendix IV:	Fuel/Air Premixer Development
Appendix V:	Catalyst Materials Development
Appendix VI:	Variability in Natural Gas Fuel Composition and Its Effects on the Performance of Catalytic Combustion Systems
Appendix VII:	Xonon Production Readiness

## List of Figures

Figure	Page
Figure ES1 – Typical Xonon® combustion system.....	2
Figure 1.1.1.1 -- Dependence of NO <sub>x</sub> formation on temperature (10 atm pressure, 20 ms residence time).....	11
Figure 1.1.1.2 -- Essential features of flame versus catalytic combustor. NO <sub>x</sub> formation accelerates above about 1500°C.....	12
Figure 1.1.2.1 -- General program approach shows integration of technology improvements into RAMD engine testing .....	13
Figure 1.3.1 – Total program expenditures.....	18
Figure 2.1.1.1 – Xonon® Catalytic Combustion System installed on Kawasaki M1A-13A .....	20
Figure 2.1.1.2 -- The Xonon® equipped Kawasaki M1A-13X unit installed at SVP .....	21
Figure 2.1.2.1.1 -- Kawasaki (KHI) M1A-13A gas turbine engine with DLN and water injection.....	22
Figure 2.1.6.4.1 – Phase I NO <sub>x</sub> emission results (30 minute averages corrected to 15 percent O <sub>2</sub> ) .....	30
Figure 2.1.6.5.1 -- Build 5 KHI-2 Xonon® 2.0 test configuration .....	32
Figure 2.1.6.5.2 – Phase II NO <sub>x</sub> emission results (30 minute average).....	33
Figure 2.1.6.6.1 -- Xonon® 2.0 and Xonon® 2.1 comparison.....	34
Figure 2.1.6.6.2 -- Phase III NO <sub>x</sub> emission results (30 minute averages).....	35
Figure 2.2.2.1 -- Load response comparison of a dynamometer and a generator for a step change in load set point.....	38
Figure 2.2.5.1.1 -- 600 kW to 300 kW load step prior to tuning Main Demand PIDs.....	41
Figure 2.2.5.1.2 -- 300 kW load step after tuning Main Demand PID's.....	41
Figure 2.2.5.1.3 -- 300 kW load step before and after increasing the kW Ramp Rate .....	42
Figure 2.2.5.1.4 -- 600 kW load step with same parameters as tuned 300 kW load step .....	42
Figure 2.2.5.1.5 -- 600 kW load step after further tuning .....	43
Figure 2.2.5.1.6 -- 1500 kW to 600 kW load step.....	44
Figure 2.2.5.2.1 -- 300 kW load rejection prior to tuning.....	45
Figure 2.2.5.2.2 -- 300 kW load rejection after tuning.....	46
Figure 2.2.5.2.3 – 600 kW load rejection with same PID parameters as the 300 kW load rejection .....	46
Figure 2.2.5.2.4 -- 300 kW load rejection (1.9 percent over-speed, -0.9 percent under-speed).....	47
Figure 2.2.5.2.5 -- 1050 kW load rejection (6.9 percent over-speed, -2.7 percent under-speed).....	47

Figure 2.2.5.3.1 -- Engine speed oscillations after load rejection and before breaker re-synchronization .....	48
Figure 2.3.3.2.1 -- Comparison of LCF results for both materials at 850 and 950 °C .....	52
Figure 2.3.3.3.1 -- 0.2 percent Yield Strength versus Temperature.....	53
Figure 2.3.3.4.1 -- Multilinear stress strain curves for Haynes 214.....	54
Figure 2.3.4.1 -- BMM finite element model .....	55
Figure 2.3.4.2 -- Heat Transfer Analysis Metal Temperature Distribution .....	56
Figure 2.3.5.1 -- Equivalent Stress in Selected Elements at Midpsan .....	57
Figure 2.3.5.2.1-- Axial deformation versus time for the One Row FE Elasto-Plastic-Creep Analysis.....	58
Figure 2.3.5.2.2 -- Maximum equivalent strains from previous cell versus time .....	59
Figure 2.4.2.1 -- Fuel/Air mixer project approach.....	62
Figure 2.4.3.1.1 -- Lobe Mixer Geometry CFD Features.....	63
Figure 2.4.3.1.2 -- Three-dimensional rendering of a complete 12-lobed mixer along with fuel pegs .....	64
Figure 2.4.3.1.3 -- In-Plane Velocity Vectors with Short-Lobe Mixer .....	65
Figure 2.4.3.1.4 -- In-Plane Velocity Vectors with Long-Lobe Mixer .....	66
Figure 2.4.3.2.1 -- Baseline Fuel-Peg Geometry and Two-Layer Computational Grid.....	67
Figure 2.4.4.2.1 -- Fuel/air sampling grid points.....	71
Figure 2.4.4.2.2 -- Measured HC concentration vs. angle and diameter.....	72
Figure 2.4.5.1.1 -- Flameholding test rig setup.....	74
Figure 2.4.5.1.2 -- Test section overview .....	74
Figure 2.4.5.1.3 -- Photograph of laser anemometry setup.....	76
Figure 2.4.5.2.1 -- Positive flameholding results showing high intensity (left) and low intensity (right) flameholding.....	77
Figure 2.4.6.2.1 -- Predictions of CO and temperature as a function of equivalence ratio using the residence time and volume of the recirculation zone .....	81
Figure 2.5.4.1 -- High Pressure Thermal Aging Facility that reproduces the pressure, gas phase composition and temperature of the actual gas turbine combustor.....	89
Figure 2.5.5.1 -- Catalytic combustion test facility schematic design. Two such high pressure rigs are available at CESI's Mountain View facility.....	92
Figure 2.5.5.2 -- Sub-scale catalyst performance (light-off) test results .....	93
Figure 2.5.5.3 -- Results of sub-scale short-term durability tests.....	94
Figure 2.6.4.1 -- Heating Value Distributions.....	98
Figure 2.6.4.2.1 -- Baseline Operating Window.....	99

Figure 2.6.4.2.2 -- Durability Limit Shift Distribution of Surveyed Gases.....	101
Figure 3.2.1.2.1 -- Worldwide prime mover orders (over 1 MW) .....	108
Figure 3.2.1.2.2 -- Estimated gas turbine market (Forecast International, 1999).....	108
Figure 3.2.1.2.3 -- Worldwide reciprocating engine sales .....	111
Figure 3.2.1.4.1 -- Comparison of net power costs in CHP duty .....	115
Figure 3.2.1.4.2 -- Comparison of yearly savings for 5 MW system: purchased fuel and power costs versus fully amortized CHP owning and operating costs.....	116
Figure 3.3.2.1 -- Schematic diagram of the catalyst module with bonded metal monolith (BMM) structures at inlet and outlet.....	125
Figure 3.3.2.2 -- Photograph of catalyst in container. See text for descriptive details.....	125
Figure 3.3.2.3 -- Catalytica Energy Systems, Inc. manufacturing facility in Mountain View .....	126
Figure 3.3.3.1 -- Floor plan of Catalytica Energy Systems, Inc. manufacturing facility in Gilbert, AZ.....	127
Figure 3.4.1.1 -- Comparison of Annual User Benefits for CHP Sites based on the SCR and Xonon® Market Penetration Rates .....	131
Figure 3.4.1.2 -- Comparison of Annual Energy Savings for CHP Sites based on the SCR and Xonon® Market Penetration Rates .....	132

## List of Tables

<b>Table</b>	<b><u>Page</u></b>
Table ES1—Program results and goals .....	4
Table 1.2.2.1 – Projected Life Cycle NO <sub>x</sub> Control Costs.....	17
Table 2.1.6.1.1 -- RAMD Values.....	27
Table 2.1.6.2.1 -- RAMD engine builds and operating hours .....	29
Table 2.1.6.4.1 – Phase I emissions results(corrected to 15 percent O <sub>2</sub> ) .....	30
Table 2.1.6.5.1 -- Phase II emissions results(corrected to 15 percent O <sub>2</sub> ) .....	32
Table 2.1.6.6.1 -- Phase III emissions results(corrected to 15 percent O <sub>2</sub> ).....	35
Table 2.3.3.1 -- Haynes 214 Treatments for Testing.....	50
Table 2.3.3.3.1 -- Fatigue testing matrix.....	53
Table 2.3.5.2.1 -- SVP Deflection vs time .....	60
Table 2.4.3.2.1-- Fuel-Peg Model Conditions and Methods.....	69
Table 2.4.3.2.2-- Airfoil fuel peg CFD simulations approach angle.....	70
Table 2.4.6.2.1 -- Reattachment length using the standard k-ε model with Chen modification ...	80
Table 2.4.6.2.2 -- Recirculation Zone Volume and Time .....	81
Table 2.5.1.1 -- Thermal sintering data comparing the loss in surface area of the current ceramic washcoat material with a new high thermal stability material .....	84
Table 2.5.3.3.1 -- Effect of hydrolysis stoichiometry and acid or base addition on the preparation of precipitated Ta-Zr oxide powders .....	86
Table 2.5.3.4.1 -- BET Surface area results for dried Ta-Zr oxide materials .....	87
Table 2.5.4.1 -- Catalysts tested in HPAR experiments at 900°C and 975°C.....	89
Table 2.5.4.1.1 -- Normalized results of the analysis for total (BET) surface area and exposed metal content for the 900°C HPAR aged catalysts.....	90
Table 2.5.4.2.1 -- Total (BET) surface area analysis for the 975°C experiment .....	91
Table 2.5.5.1 -- Catalyst performance and short-term durability test conditions.....	93
Table 2.5.5.2 --Characterization of fresh and aged catalysts .....	94
Table 2.6.3.1 -- Composition Variability of Natural Gases in the United States.....	97
Table 2.6.4.2.2 -- Maximum Allowable Dopant Levels .....	102
Table 3.1.1 – RAMD values after 8128 hours of operation .....	103
Table 3.1.2 -- RAMD emissions for 8128 hours of operation (30 minute averages corrected to 15 percent O <sub>2</sub> ) .....	104
Table 3.2.1.2.1 -- Gas turbine orders by size range (1999).....	109

Table 3.2.1.2.2 -- Gas turbine order trend (1984-1999) .....	109
Table 3.2.1.2.3 -- Gas turbine and reciprocating engine orders (1999, 1-30 MW) .....	110
Table 3.2.1.3.1 -- SB 1298 Two-Phase Emissions Limits .....	112
Table 3.2.1.3.2 -- Qualitative Emission Limits and Options .....	113
Table 3.2.1.4.1 -- Capital and operating impacts of pollution control systems .....	114
Table 3.2.1.5.1 -- Comparison of the Impacts of DLN/SCR and Xonon on CHP Market Penetration .....	117
Table 3.4.2.1 -- NO <sub>x</sub> Emission Reductions for the DLN/SCR and Xonon® CHP Market Penetration Scenarios based on Backing out Existing Boiler and Generation Technology ..	134

## Preface

The Public Interest Energy Research (PIER) Program supports public interest energy research and development that will help improve the quality of life in California by bringing environmentally safe, affordable, and reliable energy services and products to the marketplace.

The PIER Program, managed by the California Energy Commission (Commission), annually awards up to \$62 million to conduct the most promising public interest energy research by partnering with Research, Development, and Demonstration (RD&D) organizations, including individuals, businesses, utilities, and public or private research institutions.

PIER funding efforts are focused on the following six RD&D program areas:

- Buildings End-Use Energy Efficiency
- Industrial/Agricultural/Water End-Use Energy Efficiency Renewable Energy
- Environmentally-Preferred Advanced Generation
- Energy-Related Environmental Research
- Strategic Energy Research

What follows is the final report for the Durability of Catalytic Combustion Systems Project, conducted by Catalytica Energy Systems Inc. The report is entitled “Durability of Catalytic Combustion Systems.” This project contributes to the Environmentally-Preferred Advanced Generation program.

For more information on the PIER Program, please visit the Commission's Web site at: <http://www.energy.ca.gov/reseach.index.html> or contact the Commission's Publications Unit at 916-654-5200.

## **Executive Summary**

Catalytica Energy Systems Inc. (CESI) is developing a novel catalytic combustion process that produces ultra-low emissions for natural gas fired turbine engines. As part of this effort, the California Energy Commission (the Commission) sponsored development of supporting catalytic combustion technologies and on-grid demonstration of the CESI Xonon® Catalytic Combustion system. This is the final summary report covering the entire 3-year effort.

### **Background**

The high temperatures in typical combustion processes accelerate the formation of noxious oxides of nitrogen (NO<sub>x</sub>). It is well known that NO<sub>x</sub> formation increases dramatically when the temperature exceeds about 1600°C (2900°F). Traditional diffusion flame combustor flame temperatures can exceed 2200°C (4000°F) for brief periods, so it is virtually impossible to achieve ultra-low NO<sub>x</sub> levels when a turbine is fired with a diffusion flame combustor. State-of-the-art Dry Low NO<sub>x</sub> (DLN) combustion systems can operate at high single digit NO<sub>x</sub> levels; however, these systems are expensive and susceptible to flame-out or flame instability because they operate at very low fuel/air ratios. DLN combustion systems will need to be coupled with expensive exhaust cleanup systems in order to achieve NO<sub>x</sub> levels below 3 parts per million by volume (ppmv).

The catalytic combustion technology pioneered by CESI (called Xonon®) achieves ultra-low emission levels without the drawbacks found in other low emission technologies. In the Xonon® combustion system, NO<sub>x</sub> formation is reduced as the result of low combustion temperatures. The maximum combustor exit temperatures on a typical small Xonon® equipped turbine engine is 1350°C (2460°F) or lower – well below the temperatures where NO<sub>x</sub> readily forms.

A typical Xonon® combustion system is shown in Figure ES1. Engine compressor discharge air enters an annular plenum prior to entering the pre-burner. The pre-burner is a small DLN type combustor that pre-heats the combustor air up to the catalyst operating temperature. Fuel is then injected into the warm air and thoroughly mixed before entering the catalyst module. In the catalyst module, some of the fuel/air mixture is combusted through a flameless catalytic process. The combustion process continues in the burnout zone until all of the remaining un-combusted fuel is reacted.



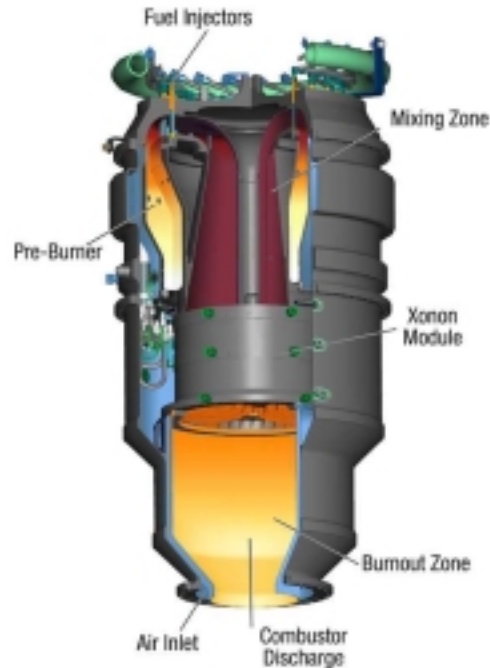


**Figure ES1 – Typical Xonon® combustion system**

### **Project Approach**

The plan entailed installing the currently available Xonon® combustion system on a 1.4 MW Kawasaki M1A-13A gas turbine. This initial configuration established the baseline system performance and the test procedures necessary to handle system failures or stoppages. Simultaneously, development efforts began on component level technology improvements. As these individual technology improvements were developed, they were incorporated into the RAMD engine test at stoppages or when appropriate.

### **Project Purpose**

The purpose of the project was three-fold:

1. To demonstrate the performance of the Xonon® combustion system in actual on-grid engine operation for up to 8,000 hours. The plan was to use a Xonon® equipped Kawasaki M1A-13A gas turbine as a platform for a Reliability, Availability, Maintainability and Durability (RAMD) test.
2. To advance the supporting technologies of the Xonon® catalytic combustion system to the point where a pre-production product could be successfully designed and fabricated. The supporting technologies investigated during this program include:
  - The control of the combustor and gas turbine system with the capability to handle load steps and full load loss;
  - The durability of the catalyst mechanical structure;
  - Fuel-air mixing and the occurrence of ignition of the fuel-air mixing upstream of the catalyst
  - The development of longer life catalyst materials; and

- The effects of the variability in fuel quality on combustor performance
- 3. To determine the commercialization potential of the Xonon® combustion system and the capability of CESI to manufacture Xonon® modules to meet predicted production demand.

CESI developed plans to address the technical issues associated with fielding a robust, low-emission catalytic combustion system for the power generation industry.

### **Technology Objectives**

The specific technical goals for the project are to:

- Demonstrate the catalytic combustion technology and the Xonon® combustor to a reliability of 98 percent and availability of 96 percent.
- Demonstrate RAMD engine emissions below 3 ppm NO<sub>x</sub>, and 5 ppm CO and UHC.
- Develop a control strategy able to meet the load following and load step performance required by the power generation industry.
- Develop a robust mechanical support system for the catalyst that will exceed 8,000 operating hours.
- Design and test an axial fuel/air premixer design for the Xonon® combustion system.
- Develop catalyst materials that will exceed 8,000 operating hours.
- Determine the effect of variability in natural gas fuel composition on the performance of catalytic combustion systems. This task involved two primary objectives:
  - 1) Survey the range of natural gas compositions found in the United States and worldwide.
  - 2) Test a catalyst system over the composition range found in the survey to observe the effects of varying natural gas composition, specifically higher hydrocarbons and diluents, on the performance of the system.

### **Economic Objectives**

The technology developed during the course of this program is projected to reduce the cost of producing electric energy in California and the rest of the nation. Much of the cost savings will result from the reduction in the cost of complying with environmental regulations. New equipment installed in California today is usually required to meet NO<sub>x</sub> and other emissions to a level of 3 to 5 ppm. Meeting these low levels will require the lean pre-mix combustion technology (commonly called DLN) coupled with the use of SCR. Table 1.2.2.1 below shows the estimated economic costs associated with various types of NO<sub>x</sub> control technologies. The data clearly show that Xonon® is the only single technology that can economically deliver <3ppm NO<sub>x</sub> emissions.

### **Project Technical Outcomes**

CESI has successfully completed the development efforts to improve the performance and reliability of selected catalytic combustion technologies and the Xonon® combustion system. Although not all of the initial goals were met with technical success, the overall program delivered significant technical and performance achievements. The outcomes for each of the technical goals are summarized in the paragraphs that follow.

## RAMD Engine Test

The RAMD test concluded with 8,128 hours of actual on-grid operation with a Xonon® combustion system. This industry leading accomplishment validates the Xonon combustion system as a viable pollution control technology for gas fired turbine applications. Table ES1 details the results of the RAMD effort. The table clearly shows that the average emission levels for NO<sub>x</sub>, CO, and Unburned Hydrocarbons (UHC) are well below the program goals. The Xonon® system also exceeded the reliability goal of but fell slightly short of the availability goal. RAMD index values for maintainability and durability were not calculated because of the replacement of several of the original components with newly designed components with enhanced performance characteristics. Based on analytical model projections that have been verified through sub-scale testing, the final combustor configuration can achieve the 8,000 hour life goal.

**Table ES1—Program results and goals**

Performance Parameter	Result
RAMD operating hours	8,128 hours (goal 8,000 hours)
NO <sub>x</sub> emissions (average at full load)	1.3 ppmv (goal < 3 ppmv)
CO emissions (average at full load)	0.9 ppmv (goal < 5 ppmv)
UHC emissions (average at full load)	1.3 ppmv (goal < 5 ppmv)
Reliability	99.2 percent (goal 98 percent)
Availability	91.2 percent (goal 96 percent)

Note: Values for maintainability and durability were not calculated

(see Section 2.1.6.1 for details)

## Control System Development

CESI completed the task to develop a fuel control system capable of accepting complete load loss without exceeding the turbine over-speed or surge limits. The control logic developed as a result of this activity improved the operational characteristics of the system in load following, load rejection and breaker auto-resynchronization modes. The control system improvements include:

- The capability to accept load steps up to 600 kW without the loss of system stability;
- The capability to survive complete load loss up to 1050 kW without exceeding over-speed limits; and
- The capability to automatically resynchronize to the power grid following a load rejection.

### **Catalyst Axial Support Analysis**

A detailed study was conducted using a combination of structural analysis and material testing to determine the durability of the axial catalyst mechanical support (designated the Bonded Metal Monolith or BMM). The fatigue analysis results show that the average calculated fatigue life is 650 cycles (50 cycles initiation and 600 cycles of propagation) , which is well within the design life (8,000 hours or approximately 100 cycles) of the BMM. These analytical results agree favorably with the actual hardware, which showed signs of crack initiation after 50 cycles (4,128 hours).

Creep analysis results show that the BMM does not meet the design life goal of 8,000 hours. Due to the low creep life of the BMM design, CESI initiated an internally funded redesign activity. The resulting axial support design is currently undergoing engine testing at the Silicon Valley Power (SVP) test facility. Early test results from the SVP site indicate that the newly designed axial support will exceed the 8,000 hour life goal.

### **Axial Fuel/Air Premixer and Flameholding Study**

A detailed study was conducted using a combination of computational fluid dynamic (CFD) analysis and cold flow rig testing to determine the feasibility of incorporating an axial fuel/air premixer into the Xonon® catalytic combustion system. The results indicate that the lobed axial mixer configurations studied will not perform better than the current Xonon® radial mixer design. Cold flow testing of the mixer effectiveness showed poor mixing directly downstream of the fuel peg locations.

A second aspect of this task was to study the effects of temperature, pressure, gas velocity and geometry on flameholding and to determine those parameters that will reduce the possibility of flameholding in future CESI premixer designs. The flameholding study concluded that flameholding transition occurs somewhere between a 0.0375" and a 0.125" step expansion. Steps less than 0.0375" were much less likely to initiate flameholding.

### **Catalyst Improvements**

Sub-scale reactor tests showed that certain new catalyst formulations demonstrated superior initial performance and short-term stability when compared to the current baseline catalyst. In addition, 8000-hour total surface area testing also showed improvement over the current catalyst system formulation. However, the long-term stability of the active metal surface was found to be inferior to that of the current baseline catalyst after exposures of 8000 hours at 900°C and 4000 hours at 950°C. Based on the long-term performance test results, it was determined that the new catalyst formulations would not be incorporated into the RAMD engine-testing program.

### **Natural Gas Variability**

The results of this task show that the current catalyst is insensitive to inerts (nitrogen and/or carbon dioxide) in concentrations up to 25 vol percent. In addition, the inclusion of higher volumes of hydrocarbon constituents increases the catalyst reactivity, causing a shift of the operating window resulting in:

- The emissions design limit being reached at a lower catalyst inlet temperature;

- The catalyst durability design limit being reached at a lower catalyst inlet temperature; and
- Movement of the homogeneous combustion front closer to the catalyst outlet face for a given outlet gas temperature and  $T_{ad}$  (Combustor exit temperature).

Relatively large amounts of higher hydrocarbon constituents do not damage the catalyst in the short term. If properly monitored, a relatively large higher hydrocarbon constituent level can actually increase long-term catalyst durability by operating at lower catalyst inlet temperatures.

### **Economic Outcomes**

Since the Xonon® technology is in the pre-production phase of development, actual economic results are not available. However, CESI has developed economic models based on industry trends, production readiness assessments, and OEM production orders. These models project that Xonon® technology can produce net power costs that are only 7-9 percent greater than an uncontrolled high-emission turbine. In areas where less than 3 ppm NO<sub>x</sub> emissions are required, Xonon® achieves the same NO<sub>x</sub> emissions levels as the DLN plus SCR option at costs that are 7-21 percent lower. See Section 3.2.1 for more details on the projected cost benefits of Xonon®.

### **Project Commercialization Potential**

On-site Energy Inc. performed a commercialization study that examined the commercial potential of the Xonon® catalytic combustion technology. Through a series of analyses, customer and OEM interviews, and marketing research, the following conclusions were reached:

- Xonon® equipped gas fired turbine engines have the potential to produce net power costs that are only 7-9 percent more expensive than an uncontrolled turbine.
- When compared to DLN combustors coupled with Selective Catalyst Reduction exhaust clean up technologies, Xonon costs are 7-21 percent lower (depending on the application).
- Environmental restrictions will necessitate the use of clean up technologies before new gas-fired applications can even be permitted. This is particularly true in California.
- Annual growth in new gas-fired turbine orders is about 13 percent per year on a compounded basis. The increase in Combined Heat and Power (CHP) applications for California alone is roughly 18.5 percent per year.
- Xonon® is positioned in the market to capture a large percentage of the growth in new gas-fired turbine applications.

### **Production Readiness**

CESI has committed significant resources to meet the projected production demands for Xonon® catalyst modules. The company has opened a new facility in Gilbert, Arizona for the manufacture and assembly of Xonon® modules. The facility is sized to meet the production demand for at least the next 5-7 years. Additional capacity, if needed, would be available at our current Mountain View manufacturing facility.

## Conclusions

CESI completed a three-year program to develop and test a pre-production catalytic combustion system on a gas fired turbine platform. The system performed well and met many of the program goals and objectives. Some additional development work needs to be completed on selected individual components in order to validate durability estimates. Some of the key overall program conclusions are:

- The Xonon® catalytic combustion system demonstrated ultra-low levels of NO<sub>x</sub>, CO and UHC emissions for 8,128 hours of on-grid operation.
- The Xonon® catalytic combustion system demonstrated a reliability of 99.2 percent (goal 98 percent) and an availability of 91.2 percent (goal of 96 percent).
- The Xonon fuel control system is now able to adjust to load loss, large load step increases and grid resynchronization without loss of stability.
- The axial catalyst support did not have the required durability to meet the 8,000-hour life goal. A new support system was designed and is currently being tested in the RAMD engine test bed.
- The new axial fuel/air mixer design did not meet the goal for mixing uniformity. As a result, the current radial swirler was kept as the primary design for the RAMD testing.
- Some new catalyst formulations showed early promise during short-term testing; however, long-term test results showed that the new formulations were inferior to the current catalysts.
- An increase in the concentration of heavy hydrocarbons shifts the catalyst operating window and moves the homogeneous combustion wave front closer to the catalyst outlet face. These changes in operational characteristics should not adversely affect the catalyst module if the proper control logic is in place.
- The Xonon® combustion technology is positioned to capture a significant portion of new pollution control business for the small to medium size gas turbine market.
- The growth in new gas fired turbine projects is projected to be 13 percent per year on a compounded basis.
- Xonon® offers several competitive advantages over other pollution control technologies. These include:
  - Lower initial capital acquisition costs;
  - Lower operational costs;
  - Shorter permitting time;
  - Ultra-low emissions (NO<sub>x</sub> < 3 ppmv, CO < 5 ppmv, UHC < 5 ppmv);
  - Xonon® is a pollution prevention technology instead of a pollution clean-up technology; and
  - Xonon® modules are recyclable and do not use the environmentally hazardous chemicals (like ammonia) utilized by emission clean up technologies.
- CESI is committed to the commercialization of Xonon® and has allocated significant financial resources to improving CESI's manufacturing infrastructure and facilities.

### **Benefits to California**

Catalytic combustion systems provide ultra-low emissions levels of pollutant species such as NO<sub>x</sub>, CO, and UHC. This allows the development of distributed power systems in urban and suburban areas throughout much of California. Today most of these areas have emission regulations sufficiently severe that gas turbines using conventional combustion systems cannot be used without the use of exhaust gas clean-up systems. One such system is selective catalytic reduction, or SCR, which catalytically reduces NO<sub>x</sub> with ammonia gas that is injected into the exhaust stream ahead of the SCR catalyst. The economies of scale of SCR systems impede its use on small gas turbines, typical of the size turbine that would be used in distributed power scenarios, as the much larger percentage of added cost (capital and operating) from SCR render power generation with small engines uneconomical. This economic penalty has largely eliminated the use of small gas turbine power generation in areas with severely restrictive emission regulations.

Catalytic combustion systems can break this paradigm by providing NO<sub>x</sub> levels as low as or lower than those provided by SCR at a cost that is significantly lower for all sizes of gas turbine generation units. This breakthrough allows the distributed power concept to become reality in areas of California. The approval for use as an alternative BACT system (in progress), requires demonstration of the practicality (*i.e.*, durability and fuel flexibility) of the catalytic combustion system. The results of this project demonstrate the ability to operate on natural gas with the range of compositions delivered to California cities, allowing gas turbines to penetrate this emerging and very important power generating market segment in California.

Program success will lead to the economic viability of small gas turbines in distributed power generation that locates generating systems at or near the point of end use. Power generation in this manner will provide, by minimizing the costs of transmission and distribution, lower electricity prices to the consumer. Also, locating the generation at the “end-of-line” in industrial or institutional facilities accommodates cogeneration, or the use of the exhaust heat from the turbine to replace heat that would otherwise be obtained from a separate burner. Cogeneration is a much more efficient method of fuel conversion, and not only consumes less fuel but produces lower emissions. Distributed power generation will also improve the reliability of the power supply network, thus avoiding widespread planned or unplanned interruptions in power delivery.

## **Abstract**

The Catalytica Energy Systems, Inc. (CESI) is developing and commercializing catalytic combustion technology for application in natural gas fired gas turbines. This technology, trade named Xonon®, achieves ultra-low emissions levels without the need for exhaust aftertreatment systems. This PIER 1 project addresses three key aspects of bringing this new technology to market:

1. First demonstration of a catalyst-equipped gas turbine supplying power to the electrical grid.
2. Further development of combustion system components for commercial service.
3. Assessment of market requirements and opportunities for Xonon application.

The primary goal of the project was to achieve 8,000 hours of grid-connected turbine operation while maintaining base load emissions levels below 5 parts per million (ppm) nitrogen oxides (NO<sub>x</sub>) and 10 ppm carbon monoxide (CO) and unburned hydrocarbons (UHC). During the extended turbine operation, other project efforts were focused on improvements in individual components of the combustion system --- fuel-air mixer, catalyst mechanical support, controls system, longer-life catalysts --- that could be incorporated in the turbine test program as it proceeded. The market requirements for applying this new technology in California and elsewhere were evaluated via interviews with a broad spectrum of stakeholders to determine the technical, regulatory, and economic drivers in the marketplace.

The successful outcome of this project is represented in the 8,128 hours of operation of a grid-connected, Xonon-equipped, 1.4 MW, Kawasaki M1A-13X gas turbine at a Silicon Valley Power site. Average emissions levels over the course of those hours were 1.3 ppm NO<sub>x</sub>, 0.9 ppm CO, and 1.3 ppm UHC. The catalytic combustion system and associated controls are now being offered for commercial purchase. The initial 3-unit sale is for installation in a government facility in Massachusetts.



## 1.0 Introduction

### 1.1. Project Background

Catalytica Energy Systems, Inc. (CESI) has been developing catalytic combustion for gas turbines since 1988 (until December 2000, under earlier corporate names of Catalytica Combustion Systems, Inc. and Catalytica, Inc.). Over this period, CESI had developed the basic technology for a radically innovative approach to the combustion of hydrocarbon fuels to achieve ultra low levels of pollutant oxides of nitrogen ( $\text{NO}_x$ ). Prior to the current program, the Xonon® technology had been developed through the following stages:

- 1) Sub-scale high-temperature rig testing at low and high pressures.
- 2) Demonstration in a full-scale combustion system on a Kawasaki Heavy Industries (KHI) M1A-13X 1.4-MW gas turbine for 1,000 hours in Tulsa, OK.

During the M1A-13X demonstration, the engine operated over the full load range of the gas turbine and demonstrated emissions levels of less than 2.5 parts-per-million (ppm)  $\text{NO}_x$  and less than 5 ppm of both carbon monoxide (CO) and unburned hydrocarbons (UHC) at full load conditions.

The pollution-prevention capabilities of advanced catalytic combustion systems will encourage the development of distributed power systems in urban and suburban areas. Today, most of these areas in the U.S. have emission regulations sufficiently severe that gas turbines using conventional combustion systems cannot be used without the use of expensive exhaust gas clean-up systems. The current exhaust clean-up system of choice is the selective catalytic reduction system or SCR. This system is mounted in the exhaust system of a gas turbine and catalytically reduces  $\text{NO}_x$  with ammonia gas that is injected into the exhaust stream ahead of the SCR catalyst. The economies of scale are such that SCR systems for small gas turbines, typical of proposed in distributed power scenarios, are a much larger percentage of the total cost than for large gas turbines. This economic penalty has largely eliminated the use of small gas turbine power generation in areas with severely restrictive emission regulations.

Catalytic combustion systems can break this paradigm by providing  $\text{NO}_x$  levels as low or lower than those provided by SCR, and at a cost that is significantly lower for all sizes of gas turbine generation units. This breakthrough is important in that it will allow the distributed power concept to become reality in areas such as California, New York and Chicago. However, approval for use as an alternative BACT system will require demonstration of the practicality (*i.e.*, durability and fuel flexibility) of the catalytic combustion system. Catalytica has developed enabling technologies that will allow gas turbines to penetrate this emerging and very important power generating market segment.

Program success will lead to the use of small gas turbines in a distributed power generation scenario that locates generating systems at or near the point of end use. Distributed power generation will provide lower electricity prices to the consumer by minimizing the costs of power transmission and distribution. In addition, locating the generation at the “end-of-line” near industrial or institutional facilities accommodates cogeneration, or the use of the exhaust heat from the turbine to replace heat that would otherwise be obtained from a separate burner or boiler system. Cogeneration is a much more efficient method of fuel conversion and

produces lower emissions. Distributed power generation will also improve the reliability of the power supply network, lessening the chances of brown-outs or a full black-out.

### 1.1.1. Technology Concept

High temperatures in a combustion process accelerate  $\text{NO}_x$  formation. The temperature dependence of  $\text{NO}_x$  production is shown in Figure 1.1.1.1 for conditions typical of a gas turbine combustor. It is evident from the curve that  $\text{NO}_x$  production increases dramatically when the temperature exceeds about  $1600^\circ\text{C}$  ( $2900^\circ\text{F}$ ). Temperatures in the hottest regions of a diffusion flame can exceed  $2200^\circ\text{C}$  ( $4000^\circ\text{F}$ ) for brief periods, so there is little possibility of achieving single digit  $\text{NO}_x$  levels when a turbine is fired with a diffusion flame combustor. If, on the other hand, the peak combustion temperature can be limited below about  $1540^\circ\text{C}$  ( $2800^\circ\text{F}$ ),  $\text{NO}_x$  levels can be less than a few parts per million. Unfortunately, at fuel-air ratios low enough to achieve such low  $\text{NO}_x$  concentrations, flames are highly unstable and are susceptible to flame-out or fluctuations which can cause severe combustor vibrations, so even a lean premixed combustor cannot operate in this most desirable low temperature range to achieve ultra-low  $\text{NO}_x$  emissions.

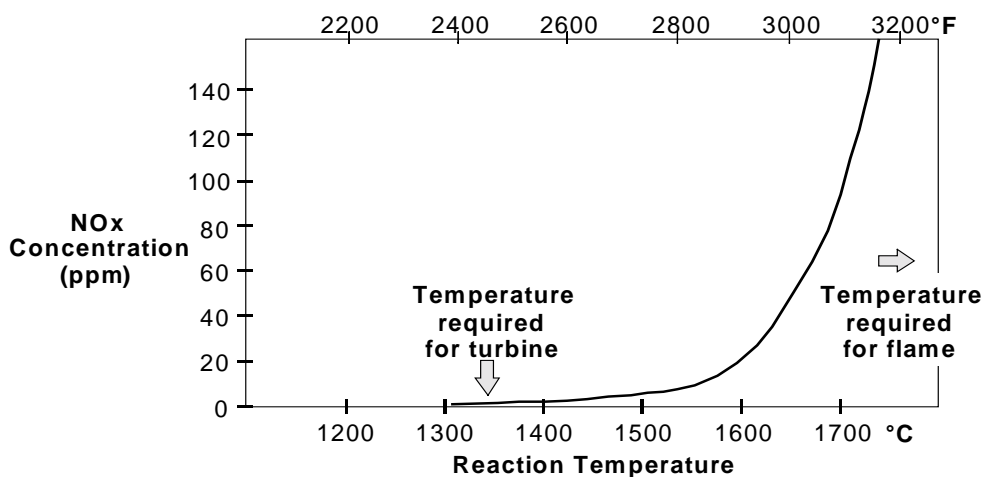
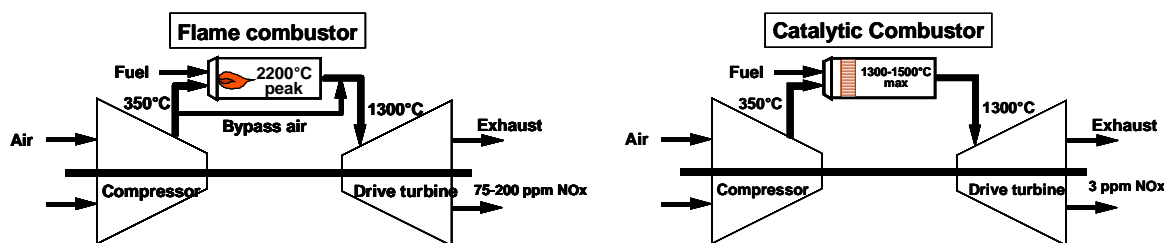


Figure 1.1.1.1 -- Dependence of  $\text{NO}_x$  formation on temperature (10 atm pressure, 20 ms residence time)

As a consequence of the situation depicted in Figure 1.1.1.1, a gas turbine with a lean premixed combustor must use an exhaust gas cleanup system to meet the NO<sub>x</sub> goals established for Environmentally Preferred Advanced Generation (EPAG) systems. Selective catalytic reduction (SCR) technology is available for this purpose, but it extends appreciably the footprint of the turbine and adds very significant costs that are reflected in the cost per kilowatt-hour (i.e., the cost of electricity) that the end user ultimately pays. In addition, SCR systems require ammonia, which presents problems in transportation and storage due to its volatility and toxicity. Urea-based SCR systems are an alternative, but they require an extra process step to convert the urea into ammonia for reaction over the SCR catalyst. SCONOX, a second commercial cleanup system, is even more expensive than SCR. The cost of an extra cleanup unit is particularly burdensome for smaller gas turbines, as the cleanup costs are higher on a dollars-per-kilowatt and per kilowatt-hour basis. The ultimate effect has been a drastic reduction in the sighting of gas turbines in California over the last ten years despite the gas turbine's well-known benefits in distributed generation and cogeneration.

In contrast to flame combustion, catalytic combustion does not involve any issues of flame stability. The fuel-air ratio entering the catalyst simply needs to be high enough to generate the desired turbine inlet temperature at full conversion of the fuel. In current small turbines the required maximum temperature at the combustor exit is typically 1350°C (2460°F) or lower; so Figure 1.1.1.1 shows that extremely low NO<sub>x</sub> concentrations are possible using catalytic combustion. The essential difference between the two approaches to gas turbine combustion is shown schematically in Figure 1.1.1.2.



**Figure 1.1.1.2 -- Essential features of flame versus catalytic combustor. NO<sub>x</sub> formation accelerates above about 1500°C**

### 1.1.2. Project Approach

Prior to this project, the KHI catalytic combustion system had been operated on a gas turbine engine and had completed a 1000-hour endurance test in Tulsa Oklahoma. This operational test identified a number of issues that needed to be resolved for the technology to be accepted by gas turbine original equipment manufacturers (OEMs). In addition to these technology issues, CESI recognized the need to demonstrate the high durability and reliability of the catalyst and combustion system that is equivalent to other major turbine engine components. CESI developed a program plan to provide the market with this demonstrated performance consisting of four steps:

- Operate the Xonon® combustion system in a KHI M1A-13X in a power generation facility for 8000 hours (approximately 1 year of continuous operation).

- Continue the rapid development of the technologies needed to meet the durability and reliability requirements for the Xonon® combustor and catalyst module.
- When the required reliability has been demonstrated, move the Xonon® combustor technology to one or more commercial sites for field-testing.

Offer the Xonon® combustor as a commercial product and begin translation of the technology to other gas turbine engines.

This current project covers items 1 and 2 from the above list and had two interdependent goals:

- Goal 1     Develop the necessary technologies to improve the durability and reliability of the Xonon® combustor and catalyst module.
- Goal 2     Develop and demonstrate the reliability, availability, maintainability and durability (RAMD) on the Xonon® equipped KHI M1A-13X.

These two goals were addressed simultaneously. The general project approach is shown schematically in Figure 1.1.2.1 below. The project is built around a RAMD engine test that is designed to test and demonstrate the durability and reliability of the combustion system. RAMD is an approach designed to measure quantitatively the R-reliability, A-availability, M-maintainability and D-durability of a system composed of many components.

The plan entailed installing the currently available combustion system on the engine for the initial testing. This initial configuration established the baseline system performance and the test procedures necessary to handle system failures or stoppages. Simultaneously, development efforts began on component level technology improvements. As these individual technology improvements were developed, they were incorporated into the RAMD engine test at stoppages or when appropriate. The overall project objective was to demonstrate RAMD performance sufficient for the target power generation market.

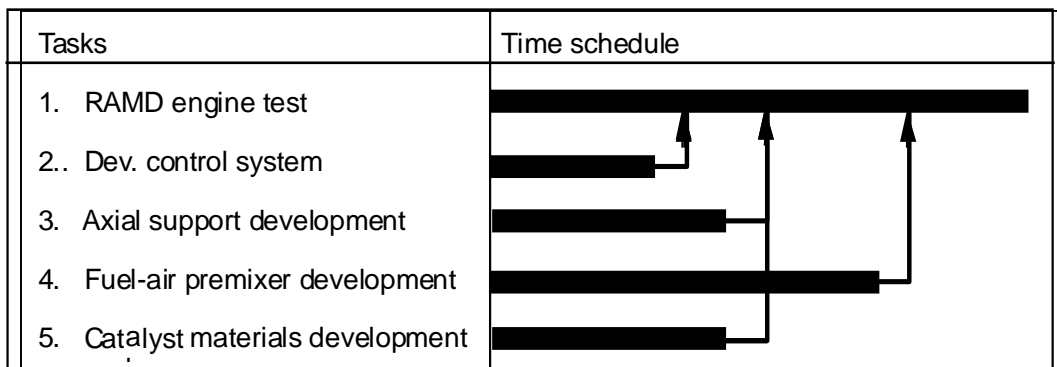


**Figure 1.1.2.1 -- General program approach shows integration of technology improvements into RAMD engine testing**

### 1.1.3. Problem Statement

The current emissions requirement for permitting a new gas fired turbine in California is generally under 9 ppm NO<sub>x</sub>, with significantly more stringent requirements (< 5 ppm) found in the San Francisco Bay Area and in the South Coast Air Quality District. The current marketplace method for achieving these levels involves the use of a Selective Catalytic Reduction (SCR) unit

of about 95 percent reduction to achieve ~ 9 ppm NO<sub>x</sub>. For levels below 9 ppm NO<sub>x</sub>, the SCR unit must be used in conjunction with an additional method of control (e.g. steam injection, lean pre-mix combustion technology). These stringent emission requirements pose significant cost burdens on power generators. Catalytic combustion, which is a pollution prevention technology, has the potential to significantly reduce the cost over that of the current state-of-the-art clean up technologies.

The scientific and engineering communities have recognized catalytic combustion for almost thirty years as a technically compelling approach to reducing NO<sub>x</sub> emissions in gas turbines. Previous efforts at developing robust catalytic combustors for gas turbines have achieved low, single-digit NO<sub>x</sub> ppm levels but have failed to produce combustion systems with suitable operating lifetimes. This was typically due to the lack of suitable high-temperature materials used for catalysts and associated catalyst support systems.

Catalytic combustors provide an economically attractive alternative, as compared to exhaust gas clean-up technologies, for the full range of gas turbine sizes. This is especially true for small turbines, which are expected to provide a considerable amount of electrical power in the distributed generation market. Before commercial acceptance, however, catalytic combustion systems need to demonstrate the reliability, availability, maintainability and durability (RAMD) required of modern power generation gas turbine systems.

#### **1.1.4. Project Purpose**

The intent of this project was to advance the technologies of catalytic combustion systems to the point where a pre-production product could be successfully designed and fabricated. To accomplish this, a number of technical issues had to be resolved. The major technical issues addressed by this project were:

- The demonstration of the Reliability, Availability, Maintainability and Durability of the entire combustion system;
- The control of the combustor and gas turbine system with the capability to handle load steps and full load loss;
- The durability of the catalyst mechanical structure;
- Fuel-air mixing and the occurrence of ignition of the fuel-air mixing upstream of the catalyst;
- The development of longer life catalyst materials; and
- The effects of the variability in fuel quality on combustor performance.

In addition to the technical issues listed above, several business related issues were also addressed in this program including:

- The capability of CESI to fabricate catalyst modules in production quantities; and
- The commercialization potential of the Xonon® catalytic combustion technology.

CESI developed program tasks to address each of the issues listed above. This project is the first part or phase of a larger multi-year program intended to move the CESI Xonon® catalytic combustion system into the market place as quickly as possible.

#### **1.2. Project Goals**

The overall objective of this project was to conduct research and development activities necessary to advance CESI's Xonon® catalytic combustor technology while meeting the PIER1 goals defined by the California Energy Commission in the original RFP. These goals are:

- 1) To reduce the costs of the proposed environmentally preferred advanced generating technology, in either a simple-cycle or co-generation mode, while maintaining or improving environmental or public health performance. Specifically, the goal is to reduce the amount by which the technology currently exceeds competitive market costs by 50 percent.
- 2) To reduce adverse environmental or public health impacts of electricity generation by at least 15 percent below current best practices (< 9 ppm NO<sub>x</sub> without SCR), while maintaining or improving cost performance.

In addition to the overall program goals listed above, there were specific technical and economic objectives as described in the sections below.

### **1.2.1. Technical Objectives**

The project tasks were conceived to directly support the development of the next generation of industrial size gas turbine systems (under 50-MW) through substantial improvements in their environmental performance. Specifically, the successful completion of this project greatly enhances ability of these size class turbines to meet the most severe NO<sub>x</sub>, CO and unburned hydrocarbons (UHC) regulations.

The project technical objectives are:

- Demonstrate the catalytic combustion technology and the Xonon® combustor to a reliability of 98 percent and availability of 96 percent.
- Demonstrate RAMD engine emissions below 3 ppm NO<sub>x</sub>, and 5 ppm CO and UHC.
- Develop a control strategy able to meet the load following and load step performance required by the power generation industry.
- Develop a robust mechanical support system for the catalyst that will exceed 8,000 operating hours.
- Design and test an axial fuel/air premixer design for the Xonon® combustion system.
- Develop catalyst materials that will exceed 8,000 operating hours.
- Determine the effect of variability in natural gas fuel composition on the performance of catalytic combustion systems.

### **1.2.2. Economic Objectives**

The technology developed during the course of this program is projected to reduce the cost of producing electric energy in California and the rest of the nation. Much of the cost savings will result from the reduction in the cost of complying with environmental regulations. New equipment installed in California today is usually required to meet NO<sub>x</sub> and other emissions to a level of 3 to 5 ppm. Meeting these low levels will require the lean pre-mix combustion technology (commonly called DLN) coupled with the use of SCR. Table 1.2.2.1 below shows the estimated economic costs associated with various types of NO<sub>x</sub> control technologies. The data clearly show that Xonon® is the only technology that can economically deliver <3ppm NO<sub>x</sub> emissions.

Table 1.2.2.1 – Projected Life Cycle NO<sub>x</sub> Control Costs

Type	NO <sub>x</sub>	5 MW Class		25 MW Class		150 MW Class	
		\$/ton	¢/kWh	\$/ton	¢/kWh	\$/ton	¢/kWh
Dry Low NO <sub>x</sub> Combustion	25 ppm	260	0.075	210	0.124	122	0.054
Xonon® catalytic combustion	<2 ppm	957	0.317	692	0.215	371	0.146
Water or steam injection	42 ppm	1,652	0.41	984	0.24	467	0.152
Low-temperature SCR	9 ppm	5,894	1.06	2,202	0.429	N/A	N/A
Conventional SCR	9 ppm	6,274	0.469	3,541	0.204	1,938	0.117
High-temperature SCR	9 ppm	7,148	0.53	3,841	0.221	2,359	0.134
SCONOX catalytic absorption	2 ppm	16,327	0.847	11,554	0.462	6,938	0.289

Source: OnsiteSycom



### 1.3. Expenditure Summary

The actual expenditures for this project are shown in Figure 1.3.1 below. These costs include the total investment by the Commission, CESI and other cost share partners. Figure 1.3.1 shows costs for the original program plan and the program replan<sup>1</sup> (Notes and References are in Section 6.0) that took place in 1999. The replan became necessary after a number of unforeseen circumstances and technical issues adversely impacted both the schedule and costs of the originally defined program. In some cases, the technical difficulties presented serious risks to successful completion of the stated goals of the program.

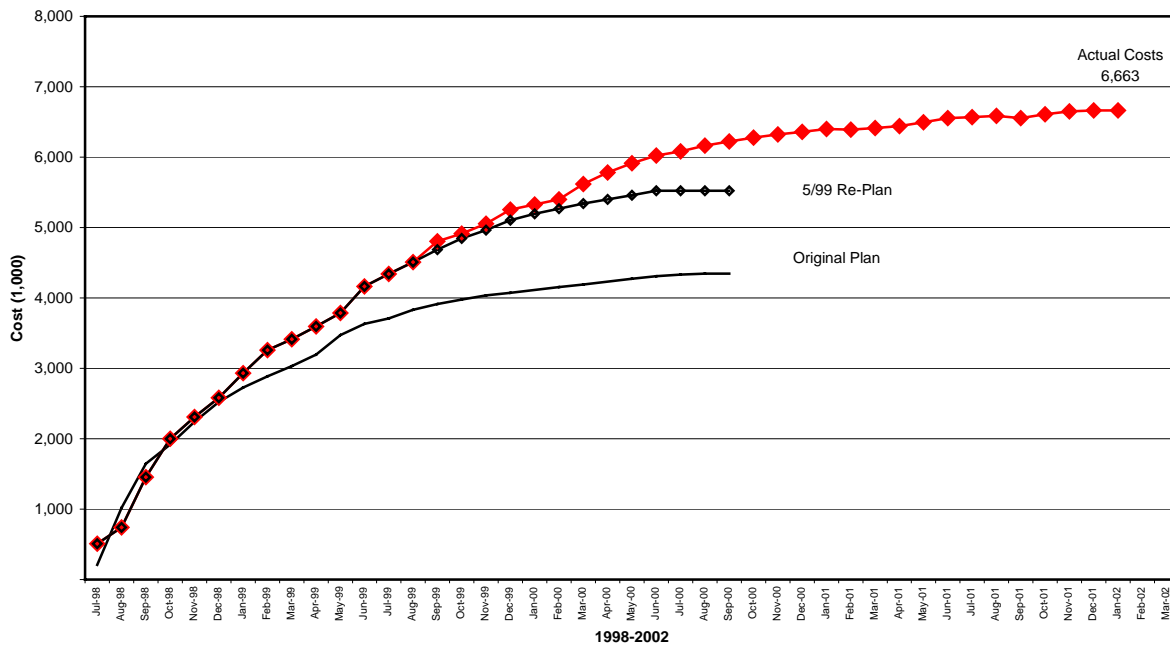


Figure 1.3.1 – Total program expenditures

### 1.4. Report Organization

The remainder of this report describes all the work done over the 3+ years of the CEC-supported PIER 1 project. Section 2 covers each of the areas of technical focus in turn, including:

- Engine testing (Section 2.1)
- Controls development (Section 2.2)
- Axial support development (Section 2.3)
- Fuel/Air premixer development (Section 2.4)
- Catalyst materials development (Section 2.5)
- Fuel composition effects (Section 2.6)

The approach, results, and implications of the technical efforts in each area are described and discussed.

The outcomes of this technology development project are considered in Section 3. The technical outcomes are summarized in Section 3.1, followed by narratives about commercialization potential (Section 3.2), manufacturing capability (Section 3.3), and benefits to the State of California (Section 3.4).

Subsequent sections cover the overall Conclusions and Recommendations (Section 4), Glossary of terms (Section 5) and Notes and References (Section 6).

Appendices A through G follow at the end of the document. They contain detailed information, both in text and figures, which may interest the inspired reader but is not essential for understanding the reported work. The main text of the report contains references to these Appendices at the appropriate locations.

A separately numbered set of Appendices (I through VII) is also part of the complete documentation of this project. These Appendices contain the full texts of the Progress Reports written at the completion of each major project task. The contents of those Progress Reports form the basis for the technical commentary in this Final Report. In most cases, the Final Report contains fewer details than the original Progress Report. For the most thorough treatment of a particular Final Report topic, then, the reader is directed to the corresponding task report in the separately numbered Appendices I – VII.

## 2.0 Approach

### 2.1. RAMD Engine Testing

Further details of the engine-testing program are provided in Appendix II: RAMD Testing and Control System Development.

#### 2.1.1. Introduction

Catalytic combustion has been in development for several years at CESI. Hundreds of hours of rig and simulated engine testing have validated the various design features of the catalytic combustion system. The results from these tests combined with extensive analytical design activities resulted in a fully functional catalytic combustion system capable of meeting the stringent project emissions targets ( $< 3 \text{ ppm NO}_x$ ). The resultant catalytic combustion system as installed on a Kawasaki M1A-13A gas turbine engine is shown pictorially in Figure 2.1.1.1.

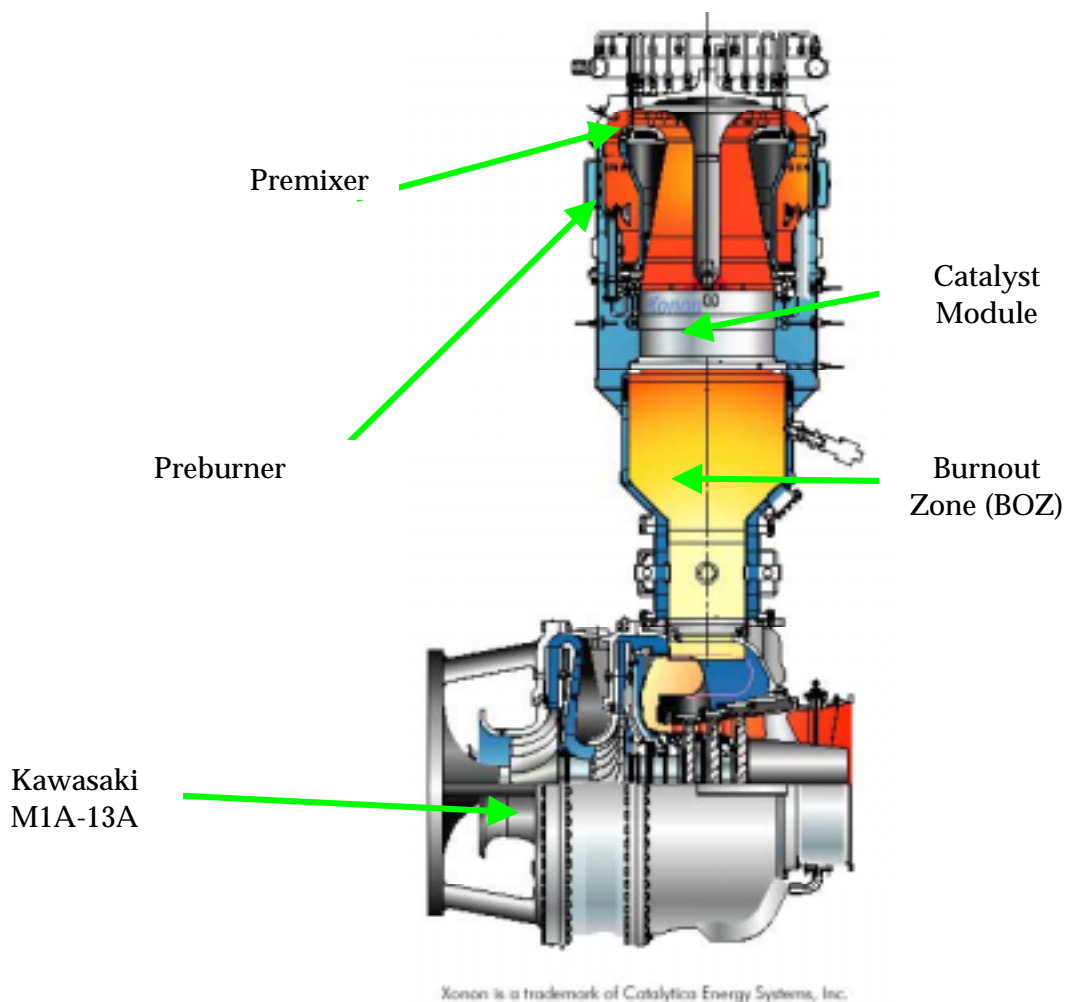


**Figure 2.1.1.1 – Xonon® Catalytic Combustion System installed on Kawasaki M1A-13A**

Prior to the current program, an earlier configuration of the combustion system (the KHI-1 prototype) had operated in excess of 1,000 hours in testing performed in Tulsa, Oklahoma. This

test provided valuable information regarding the initial durability of the catalyst and other components of the combustion system. The next step towards commercialization was to demonstrate the durability and reliability of Xonon®, including its ability to operate unattended for an extended period (8,000 hours).

The Xonon® 2.0 combustion system shown in Figure 1.1 consists of a preburner, a fuel/air premixer, a two stage catalyst module and a homogeneous burnout zone. The preburner preheats the air to catalyst operating temperatures. The premixer thoroughly mixes the warm air and fuel prior to entering the catalyst module. In the catalyst module, the fuel air mixture is partially converted in a flameless combustion process. The remaining reaction occurs in the homogeneous burnout zone before the hot product gases enter the turbine.

CESI purchased an M1A-13A Kawasaki gas turbine engine and installed it on a site owned by the Silicon Valley Power (SVP) Company located in the City of Santa Clara as shown in Figure 2.1.1.2 (Note: a Xonon® equipped M1A-13A is denoted as a M1A-13X). SVP provided financial assistance to the project by providing low cost fuel and reduced rental charges. The power produced was used on site and exported to the local grid. The intent was to exercise the system through a rigorous set of duty cycles consistent with actual industrial operation. This testing covered over 8,000 hours during which the emissions and performance were continuously monitored. In addition, data used to calculate the reliability, availability, maintainability, and durability were gathered and analyzed.

**Figure 2.1.1.2 -- The Xonon® equipped Kawasaki M1A-13X unit installed at SVP**



### 2.1.2. Approach

The project is built around a RAMD engine test that is designed to test and demonstrate the durability and reliability of the combustion system. RAMD is an approach designed to measure quantitatively the R-reliability, A-availability, M-maintainability and D-durability of a system composed of many components. The durability engine test ran nearly continuously with system failures or stoppages recorded and analyzed. Development efforts, performed in parallel, were initiated on technology improvements. As these technology improvements were developed, they were incorporated into the RAMD engine test at stoppages or when appropriate. The overall objective was to reach the end of the project with demonstrated RAMD performance and emissions levels suitable for the target power generation market.

### 2.1.3. Test Bed Selection

Kawasaki Heavy Industries Limited (KHI) produces the rugged M1A-13A 1.4-MW industrial gas turbine which is intended to be packaged as a cogeneration unit producing both electric power and steam (see Figure 2.1.2.1.1). It has a modest thermal efficiency of 25.5 percent (heat rate 13,400 Btu/kW-hr) and is configured with a single external can-type combustor that is readily accessible. The M1A-13A has a pressure ratio of approximately 9.3 to 1, which is comparable to that found in many other industrial gas turbines in the 1 to 6-MW range. The low mass flow (8.2 kg/s) allows the catalytic combustor to be maintained as a small system typical of large rig test units thus reducing the cost of the total system. A low firing temperature of 1004°C makes the engine ideal for catalytic combustion since the modest temperatures in the gas-phase burnout zone (BOZ) allow the use of existing liner cooling technologies.

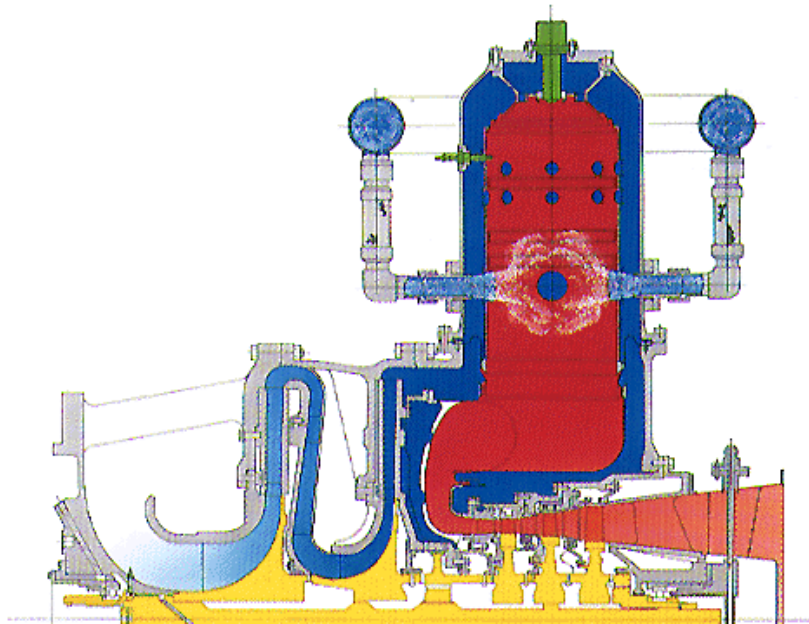


**Figure 2.1.2.1.1 -- Kawasaki (KHI) M1A-13A gas turbine engine with DLN and water injection**

The M1A-13A engine configuration is an ideal platform for the implementation of the Xonon® catalytic combustion system. The external can combustor configuration does not have the

physical size constraints found with other types of combustion systems. This feature allows more flexibility in the size and configuration of the combustion system design. Because of this flexibility, the Xonon® 2.0 catalytic combustion system, although somewhat larger than the original combustion system, is easily adaptable to the M1A-13A engine single-can configuration.

## **2.1.4. Description of Testing Procedures**

### **2.1.4.1. Engine Monitoring**

The gas turbine exhaust emission levels were monitored at one-second intervals and averaged over the course of 15-minute periods. Oxides of nitrogen (NO<sub>x</sub>), carbon monoxide (CO), and unburned hydrocarbons (UHC) were the primary pollutant species monitored and measured. All emissions were verified by an annual relative accuracy test audit (RATA) per federal procedures described by 40CFR60 Appendix B. The species concentrations, expressed as concentration by volume on a dry sample basis [e.g., parts per million by volume, dry (ppmvd)] were measured using the following techniques:

- NO<sub>x</sub>: Gas phase chemiluminescence;
- CO: Non-dispersive infrared (NDIR) photometer;
- Unburned Hydrocarbons (UHC): Flame ionization detector (FID);
- O<sub>2</sub>: Paramagnetic detector; and
- Total Hydrocarbons (THC): Flame Ionization Detector (FID).

The fuel flow was measured and compared to that obtained from an exhaust species carbon balance (EPA Method 19). Natural gas usage was measured with a coriolis type flow meter.

The catalytic combustion system was thoroughly instrumented with miniature thermocouples and pressure taps. The gas temperatures at the preburner outlet, catalyst inlet, catalyst inter-stage and catalyst exit were monitored using type-N thermocouples. Static pressure taps were positioned so that the pressure drops across all three of the main components--the preburner, fuel-air premixer and catalyst bed--were determined. Dynamic pressures were measured using Kistler brand pressure probes. Fuel-air ratio gas sampling used fixed rakes (sampling isokinetically) located immediately upstream of the catalyst module inlet. A near infra-red (IR) camera was mounted to view the exit face of the catalyst module through a quartz window in the burnout zone leading to the combustor scroll and turbine inlet nozzle vanes. Although the IR camera was not routinely calibrated to give accurate temperature measurements, it enables the temperature uniformity of the catalyst module to be continuously monitored.

The turbine system is fully instrumented to collect performance parameters for monitoring and control. A separate continuous emissions monitoring system (CEMS) measures pollutant emissions in the engine exhaust stack, and provides this information to the main control system. Data for all parameters are recorded and stored at one-second intervals. Data reporting to demonstrate regulatory compliance is handled independently. Sections 2.1.5.4 – 2.1.5.6 present the emissions performance data from normal operation of CESI at Silicon Valley Power BAAQMD Plant No. 11840, Permit No. 18547, Source No. S-1.

In addition to the performance data, some of the data records are tagged with a code, indicating the occurrence of an “event” during the period in which that record was being collected. Depending on the nature of these events, certain of these records have been identified as inappropriate for inclusion into the emissions results. These records are then highlighted and tagged with the appropriate event code and stored in the data collection system.

For purposes of this data presentation, an “event” is defined as any occurrence outside of normal controlled operation, which might impact the operation or performance of the turbine facility. Specifically, when the indicated exhaust emissions do not accurately represent the actual emissions produced by the facility, or when operating conditions are not representative of typical “normal” steady-state operation at the maximum design load, these periods are classified as “events.” Examples of events not included in the emission averages would be system calibration, engine start up and shutdown. It is important to note that “events” as they relate to emission data collection may or may not coincide with “events” used to calculate reliability.

An Event Criteria data sheet was used to categorize all of the observed events by keyword, and describes each event in sufficient detail to explain the treatment of data collected during the period of the event. The Event Log lists each observed event during the entire period of the data collection, including any additional comments to further explain the particular event. Specific occurrences of the events are indicated by keyword in the data table along with the parameter. .

A detailed test log was kept to track engine operating conditions and to record any testing anomalies. If an operating event occurred, the cognizant test engineer would evaluate the event and determine the appropriate course of action. If the event occurred when the testing was unmanned, the test cell control logic would evaluate the event and contact a test engineer through an automated paging system. If the event were deemed severe, the test cell control logic would automatically shut down the engine.

#### **2.1.4.2. Engine Test Cycle**

The Xonon® 2.0 combustion system was designed to operate efficiently at or near 100 percent load conditions. While the engine could operate at partial load, the system was optimized for fully loaded 100 percent speed conditions for both performance and low emissions. Although the Continuous Emission Monitoring System (CEMS) measures emissions during the entire engine cycle (from start to stop), inherent sampling delays in the analyzers make it difficult to gather meaningful transient data. All of the RAMD emissions data summarized for this report are at full engine load conditions. This strategy is in conformance to the proposed amendment to part 51 of Chapter I of Title 40 of the Code of Federal Regulations as to the demonstration of pollution control technologies.

If a Xonon® combustion system is to be operated at varying loads (i.e., less than full load), the combustor would need to be equipped with an air by-pass valve allowing some of the combustor air to be diverted from the core combustion flow. The by-pass valve would also be necessary to meet partial load emission requirements.

### 2.1.5. RAMD Definitions

RAMD (Reliability, Availability, Maintainability, Durability) is a program that is supported and recognized by a number of important third-party organizations including the California Air Resources Board, the California Energy Commission, the U.S. Department of Energy, the U.S. Environmental Protection Agency, the Electric Power Research Institute, and the Gas Technology Institute. The primary functions of the CESI RAMD effort were to:

- Define and update the requirements of the development program;
- Predict reliability improvement;
- Quantify demonstrated reliability;
- Apportion unreliability;
- Identify pathways to attain reliability goal;
- Quantify the importance of each problem; and
- Track problem resolution.

Complete definitions for all the parameters used in the calculation of RAMD values can be found in the Glossary and Appendix B at the end of this report.

#### 2.1.5.1. Reliability

Reliability is defined as the percent of time in the period of interest during which the unit is not in a forced outage state. The standard suggests the use of forced outage rate (FOR) as a measure of unreliability. Reliability is the complement to this value.

Reliability (RF) = 1 – Forced Outage Rate (FOR)

$$\begin{aligned} & \text{Period Hours (PH) – Forced Outage Hours (FOH)} \\ & = \frac{\text{Period Hours (PH)}}{\text{Period Hours (PH)}} \end{aligned}$$

Substituting the expression for period hours,

$$\begin{aligned} & \text{SH} + (\text{RSH} + \text{POH} + \text{MOH}) \\ \text{Reliability (RF)} = & \frac{\text{SH} + (\text{RSH} + \text{POH} + \text{MOH}) + \text{FOH}}{\text{SH} + (\text{RSH} + \text{POH} + \text{MOH}) + \text{FOH}} \end{aligned}$$

Note that since FOH ≥ 0, any non-zero time logged as RSH, POH or MOH will result in a net increase in reliability, since the net increase relative to the numerator will be greater than the net increase relative to the denominator, resulting in a larger quotient.

The goal of this program is to meet a reliability of at least 98 percent.

#### 2.1.5.2. Availability

The percent of time in the period of interest in which the unit could be operated to meet the test objectives



Service Hours (SH) + Reserve Shutdown Hours (RSH)

$$\text{Availability (AF)} = \frac{\text{Service Hours (SH) + Reserve Shutdown Hours (RSH)}}{\text{Period Hours (PH)}}$$

The goal of this program is to meet an availability of at least 96 percent before replacement is required.

#### 2.1.5.3. Maintainability

The maintainability of the test catalytic combustor will be measured as the mean time to repair or replace (MTTR). MTTR is defined as the sum of the products of the average part failure rate and the part repair or replacement time divided by the sum of the part failure rates.

The mathematical model for calculating the MTTR is:

$$\text{MTTR} = \frac{\sum(\lambda * R_p)}{\sum(\lambda)}$$

Where  $\lambda$  = average part failures per thousand hours

$R_p$  = repair time required to perform a corrective maintenance action in hours.

The data obtained was to be used to identify repair technologies and fault isolation techniques.

The initial maintainability design criteria (those items designed into the system) included:

1. Reparability,
2. Simplicity of design,
3. Availability, and
4. Modularity.

The goal of this program is to meet a maintainability index of 8,000 hours before replacement is required.

#### 2.1.5.4. Durability

The durability of the catalyst module and the combustion system is defined as the ability to continue to meet the performance goals after a specified extended period of time. In essence the system must meet and go beyond all RAM requirements. For the purposes of this project this extended time period will be defined as MTBO or the reduced hours defined by the availability. Durability is thus the actual time to overhaul or replacement divided by either the defined MTBO (8,000 hours) or the reduced number of hours that defines the availability goal (7,680 hours @ 96 percent availability). To be considered durable the combustion system would have to exhibit a number greater than one (or 100 percent).

If the combustion system continues to operate and meet the required performance after the 8,000 or 7,680 hours used as the measure, it will enter the durability phase of the test program. Testing will be continued until such time as the gas turbine exhaust  $\text{NO}_x$ , CO or UHC concentrations exceed certain levels. To provide some definitions of these levels the  $\text{NO}_x$

concentration used for evaluation purposes will be 3 ppmvd, the CO 10 ppmvd, and the UHC 10 ppmv (dry). If these levels are exceeded the catalytic combustor performance will be considered degraded to the point that it requires replacement. The hours accumulated at this point divided by the MTBO or the 7,680 hours value will be the measure of the system durability. This is sometimes expressed as one (1) subtracted from the latter value and the result expressed as a percentage.

## **2.1.6. Test Results**

### **2.1.6.1. RAMD Calculations**

A key objective of the ongoing SVP operation has been to validate the reliability, availability, maintainability, and durability of the catalyst-equipped system. The performance of the Xonon® system averaged over 8,100 operating hours is summarized in Table 2.1.6.1.1. The program exceeded the goal for reliability (goal – 98 percent) and fell short on availability (goal – 96 percent). The lower availability value is primarily due to higher than anticipated accumulation of reserve shutdown hours (RSH).

The values for maintainability and durability were not calculated due to the earlier than expected replacement of some system hardware. Maintainability is a function of the average part failure rate and repair times. Since several key components were replaced with new designs during the program due to performance limitations (most notably the axial support) or the opportunity to incorporate design improvements (catalyst foil pack), meaningful maintainability values are difficult to calculate. Similarly, the change out of several key components makes the durability calculations difficult to interpret. Accurate maintainability and durability values can be determined once the design is set and time begins to accumulate on multiple units.

**Table 2.1.6.1.1 -- RAMD Values**

<b>RAMD Values (8128 hours)</b>	
<b>Reliability</b>	99.2 percent
<b>Availability</b>	91.2 percent
<b>Maintainability</b>	NA
<b>Durability</b>	NA

### **2.1.6.2. Combustor Configuration**

The RAMD test program accumulated 8,128 hours of on-grid power generation over the course of two years. The intent was to accumulate operating hours as quickly as possible with minimal interruption due to planned or unplanned shutdowns. The RAMD tests were periodically interrupted to perform development tests on sub-systems including the combustion control system, automated bypass integration, premixer and the catalyst container components. Other non-combustion system test interruptions include those related to test cell and computer/communication upgrades.

The RAMD hours were primarily accumulated on four (4) combustor builds. The testing occurred in three phases with new or reworked components/systems implemented during each phase. Table 2.1.6.2.1 shows the phase, engine build and hour accumulation for the entire RAMD test program. Discontinuity in the numbering of the combustor builds is due to the intervening development tests mentioned in the previous paragraph.

**Table 2.1.6.2.1 -- RAMD engine builds and operating hours**

	Build	RAMD Hours	Build Hours
Phase I	KHI-2 build 3	0 - 2064	2064
	KHI-2 build 3A	2065 - 4128	2064
Phase II	KHI-2 build 5	4129 - 7356	3228
Phase III	KHI-2.1 build 1F	7357 - 8128	772
Total RAMD Hours			8128

#### **2.1.6.3. Emissions Measurements**

The exhaust emissions were monitored with an ML661 extractive CEMS specifically designed for industrial applications incorporating proven analyzers that provide exceptional stability and accuracy. The data acquisition system (DAS) records data and generates reports. The basic function of the ML661 extractive CEMS is to provide emissions data that can be used for process control and/or for compliance with local, state and federal regulations. At a minimum, the ML661 satisfies the requirements of the US EPA 40 CFR.

The ML661 system is designed for 24-hour continuous automatic operation. There are several different modes of operation, all controlled by a General Electric GE 90-30 Programmable Logic Controller (PLC) mounted inside the CEMS rack. Except during calibration mode, which occurs every 24 hours, the system is in the sample mode of operation, with sample gas routed to all analyzers. During each 24-hour period, approximately 23 hours and 45 minutes are available for sampling and 15 minutes are dedicated to an automatic calibration check.

The following emissions measuring equipment was used for the RAMD test program:

- CO: ML 9832 Nondispersive Infrared Absorption Analyzer
- CO<sub>2</sub>: ML 472 (Servomex 1415) Nondispersive Infrared Photometer
- NO<sub>x</sub>: ML 9841AS Gas-Phase Chemiluminescence Spectroscopy Analyzer
- Dry O<sub>2</sub>: ML 422 (Sevomex 1420) Paramagnetic Analyzer
- THC: Rosemount 400A Flame Ionization Detector

#### **2.1.6.4. Phase I Emissions Results**

The emission levels were measured and recorded at one-second intervals. The raw one-second interval data were averaged over the course of 30-minute blocks of time. Table 2.1.6.4.1 shows a summary of the averaged emission results for NO<sub>x</sub>, CO and UHC. In addition, data were summarized in one hour and three hour rolling averages. All emission data are corrected to 15 percent oxygen. The table shows that the average emission level for each constituent is quite low and within the respective program goals (NO<sub>x</sub>: 3.0 ppm, CO: 5.0 ppm, UHC: 5.0 ppm).

Table 2.1.6.4.1 – Phase I emissions results(corrected to 15 percent O<sub>2</sub>)

	30 minute averages (ppm)			1 hour rolling averages (ppm)			3 hour rolling averages (ppm)		
	Min	Avg	Max	Min	Avg	Max	Min	Avg	Max
<b>NO<sub>x</sub></b>	0.5	1.3	2.9	0.5	1.3	2.9	0.5	1.3	2.8
<b>CO</b>	0.0	1.2	12.5	0.0	1.2	12.5	0.1	1.2	9.6
<b>UHC</b>	0.0	1.0	9.1	0.0	1.0	9.0	0.0	1.0	8.8

Figure 2.1.6.4.1 is a graph showing the 30 minute averaged NO<sub>x</sub> data versus testing date. The data clearly show that the NO<sub>x</sub> level never exceeded the 3.0 ppm goal. Figure 2.1.6.4.1 also shows that the NO<sub>x</sub> levels began to increase during the colder months. In early operation (June through September, 1999), the load and ambient temperature were both high, and NO<sub>x</sub> performance was uniformly very good. In October, the ambient temperature began to drop, and by the end of the month, NO<sub>x</sub> levels were periodically reaching levels over 2 ppm, and CO emissions were also exceeding normal operation levels.

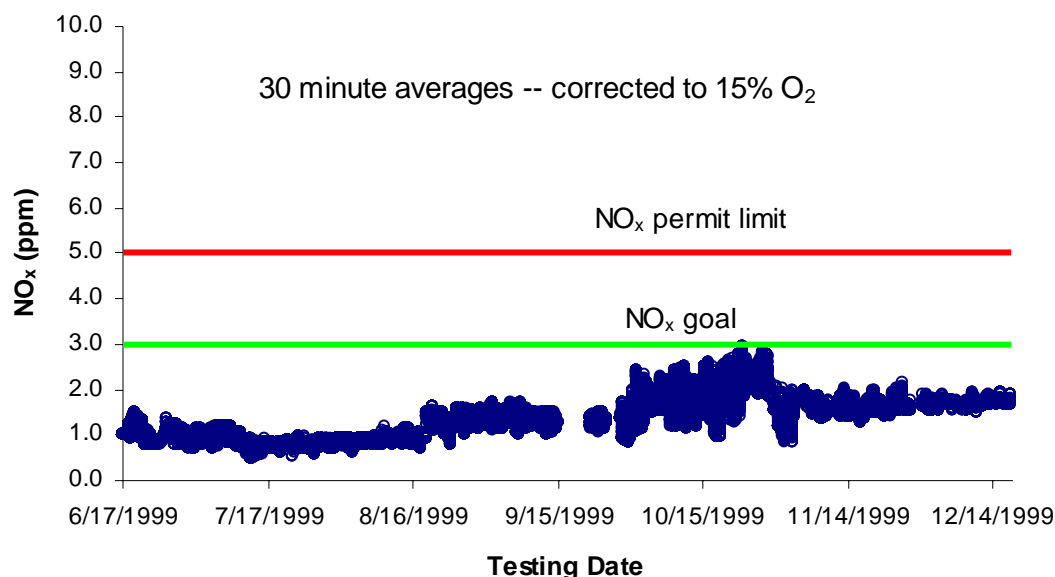


Figure 2.1.6.4.1 – Phase I NO<sub>x</sub> emission results (30 minute averages corrected to 15 percent O<sub>2</sub>)

After some investigation, it was determined that the probable cause of the high CO was due to a capacity limitation of the gearbox. As ambient temperature drops, the power generation capacity of the turbine increases, but the gearbox capacity does not change. So at the lower ambient temperatures, the turbine and combustor systems operate at part load conditions. Since the combustion system was not optimized for the widest turndown range, high CO emissions resulted.

The higher NO<sub>x</sub> emissions can also be attributed to the gearbox capacity limitation that effectively operates the engine and combustor at part load conditions. Under part load conditions, the preburner outlet temperature is higher than at base load conditions. Since the primary source of NO<sub>x</sub> is from the preburner, the higher outlet temperature of the preburner resulted in higher NO<sub>x</sub> emissions. In addition, a portion of the higher NO<sub>x</sub> can be attributed to the performance requirements at low ambient temperatures. In order for the preburner to maintain a constant outlet temperature, the temperature rise across the preburner must be higher for the lower ambient temperatures. The higher temperature rise results in higher NO<sub>x</sub> emissions from the preburner.

A possible solution to the partial load operation limitation is the incorporation of a combustor bypass valve. During partial load conditions, the combustor bypass valve is opened and combustor airflow is reduced. The fuel/air ratio within the catalyst increases, resulting in improved BOZ efficiency and lower emissions. This theory was tested on October 27<sup>th</sup> when the unit was shut down to exchange the original transition piece between the engine and combustor with another that had a larger liner effective area. The effect of this change was the same as partially opening a bypass valve. NO<sub>x</sub> emissions dropped over 1 ppm and the CO dropped over 4 ppm at the same ambient temperature. Based on these results, CESI incorporated a bypass valve system in the Xonon® 2.1 combustor configuration.

Figure C1 in Appendix C shows the 30-minute averaged data for CO. The CO data shows non-conformance to the program goal of < 5.0 ppm in a relatively large percentage of the data points. In addition, the CO levels exceeded the permit allowances of < 10.0 ppm on two separate occasions. The preburner/catalyst fuel split and the BOZ residence time primarily determine the level of CO emissions. Development work on the preburner/catalyst fuel split issue, which is determined by the control system logic, continued during subsequent RAMD testing phases. Work on lengthening the BOZ residence time, which requires hardware changes, is currently being pursued under a company-funded effort.

Figure C2 shows the 30-minute averaged data for UHC. The figure shows that the UHC levels exceed the 5 ppm goal on a handful of occasions and never exceeded the 10 ppm permit levels.

#### 2.1.6.5. Phase II Emissions Results

The primary purpose of this build was to integrate design improvements and hardware changes based on Phase I test results. The major hardware changes are shown in Figure 2.1.6.5.1 below. The key change for build 5 was the new generation 2.0 catalyst module with improved aging characteristics.

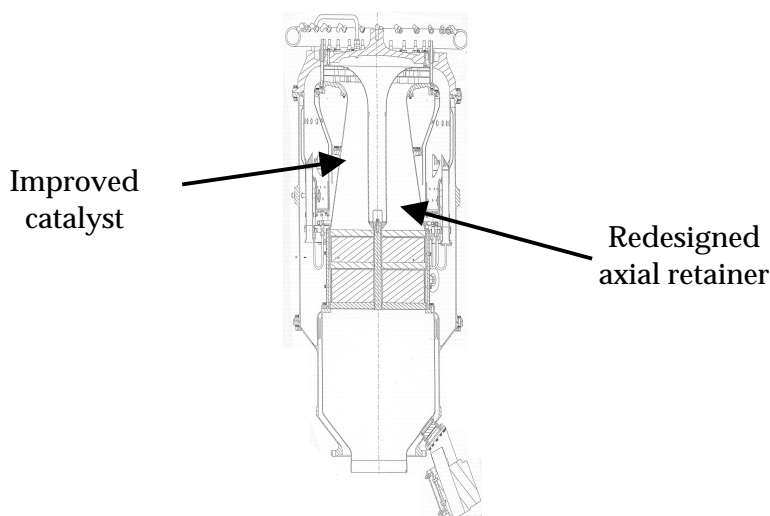


Figure 2.1.6.5.1 -- Build 5 KHI-2 Xonon® 2.0 test configuration

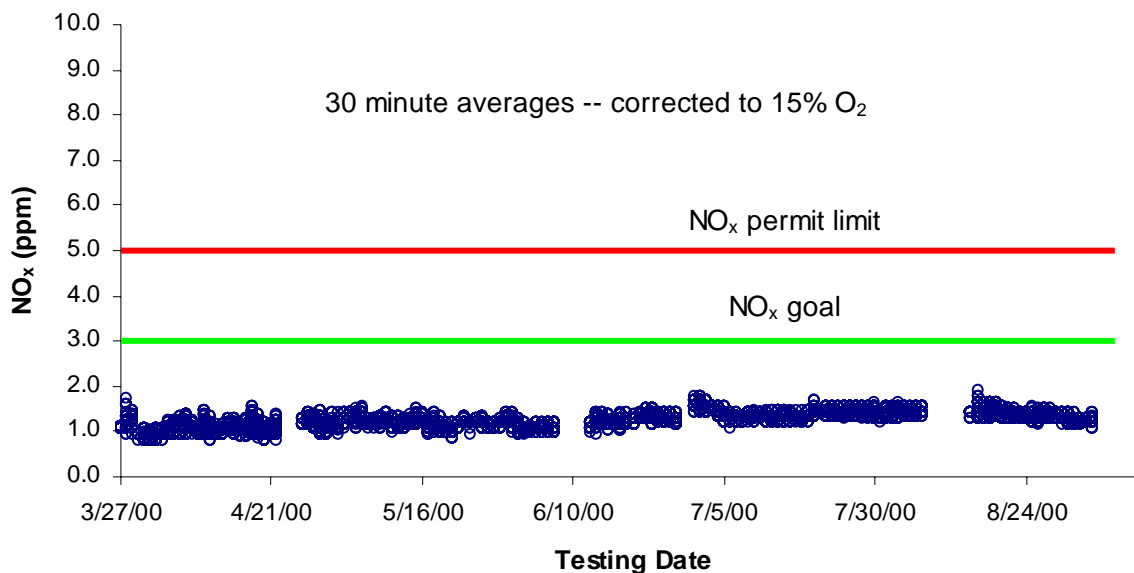
Table 2.1.6.5.1 shows a summary of the emissions results for NO<sub>x</sub>, CO and UHC during Phase II. The averaged data show that all emission levels are quite low and well within the program targets. In fact, the average emission levels are modestly lower than those measured during the Phase I testing. Figure 2.1.6.5.2 is a graph showing the 30-minute averaged NO<sub>x</sub> data versus testing date. The data show that the overall NO<sub>x</sub> levels were lower than those seen during the Phase I testing and the level never exceeded the 3.0 ppm goal.

Table 2.1.6.5.1 -- Phase II emissions results(corrected to 15 percent O<sub>2</sub>)

	30 minute averages (ppm)			1 hour rolling average (ppm)			3 hour rolling averages (ppm)		
	Min	Avg	Max	Min	Avg	Max	Min	Avg	Max
<b>NO<sub>x</sub></b>	0.8	1.2	1.9	0.8	1.2	1.8	0.8	1.2	1.7
<b>CO</b>	0.0	0.5	94.5	0.0	0.5	73.4	0.0	0.5	25.9
<b>UHC</b>	0.0	0.6	7.6	0.0	0.6	5.2	0.0	0.6	3.5

Figure C3 in Appendix C shows the 30-minute averaged data for CO. The CO data shows fewer non-conformance points ( $> 5.0$  ppm) when compared to those seen in the Phase I testing. However, the data also shows three days where very large excursions ( $> 30$  ppm) were observed. In each case, these short-term excursions were due to modifications being made to the control system logic that determined the preburner/catalyst fuel split.

Figure C4 shows the 30-minute averaged data for UHC. Only one data point exceeds the 5 ppm emission goal.



**Figure 2.1.6.5.2 – Phase II NO<sub>x</sub> emission results (30 minute average)**



#### 2.1.6.6. Phase III Emissions Results

The primary purpose of this build was to install the combustor air by-pass system and to integrate improvements in the preburner and catalyst module container. The major hardware changes are shown in Figure 2.1.6.6.1. These changes were implemented in order to improve operational characteristics of the system, improve the life of the catalyst container and to ease assembly/replacement of the catalyst module. Operationally, the by-pass system increases the part load capability, and the modifications to the preburner improve the part load stability.

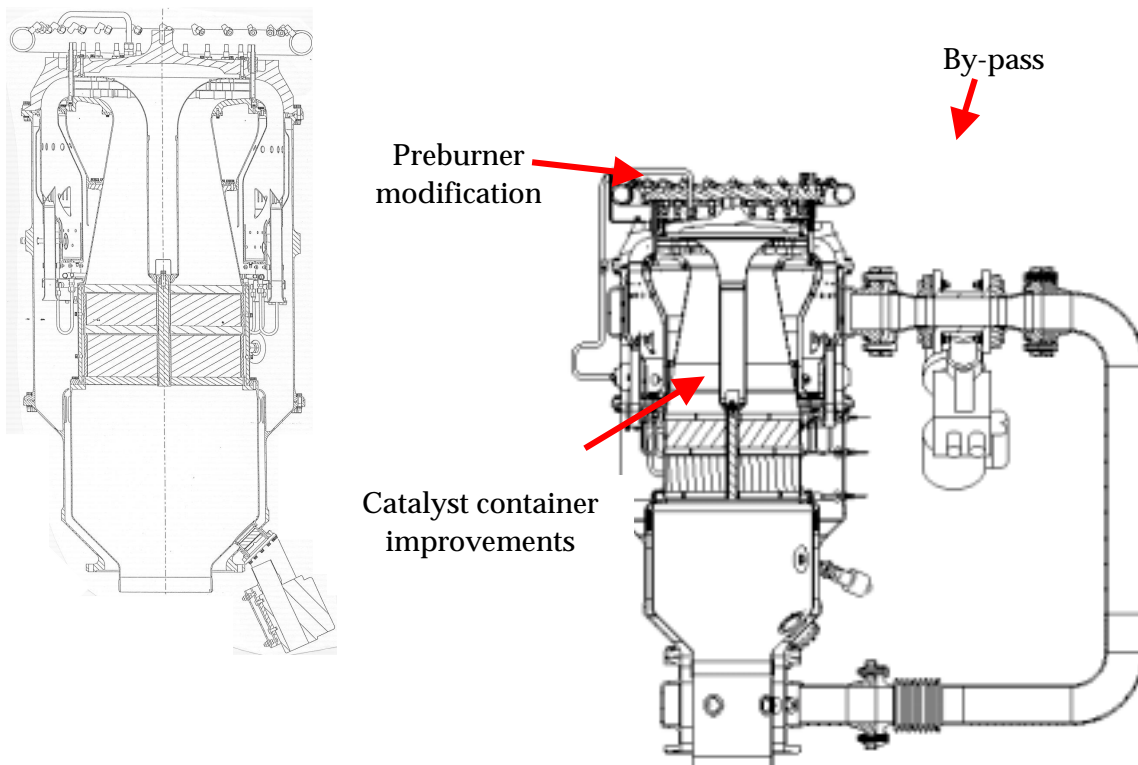


**Figure 2.1.6.6.1 -- Xonon® 2.0 and Xonon® 2.1 comparison**

Table 2.1.6.6.1 shows a summary of the emissions results for NO<sub>x</sub>, CO and UHC. As in the case of the Phase I and Phase II results, the averaged data show that all emission levels are quite low and well within the program targets. In fact, the average emission levels are lower than those measured during either the Phase I or Phase II testing. Figure 2.1.6.6.2 is a graph showing the 30-minute averaged NO<sub>x</sub> data versus testing date. The data show that the overall NO<sub>x</sub> levels are comparable to those seen during the Phase I testing, and the level never exceeded the 3.0 ppm goal.

Table 2.1.6.6.1 -- Phase III emissions results(corrected to 15 percent O<sub>2</sub>)

	30 minute averages (ppm)			1 hour rolling averages (ppm)			3 hour rolling averages (ppm)		
	Min	Avg	Max	Min	Avg	Max	Min	Avg	Max
<b>NO<sub>x</sub></b>	0.7	1.1	1.6	0.7	1.1	1.5	0.8	1.1	1.5
<b>CO</b>	0.0	0.4	11.3	0.0	0.4	5.5	0.0	0.4	5.5
<b>UHC</b>	0.0	0.4	5.0	0.0	0.4	3.5	0.0	0.4	3.0

Figure C5 in Appendix C shows the 30-minute averaged data for CO. The CO data shows fewer non-conformance points (> 5.0 ppm) when compared to those seen in either the Phase I or Phase II testing. The figure shows that the CO levels exceeded the target and permit values on one testing day. As discussed in section 2.1.6.4, this short-term excursion was due to modifications made to the control system logic controlling the preburner/catalyst fuel split.

Figure C6 shows the 30-minute averaged data for UHC. The UHC emissions are lower than those measured during the previous test phases, and the level never exceeded the 5 ppm emission goal.

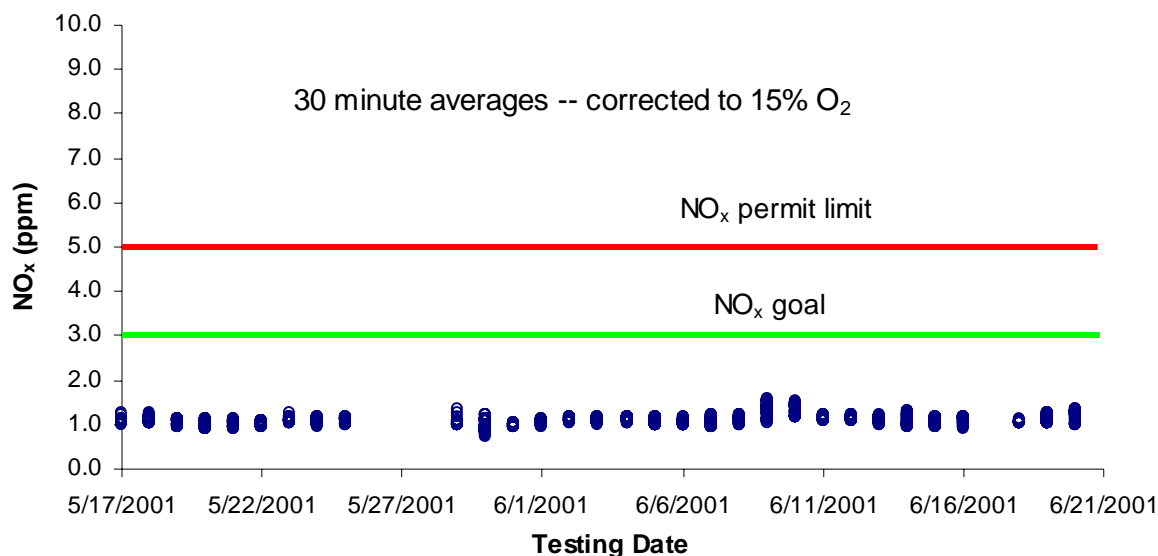


Figure 2.1.6.6.2 -- Phase III NO<sub>x</sub> emission results (30 minute averages)

### 2.1.7. Conclusions

The key findings for this task include:

- The RAMD engine program accumulated 8,128 on-grid operating hours utilizing a catalytic combustion system that was built/modified 4 times over the course of total operation. Reliability was calculated at 99.2 percent, which exceeded the goal of 98 percent. Availability was calculated at 91.2 percent, which fell short of the 96 percent goal. Maintainability was not calculated because the values for “average part failure rate” and “mean time to repair or replace the part” are not meaningful when design changes are made if a part fails. Likewise, Durability goals were not met due to the replacement of several key components during the course of the program. Based on the data collected that validate our model projections, the final combustor build can demonstrate the 8,000 hour life goal.
- NO<sub>x</sub> levels were quite low during the course of the entire test program and never exceeded 3.0 ppm (on a 30-minute average basis). All emission data are summarized at full-load design-point conditions. Emission values at part load, starting and shutdown may exceed the target levels.
- Overall average CO levels were well below the target goal of 5 ppm; however, on several occasions, especially early in the test program, the 30-minute average emission values exceeded the permit levels of 10 ppm. Changes in the control system implemented in subsequent test phases lowered the CO to acceptable levels.
- Overall average UHC levels were well below the target goal of 5 ppm, however, on a handful of occasions early in the test program, the 30-minute average emission values exceeded the target level of 5 ppm. Changes in the control system implemented in subsequent test phases lowered UHC emissions to levels below 5 ppm.
- The control system development activity produced new control logic to improve turndown, load shedding and emission control. It is clear that advanced controls development is critical to the success of the Xonon® combustion technology.
- The axial support structure had to be replaced after 4,000 hours due to poor durability. The Phase II testing incorporated a new axial support structure design developed outside of the PIER 1 program. The replacement of the axial support did not affect the Reliability or Availability of the Kawasaki Gas Turbine Generation system since the replacement occurred at a scheduled shutdown. Operating hours to date compared to the analytical model of the new support structure indicate the new support structure will exceed the durability goals of the combustion system.
- Both the Phase I and Phase II/III catalyst showed good durability up to 4,000 hours. However, it became clear that a new catalyst design being developed in a separate program at the CESI R&D center had aging characteristics that were better than the catalyst used during Phase I. The turbine-mounted combustor is the best place to assess and demonstrate long-term catalyst durability; so the original Phase I catalyst was replaced with the improved catalyst during Build 5. The second-generation catalyst accumulated 4,000 hours while exhibiting good emissions performance. Additional testing is currently underway to prove adequate emissions performance up to the 8,000-hour performance target.

- The inclusion of an automated combustor by-pass system will quite likely be necessary to meet the turn-down emissions requirements for future Xonon® applications. This will be particularly important for engine applications that operate a significant percentage of their duty cycle at part-load conditions and without the capacity to vary the engine air flow with compressor inlet guide vanes. The inclusion of a bypass system may be necessary in order to meet certification requirements in such situations.
- The overall project objective of demonstrating adequate RAMD performance has been met through a combination of demonstrated operating hours and modeling. The data collected during both phases of operation were used to validate our model projections (catalyst aging, axial support structure creep, liner temperatures for thermal cycle fatigue, etc.) to 8,000 hours of operation. The success of these efforts is evidenced by the decision of Kawasaki Heavy Industries to pursue commercialization of the Xonon system via their introduction of the M1A-13X gas turbine.
- The ISO heat rate for the Xonon-equipped engine at Silicon Valley Power (SVP) is approximately 15,700 BTU/kW-hr. It is important to note that the engine installed at SVP was purchased used and has a very poor performing engine (compressor efficiency was termed “marginal”). The higher reported heat rate **cannot** be directly compared to the baseline Kawasaki gas turbine heat rate of 13,400 BTU/kW-hr. The heat rate of the engine installed at SVP has not been measured with a standard Kawasaki combustor.

## 2.2. Control System Design

Further details of the control system development effort are provided in Appendix II: RAMD Testing and Control System Development.

### 2.2.1. Introduction

The fuel control for the catalytic combustion system differs significantly from conventional gas turbine combustors. There are two distinct fuel flows. Part of the fuel is used in a preburner system to heat the compressor discharge air to a temperature around 450°C (840°F). The main fuel is injected into this hot vitiated air in a specially designed mixing section. This premixer is located upstream of the catalyst module inlet. When any change in load occurs, including a sudden load loss, the total fuel flow is changed and the split of fuel between the preburner and the catalyst must be changed to maintain the catalyst within its operating window.

The current control system incorporates some elements of “feed forward”, or predictive control strategies, to allow more precise control. Previous testing during the Xonon®1 demonstration had proceeded to the point where load steps of +100 percent and -60 percent could be controlled without exceeding the gas turbine operating limits. Demonstration of a load step from 100 percent to 0 percent could not be accomplished due to the slow response of the dynamometer.

### 2.2.2. Approach

The objective of this task was to develop a fuel control system capable of accepting complete load loss without exceeding the turbine over-speed or surge limits. An important part of any power generation system is the ability to handle “upsets” in the distribution system and quickly come back on line. The desirable attributes are:

- Ability to follow the load requirement and to handle sudden load changes while not exceeding the turbine over speed or under speed limits.
- If the grid or load connection is suddenly lost, the system must be able to quickly cut back the turbine power (fuel flow) without exceeding the over-speed limits set by the gas turbine manufacturer.
- In the case of sudden load loss, it is also highly desirable for the turbine to go to a spinning idle condition, or Full Speed No Load (FSNL), rather than a complete shut down, allowing the system to come back on line quickly.

Previous testing and the development of the KHI gas turbine control system were performed in a test cell with a water brake dynamometer. This type of dynamometer load has a relatively slow response to load change inputs. For example, a step load change signal from 100 percent load to 0 percent load occurs over a period of about two seconds for the dynamometer compared to a nearly instantaneous loss in load for the generator open circuit situation as shown in Figure 2.2.2.1. Substantially faster control system performance would be required to handle load loss from a generator. The control system had been developed to handle full load steps with the available dynamometer system, but further development and testing was required to evaluate the effects of the shorter response time associated with actual on-grid operation. This work was done for this task at the SVP engine test facility.

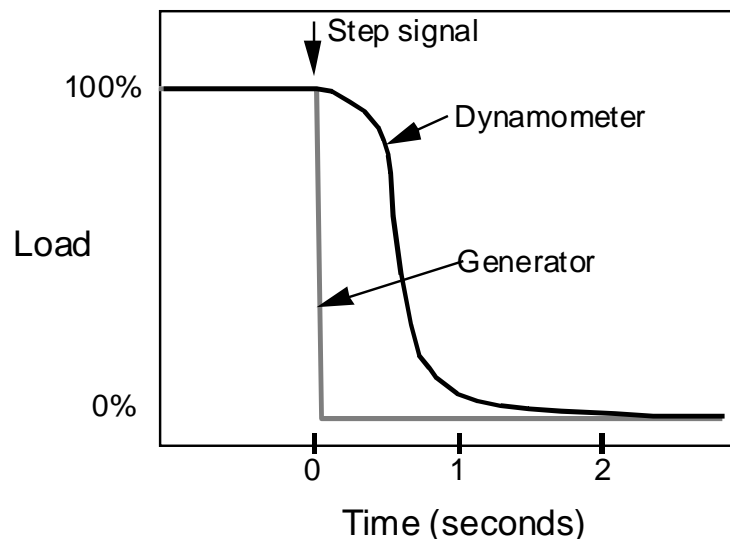


**Figure 2.2.2.1 -- Load response comparison of a dynamometer and a generator for a step change in load set point**

### **2.2.3. Concept Development**

It was originally believed that a model-based control strategy would be required to achieve the performance required by the power generation industry. This model-based control strategy would be a mathematical model of the turbine, combustor and catalyst to predict the control settings. This strategy had been applied to the control of some gas turbine systems, especially low NO<sub>x</sub> lean premix combustion systems. The mathematical model was then to be combined with the current control strategy to produce a fully predictive control system for the KHI engine.

## **2.2.4. Control System Design**

### **2.2.4.1. Simulation Studies**

As part of the development of the engine model, it would be necessary to compare the model predictions with the engine performance. Running the model against the system at the Santa Clara facility would allow one to tune the model so that it could be used as a simulator to test various control strategies and adjustments before being implemented online.

### **2.2.4.2. Implementation on KHI Engine Control System**

After the model-based control strategy had been developed, it was to be implemented on the engine and a full test program executed to further develop the system and to demonstrate the required performance. The work in this task was to include:

- a. Installing the model-based control algorithm in the Santa Clara KHI control system.
- b. Develop the system as required to permit operation of the facility.
- c. Run performance tests to establish the required capability.

### **2.2.4.3. Program Replan**

Due to unforeseen events and issues in setting up the Santa Clara facility, a “Technical and Cost Replan” was subsequently submitted to the Commission in May 1999. The following describes the deviations from the original plan as it pertains to the Fuel Controls Development.

As a supporting task to the shakedown of the facility and combustor performance mapping, substantial development of the synchronization, breaker and combustor control systems was required to provide stable and reliable operation on the power grid. In addition, control algorithms were developed to handle the operation of the combustor while maintaining low emissions levels, and some testing was conducted with rapid programmed load changes. This work suggested that the best approach to achieving an operating system with the required performance would be to utilize the existing control algorithm, with added control logic as necessary to handle large load excursions. This is in contrast to implementing a new model-based control strategy.

At the time of the replan, the existing control system allowed for reliable, extended operation of the facility with low emissions and under normal operating conditions. This system provided acceptable performance during startup, shutdown, loading and unloading under controlled conditions, in addition to some load step capability as required for combustor and system testing.

In order to complete development of the control system to achieve acceptable load step control under typical commercial operating conditions, a subsequent phase of testing was planned. This testing was to commence after substantial operating time had been logged on the RAMD test, and would identify control parameters and possibly additional logic required to meet the required performance targets for load steps.

### **2.2.5. Control System Development and Testing**

Many of the test runs overlapped each other in order to make the best use of the engine test availability. In order to present these in an organized manner, test runs have been grouped by mode of operation than rather than chronologically.

#### **2.2.5.1. Load Following**

Load following is the ability to react to changes in system load. This can be either a response to load going on-line or off-line in an islanded system (such as in an industrial plant), or dispatched requests when connected to the grid. A characteristic of a well-controlled turbine-generator set is its ability to make large load steps without losing stability. These tests addressed a wide range of load levels and step changes in order to tune various parameters that control both stability and ramp rates.

One of the first efforts was to be sure that the system returned to a stable, steady state condition after each load step. After preliminary observations through a full range of loads, it was apparent that improvement in load stability was greatly needed. After some investigation, it was determined that there are two rate-limiting factors in the engine control logic. One factor determines the main fuel flow ( $W_{f,main}$ ) demand based on speed droop, and the second factor is the Proportional, Integral and Derivative (PID) parameters of the main fuel valve driver. It was subsequently found that the  $W_{f,main}$  demand PID output is slower than that of the main fuel valve driver, and is therefore the appropriate set of parameters to tune.

To simplify matters, the first stability tests were run on 300 kW load steps from 600 kW to 300 kW. The initial load plot is shown in Figure 2.2.5.1.1. After many runs from 600 kW to 300 kW while tuning all three Main Demand PID terms, this load step was much more stable as can be seen in Figure 2.2.5.1.2. The next objective was to speed up the load change by changing the kW ramp rate. As could be expected, this introduced some instability that had to be eliminated by simultaneously re-tuning the Main Demand PID parameters as before. The result is shown in Figure 2.2.5.1.3. Load steps were then increased to 600 kW for a 900 kW to 300 kW load change to verify the changes on the smaller load test will perform well for a larger step. An initial run is shown in Figure 2.2.5.1.4. After several tuning runs with the 600 kW load step, the improvements in speed and stability are apparent in Figure 2.2.5.1.5.

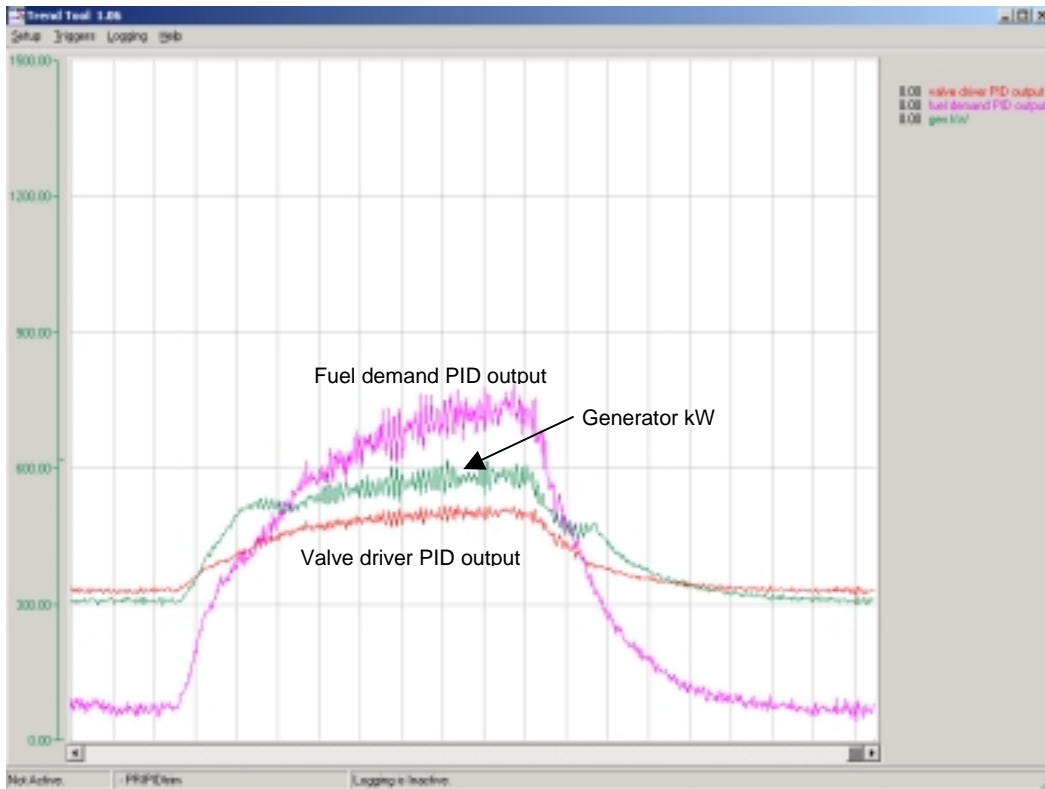


Figure 2.2.5.1.1 -- 600 kW to 300 kW load step prior to tuning Main Demand PIDs

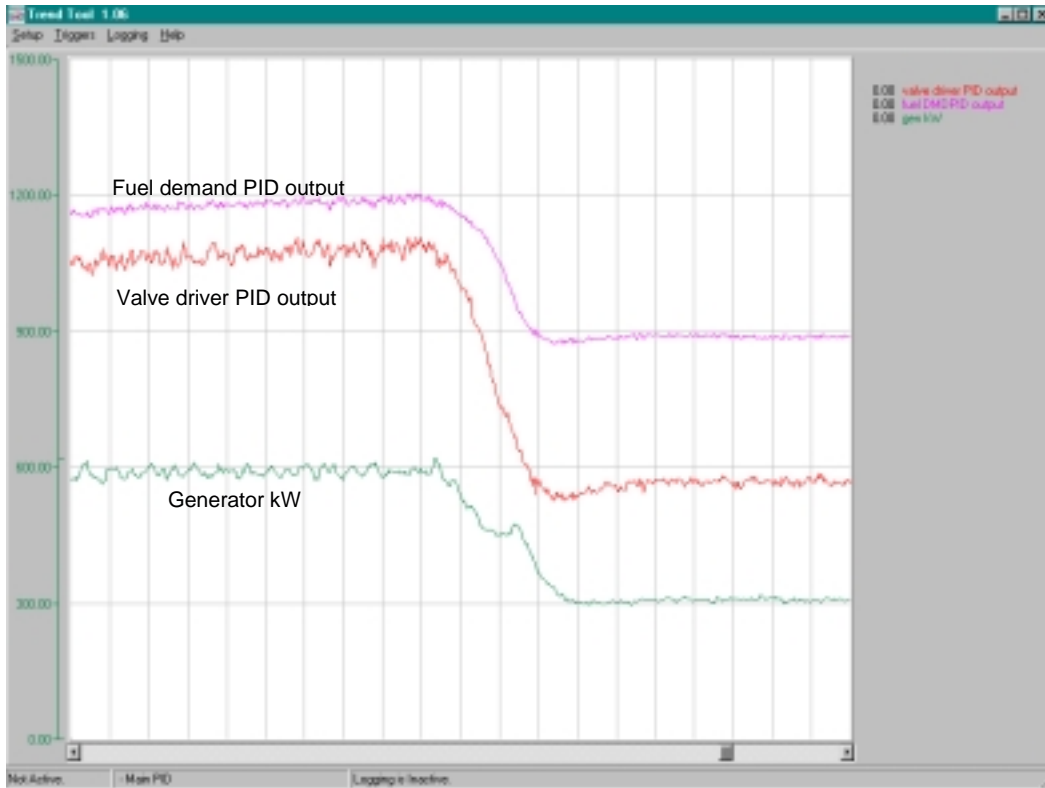


Figure 2.2.5.1.2 -- 300 kW load step after tuning Main Demand PID's



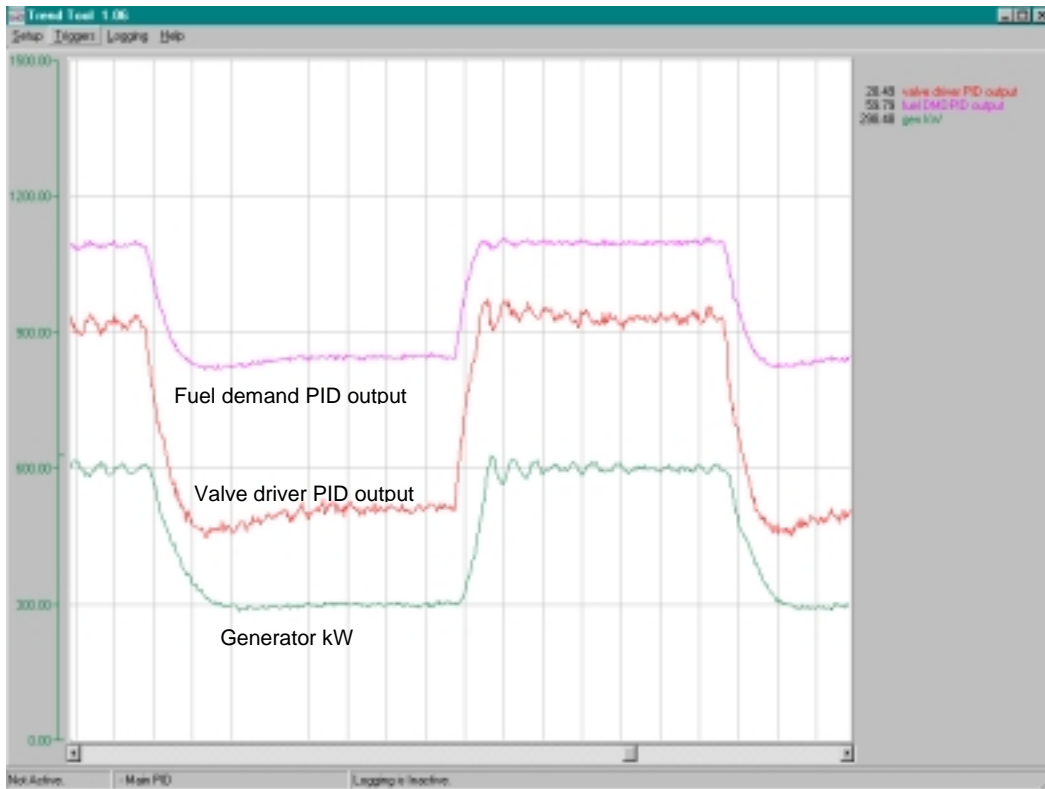


Figure 2.2.5.1.3 -- 300 kW load step before and after increasing the kW Ramp Rate

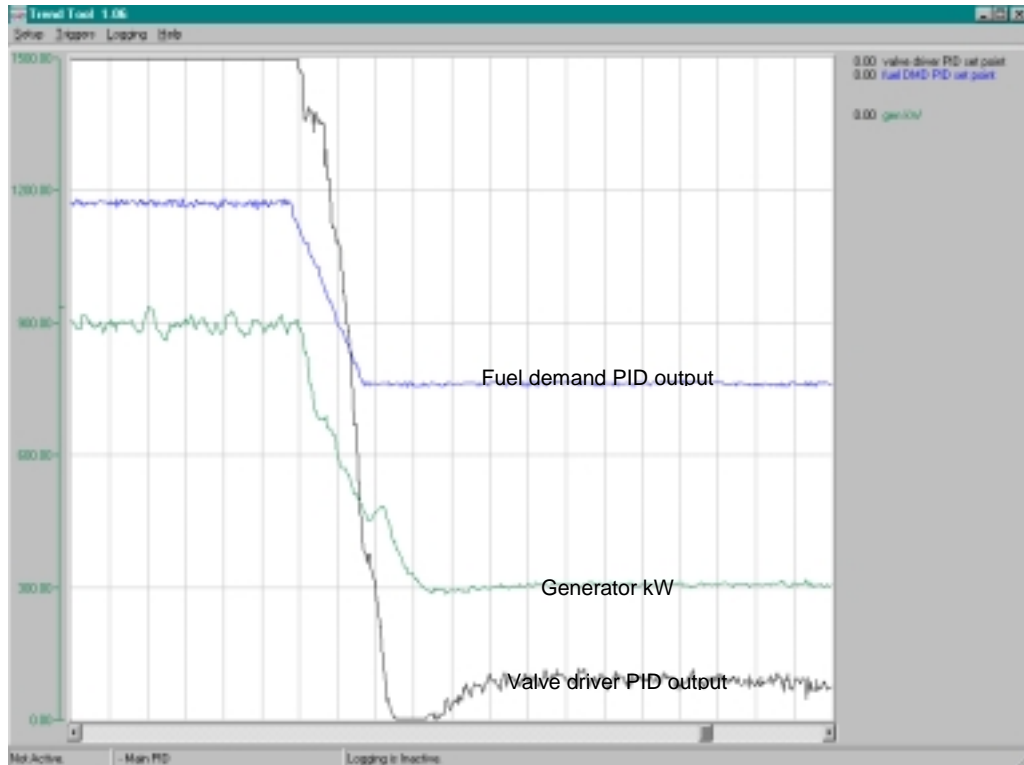
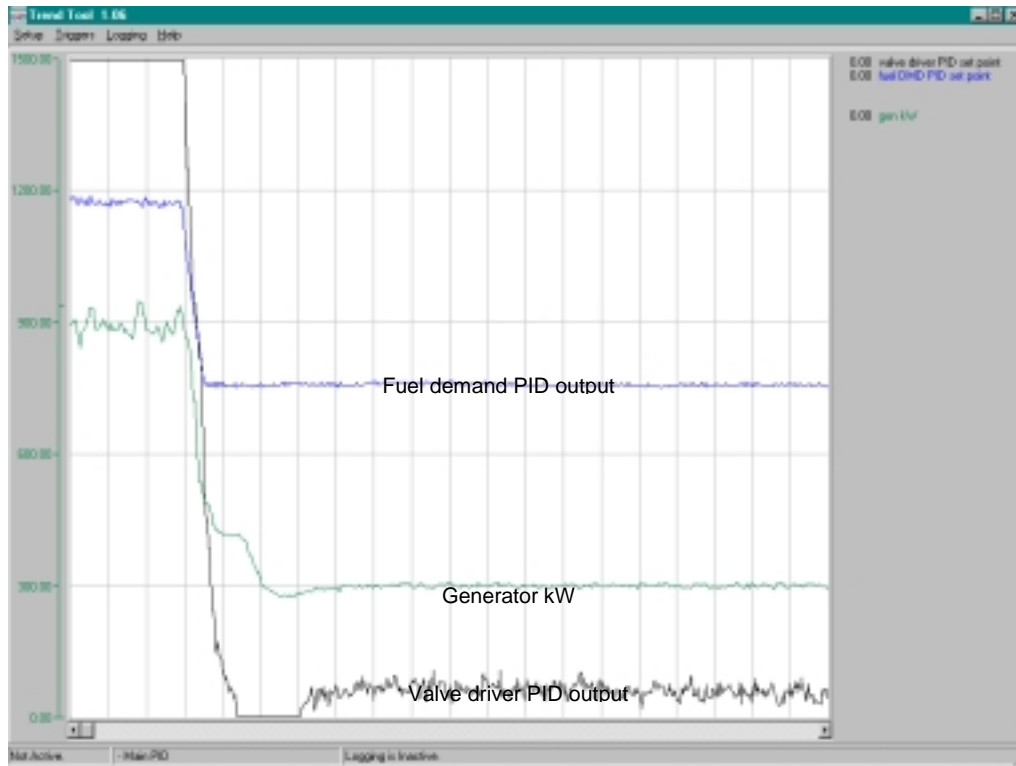


Figure 2.2.5.1.4 -- 600 kW load step with same parameters as tuned 300 kW load step



**Figure 2.2.5.1.5 -- 600 kW load step after further tuning**

The next set of load following tests was to examine intermediate load steps from 1500 kW (~full load) all the way down to 300 kW. The machine was first ramped up to 1500 kW, and then reduced to 1200 kW, 1000 kW, 800 kW, 600 kW and finally 300 kW. At 1200 kW through to 600 kW, it was very noisy and the oscillations would not stabilize. Once down to 300 kW, the load plot was significantly more stable.

One interesting phenomenon to note is that as load is increased the instabilities are not as apparent as they are on downward ramps. One possible explanation for this is the existence of acceleration torque during loading, which is not present during unloading. This is an issue that should be explored, however, it was not done during this phase of testing since we were able to dampen these oscillations by tuning the various parameters as discussed below.

Testing resumed with a load change from 1500 kW to 600 kW, as shown in Figure 2.2.5.1.6. An overshoot to ~533 kW occurred with the activation of the preburner's primary stabilizing logic. After on-line tuning of the PID parameters it was possible to reduce the swings to about +/- 50 kW swings.

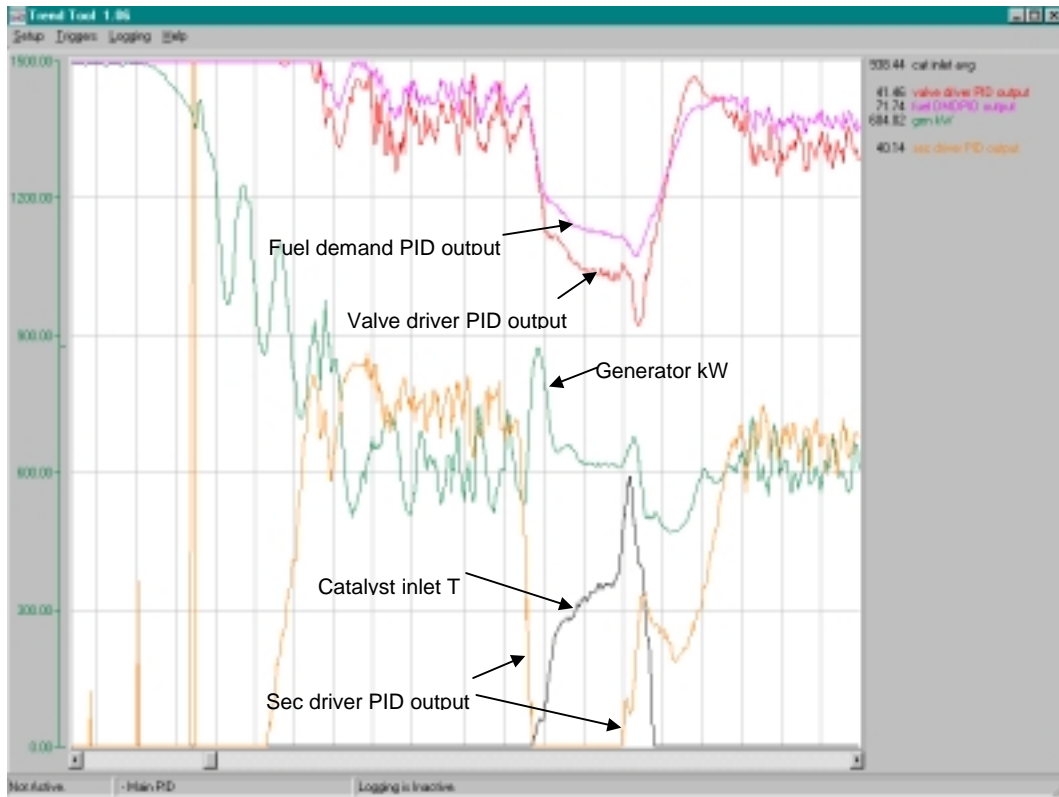


**Figure 2.2.5.1.6 -- 1500 kW to 600 kW load step**

After some investigation, we concluded that the following chain of events was the cause of the instabilities. When the load is reduced, the secondary fuel begins to increase resulting in higher secondary zone efficiency. This initiates an oscillation load (rather than a smooth curve). The sudden change in secondary zone combustion efficiency also activated the primary zone stabilization module reducing the oscillations. However, when this primary zone stabilization ends, the performance becomes very unstable again. The load is already unstable before the secondary zone efficiency jumps from low to high further aggravating the problem. The primary stabilization module causes the catalyst inlet temperature to rise (i.e. by increasing the primary fuel, the fuel fed into the secondary burns more efficiently). A stable point is reached quickly, but this stability is lost as the primary fuel flow is reduced after the primary stabilization sequence ends.

As a solution, the preburner operating curve was changed to increase the preburner outlet temperature (which is controlled by the secondary fuel flow) at the point where the stability is lost. This seemed to substantially lower the amplitude of the oscillations.

### **2.2.5.2. Load Rejection**

Load rejections occur when the generator breaker opens and the load drops instantaneously resulting in the engine being in a Full Speed No Load (FSNL) state. Issues that arise are primarily associated with engine over-speed and under-speed conditions which occur when the fuel control system must suddenly adjust to a no load condition.

As in the previous tests, smaller steps were taken first to minimize potential damage to the machine. The initial load rejections were from 300 kW. In the first test, using the new PID parameters from the load following tests, the system went into uncontrollable oscillations when the breaker was opened at 300 kW. The proposed solution was to create two separate sets of PID parameters; one set would control while the breaker was open and the other set would control while the breaker was closed.

The first load rejection with the new dual PID parameters logic in place was from 300 kW. This resulted in numerous oscillations in speed, which eventually smoothed out after about 40 seconds, as shown in Figure 2.2.5.2.1. Figure 2.2.5.2.2 shows the effect of tuning the PID parameters after additional load rejections from 300 kW. Figure 2.2.5.2.3 shows a 600 kW load rejection with the same PID parameters as above. Additional tuning of the PID parameters was performed to minimize the over-speed/under-speed excursion and the time to stabilize the turbine at FSNL. The key target was to ensure turbine speed would not exceed the OEM recommended 108 percent speed. Load rejections were performed from 300 kW, 600 kW, 900 kW, and 1050 kW load levels, and are shown in the Figures 2.2.5.2.4 and 2.2.5.2.5.

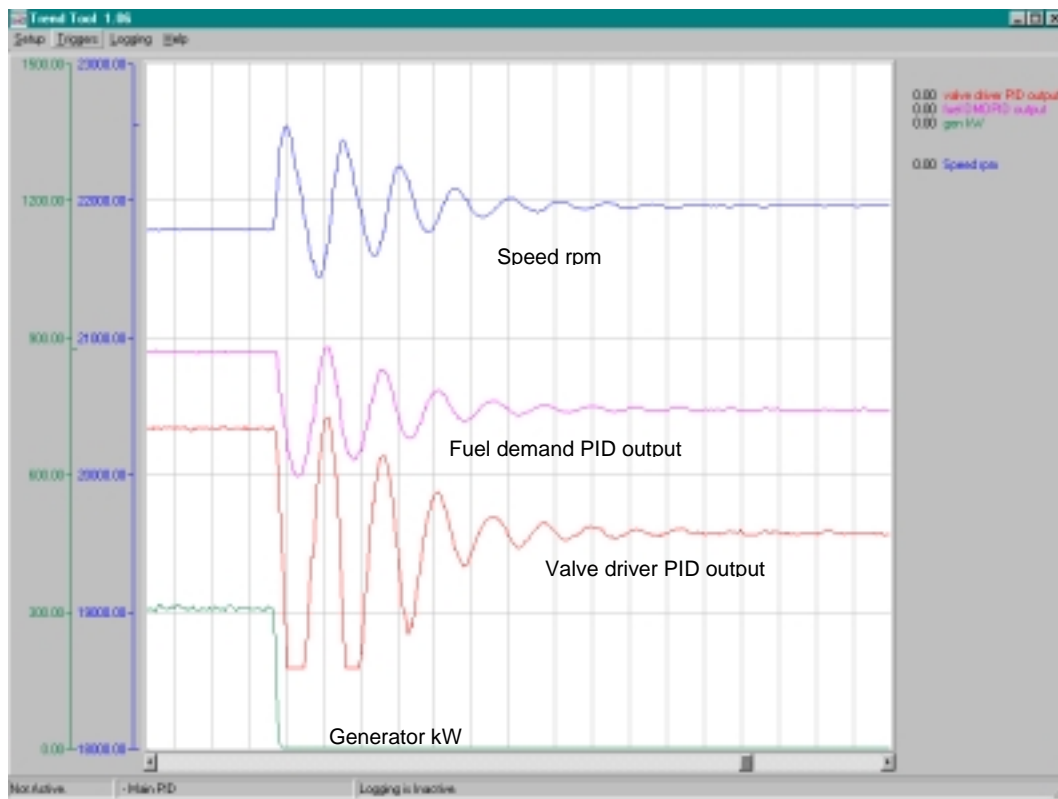


Figure 2.2.5.2.1 -- 300 kW load rejection prior to tuning

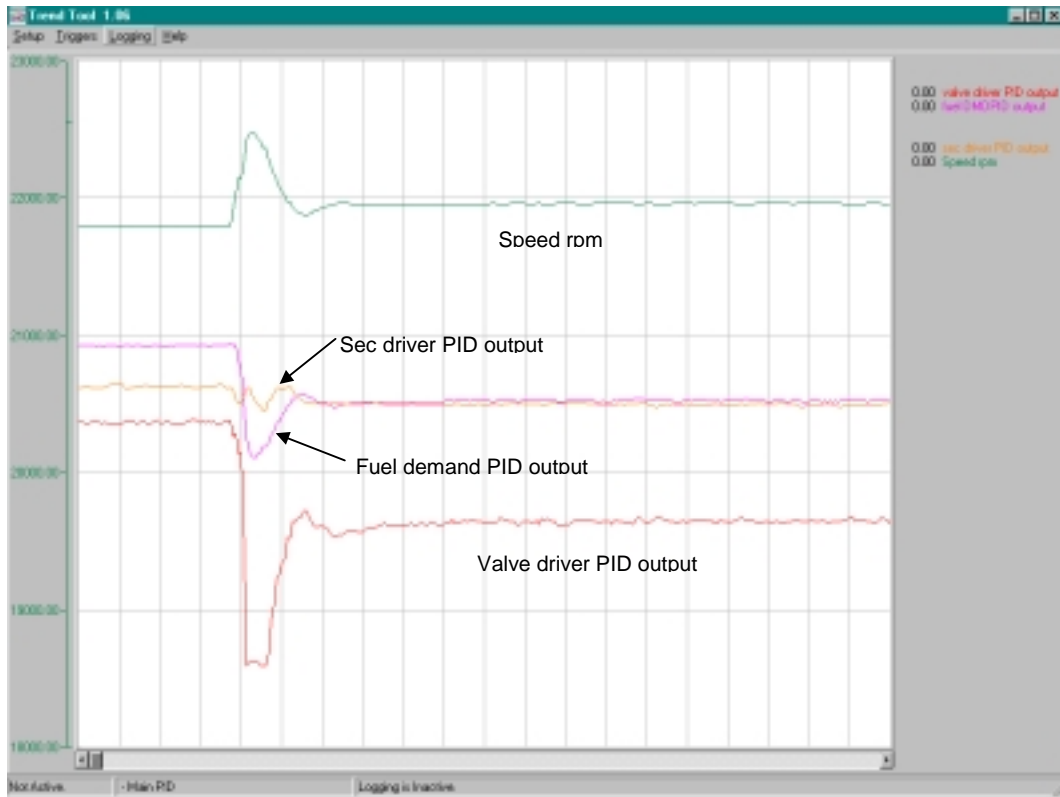


Figure 2.2.5.2.2 -- 300 kW load rejection after tuning

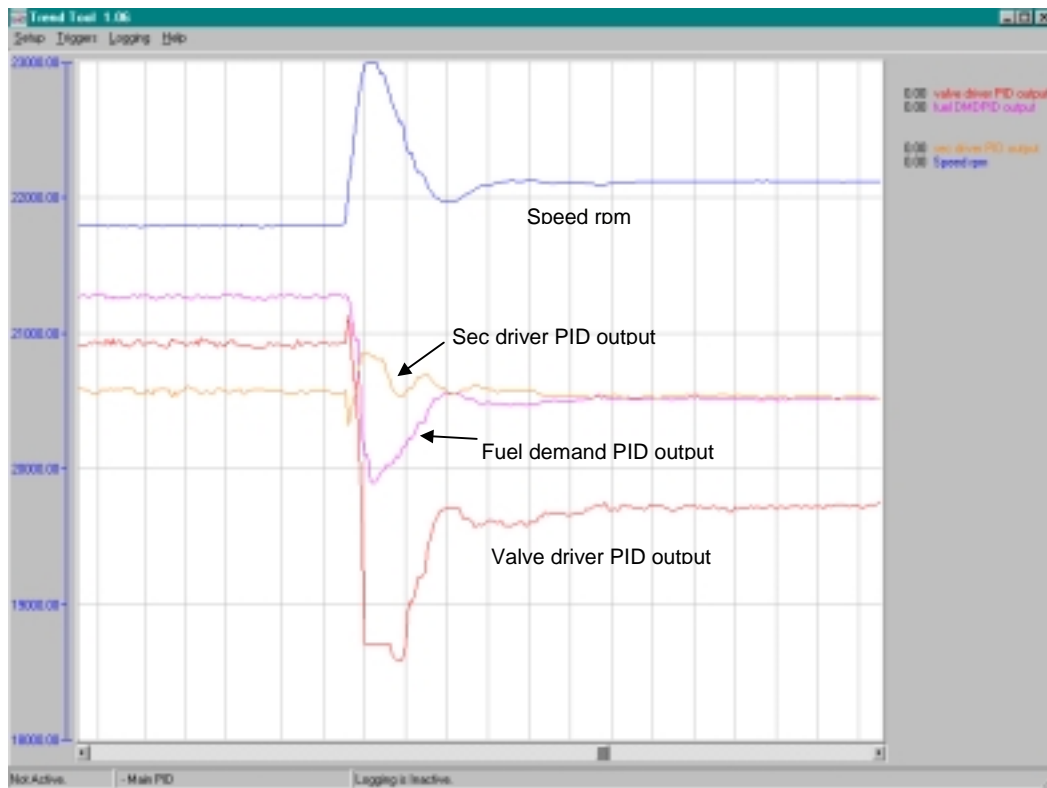


Figure 2.2.5.2.3 – 600 kW load rejection with same PID parameters as the 300 kW load rejection

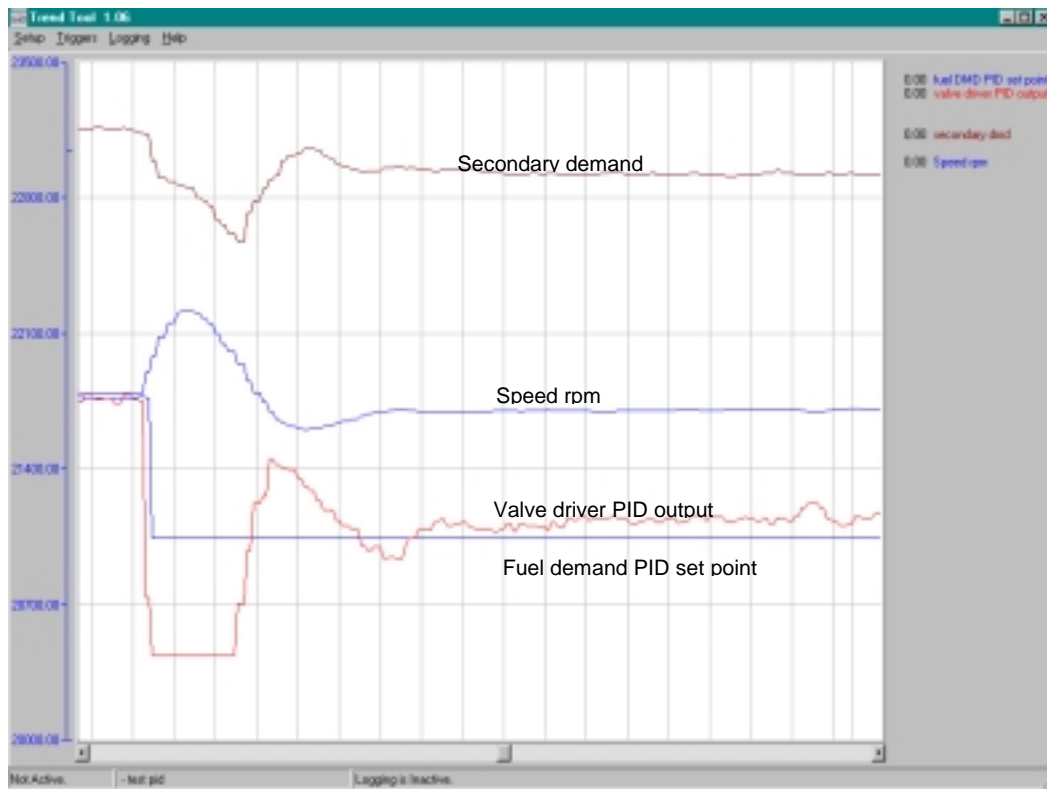


Figure 2.2.5.2.4 -- 300 kW load rejection (1.9 percent over-speed, -0.9 percent under-speed)

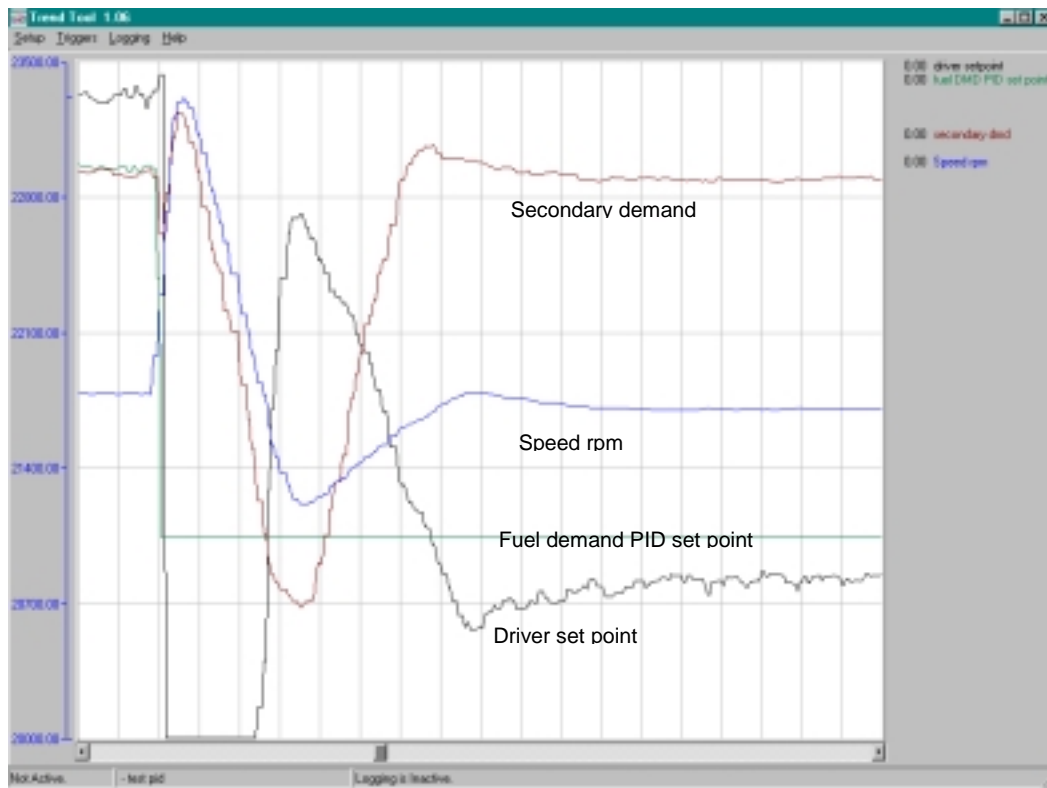


Figure 2.2.5.2.5 -- 1050 kW load rejection (6.9 percent over-speed, -2.7 percent under-speed)

### 2.2.5.3. Breaker Auto-Resynchronization

Following a load rejection, it is desirable for the machine to automatically resynchronize with the grid. In order for a generator to synchronize with the grid the rotational frequency of the shaft must match the frequency of the grid within  $\pm 0.5$  Hz. With an engine speed of 21800 rpm, this corresponds to  $\pm 181.67$  rpm in engine speed. The system dynamics during an unload results in a time lag before the engine speed settles to steady state. These speed oscillations must fall within the specified rpm range for successful grid resynchronization to occur. Since a resynchronization won't occur until a by-pass relay has timed out, the timeout delay can be used to allow sufficient time for the engine speed to stabilize.

Several load rejections were performed to determine the time it takes for stabilization. Figure 2.2.5.3.1 shows one of these test runs. It was determined that the timeout delay needs to be at least 15 seconds before the generator frequency stabilizes to within  $\pm 0.5$  Hz of the grid frequency.

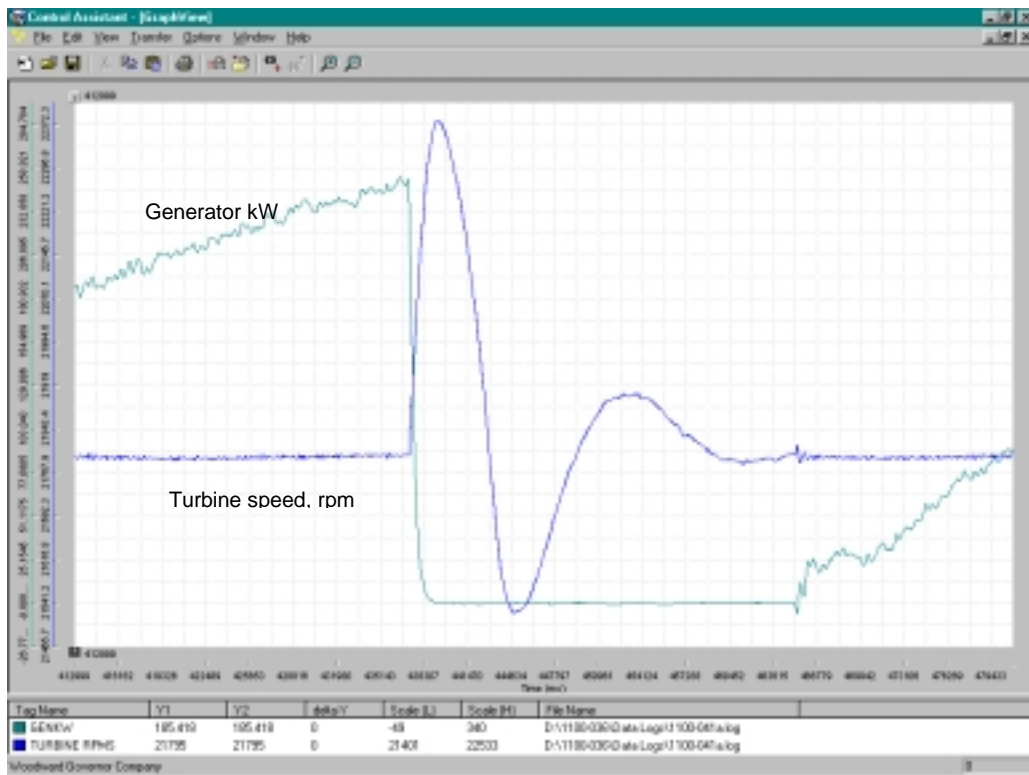


Figure 2.2.5.3.1 -- Engine speed oscillations after load rejection and before breaker re-synchronization

### 2.2.6. Conclusions

The key findings for this task include:

- Instabilities that occurred during 300 kW and 600 kW load steps were successfully eliminated by tuning the Main Demand PID parameters.

- Part load instabilities were eliminated by modifying the operating curve to increase the preburner outlet temperature, avoiding a region where the primary stabilization module cycles on and off.
- Main Demand PID parameters were tuned to prevent exceeding over-speed limits when rejecting load from 300 kW, 600 kW, 900 kW, and 1050 kW.
- After a load rejection, the timeout delay before automatically re-synchronizing to the grid was adjusted such that there was sufficient time for the generator frequency to fall within  $\pm 0.5$  Hz of the grid frequency.

Future activities will involve the development of control system features required to operate at ultra-low emissions across a much larger load range.

### **2.3. Axial Support Development**

A more detailed discussion of the mechanical analysis of the axial support can be found in Appendix III: Combustion Catalyst Axial Support Mechanical Durability.

#### **2.3.1. Introduction**

This section describes work completed to predict the mechanical durability of the catalyst axial support referred to as the BMM (bonded metal monolith). This component is critical to the operation of the gas turbine combustion system and must survive over 8,000 hours at high temperature and constant mechanical load. Limited operating experience exists for this unique application creating a need to develop a methodology for predicting and designing for long-term durability.

The function of the axial support is to restrain the catalyst foils from movement due to the force of the combustion gas flow. The contact pressure against the catalyst foils must be sufficiently low to avoid locally deforming the foils. Because the restraint must occur at the exit of the combustion gas from the catalyst, the axial support operates at very high temperature. Also, minimal airflow must be blocked to avoid flow disturbances. To accomplish these objectives, a high temperature alloy foil honeycomb is employed which distributes the contact load over the face of the catalyst foil roll and exhibits very low flow blockage.

Durability issues for the axial support are the same as those found in other gas turbine engine components, which include:

- Permanent deformation (due to creep and plasticity);
- Low cycle fatigue (due to thermal and mechanical loading); and
- Oxidation (an important issue, however it is not addressed in this study).

#### **2.3.2. Approach**

A combination of structural analysis and material testing was selected as the best method for determining the durability of the BMM. Although it is usually desirable to determine the durability of components by testing them under actual engine conditions, this approach was not deemed practical for several reasons. First, the temperature distribution and pressure loading



were found to be very difficult to reproduce in a suitable test configuration. Second, the length of time required for the durability test was greater than 8,000 hours (approximately one year of around the clock operation), which would tax our ability to meet the facility and support personnel requirements. Acceleration of the durability test was considered, however, it was ruled out due to the possibility that it might add uncertainty to the results.

Due to the lack of suitable material data, the effort for this task included a limited material specimen test program designed to provide high-quality data at relevant load and temperature conditions. The published data were reviewed and utilized when possible; however, the bulk of the data did not adequately model the BMM honeycomb material. Specifically, the data did not address the thin cross-section of the foil or the effect of the brazing and pretreatment processes. All of these factors are believed to significantly affect the material properties.

The structural analyses relied on extensive use of finite element modeling due to the complex geometry and the presence of thermal loads. It was discovered that the stress distribution within the honeycomb varied greatly due to geometric factors. Since small increases in peak stress levels can dramatically reduce fatigue life, it was necessary to assess the plastic and creep strain throughout the entire operating range. Constitutive material property data determined from the material property testing results were input into the finite element model to further improve the stress and life predictions.

### 2.3.3. Material Property Data

The current base material for the BMM is Haynes 214 (designated H214 hereinafter), a high temperature NiCrAl superalloy. Limited material property data for this alloy were published in publicly available literature provided by Haynes International Inc. However, this information is typically averaged data and may not be representative of the thin foil used in the BMM honeycomb. In addition, the BMM uses a brazed, pretreated, and heat-treated material that may have significantly different properties from the base material. [The details of the pretreatment are proprietary and are not included in this report.] Consequently, it was deemed critical to obtain detailed material properties for foil that had been exposed to the braze cycle and to the intended other treatments. The testing was done by Materials Characterization Laboratories (MCL) in Scotia, NY.

**Table 2.3.3.1 -- Haynes 214 Treatments for Testing**

<b>Material</b>	<b>Elastic-plastic</b>	<b>Creep</b>	<b>Fatigue</b>
<b>Base case</b>	X		X
<b>Heat treated</b>	X		
<b>Pretreated</b>	X	X	X
<b>Pretreated and brazed</b>	X	X	

The elastic-plastic, fatigue, and creep testing were completed for the material treatments listed in Table 2.3.3.1. The creep tests were done with two similar pretreated materials, one that had been through the braze cycle and one that had not. The objective was to test the pretreated H214 for a duration of 4000 to 8000 hours, while the brazed counterpart would be run for a shorter duration of 2000 hours. The short duration would provide adequate evidence if the two materials were significantly different.

The “Base case” indicates testing an as-received H214 foil from Haynes and exposing it to a brazing thermal cycle without any actual brazing. The “Heat treated” designation indicates having a pretreatment in 1-atm air at 1,920°F (1,050°C) for 10 hours, thus ensuring the formation of a protective alumina layer. “Pretreated” indicates addition of an extra pretreatment step in the H214 processing. Finally, the “Pretreated and brazed” sample had two foils brazed together along their center-span.

The elastic-plastic and creep tests were done with a 0.010-inch thick foil, while the fatigue testing was done on a 0.090-inch thick sheet. The increase in thickness for the fatigue testing was necessary to prevent buckling when the specimen was compressed after tensile yielding at the high strain needed to cause fatigue.

#### **2.3.3.1. Creep Testing**

Due to a limited number of creep testing machines, only the pretreated H214 was tested at stresses of 500 and 1000 psi, with each stress applied at 1562°F (850°C), 1652°F (900°C), and 1742°F (950 °C).

As the testing progressed, it became apparent that the creep rates of several of the samples were inconsistent. All the samples, with the exception of two (1562°F/1000 psi and 1652°F/1000psi), appeared to be elongating normally. The “normal” samples had the classic primary creep portion, along with the more stable secondary creep portion. The two “abnormal” samples exhibited elongation rates higher than the rest of the samples, so these tests were stopped due to the possibility of defects in either the sample material or experimental set-up itself. The two samples were then re-tested which produced similarly inconsistent results.

After careful evaluation and inspection of the equipment and in-progress results, it was determined that the thin foils combined with stick-slip phenomenon with the mechanical extensometer were causing the unexpected results. Consequently, all testing was stopped and the elongation checked manually. In all the samples with greater than 2500 hours, the elongation checked manually proved to have a creep strain of two to three times greater than the extensometer reading at the time the sample was stopped. This corroborated the theory that the extensometer was inaccurate, and that the foils were creeping at much higher rates than expected.

At this point, there were several adjustments that could be made in future testing. The samples could be increased in thickness and/or width to increase the load relative to the extensometer, or the extensometer could be eliminated altogether. However, there is undocumented evidence that material with only 2 or 3 grains through the thickness can have significantly higher creep rates than thicker samples. This is caused by the relative freedom for the grains to shear. Previous examination of a service-exposed BMM showed 2 or 3 grains through the wall.

Therefore, it was again decided that thickness could not be increased without compromising the applicability of the results. The widest sample that MCL can accommodate on their creep machines is 0.4 inches at the gage section. This is an increase of 1.6 times the width from the current 0.25 inches. This higher width translates to an increase in load of 1.6 times which was not considered enough to overcome the stick-slip uncertainty.

Eliminating the extensometer was the best option to remove the stick-slip unknown. The main drawback to this approach is that continuous points will not be obtained, and that the primary creep might be missed. Discrete points were obtained by stopping to measure elongation at selected intervals. Plots of creep strain versus time at 850, 900 and 950°C can be found in Figures D1-D3 in Appendix D.

### 2.3.3.2. Fatigue Testing

The fatigue testing of H214 samples was done at Mar-Test (a division of MCL). Two variations of the same material were tested, an H214 sample exposed to the braze cycle, and a pretreated H214. Each specimen had a thickness of 0.090 inches, and was run at 1,562, 1,650, 1740 and 1,830°F (850, 900, 950, and 1000 °C). Three strain ranges per temperature, an R Ratio = +1 and two-minute tensile hold were part of the test matrix. Strain ranges were chosen to obtain failures between 100 and 1000 cycles. Figure 2.3.3.2.1 shows the results of the fatigue tests for both material variations.

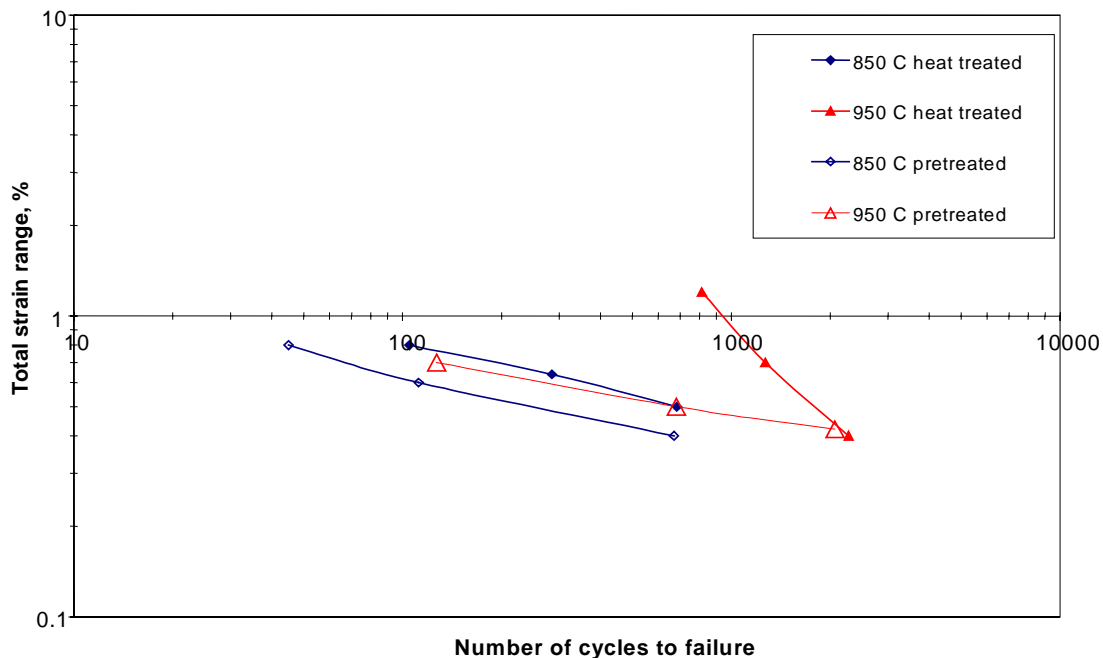


Figure 2.3.3.2.1 -- Comparison of LCF results for both materials at 850 and 950 °C

Note that across every temperature, the pretreated H214 had lower LCF life than the heat-treated H214. The best results for comparing the two types of materials were chosen at 850 and 950 °C. Note that the pretreated material at 950 °C has its low-cycle fatigue curve nearly on top of the heat-treated material at 850 °C. It is obvious that the fatigue properties of H214 are reduced when it is pretreated. For example, at a strain range of 0.7 percent, the pretreated H214

had 127 cycles to failure, whereas the H214 that was exposed to the braze cycles had 1270 cycles to failure. However, as the strain range was reduced, the difference in cycles to failure between the pretreated and non-pretreated became smaller.

### 2.3.3.3. Elastic-Plastic Testing

Four variations of the H214 foils were tested at MCL as shown below in Table 2.3.3.3.1. Each material was run at 875, 925, and 975°C, with three tests at each temperature. Initial test results have been completed, but further tests will be needed to ensure data quality. The results of the testing are shown below in Figure 2.3.3.3.1.

**Table 2.3.3.3.1 -- Fatigue testing matrix**

Material	Designation
Untreated H214	1T
Heat treated H214	1BT
Pretreated H214	2T
Brazed H214	3T

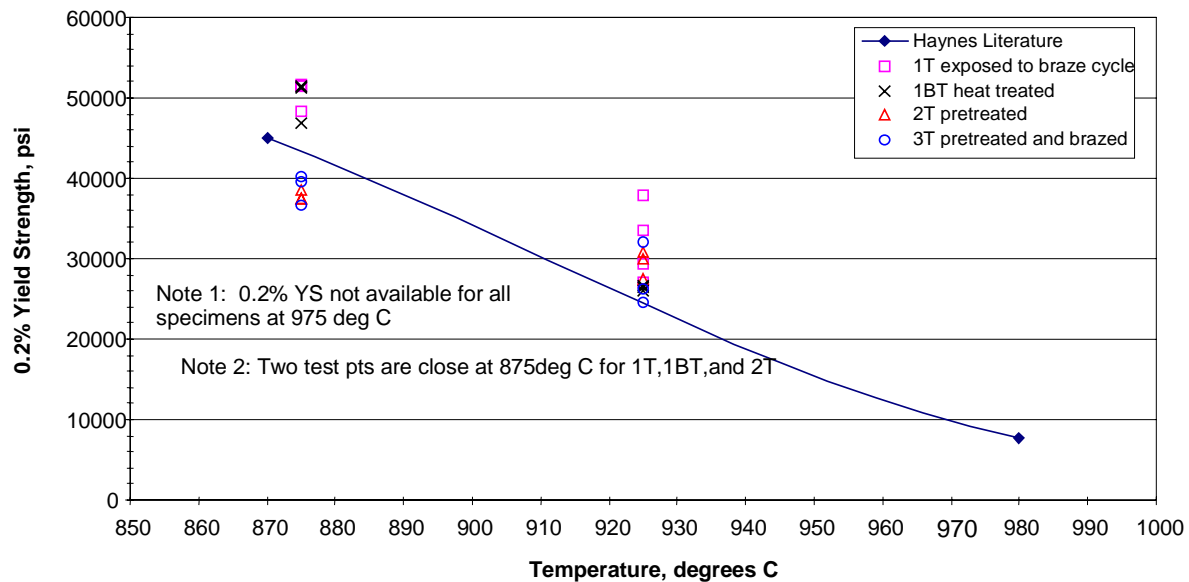


**Figure 2.3.3.3.1 -- 0.2 percent Yield Strength versus Temperature**

### 2.3.3.4. Material Constitutive Model for Structural Analysis

The constitutive models for the H214 material used in the finite element structural analysis were obtained from readily available supplier literature and from the test results detailed in the previous discussions. The elastic plastic multilinear stress strain curves as used in the

constitutive models are shown in Figure 2.3.3.4.1. Metal temperatures between input curves are linearly interpolated.

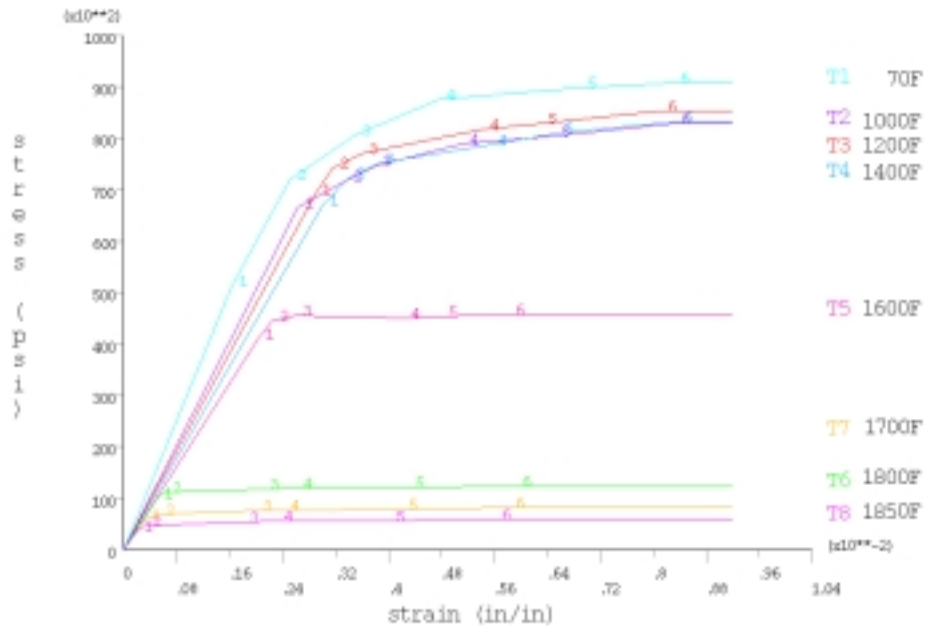
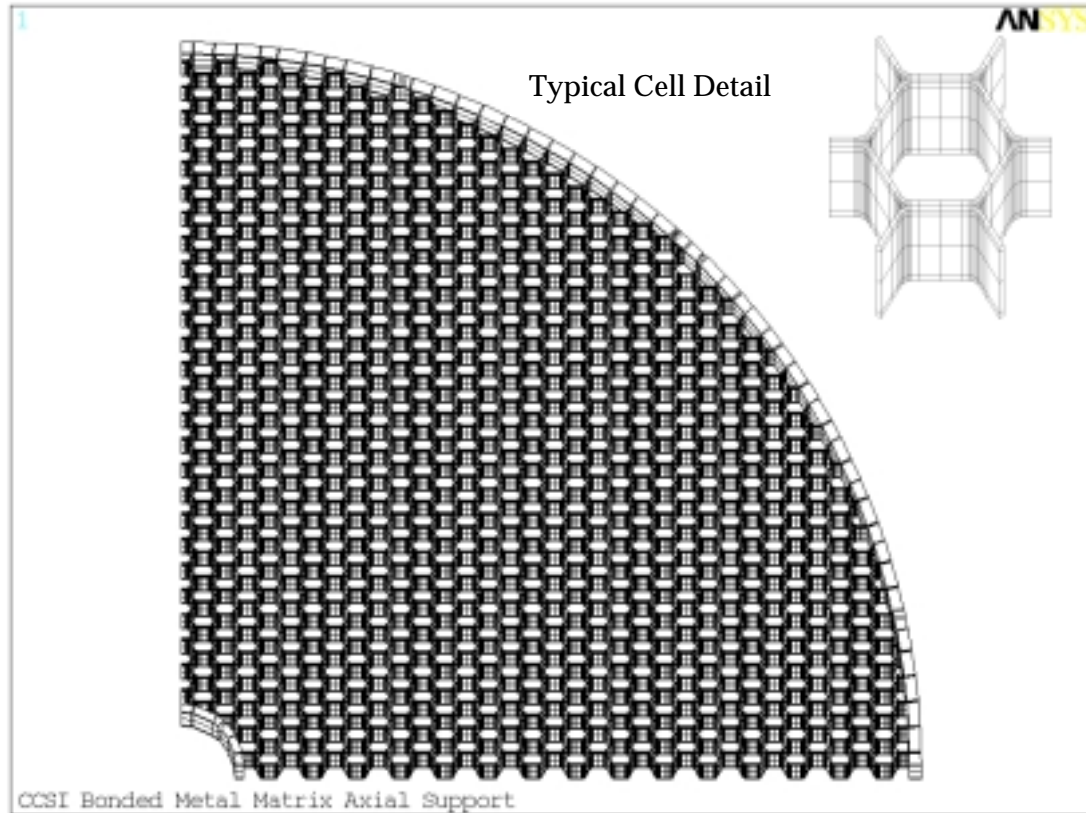


Figure 2.3.3.4.1 -- Multilinear stress strain curves for Haynes 214

#### 2.3.4. Structural Analysis

The finite element mesh is shown in Figure 2.3.4.1. The model is constructed of predominately 8-noded hexahedral elements for accuracy with high computational efficiency. The large aspect ratio of the honeycomb geometry due to the thin foil relative to the BMM diameter and height, along with the minimum cyclic symmetry of a quarter sector results in a large number of elements. This model contains 158,484 elements and 319,700 nodes. Several meshes were analyzed to arrive at this construction, which obtains optimal accuracy with the minimum number of elements.

Brazing of the corrugated foils to construct the honeycomb creates radii at the joints between foil pairs. This radius was measured on numerous joints and found to be about 0.020 inches. In addition, the finite element analysis was run with 0.005 inch larger and smaller radii, and the calculated variation in the stresses was not significant.



**Figure 2.3.4.1 -- BMM finite element model**

The metal temperature distribution applied to the thermal stress analyses was obtained from infrared imaging of the catalyst module during turbine operation at Silicon Valley Power. These temperatures as applied to the finite element model are shown in Figure 2.3.4.2. This is an approximation of the actual temperature measurements, which matches the hottest radial line and assumes that distribution over the quarter sector. This is considered fairly accurate though a slightly conservative loading for the stress analysis. Assuming that the worst radial gradient exists all around the circumference will produce slightly higher stress than the actual condition with a less severe gradient at most circumferential locations.

Mechanical loading on the axial support is due to edge contact from the catalyst foils, which sustain a fluid pressure loss. Uniform pressure rather than discrete foil contacts were used to represent this edge load. Because the contacts are at most .040 inches apart, this approximation is considered reasonable. The pressure drop across the entire cross section used in these analyses was 1.0 psi and the uniform pressure load on the honeycomb edge was then 7.8 psi. Symmetry restraint conditions are applied at each cut boundary on the inner and outer diameters. Axial restraint is applied at the outer and inner diameter to represent the contact conditions within the assembled catalyst module.

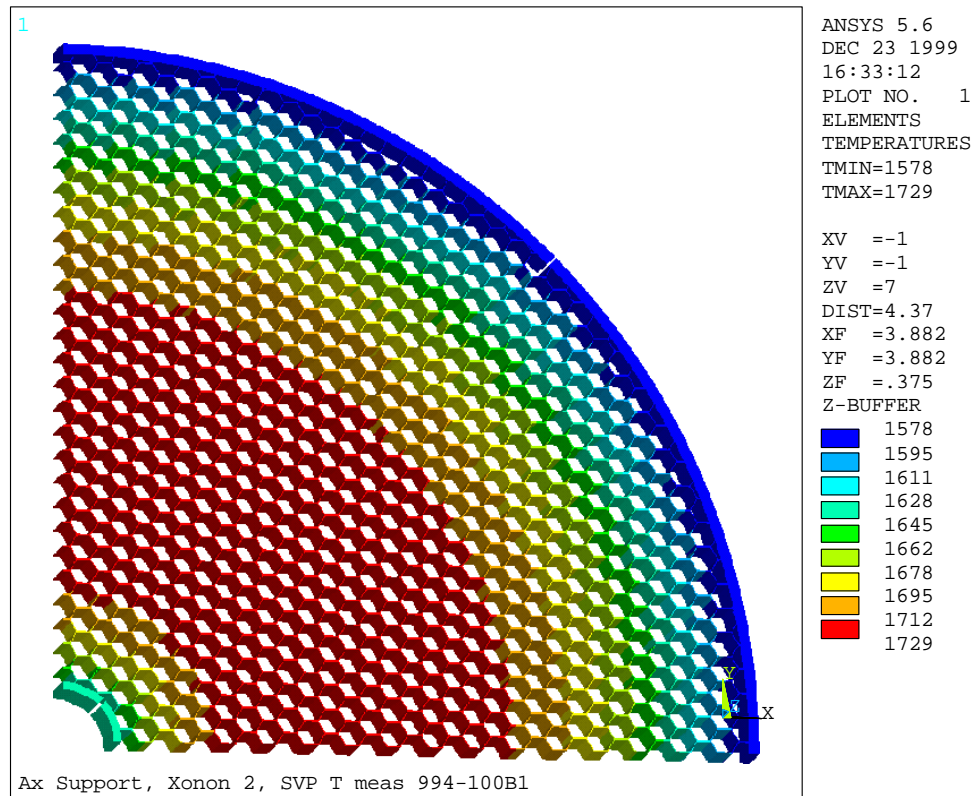


**Figure 2.3.4.2 -- Heat Transfer Analysis Metal Temperature Distribution**

### 2.3.5. Analysis Results

Stresses due to the thermal gradients and mechanical loading determine the number of load cycles necessary to cause low cycle fatigue. Stress is highest near the thermal expansion slots in the outer band. Peak equivalent stresses due to the thermal and pressure load in the honeycomb cells within the sector are shown in the Figure 2.3.5.1. The maximum stress is in the center slice at the outer diameter, adjacent to the thermal expansion slot and is the likely location of initial low cycle fatigue.

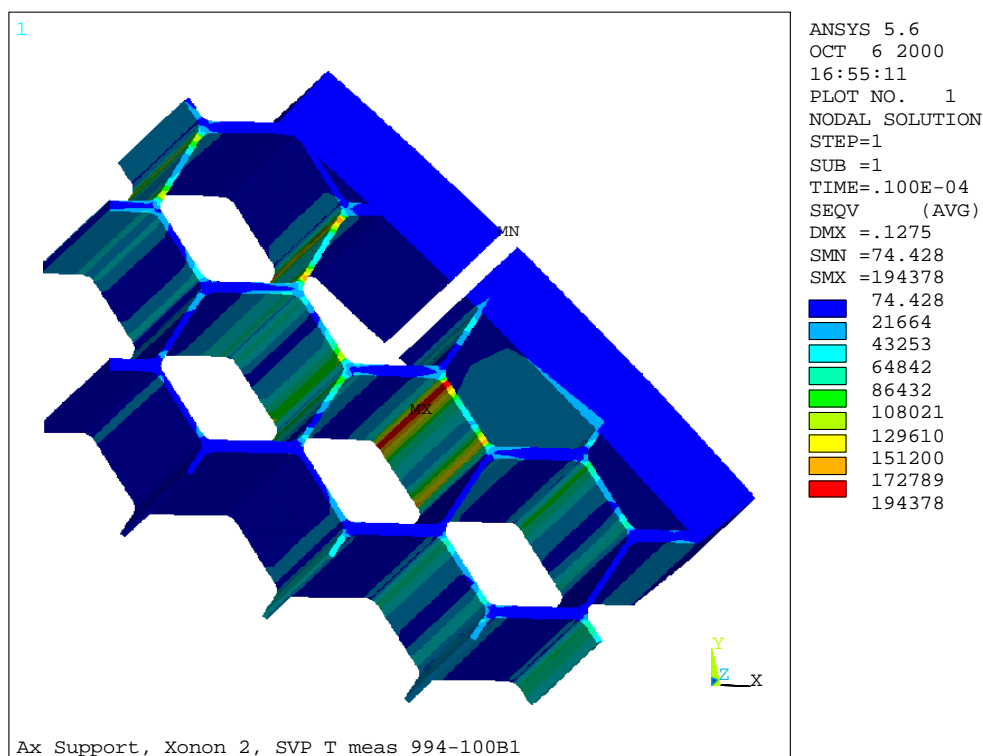


Figure 2.3.5.1 -- Equivalent Stress in Selected Elements at Midpsan

#### 2.3.5.1. Fatigue Analysis

Using the previously reported fatigue data for pretreated H214 at 900°C and 194 ksi, the number of cycles to fatigue failure is predicted to be less than 50. Fatigue cracks have been observed at this location after operation of more than 50 starts. However, this condition does not cause a durability concern since the structural integrity is not compromised by a single or even multiple cells separating near the thermal expansion slots. These cracks would need to extend along a significant portion of the outer ring to cause lack of support for the catalyst. If the initial cell wall fatigues in 50 cycles, then the adjacent cells acquire additional strain and fatigue (though at slightly lower rates), well over 600 cycles are required to connect between the expansion slots. This is very conservative since the more cells crack, the lower the fatigue stress becomes. Another possibility, though even less likely, is that a section of honeycomb becomes liberated as a closed loop of cracks form. There is insufficient stress away from the slot to cause this event.



### 2.3.5.2. Creep Analysis

The combined effect of thermal stress exceeding yield and mechanical stress high enough to drive creep can also cause cyclic ratcheting. Ratcheting causes additional deflection due to load and unload cycles. It is possible for this ratcheting of the deflection to continue indefinitely or to 'shakedown' and stop once the strain-state has reached a certain condition. The results of this section revealed the importance of including load cycling and plasticity in addition to creep in the prediction of permanent deflection.

A nonlinear FE analysis of the one row model with the inclusion of plasticity and creep material behavior was completed. Loading was applied as a linear ramp over 72 seconds similar to how the turbine is started. This was done gradually in 50 steps in order to allow plastic deformation to redistribute. Next, the load was held constant for 200 hours while creep strain accumulated. The load was removed analogous to the load application method. This cycle was repeated eight times.

Axial deformation versus time results provide the most evidence for evaluating axial support creep damage and can be easily compared to field measurements. Computed axial deformation versus time is plotted in Figure 2.3.5.2.1 near the mid-span between the inner and outer rings. At each 200-hour increment, the deflection appears to step change due to the relatively short time required in removing and applying load. Note that the results are step-wise linear rather than continuous in nature. This occurs because results at discrete times are stored in the solution to reduce use of computer disk space. After 1,600 hours the FE analysis computes .020 inches of permanent axial deformation. Each 200-hour increment increases the deflection by .0022 inches.

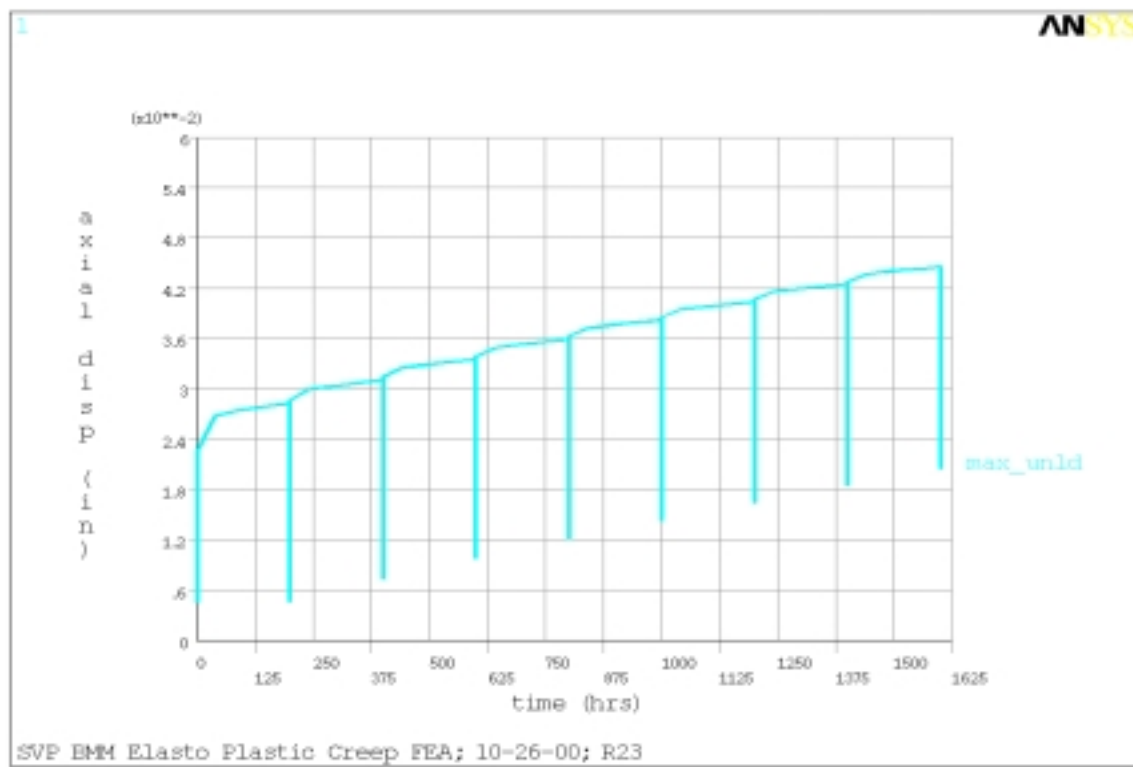


Figure 2.3.5.2.1-- Axial deformation versus time for the One Row FE Elasto-Plastic-Creep Analysis

The maximum strains from the above honeycomb cell are plotted versus time in Figure 2.3.5.2.2. There is reversal of the plastic strain and subsequent change in the creep rate at each start up and shutdown. This will significantly increase the amount of deformation due to load cycling during operation.

At each shutdown, the reversal of plasticity results in ratcheting of the deformation upon restarting. This deformation mechanism is considered very detrimental to most designs since deformation is added with each load cycle regardless of operating time. As can be seen in Figure 2.3.5.2.2, each start-stop adds approximately .0003 inches of axial deflection compared to continuous operation without a stop. Fifty starts results in 0.015 inches of additional permanent deflection, which is considerable when compared to the computed deformation. Not only is significant deflection added, but also the ability to predict the behavior is much more difficult because the material constitutive model must precisely represent the characteristics of the yield surface.

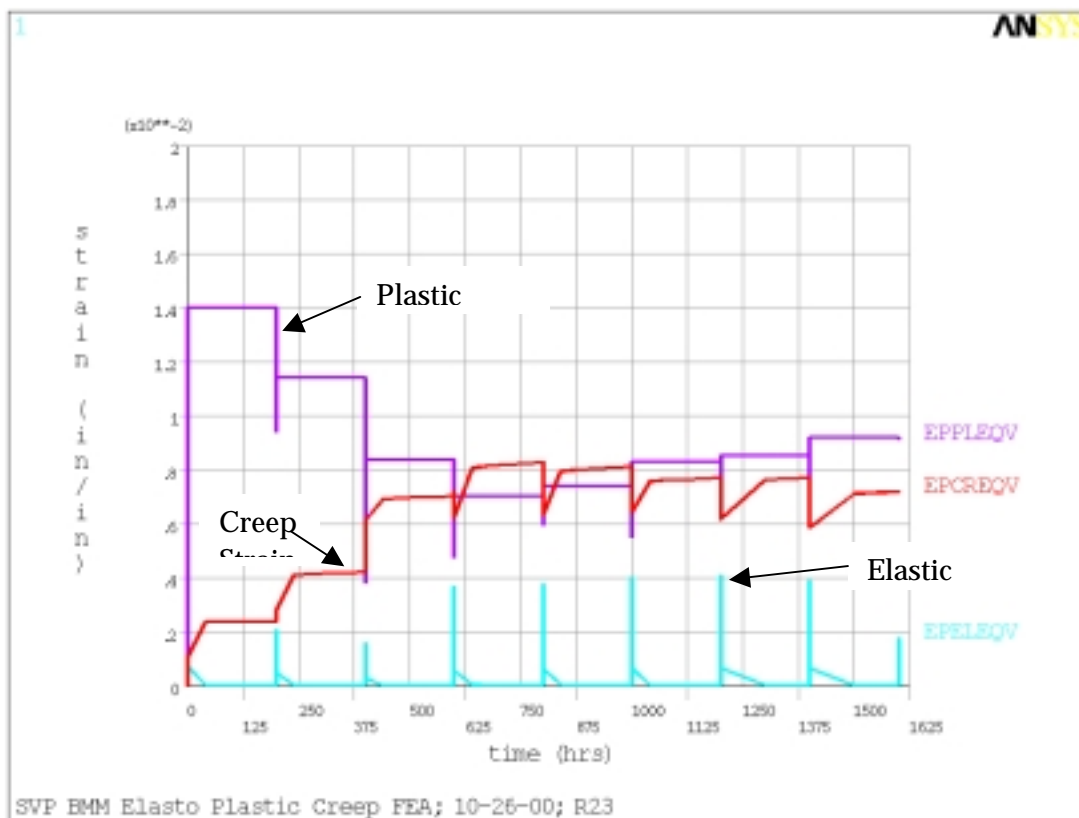


Figure 2.3.5.2.2 -- Maximum equivalent strains from previous cell versus time

Measurements of an operating Xonon® combustion system at Silicon Valley Power were taken over 4,129 hours of operation with approximately 50 starts. The maximum axial deflection, which occurs near midspan between the center and outer diameter, is summarized in Table 2.3.5.2.1. Extrapolating the analytical prediction to 4,165 hours, assuming the deformation rates continue:

$$\begin{aligned}
 &0.020 && \text{Computed deflection 1,600 hrs, 8 starts} \\
 &+ (4165-1600) * (.0022 - .0003) / 200 && \text{Creep rate minus ratcheting times added hours} \\
 &+ (50-8) * .0003 && \text{Ratchet rate time added starts} \\
 &0.057 \text{ inches}
 \end{aligned}$$

The analytical prediction has underestimated the deformation seen in operation by 2.7 times ( $0.154/0.057 = 2.7$ ). The reason for this discrepancy can be attributed to the material data used to formulate the constitutive equations. As discovered in the material creep testing, foil may have a considerably higher creep rate than that found in sheet material. For the honeycomb foil with as few as three grains through thickness, creep resistance is weakened considerably and a 2.8 increase in creep rate was seen in short term testing. The material constitutive equation for this analytical prediction was based upon the more creep resistant sheet data.

**Table 2.3.5.2.1 -- SVP Deflection vs time**

<b>Time (hrs)</b>	0	1107	1408	2065	3056	3180	4129.1
<b>Axial Defl (in)</b>	0	0.092	0.107	0.115	0.126	0.136	0.154

### 2.3.6. Conclusions

The key findings for this task include:

- The fatigue analysis results show very good agreement with fatigue cracking observed in actual engine hardware.
- The analysis was unable to predict the permanent deformations (creep) observed on actual hardware. Clearly, the primary cause of this discrepancy is the lack of reliable material data.
- Achieving an accurate prediction of permanent deformation will require measuring creep strain of the actual foil at engine operating stresses and temperatures.

## 2.4. Fuel/Air Premixer Development

The pre-mixer development work is described more fully in Appendix IV: Fuel/Air Pre-Mixer Development.

### 2.4.1. Introduction

CESI conducted a study to design, develop, and test a mixer / fuel injection system for an axial flow combustor. In order for a catalytic combustor to have acceptable performance, an axial flow mixer must provide a fuel/air mixture with uniform composition, velocity and

temperature to the catalyst with mixing occurring over a very short distance and with a low-pressure drop.

The mixer that was developed was a lobed forced mixer that can achieve good mixing over a relatively short distance. The fuel pegs chosen for this mixer were an airfoil design, which reduces dynamic pressure losses and flow recirculation, thus decreasing the potential for flameholding. The primary benefit of this design is reduced package size for an axial flow combustor without decreasing catalyst life. The design focused on the CESI Xonon® 1.0 catalytic combustion system for the Kawasaki M1A-13X gas turbine, since this was the most readily available engine test bed at the time.

The following steps were completed for this study:

- A background literature search to determine the best mixer configuration to pursue for this study.
- Computational Fluid Dynamics (CFD) analyses of various lobed mixer and fuel peg parameters in order to determine the optimum geometry for the final design.
- Experimental and computational analyses to better understand flame holding mechanisms for this mixer design and future design iterations.
- Cold flow rig testing of the final mixer / fuel peg designs to determine the fuel/air mixing characteristics of the mixer.

### 2.4.2. Approach

The axial fuel/air premixer development approach is summarized in the following diagram:

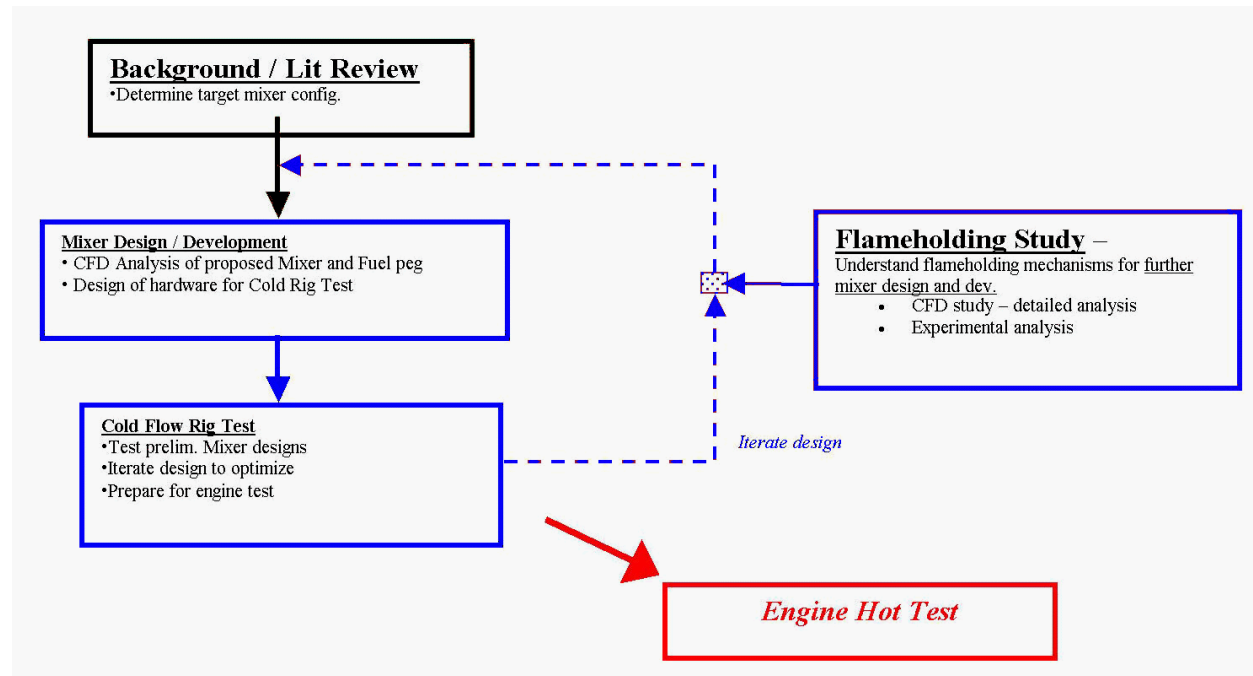


Figure 2.4.2.1 – Fuel/Air mixer project approach

The steps depicted in Figure 2.4.2.1 are described in detail below:

- A background data search and literature review was first conducted in order to determine the most suitable mixer configuration. A review of previous studies led to the selection of a lobe forced mixer primarily due to its short mixing length. An airfoil design for the fuel peg was selected based on the requirements for low flow recirculation and minimum pressure loss.
- Once the hardware selection was completed, mixer and fuel peg designs were optimized through detailed CFD analyses. Cold flow test hardware was procured once the final designs were established.
- In parallel, experimental and computational analyses were performed in order to better understand flameholding mechanisms. This information was useful for this mixer design and future design iterations.
- Cold flow rig testing was performed to determine the mixer effectiveness.
- In the end, the predicted performance of the mixer design derived from the computational and experimental work was no better than the radial mixer currently in use on the turbine combustor. Consequently, CESI and the Commission concurred that the engine hot test would not be pursued.

### 2.4.3. CFD Analysis

#### 2.4.3.1. Lobed Mixer CFD

A computational simulation was conducted to study the feasibility and establish design guidelines for using a lobed mixer in a catalytic combustor. The lobed mixer would be used to assist mixing of the main fuel with the preheated preburner exit air. Simulations were conducted with varying lobe lengths and numbers of lobes. The lobe shapes were generated through the rotation of a sine curve through  $360^\circ$ . The centerline of the lobed mixer was located half way between the combustor center-body and the combustor wall. The Xonon® 1.0 flow path was used, with inlet flows mapped from separate preburner solutions conducted without the radial mixers.

The computational meshes were generated by hand and consisted of approximately 600,000 computational cells (Figure 2.4.3.1.1). Highly accurate physical property and turbulent viscosity models were used based upon experience with earlier radial mixer simulations. Model results showed that the initial design based upon literature results did not provide sufficient penetration from the lobe exits to the walls of the combustor. The lobe length was increased for subsequent simulations, and adequate penetration was obtained.

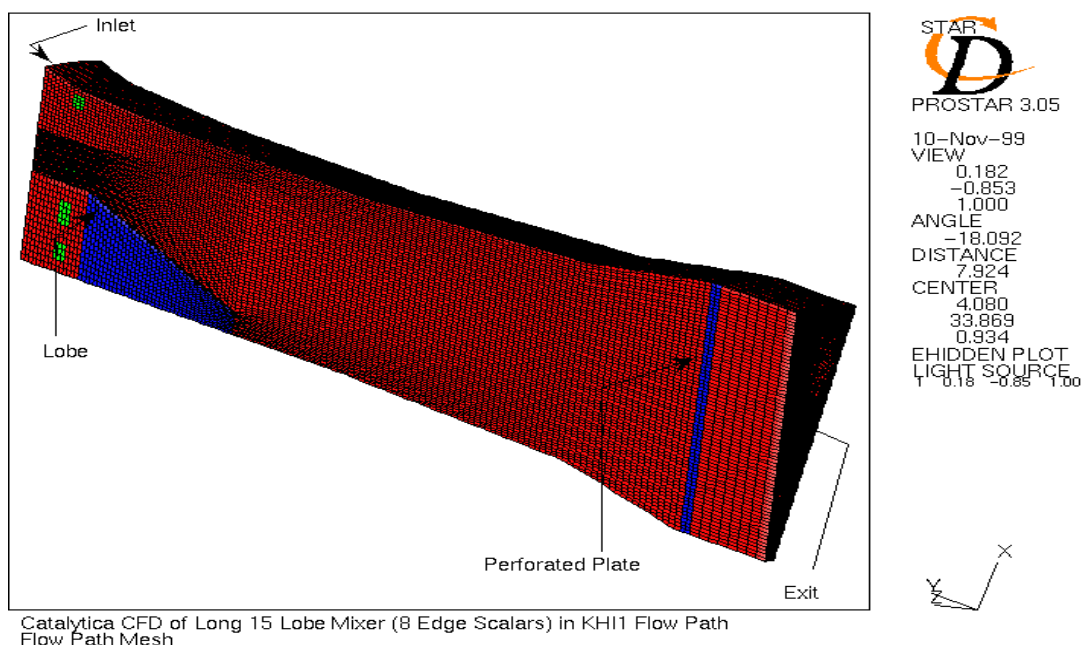


**Figure 2.4.3.1.1 -- Lobe Mixer Geometry CFD Features**

Mixers with 10, 12 and 15 lobes were simulated. Figure 2.4.3.1.2 shows a rendering of a 12-lobed mixer solid CAD model. The mixing effectiveness increased as the number of lobes was increased. Most of this improvement is believed to be due to the implied increase in the number of fuel injection points, i.e., eight or sixteen for each lobe required for symmetry.

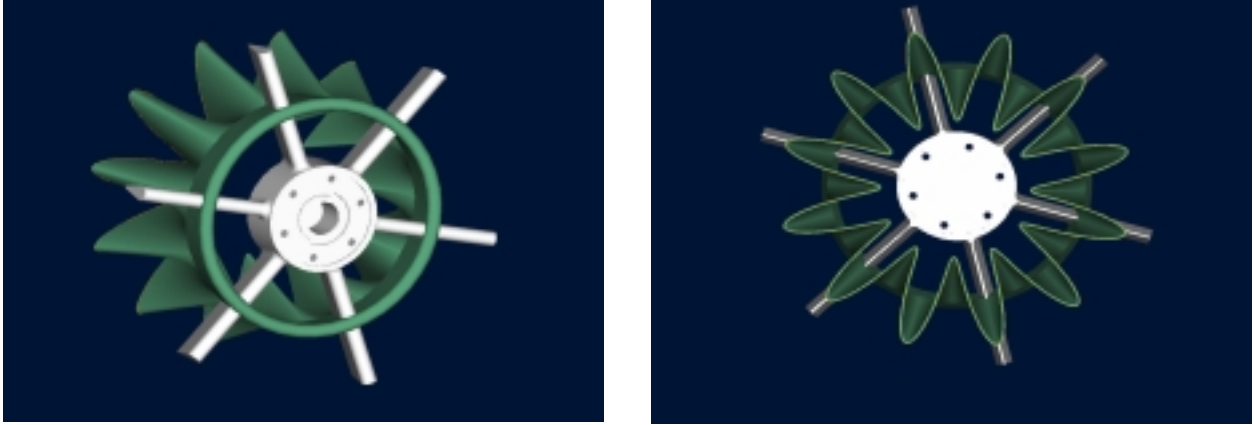


**Figure 2.4.3.1.2 -- Three-dimensional rendering of a complete 12-lobed mixer along with fuel pegs**

Comparison of the lobed mixer results with the CFD results for the atmospheric pressure 3-Stack radial mixer model indicate that the current designed lobed mixer will not provide the degree of fuel/air uniformity provided by the radial mixer. The lobed mixer does not have the mixing driving mechanisms of strong swirl and counter-flow provided by the current radial mixer. The lobed mixer shows promise, however, as an alternate mixer, especially for axial flow combustors where a radial mixer might be difficult to design and install.

The first simulation was made with an assumption that a high Reynolds number turbulence model was appropriate. A second simulation was made with a low Reynolds number turbulence model, which required a refined grid. These two simulations produced similar results, thus indicating that the high Reynolds number turbulence model was suitable.

The inlet boundary condition was taken from a previous run of the KHI premixer geometry with the radial mixers removed. This provided an inlet boundary condition that was then mapped to the inlet boundary of all simulation runs. The inlet boundary was essentially isothermal, but did have variation in the inlet axial and radial velocity components, and in the turbulence parameters  $\kappa$  (kappa – turbulent kinetic energy) and  $\epsilon$  (epsilon – rate of turbulence dissipation).

A key result of this simulation is shown in Figure 2.4.3.1.3. The main observation can be seen in the top portion of this figure. This shows that the fluid flowing outward through the upward directed lobe is not reaching and mixing with the flow approaching axially from the upstream (left). The outward flowing air through the lobe is not penetrating to the wall, or in the nomenclature of mixers, this is an under-utilized case. Ideally, the momentum of the fluid flowing outward through the lobe would cause it to approach the surface very closely.

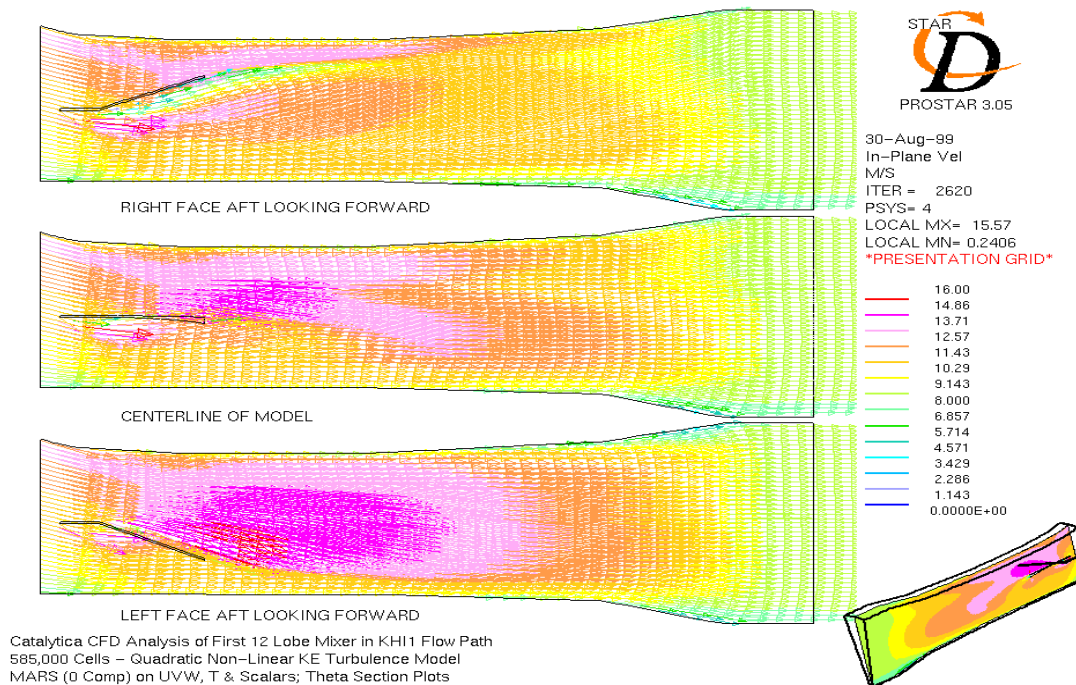


**Figure 2.4.3.1.3 -- In-Plane Velocity Vectors with Short-Lobe Mixer**

The second simulation made was with a 12-lobe mixer with the same location and half-angle, but with the lobes being extended downstream and outwards from the lobe centerline. The lobes were extended to within about one-half inch from the combustor wall and center-body. A plot similar to the previous plot can be found in Figure 2.4.3.1.4. In this case, as well in other cases run with longer lobes, the lobe jet penetration to the wall was very good. Since the penetration concern was adequately addressed with this first modification, all future runs were made with this longer lobe.

After obtaining a solution for the 12-lobe mixer that met the jet penetration requirement, computer models were also generated for 10-lobe and 15-lobe designs. The next important factor that was investigated was the mixing between the fluid inside and outside of each lobe. There are several ways to examine the mixing between the two streams. One way is to compare the in-plane velocities normal to the bulk axial flow direction. The in-plane velocities are shown in Figures E1, E2 and E3 in Appendix E for 10, 12 and 15 lobe models respectively. Little difference can be seen between these plots. In general, the degree of mixing (i.e., the cross-planar velocities) is low compared to the radial mixer currently in use in Xonon® 2.0.



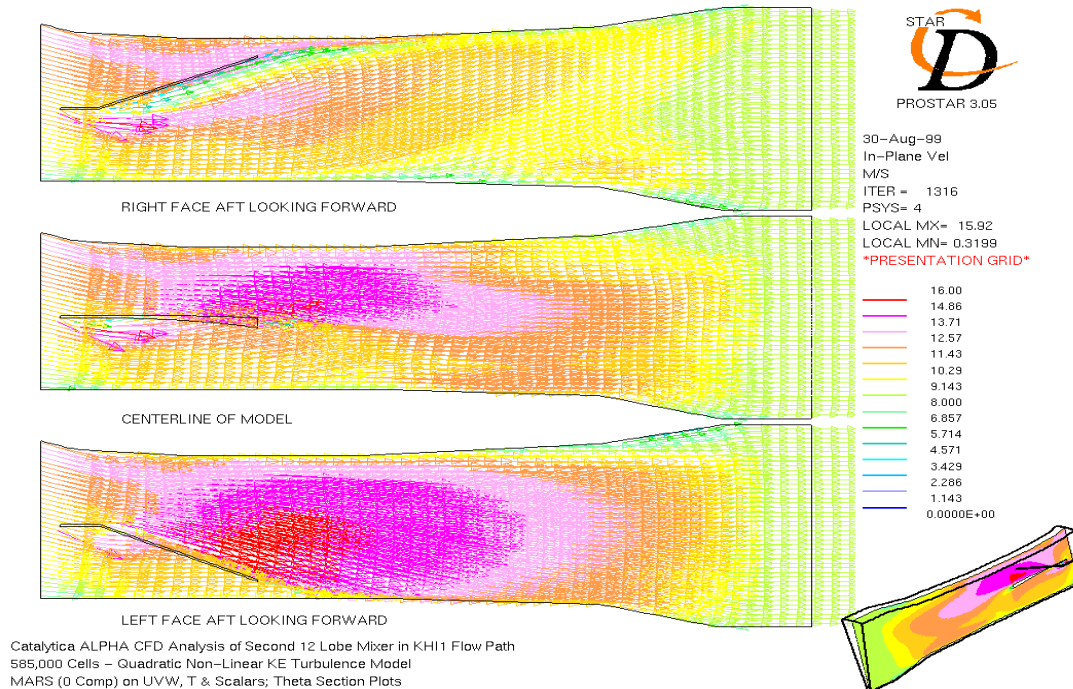


**Figure 2.4.3.1.4 -- In-Plane Velocity Vectors with Long-Lobe Mixer**

#### 2.4.3.2. Fuel Peg CFD Analysis and Design

For good fuel and air mixing, it is important to obtain a good fuel distribution from the fuel injection system. This can be interpreted to mean obtaining a uniform fuel distribution and/or to inject the fuel in such a manner as to take maximum advantage of the mixing capability of the lobed mixer. Obtaining uniform fuel and air mixing only from the fuel injection system would be difficult, since a very large number of fuel injection points would be required.

The method of choice for fuel injection utilizes an airfoil shaped fuel peg as shown in Figure 2.4.3.2.1. The cross-section is that of a circular tube with a triangular shaped faring welded onto the downstream side. Fuel injection holes are drilled perpendicular to the dominant air flow direction and the fuel peg. This provides small, high velocity jets of fuel, normally natural gas, to penetrate and mix with the air. The depth of fuel penetration is calculated by a method developed by CESI. The mixer then is used to increase the fuel and air uniformity.

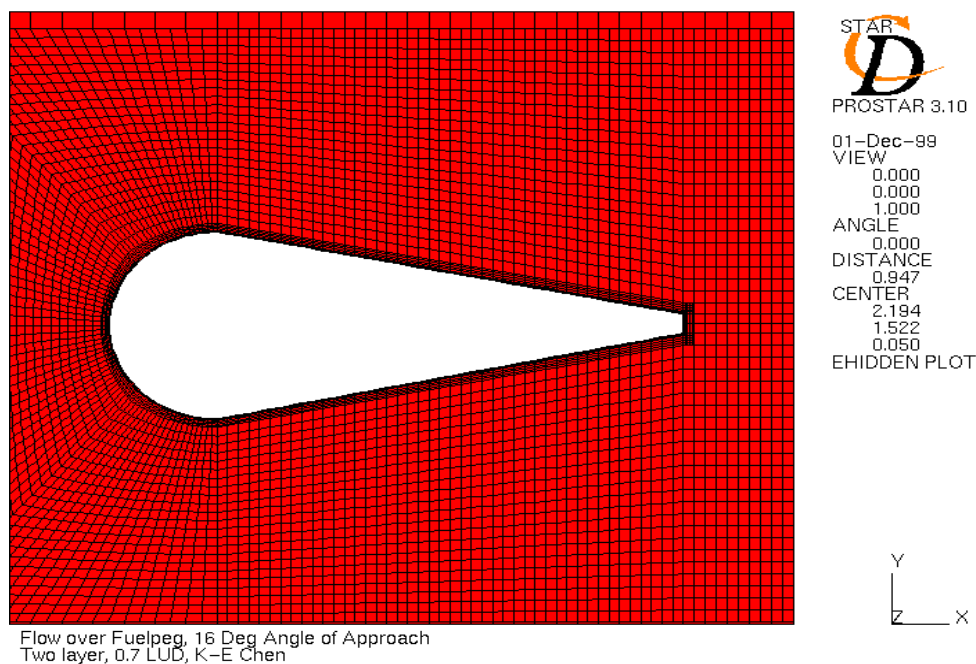


**Figure 2.4.3.2.1 -- Baseline Fuel-Peg Geometry and Two-Layer Computational Grid**

The current fuel peg design works well for fuel injection. However, the blunt upstream surface combined with the sharp transition from round to flat side surface and the flat sides of the faring could allow a recirculation zone to form. The recirculation zone *per se* is not a problem. However, a recirculation zone in an area containing a combustible mixture could act as a flameholder if ignited.

The current fuel peg design has the general shape of an airfoil. However, airfoils, as used on airplane wings, are specially designed so as to minimize formation of recirculation zones. An airfoil must allow flow over both the top and bottom surfaces at a range of angles of approach without forming recirculation zones. As the approach angle is increased, the surface area on the top of the wing is increased. Thus the air velocity is increased compared to the bottom velocity, and lift is generated. Recirculation zones increase drag, and if sufficiently severe, result in the loss of lift (stall). Therefore, an airfoil design has been investigated as an alternate shape for the fuel peg that would decrease the possibility for setting up recirculation zones. Constraints inherent in the design of the fuel pegs include:

- Gas velocity through the fuel peg should be less than 100 feet/sec.
- Pressure drop across the fuel peg fuel jets should be approximately 10 percent.
- Location and orientation of the fuel pegs and lobed mixer must be compatible with the existing Xonon® 1.0 combustor.

A fuel peg needs to be symmetrical, whereas most wings are not symmetrical --- having more surface area on the top than on the bottom. The types of airfoils selected for investigation were the NACA00nn varieties. The “00” indicates that the airfoil shape is symmetrical and the “nn” indicates the airfoil maximum thickness as a percentage of the chord length.

The base case fuel peg design was based upon a prior CESI design. This design consists of a circular stainless steel tube approximately 0.5" O.D. A triangular shaped faring is attached to the downstream side of the tube. The model domain consists of a two-dimensional cross-section of the fuel peg located in a rectangular area 3" wide by 10" long. A symmetry boundary is used for the front and back faces of the single cell thick model. These faces are shown as "into" and "out of" the plots, and are not normally seen. Cyclic boundaries are used on the side boundaries. This is the most suitable boundary type (without extending the boundary outward until a stagnation boundary could be used).

Initially, several turbulence models were used, including the  $\kappa$ - $\epsilon$  model, the  $\kappa$ - $\epsilon$  quadratic model and a  $\kappa$ - $\epsilon$  cubic model. It was found that when flow separation was present, the angle of approach at which flow separation occurred was much higher than indicated from airfoil data.<sup>2</sup> After consultation with CFD experts at Combustion Science and Engineering (CSE), it was concluded that none of the available turbulence models was adequate to predict flow separation under these conditions. Therefore, a two-layer model was required.

The baseline fuel peg and each of the airfoil design fuel pegs were modeled under the same conditions, as summarized in Table 2.4.3.2.1. Each fuel peg was initially modeled with air entering at a 0° angle of approach at 14 m/s. The converged result from each iteration was used as an initial condition for the subsequent simulation, which was run at a larger angle of approach. The approach velocity was held constant, and only the approach angle varied. This technique could present problems to the model due to the small model domain if either symmetry or stagnation boundary conditions were used. However, the cyclic boundary condition provided a good solution because the flow and angle out of one side was matched by the flow and angle into the opposite side of the computational grid. (These edges are located along the top and bottom sides of the fuel peg plots.)

**Table 2.4.3.2.1-- Fuel-Peg Model Conditions and Methods**

<b>Fluid Properties</b>	<b>Air</b>
Equation of State	Ideal Gas (MW 28.96)
Molecular Viscosity	Constant (1.81E-5 kg/ms)
Specific Heat	Constant (1006 J/kgK)
Thermal Conductivity	Constant (0.02637 W/mK)
Exit Pressure	9.E+5 Pa
Turbulence Model	$\kappa\text{--}\epsilon\text{v}\epsilon\eta\text{X/}$
Two-Layer Model	Norris and Reynolds
<b>Inlet</b>	
Temperature	750 K
Density	4.237 kg/m <sup>3</sup>
Kappa, $\kappa$	2
Epsilon, $\epsilon$	80
<b>Solution</b>	
Solution Algorithm	SIMPLE (steady state)
Equation Method	MARS – 0.5 compression
Under-relaxation	0.7 U, V, $\kappa$ , $\epsilon$ ; 0.1 P

The baseline fuel peg has a thickness to length ratio of 0.375, which would match the thickness to chord length of a NASA0037 airfoil. For a given chord length and “shape”, as an airfoil’s thickness is increased so is the tendency for flow separation. Therefore, airfoil shapes used covered the range of 0.27 to 0.36 corresponding to NACA0027 to NACA0036 in three percent increments. The current fuel peg length of 1.385” was held constant for all runs, with only the thickness varying. Table 2.4.3.2.2 shows all the cases analyzed.

**Table 2.4.3.2.2-- Airfoil fuel peg CFD simulations approach angle**

<b>Airfoil</b>	<b>10°</b>	<b>12°</b>	<b>14°</b>	<b>16°</b>	<b>18°</b>
<b>NACA0027</b>			X		X
<b>NACA0030</b>			X		X
<b>NACA0033</b>		X		X	
<b>NACA0036</b>	X		X		

## **2.4.4. Cold Flow Testing of Premixer**

### **2.4.4.1. Background**

The purpose of the Lobed Mixer Cold Flow rig test was to characterize the mixing capabilities of a twelve-lobe mixer developed from CFD analysis in a cold-flow test facility. This facility allows operation at conditions scaled from the Xonon® 1.0 combustor flow-path. The velocity vectors will be measured with a wedge probe. A mixture of natural gas and air will be injected through the fuel pegs, and the fuel concentrations measured upstream of the simulated catalyst will be used to determine uniformity of fuel and air mixing.

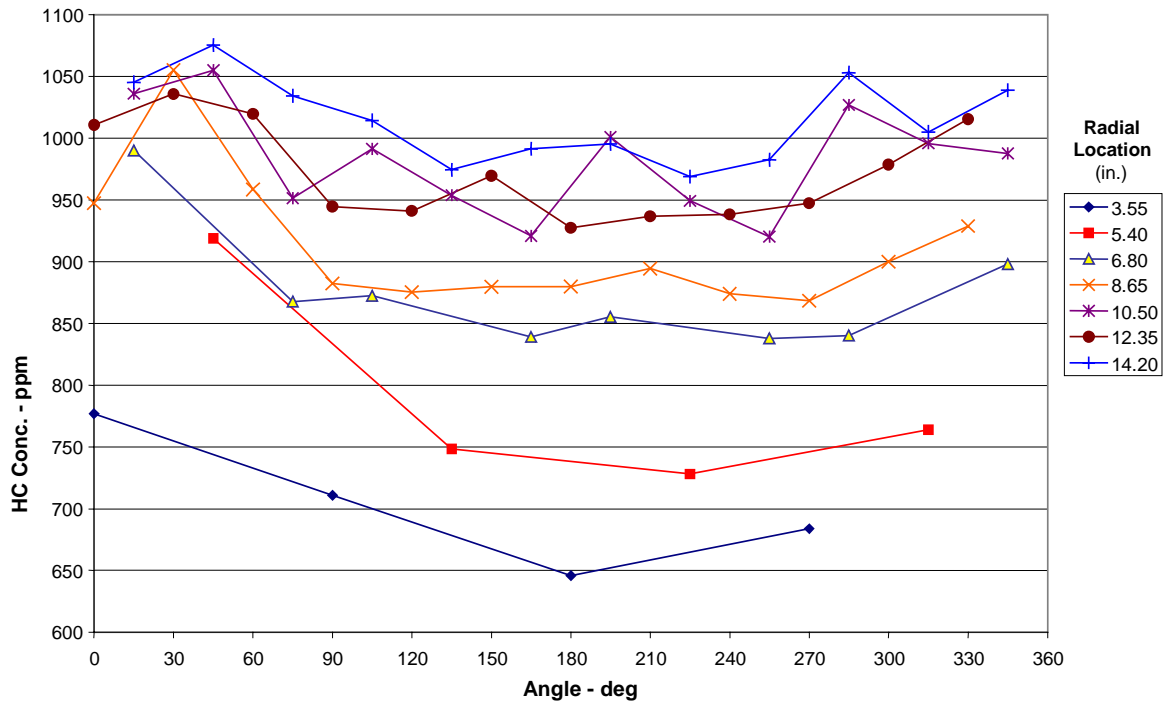
The lobed mixer design has been developed for possible use in the Xonon®1.0 combustor flow-path. The lobed mixer is an axial flow mixer, as contrasted to the radial mixers used in current CESI designs including Xonon® 2.0 and Xonon® 2.1. The mixer and fuel pegs were designed using CFD simulations as described in the previous section.

Figure 2.4.3.1.2 is a depiction of the lobed mixer to be tested. The unit consists of the lobed aerodynamic piece attached to a combined strut support/fuel injector part. The radial struts support the unit in the cold-flow rig. Figure E 4 (Appendix E) shows a notional cross-section of the lobed mixer installed in the cold-flow rig. Fuel was supplied to the central hub and out to the radial struts, and then injected through holes upstream of the lobe. The catalyst inlet was simulated with a round perforated sheet.

The fuel pegs tested have a cross section based upon the airfoil design discussed in Section 2.4.3. CFD modeling has shown that this design shows significantly more resistance to flow separation than the standard design currently being used. This resistance to separation at higher approach angles indicates that the fuel peg will be less likely to act as a flame holder.

### 2.4.4.2. Test Results

Figure 2.4.4.2.1 shows a cross-sectional plot of sampling locations, with the 0° location located at top dead center. The fuel pegs are shown by the magenta lines at 0°, 30°, up to 330°. The fuel pegs are located midway between the inner and outer directed lobes. The fuel pegs are symmetric, so the central angles between fuel pegs represent lines at which the jets from the fuel pegs collide.



**Figure 2.4.4.2.1 -- Fuel/air sampling grid points**

Figure 2.4.4.2.2 shows a plot of the Hydrocarbons (Natural Gas) concentration in ppm versus location. Note that there is a decrease in HC concentration from the outer sampling points toward the innermost sampling points. This concentration gradient is seen around the full 360° cylindrical cross-section. The concentration varies from 650 ppm at the center to 1075 ppm at the outer edges. The average concentration is 930 ppm, giving a maximum of +16 percent and a minimum level of -30 percent. This non-uniformity is greater than would be acceptable for use in a catalytic combustor. However, the inner to outer gradient can be relatively easily adjusted by modifying the size and/or location of the fuel injection points. This would provide more fuel to the low concentration center and/or less to the higher concentration outside.

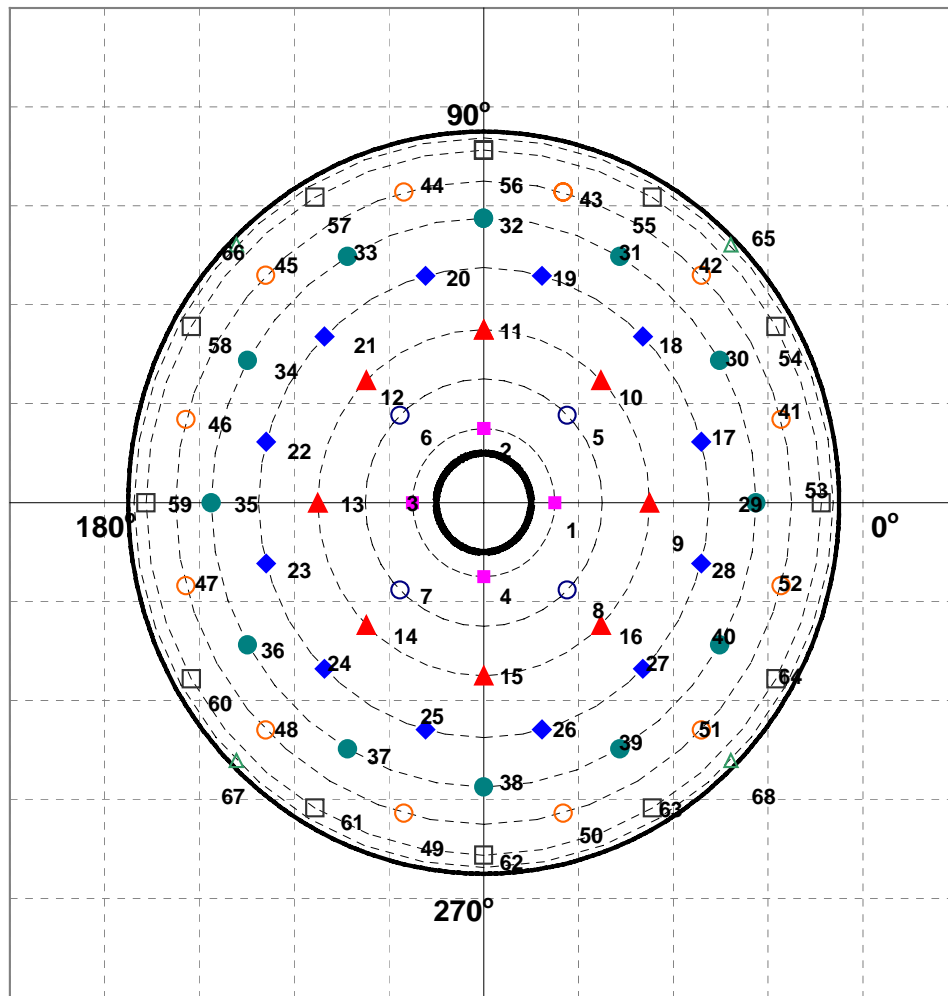


Figure 2.4.4.2.2 -- Measured HC concentration vs. angle and diameter

If Figure 2.4.4.2.2 is studied in detail, there are “lighter” (higher concentration) areas and “darker” (lower concentration) areas around the outer perimeter of the sampling area. It should be noted that the lowest concentrations of fuel occur at angles of 90°, 120°, 180°, 210°, 240° and 270°. From Figure 2.4.4.2.1, it can be seen that these points are directly downstream of the fuel pegs.

## 2.4.5. Flameholding Study

### 2.4.5.1. Background

The aim of this study was to obtain a fundamental understanding of the mechanisms of flameholding in fuel/air premixing passages for advanced lean burn gas turbine concepts. In such systems, there is a risk of autoignition, flashback, and flameholding within the premixing passage. This particular study examines the effects of geometric disturbances in the flow path on the flameholding potential of the premix passage. The design and fabrication of a semi-independent test rig to provide an experimental model of a lean burn fuel/air premixing

passage comprised a significant portion of the overall effort. While the vessel is self-contained, it relies upon facility supplied preheated air and cooled exhaust capabilities for operation.

In order to simulate the environment of a premixing passage for a natural gas fired gas turbine, both high pressures and high temperatures are required. To generate these conditions the University of California Irvine Combustion Laboratory (UCICL) High Pressure Facility is employed. The facility is capable of generating a preheated airflow at temperatures up to 1200 F and at pressures exceeding ten atmospheres. The maximum flow rate from the facility exceeds three lb/sec.

The experimental geometric conditions included sudden expansion (steps), gradual expansion (ramps) and channels. Note that, although the aforementioned geometries were fabricated, the emphasis for this phase of testing was directed at the sudden expansion type geometries. This was felt to (1) provide the most likely scenario for flameholding, and (2) provide the closest approximation to the type of perturbations found along the walls in practical premixing devices for a variety of manufacturing approaches. The facility was designed, however, to allow the additional parametric geometries to be evaluated.

The facility connection for the preheated airflow is a four-inch, 600-lb ANSI standard flange fitting. This fitting is reduced to a two inch, 600-lb flange fitting to more closely match the premixing duct dimensions. Connection to the test rig is made by a two-inch steel braided flex hose, which joins the reduced facility connection with a flow conditioner (Vortab). The flow conditioner serves to provide a uniform velocity profile upstream of the natural gas injectors and test section. The next section makes a transition from the circular cross-section of the flow conditioner to the semi-square cross-section of the premixing passage. At this point natural gas is injected axially with the flow stream. Finally, a 12-inch mixing length provides some time for mixing of the gas before entering the test section. It is within this mixing length that upstream pressure readings of the vessel are taken. A turbulence grid can be added immediately upstream of the fuel injection section. Actual turbulence levels are determined by laser anemometry. All connections between individual components are made by 600-lb flange connections. The gaskets between connections upstream of the flow conditioner are ceramic filled, wire wound gaskets. Gaskets downstream of the flow conditioner are self-energizing metallic ring seals. These special seals are used in order to eliminate the gap between components that a normal wire wound gasket would create. By eliminating the gaps a more uniform flow condition at the inlet to the test section is provided. Additionally, the gaps would be a possible location for flameholding upstream of the test section. Figure 2.4.5.1.1 presents a photograph of the inlet/mixing section. Flow is moving from the right to left in this photograph.



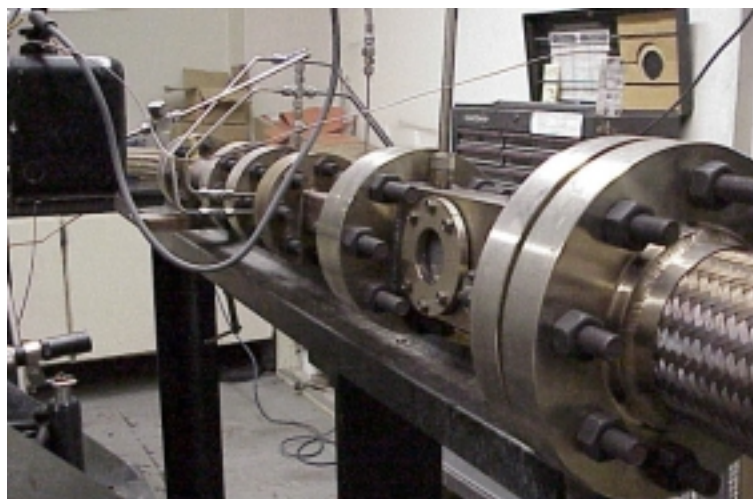


**Figure 2.4.5.1.1 – Flameholding test rig setup**

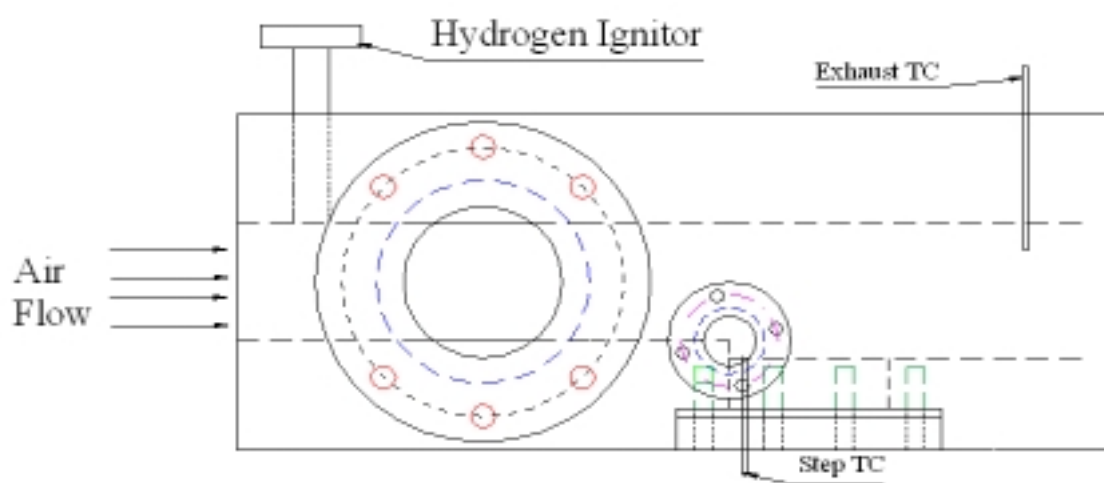


**Figure 2.4.5.1.2 – Test section overview**

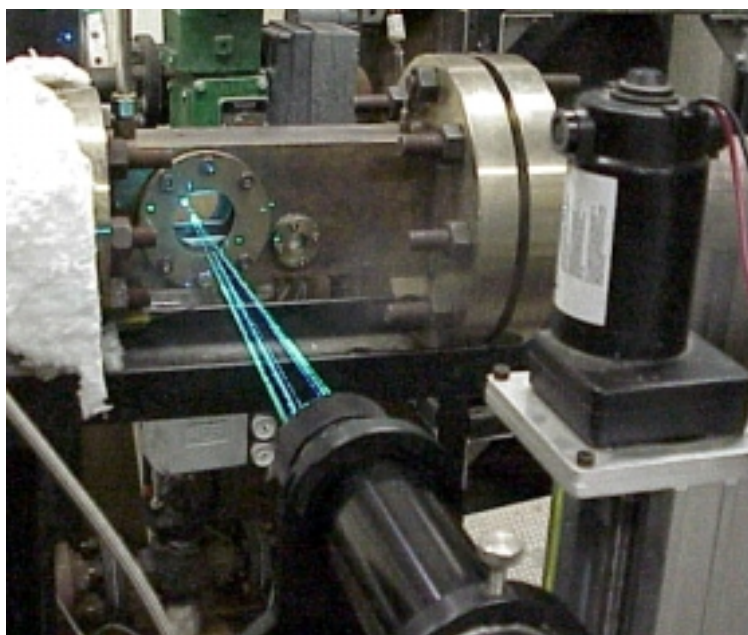
Figure 2.4.5.1.2 shows a schematic of the test section. The main block of the test section provides pressure and flow constraint as well as providing mounting locations for the other components. The hydrogen igniter, provided by CESI, injects a premixed hydrogen/air flame into the test section. Ignition is upstream of the geometric disturbance and is termed “soft ignition”. This method of ignition is used since it is considered more representative of actual autoignition conditions in a premixing passage. A premixed hydrogen flame is used to ensure full penetration and, therefore, complete ignition across the cross-sectional area of the premix duct. It is important to have complete ignition so as to ensure that high-energy radicals reaching the geometric disturbance and are not trapped upstream in high cross-flow situations. The three-inch windows allow for laser anemometry measurements and visual confirmation of hydrogen igniter operation. A thin piece of ceramic paper is placed between the test section and the

window to prevent fracturing of the window from thermal expansion of the metal. Fused quartz is used for these windows due to its high thermal shock resistance. A one-inch fused-quartz window is placed at the geometric disturbance to provide visual confirmation of a flameholding situation, and it helps to identify the location of the stabilized flame. The geometric disturbance is generated by an insert, which is placed in the test section and creates an expansion, contraction, channel, or transition angle. A thermocouple is placed in the insert to measure temperature at the disturbance to provide an indication of flameholding. Finally a thermocouple is placed at the exit of the main block to indicate if flameholding is taking place somewhere upstream.

The detection of the flameholding was accomplished visually. A small video camera was positioned to view the region from the main view port and the step view port. Flameholding was also monitored by a thermocouple at the step and by the post step thermocouple. The post step thermocouple and the visual indication were relied upon to provide the necessary information.

The measurement of the fuel distribution was accomplished using a special sampling section installed between the mixing section exit and the test section just for this measurement (it was not in place for the actual flameholding experiments). Nine evenly spaced discrete points (sample probe points) were monitored. The flow from each probe was sequentially fed to a high range Flame Ionization Detector (FID) hydrocarbon analyzer, which measured the concentration at each of the points.

The measurement of the velocity field within the inlet section was measured using laser anemometry. A two-component fiber optic system was installed onto a traverse system to provide two degrees of freedom. A photograph of the setup is shown in Figure 2.4.5.1.3. In the foreground is the two-component transceiver unit that serves to create the sample volume where four laser beams intersect as well as to collect the scattered light.



**Anemometry**

**Figure 2.4.5.1.3 – Photograph of laser anemometry setup**

A custom high volume seeding system was developed specifically for this project. It utilizes 1-micron alumina particles that are injected via a slurry solution using a twin-fluid atomization process. With the high preheat provided by the system, the water is easily vaporized, leaving the dry particles that serve to scatter the laser light.

A statistically developed set of experiments (design of experiments - DOE) was designed to conduct the testing in the most efficient manner. After review of the possible testing that could be accomplished with the parameters provided it was decided to focus upon the cases with the sudden expansion for the purpose of the present study. This results in a total of 6 parameters for study (expansion height, temperature, pressure, velocity, turbulence, and equivalence ratio). As a result, a  $2^6$  two-level, full factorial experiment was generated, resulting in 64 total cases. In addition, 5 center points were added to assess pure error and curvature in the response.

#### **2.4.5.2. Test Results**

Upon the conduct of shakedown testing, the “design space” (i.e., the limits in the ranges for each parameter) was modified somewhat. It was found, for example, that the system could not support flow rates in excess of 0.8 lbs/sec at seven atmospheres. Since the limitation affected only two out of 18 tests, the two out of range tests were conducted at lower velocities. Pre-heating was another significant issue. While the facility is capable of heating large flows of air (0.1 to 1.5 lbs/sec), it is not well suited for high preheats of small mass flow rates. This set the

low velocity limit at 100 ft/sec to prevent overheating the heater elements. As a result of the shakedown tests, turbulence intensity was dropped as a parameter and a new matrix was generated based on the constraints determined.

Positive and negative results were determined visually. Figure 2.4.5.2.1 shows two cases where positive flameholding was observed. In the left photograph the flameholding is very bright and intense. The photograph on the right also shows a stabilized flame but at a much lower intensity. Flow conditions as well as step geometry are believed to determine the intensity of the flame.

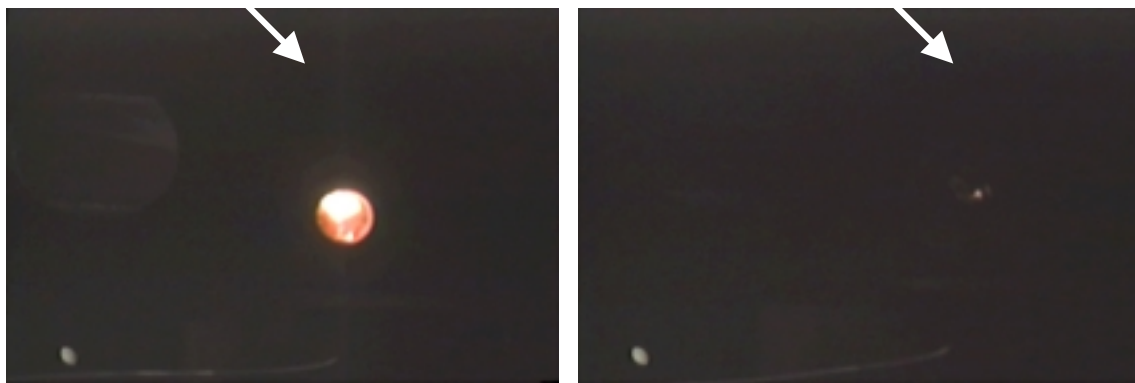


**Figure 2.4.5.2.1 – Positive flameholding results showing high intensity (left) and low intensity (right) flameholding**

Some anomalies were observed during testing. The most prevalent of these was flameholding upstream of the step. The test section introduces small disturbances upstream of the step. Two of the most notable disturbances are at the igniter end and at the window interface to the cross-section. During some tests the flame held at these disturbances. If the flame was determined to be holding upstream, the test was disregarded and rerun until the upstream flame blew off. Another anomaly that was observed was the fluctuation of the system pressure controller. For a set system pressure, the controller indicated an oscillating pressure. At 7 atm the average deviation was 2 percent of the mean. At 2 atm the deviation was roughly 4 percent.

Additional observations were made throughout the course of testing which are noted here as part of the screening results.

- Low air speeds of about 20 ft/s, especially when combined with high equivalence ratios, lead to a detonation in the vessel.
- Preheated air-flows should be greater than 0.1 lbs/sec to avoid low flow shut off of the heaters. This is an issue associated with limitations of the facility.
- Higher air-flow rates create a minimum static pressure in the vessel. This should be less than 14 psig for flows less than 1.2 lbs/sec. Again, this aspect is specific to the current facility.
- The hydrogen igniter does not fully penetrate the stream for high flow speeds. It does, however, seem to propagate across the tube by the time it reaches the step.

- There is a transition range for varying equivalence ratios such that a flame will hold strongly at a high ER, blow out at low ER, and hold with instability at median ratios.

As mentioned previously, the planned  $2^6$  factorial test matrix was not fully executed. This was due to inability to generate sufficient discrimination in turbulence levels. As a result, a sub-matrix was designed and tested that held the turbulence level constant. The basic test plan was reduced to a  $2^5$  factorial (temperature, pressure, step height, equivalence ratio, velocity), with some centerpoints.

The observed flameholding results are presented in Table E1 (Appendix E, p. E4). In the “result” column, most of the cases have a weak extinction limit listed. For these cases, flame holding was observed above or at this limit but not below this limit. Some cases do not have a weak extinction limit listed. This is due to the configuration failing to hold a flame at an equivalence ratio of less than or equal to 1.0. Since the test results revealed variation in the fuel distribution, the detailed measurements were evaluated and it was determined that the equivalence ratio near the step was approximately 70 percent of the overall equivalence ratio. As a result, a “corrected measured WE limit” is also presented in Table E1, which is simply 70 percent of the actual overall average. Table E1 also has a column for repeated measurements. These results were obtained several weeks apart with substantial tear down of the facility in between.

## **2.4.6. Flameholding Study -- Simulation & Analysis**

### **2.4.6.1. Background**

In both lean, premixed combustion and catalytic combustion systems, mixing of the fuel and air is a fundamental issue. In these systems, the ability to rapidly mix the fuel and air is critical. However, premixed fuel and air systems also present the potential for flameholding at locations of separated flow, in cavities or recesses, or in the wake behind bluff bodies. Flameholding in unintended locations can lead to component burnout or damage. This task examines flameholding within premixer passages from both a computational and experimental perspective.

Combustion Science and Engineering, Inc. was tasked by CESI to analyze the differences in two possible experimental geometries that may be used to examine the issue of flameholding in a fuel/air mixing duct. CFD models were used to model both 1-inch and 2-inch square ducts and to determine recirculation times for the region of separated flow directly downstream of the step. The recirculation time was then utilized in a previously developed analytical technique to determine if predicted recirculation zones or regions of separated flow have flameholding potential. This technique utilizes the CFD flow field predictions as inlet conditions to a Perfectly Stirred Reactor (PSR) model. The PSR model allows for the utilization of a comprehensive, chemical kinetics reaction scheme to predict the potential for flameholding.

The two proposed test sections were modeled using a commercial CFD code, STAR\*CD<sup>3</sup>. STAR\*CD is a general-purpose CFD code that uses the finite volume method. In this approach, the domain is divided into numerous discrete control volumes, or cells. STAR\*CD is capable of analyzing a wide variety of meshes, from completely structured hexahedral meshes to fully unstructured meshes. The mesh can

be composed of the usual cell types (e.g. hexahedral, prism, pyramid, and tetrahedral) as well as polyhedral cells. These cell types can exist in the mesh individually or simultaneously in any combination. For this modeling effort, only hexahedral cells were used.

The conservation equations solved in the problem (momentum, mass, energy, etc.) are discretized for each control volume. The derivatives are evaluated with reference to the cell in question and its neighbors. This results in a set of non-linear equations that are solved by iteration. The efforts required to solve these equations are influenced by the number of cells, the number of conservation equations being solved, the type of solver and the computer system being used. STAR\*CD has a number of physical and numerical modeling capabilities, which are too numerous to describe adequately in this report.

Both two-dimensional and three-dimensional models were constructed for this study. The three-dimensional models were used to determine if spanwise flow would greatly affect the recirculation time of the mixing zone. The three-dimensional models consisted of approximately 390,000 cells. The two-dimensional models used symmetry plane boundary conditions in the axial direction, which reduced the number of cells to approximately 15,000. High cell densities were used in regions of interest such as areas of flow separation. A two-layer model<sup>4</sup> was used in the wall region for better resolution and more accurate representation of the boundary layer. Turbulence was modeled using the standard k- $\epsilon$  model with and without the Chen's modification for high-shear flows<sup>5</sup>.

Identical inlet conditions were used for both the one-inch and two-inch test sections. The inlet flow velocity was 50 ft/s with a prescribed turbulent intensity of 20 percent. The pressure and temperature of the model was 9 atm and 850 °F respectively. The step height was fixed at 0.25 inches for both models. Adequate distance before and after the step was used (and proved necessary) to ensure fully-developed flow at the step and non-separated flow at the exit. The Reynolds numbers ( $Re = V \cdot D / \nu$ ) are based on the hydraulic diameter (i.e.  $2 \cdot \text{height}$ ) of the inlet, and the aspect ratio is the ratio of the outlet height to the inlet height.

#### **2.4.6.2. Analysis Results**

Accounting for the effects of scale, little difference on the flow field for either test section is seen as a function of distance from the wall, indicating that no large-scale spanwise flow movement is predicted. This is not unexpected, since k- $\epsilon$  models will not predict the vortical structure and subsequent boundary layer movement of these flows. However, experimental evidence has shown that for lower Reynolds flows (flows less than  $Re = 6600$ ) significant spanwise flow can be induced<sup>6</sup>.

Flow reattachment lengths downstream of the step were measured for both the 2-D and 3-D models. These lengths can be compared with values measured experimentally for similar flow geometries and provide an idea of the accuracy of the model. These lengths were determined by identifying the location of inflection of axial wall shear stress. Based on these distributions, non-

dimensional reattachment lengths (distance from step/step height) are shown in Table 2.4.6.2.1. Results using the standard k- $\epsilon$  model using the Chen modification are included in the table. The Chen model was developed specifically for regions of high shear and improved these predictions considerably. Without the Chen modification, reattachment lengths were approximately 25 percent shorter than those shown in Table 2.4.6.2.1.

**Table 2.4.6.2.1 -- Reattachment length using the standard k- $\epsilon$  model with Chen modification**

Section Size	Reattachment Length ( $X_r/H_s$ )	
	2-D	3-D
<b>1-inch x 1-inch</b>	6.56	6.88
<b>2-inch x 2-inch</b>	6.04	6.09

These lengths are very similar to those reported in the literature. Armaly<sup>17</sup> reports that for flows with Reynolds numbers above ~6600, the non-dimensional reattachment length is fairly constant at approximately 6.0. However, Chen and Jaw<sup>7</sup> state that the non-dimensional reattachment length is close to 7.0. Chen and Jaw also state that most standard k- $\epsilon$  models under-predict the reattachment length by at least 20 percent. The thickness of the boundary layer relative to the step height is an important concern for these models. For the 1-inch square section, the boundary layer was estimated to be approximately 15 percent of the step height, while for the 2-inch square section the boundary layer was a smaller percentage (10 percent) of the step height. Since the k- $\epsilon$  model does not handle flow in the boundary layer properly, much of the important information concerning the flow in the recirculation zone may be lost in this boundary layer thickness. This finding indicates that it is important to use the largest test section possible when experimentally obtaining comparison data in order to reduce the inherent errors of the models.

Overall, the 2-inch section predicts more significant spanwise flow behind the step than the smaller section. This may be due to the boundary layer thickness issue discussed previously. One important point to note is that experimental studies<sup>8</sup> have shown that if the expansion ratio (defined as the ratio of outlet height to inlet height) is equal or less than 1.5, turbulent flow is steady and separation is also symmetrical in a symmetric backward facing step. However, at expansion ratios greater than 1.5, the flow may become unsteady and unsymmetrical. The expansion ratios chosen for this validation should avoid these problems.

Utilizing the analytical technique developed previously for CESI, the flameholding potential of the predicted recirculation zones were analyzed. As described above, the flameholding analysis uses a comprehensive chemical kinetic mechanism and the flow characteristics of the recirculation zone. The CFD model results are used to obtain the parameters relating to the fluid mechanics. Table 2.4.6.2.2 presents the predicted recirculation time and recirculation zone volume for both the 2-D and 3-D models. The results of the flameholding analysis for both the 1-inch and 2-inch sections are shown in Figure 2.4.6.2.1. The plot contains predictions of CO and

temperature as a function of equivalence ratio using the residence time and volume of the recirculation zone shown in Table 2.4.6.2.2.

**Table 2.4.6.2.2 -- Recirculation Zone Volume and Time**

	Test Section Model	Recirculation Zone Volume (in <sup>3</sup> )	Recirculation Time (msec)
<b>1-inch x 1-inch</b>	2D	0.00957	20.097
	3D	0.13209	20.984
<b>2-inch x 2-inch</b>	2D	0.01314	20.930
	3D	0.21820	20.343

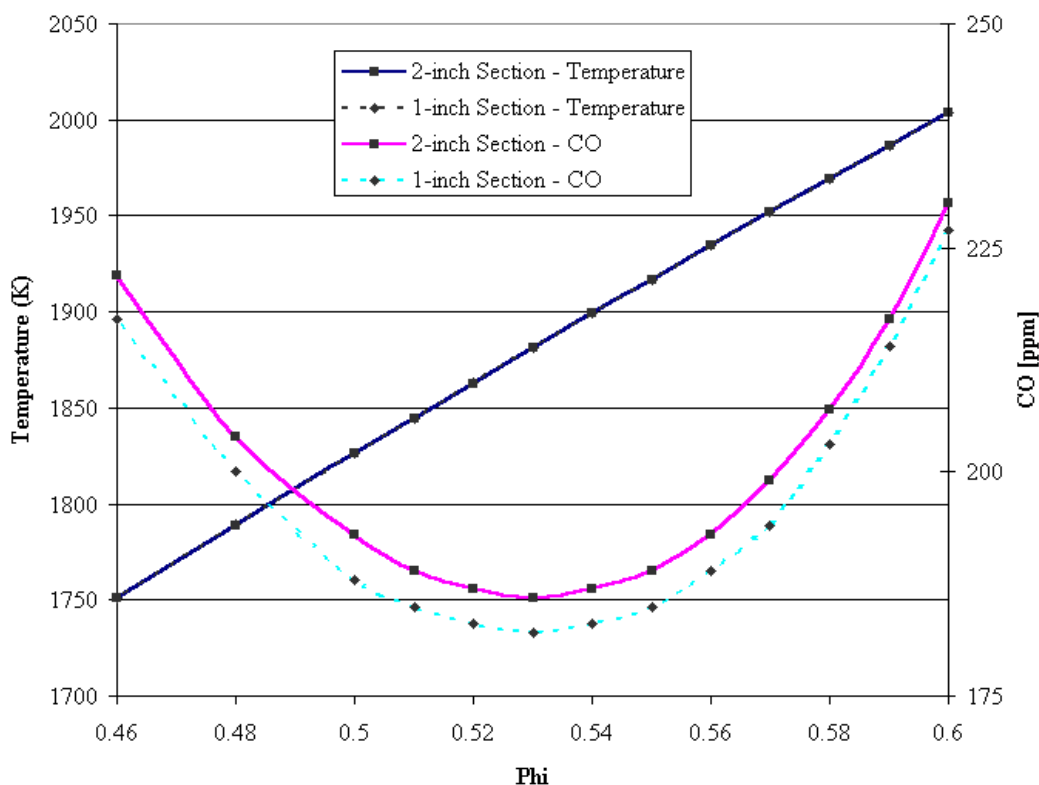


**Figure 2.4.6.2.1 -- Predictions of CO and temperature as a function of equivalence ratio using the residence time and volume of the recirculation zone**

As can be seen in the figure, very little difference in the flameholding potential is predicted for the various test section sizes. Using the flameholding criteria described above, the minimum equivalence ratio necessary for flameholding is approximately 0.485 to 0.53 for the 1-inch



section and 0.49 to 0.53 for the 2-inch section. The fairly short recirculation times raise the minimum equivalence ratio necessary for flameholding.

One-inch and 2-inch square sections containing a sudden expansion were modeled to determine the predicted differences in the flowfield and in the flameholding potential. Very little difference in the flowfield, other than the effect of scale, is predicted for these sections. Flameholding potential was also very similar for both test sections. From a modeling standpoint though, concerns about the ability of the k- $\epsilon$  model to adequately predict the recirculation zone and boundary layer velocities profiles reinforce the need for the experimental program to utilize the largest test section possible.

#### **2.4.7. Conclusions**

The key findings for this task include:

- Fuel-air measurements from cold flow testing of the initial mixer design indicated that additional development of the mixer was needed before on-engine testing could be justified. Although the original proposal specified that engine hot-testing of the new mixer would be completed, CESI and the Commission concluded that the technical and financial resources should be redirected to other program tasks.
- Additional work will be required in order that the CESI axial premixer technology can be fully developed.
- The strength of the secondary flows and turbulence levels observed in the analyses of these lobed mixer configurations suggests that they will not perform at the same level as the 3-stack mixer design.

Preliminary indications are that a greater number of lobes produce slightly better mixing. However, this result may be due to the larger number of implied fuel injection locations with an increasing number of lobes.

- The scalar mixing results suggest that a fuel injection pattern can be developed that would produce a reasonably well-mixed flow entering the catalyst. However, the results also suggest that the robustness of this design may be limited given the isolated nature of the flow cells produced by the lobes and the relatively weak secondary flow and low turbulence levels.
- The best choice for the shape of an airfoil fuel peg is the shape of an NACA0030. However, the flow area for natural gas through the fuel-peg decreases as the fuel peg thickness is decreased. As the area is decreased the gas velocity through the fuel peg increases. If the NACA0030 airfoil design would require a maximum gas velocity above 100 fps, then the NACA0033 airfoil is an acceptable compromise.
- The mixer cold flow test showed the lowest concentrations of fuel occurred at angles between 90° and 270° and directly downstream of the fuel pegs. This sector (90° to 270°) is consistent with an overall skew in the flowfield. However, the low concentrations, which match the fuel peg locations, indicate that little mixing is occurring in the circumferential direction.
- Step heights seem to have weak influence on the WE limits of a positive, flameholding case. This is seen in the similar results for the 0.125" and 0.25" step. The mechanism for

flameholding appears to exhibit a sharp transition that occurs somewhere between 0.125 and 0.0375" step expansion. Further, it is reasonable to avoid flameholding by using perturbations that are on the order of 0.0375" and less.

- Velocity and Pressure have the greatest effect on WE limits. The lack of temperature dependency is attributed to the relatively narrow range of temperatures studied.

Higher pressures, higher temperatures, and lower velocities lead to lower WE limits, though the effect of velocity was found to depend upon the pressure. In particular, velocity effects are diminished at lower pressures.

## **2.5. Catalyst Materials Development**

More details of the materials development effort are contained in Appendix V: Catalyst Materials Development.

### **2.5.1. Introduction**

One of the key material issues affecting the operability and life of a combustion catalyst is the thermal stability of the washcoat-catalyst system. The washcoat-catalyst is a porous layer of a ceramic oxide applied to the thermally conductive high-strength metal foil that serves as a support. Catalytically active metals and oxides, in our case platinum group noble metals (PGM), are dispersed within the porous washcoat layer. The thermal stability of the washcoat material is typically expressed as loss in the washcoat surface area with time at the operating temperature and conditions of the catalyst in the engine. Previous exploratory work performed at Catalytica identified several washcoat materials with substantially better thermal stability than the current formulation (Table 2.5.1.1 --- Note: "BET" stands for Brunauer, Emmett, and Teller, developers of the surface area measurement technique). The superior sintering resistance (more correctly described as coarsening resistance) of the new material is shown by its substantially higher surface area compared with CESI's standard stabilized support and a commercial non-stabilized zirconia supporting oxide after 75-hours exposure to humid air (~10-vol percent added water vapor) at elevated temperature.

**Table 2.5.1.1 -- Thermal sintering data comparing the loss in surface area of the current ceramic washcoat material with a new high thermal stability material**

<b>Catalyst Formulation</b>	<b>Catalyst Description</b>	<b>BET Area fresh (m<sup>2</sup>/g) calcined in air 1000°C</b>	<b>BET Area aged (m<sup>2</sup>/g) 10-vol percent H<sub>2</sub>O 1035°C</b>
CESI standard hot-stage catalyst	stabilized supporting oxide	41	1.9
Developmental material (CESI)	tantalum-zirconium oxide support	28	15
Zirconia reference	commercial zirconia oxide support	7	4.3

These data show that the tantala-zirconia developmental washcoat material may provide substantially improved performance for the catalyst under the operating conditions of the catalyst in a gas turbine, 900 to 1000°C with higher levels of water vapor. However, several issues need to be resolved before this material can be used in an engine combustor:

- **Commercially viable processing** - The preparation procedures for the washcoat ceramic material have only been developed for small scale (1 to 2 grams) and need to be scaled to 500 to 1000 grams to prepare enough material for detailed and large scale testing.
- **Thermal stability of catalysts** - Long term laboratory aging tests should be performed to evaluate the stability of the new washcoat material and of supported noble metal catalysts prepared with the new material.
- **Application and adhesion to foils** - There is a need to develop procedures to apply the new material to the substrate foils and to achieve the required adhesion and washcoat strength.

## **2.5.2. Approach**

The major objective of this effort was the preparation, aging, and sub-scale performance testing of combustion catalysts using the new washcoat material. The approach taken for the catalyst materials development program is detailed below:

- Evaluate new chemical approaches to the production of the developmental washcoat material and prepare test quantities of the ceramic material.
- Using the research catalyst production system at CESI's Mountain View facilities, prepare test samples of coated foil. These samples were processed in the same manner as the typical engine catalyst.
- Evaluate the test samples for cohesion and adhesion properties using the CESI developed "Abrasion Test Procedure". As needed, prepare epoxy mounted and sectioned samples for analysis by scanning electron microscope (SEM).

- Prepare test quantities of new ceramic washcoat powder that was used in the preparation of catalyst powders and pretreated in a manner similar to the target commercial catalyst foils.
- Prepare catalyst coated metal foil samples pretreated in a manner similar to the target catalyst. The metal substrate foil in this case was to be a NiCrAl superalloy.
- Age the above samples in the high-pressure aging reactor (HPAR) system at the expected conditions of operation in the gas turbine combustor.
- Remove samples periodically and characterize these samples for total washcoat surface area and specific surface area of the active catalyst component (exposed platinum group metal, PGM).
- Prepare sub-scale (50-mm diameter) catalyst systems incorporating the new ceramic support materials.
- Determine catalyst performance over the gas turbine operating conditions from start up and through the load range to full load. Compare performance of the new catalysts with the performance of the current commercial catalyst.
- Perform extended tests after establishing stable performance. These tests lasted 100 to 200 hours in duration with periodic evaluation of the catalyst “reactivity”.
- After completion of these tests, the catalyst systems were characterized by surface area measurements and SEM and the surface area data was compared with the data from the thermal aging work performed in a previous step.

### **2.5.3. New Ceramic Materials Development**

The new material was originally prepared by a sol-gel process. Sol-gel chemistry involves the slow hydrolysis of metal alkoxide reagents in very dilute alcohol solutions. Careful mixing and supercritical drying are typically required. This process limits the quantity of highly porous solid that can be prepared in a given size vessel. Several new chemical approaches that are readily adapted to larger scale processing were evaluated to obtain the desired ceramic material. The process evaluation included investigating the following:

- The effect of the hydrolysis and precipitation processes;
- The effect of H<sub>2</sub>O concentration and acid/base catalysis;
- The effect of precipitation by microfluidization; and
- The effect of drying technique.

#### **2.5.3.1. Effect of hydrolysis and precipitation processes**

Molecular-scale homogeneity of the two metal components is thought to be the primary source of the exceptional surface stability in the previously prepared Ta-Zr aerogels. Slow hydrolysis under acidic or basic conditions in dilute solutions typically produces a clear gel, while rapid hydrolysis in concentrated solutions under neutral conditions typically produces a cloudy (heterogeneous) suspension. A preliminary precipitation experiment was performed (using conditions and starting reagents similar to the aerogel preparation) to produce what was expected to be a mixed phase of the two oxide precipitates. This heterogeneous material was intended to validate the technique of producing homogeneous material by the aerogel method.

After oven drying and calcination, the precipitated Ta-Zr mixed oxide showed a homogeneous crystalline phase as determined by x-ray diffraction (XRD) analysis. It also showed a specific surface area equal to sol gel preparations that were also oven dried (xerogels) and approximately half of the best aerogel preparation. Since near homogeneity apparently was achieved with this simple precipitation technique, we investigated changes to the conditions of the precipitation method to enhance the initial surface areas of the homogeneous precipitate.

### 2.5.3.2. Precipitation by Microfluidization

Differences in relative condensation rates of the two metal alkoxides necessitate rapid mixing to create a fine-grained co-precipitate. Microfluidization introduces sub-microsecond mixing through a micro orifice. Initial experiments were conducted using a dual chamber (Microfluidics) microfluidizer designed by Catalytica's Advanced Technologies program.

The results for the precipitated Ta-Zr mixed oxide were conclusive and indicate that precipitates produced by microfluidization are superior to those precipitates produced by the drop method after 1000°C calcination. The microfluidization technique is therefore a viable alternative to slow mixing methods with the additional advantage that mixing and hydrolysis time is shortened by an order of magnitude.

### 2.5.3.3. Effect of H<sub>2</sub>O concentration and acid/base catalysis

Reaction parameters such as water concentration, acid and base catalysts were manipulated to explore the effect of these parameters on surface area stability. Table 2.5.3.3.1 lists the results from this study.

**Table 2.5.3.3.1 -- Effect of hydrolysis stoichiometry and acid or base addition on the preparation of precipitated Ta-Zr oxide powders**

Run #	H <sub>2</sub> O X stoich.	μL conc. HNO <sub>3</sub>	μL conc. NH <sub>4</sub> OH	SA 1000°C (M <sup>2</sup> /g)	SA 1035°C in steam (M <sup>2</sup> /g)
1020-105-1	10	-	-	20	10.2
1020-105-2	10	375	-	12	5
1020-105-3	10	-	375	13	-
1020-105-4	3	-	375	20	-
1020-105-5	5	-	-	12	-
1020-105-6	20	-	-	20	-
Aero gel std.	3	375	-	28	15
Xerogel	3	375	-	12.4	6.7

The total specific BET (N<sub>2</sub>) surface area measurements for the precipitates (runs 1020-105-1 through 1020-105-6) following calcination in ambient air at 1000°C and humid air at 1035°C lead to the following conclusions:

The water adjustment had the biggest effect on resulting surface area.

Neither acid nor base catalysis is necessary.

The best precipitated materials maintained surface areas within 25 percent of the measured surface area of the aerogel catalyst.

- The high surface area precipitates exceeded the surface area measured for xerogels after 1000°C calcination (previously, xerogels have been shown to be homogeneous by XRD).

#### 2.5.3.4. Effect of drying technique

The method used to remove the solvent from the precipitate could be a factor in stabilizing the initial surface area. Reducing the amount of surface tension and partial pressure in the interstitial pores can help to maintain the integrity of these pores and increase the surface area of the dried powder. Vacuum drying and supercritical drying (SCD) could help to maintain surface area. Two drying experiments were performed to assess the effectiveness of these techniques.

Upon completion of the two drying experiments, 2-gram samples of each of the white powders were calcined at 1000°C for 10-hrs. The resulting crystalline solid powders were submitted for total surface area analysis by BET (N<sub>2</sub>) physisorption (Table 2.5.3.4.1). The supercritically dried material was additionally calcined at 1035°C in humid air (10-vol percent H<sub>2</sub>O) for an additional 75-hrs.

**Table 2.5.3.4.1 -- BET Surface area results for dried Ta-Zr oxide materials**

<b>Dried Sample</b>	<b>1000°C/10-hrs with ambient air</b>	<b>1035°C/75-hrs with 10 percent H<sub>2</sub>O</b>
	<b>SA</b>	<b>SA</b>
<b>Vacuum dried 886-147-1</b>	21 m <sup>2</sup> /g	---
<b>Supercritically dried 886-147-2</b>	26 m <sup>2</sup> /g	13.5 m <sup>2</sup> /g

The results show that the drying step does play a role in producing materials with relatively high initial surface areas. The supercritically dried material after calcination at 1000°C has a surface area that is at least 25 percent greater than oven or vacuum dried material. The results for the supercritically dried powder after 1035°C calcination in humid air are comparable to our best aerogel material with similar composition.

Based on the results from the processing evaluation studies, the microfluidized, supercritically drying preparation technique was selected for production of a large batch of the new washcoat material to be used in subsequent sub-scale testing.

#### **2.5.4. Thermal Stability Testing of New Catalyst Materials**

The thermal stability of catalysts is a critical property that governs the useful life of a combustion catalyst module in operation. CESI has developed a system of four high pressure, high temperature, isothermal reactors (Figure 2.5.4.1) that expose catalytic foils, washcoat powders, and component powdered materials to a simulated combustion environment. The environment within the vessel reproduces the typical gas composition, including oxygen, water vapor, and even trace sulfur oxide present within the washcoat of a gas turbine catalyst module. The differences between the simulated and engine environment, i.e., the lower gas flow rate and the lack of thermal gradients caused by combustion of fuel, are not considered significant. Samples of catalysts used in engine tests (2900-hr) have specific surface areas and specific amounts of exposed noble metal (the active component in combustion catalysts) that follow the values expected from the High Pressure Aging Reactor (HPAR) tests. These reactors were used to examine the thermal stability of the new Ta-Zr oxide washcoat materials. Table 2.5.4.1 shows the HPAR test matrix for the thermal stability testing.

Two separate tests were performed under two different temperatures, 900°C and 975°C both at a pressure of 10 atmospheres. The catalyst powders were loaded into ceramic crucibles for ease of sampling and placed in the HPAR. After each time interval, the crucibles were removed from the reactor, and a portion of the catalytic material was removed for analysis. The portions (~1-gm each) of each powder were characterized at progressive intervals from 4 to 8000 hours for the 900°C run and from 30 to 4000 hours for the 975°C run. The specific BET (N<sub>2</sub>) surface area and the amounts of active PGM (via H<sub>2</sub> titration following reduction) were measured for each sample as shown in the following table and figures.

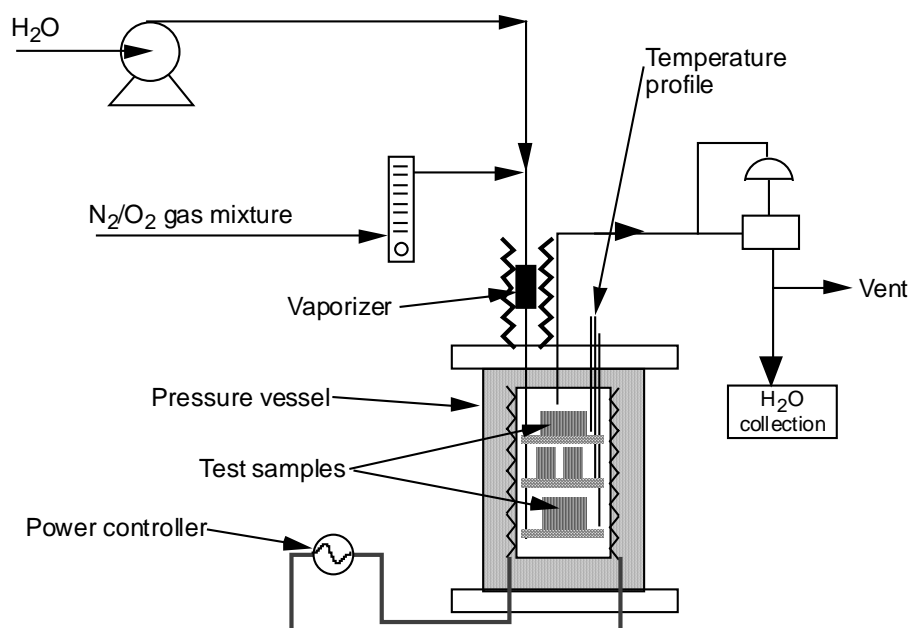


**Figure 2.5.4.1 -- High Pressure Thermal Aging Facility that reproduces the pressure, gas phase composition and temperature of the actual gas turbine combustor**

**Table 2.5.4.1 -- Catalysts tested in HPAR experiments at 900°C and 975°C**

<b>Washcoat material</b>	<b>Catalyst form</b>	<b>Final calcination temperature, time</b>	<b>HPAR temp 900°C</b>	<b>HPAR temp 975°C</b>
Std supporting oxide	powder	1000°C, 10 hours	X	X
Std supporting oxide	monolith	950°C, 10 hours	X	X
Ta-Zr oxide	powder	1000°C, 10 hours	X	X
Ta-Zr oxide	monolith	1000°C, 10 hours		X



#### 2.5.4.1. 900°C HPAR results

The results for 900°C HPAR tests (Table 2.5.4.1.1) show that catalysts prepared from the new Ta-Zr oxide initially had lower specific BET surface area than the CESI standard washcoat materials. But compared with our current washcoat material (Figure F1 in Appendix F) they show superior surface area after aging for 1000 hours under simulated combustion conditions. This result is in agreement with previous results for high temperature calcination of Ta-Zr oxide powders in air and humid (10-vol percent H<sub>2</sub>O) air. The current result simply shows that the additional of PGM in the prepared catalyst does not change the improved stability of the new supporting oxide material.

Unfortunately the new washcoat oxide does not stabilize the active noble metal phase relative to our current washcoat material (Figure F2). After 8000-h aging under simulated combustion conditions at 900°C, the active component areas for the catalyst powder prepared using the new supporting oxide is almost the same as the catalysts prepared from the current material.

**Table 2.5.4.1.1 -- Normalized results of the analysis for total (BET) surface area and exposed metal content for the 900°C HPAR aged catalysts.**

Catalyst Description	Parameter	Aging Time (h)								
		4	20	62	318	1000	2000	4000	6000	8000
CESI std powder	BET SA (m <sup>2</sup> /gm)	22.7	21	19	12.7	8.4	7	6	5	4.4
	Exposed metal (μmol_PGM/gm)	12.7	11	10	6.6	4.9	2.7	1.6	1.2	2.1
CESI std monolith	BET SA (m <sup>2</sup> /gm)	17.4	16	14.4	10.2	6.1	5.5	4.9	4.7	4.4
	Exposed metal (μmol_PGM/gm)	8	7.7	7.1	6.2	4.3	1.9	1.3	1	0.7
Ta-Zr oxide powder	BET SA (m <sup>2</sup> /gm)	--	14.3	--	9.1	8.5	7.4	7.1	--	--
	Exposed metal (μmol_PGM/gm)	--	5.4	--	1.7	1.4	1.1	0.7	--	--

#### 2.5.4.2. 975°C HPAR results

The results for the 975°C HPAR tests (Table 2.5.4.2.1) show very similar trends as the 900°C results. Catalysts prepared from the new Ta-Zr oxide washcoat again show lower specific BET surface area initially, but begin to show superior surface area after aging only 1000-h under simulated combustion conditions compared with our current washcoat material (Figure F3). As in the case with 900°C test results, the new washcoat supporting oxide does not stabilize the active noble metal phase relative to our current washcoat material (Figure F4). After 4000-h aging under simulated combustion conditions, the active component areas for the catalyst powder prepared using the new supporting oxide are almost the same as the catalysts prepared from the current material.

Table 2.5.4.2.1 -- Total (BET) surface area analysis for the 975°C experiment

Sample time (hours)	Type C3a (m <sup>2</sup> /g)	Type C3b (m <sup>2</sup> /g)	Type C3c (m <sup>2</sup> /g)	Type C3d (m <sup>2</sup> /g)	Type D2a (m <sup>2</sup> /g)	Type D2b (m <sup>2</sup> /g)	Type D1b (m <sup>2</sup> /g)	Type D3a (m <sup>2</sup> /g)	Type D3b (m <sup>2</sup> /g)
1	1.00	1.00	1.00	1.00	1.00	1.00	1.00	1.00	1.00
30	0.60	0.56	0.51	0.53	0.30	0.36	0.62	0.83	0.72
100	0.32	0.28	0.24	0.29	0.16	0.19	0.52	0.74	0.60
300	0.20	0.18	0.20	0.19	0.10	0.12	0.44	0.57	0.49
1000	0.13	0.13	0.11	0.14	0.07	0.09	0.35	0.33	0.38
2000	0.10	0.11	0.10	0.10	0.06	0.07	0.32	0.24	0.35
4000	0.07	0.07	0.09	0.09	0.05	0.00	0.28	0.15	0.31

#### 2.5.5. Catalyst Performance Testing

Since the catalyst in the Xonon® technology operates adiabatically and the flow is restricted to small channels, the performance of a small diameter plug (e.g., 2-in.) of catalyst fully simulates the operation of the full-scale (e.g., 16-in) system. Therefore CESI's sub-scale catalyst test facility (Figure 2.5.5.1) reproduces the conditions of pressure, temperature, gas composition, and air flow present in a commercial gas turbine combustor. For the catalyst performance tests, a 2-inch (50mm) diameter catalyst is assembled and installed in the test section. An air compressor and the electric air heater reproduce the temperature, pressure and flow conditions representative of air entering the combustor from a gas turbine compressor. The catalyst is then tested under the cycle conditions that represent the expected operating conditions of a particular gas turbine.

Catalysts prepared as described above using the new ceramic washcoat material were tested under the conditions expected in the Kawasaki M1A-13X gas turbine using the catalyst test facility.

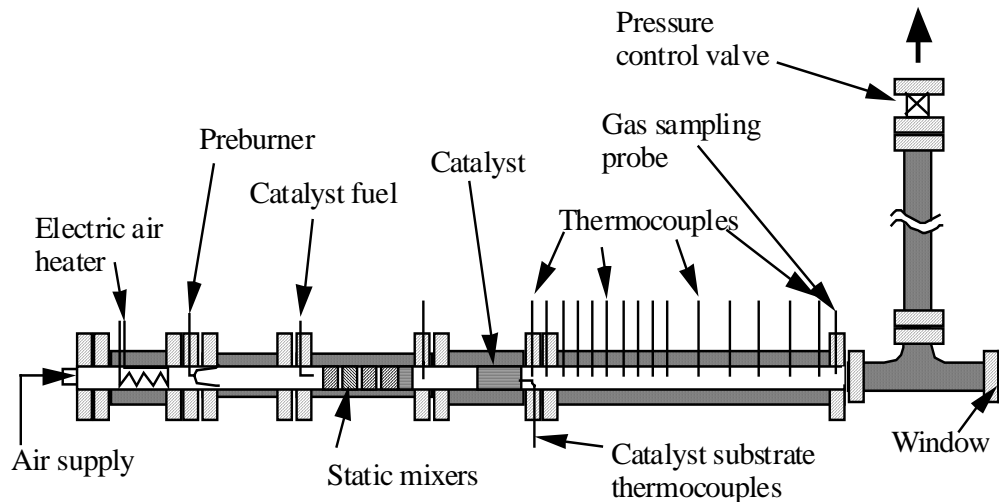


**Figure 2.5.5.1 -- Catalytic combustion test facility schematic design. Two such high pressure rigs are available at CESI's Mountain View facility.**

The monolith parameters targeted for preparation were those used for the second stage of the Kawasaki M1A-13X catalyst system. The new washcoat powders were prepared and applied to the foils as described above in Section 2.5.3. The final washcoat loading was 6.74 mg/cm<sup>2</sup> foil surface area. A standard first stage catalyst, an early design for the Kawasaki M1A-13X catalyst module, was used in series (upstream) of the new monolith for all tests. Both stages were instrumented with thermocouples, rolled to 2" diameter, and installed into the subscale test facility for investigation of performance and short-term durability.

Light-off tests were performed to determine initial light-off temperatures (LOT) for both stages. This test was followed by a 300-hour durability test of catalyst performance at Kawasaki M1A-13X turbine full-load conditions. Periodic light-off tests were performed to track catalyst activity as a function of reciprocal temperature versus time. Table 2.5.5.1 displays the conditions for each type of test. Figure 2.5.5.2 shows the light-off test results for the stage 2 catalytic monolith prepared using the new Ta-Zr mixed oxide material (labeled as *Ta-ZrO<sub>2</sub> catalyst '98*). The current system was identical to the monolith system previously tested in 1995 using sol-gel derived Ta-Zr oxide research materials as a support in stage 2 (labeled as *Ta-ZrO<sub>2</sub> catalyst '95*). Also included in the figure are test results for a catalyst prepared using the current commercial support (labeled as *baseline catalyst '98*) and the corresponding previous baseline catalyst (labeled as *baseline catalyst '95*). The figure clearly shows that the initial and short-term performance of catalyst prepared using the new Ta-Zr supporting oxides are superior to those of the current commercial materials.

**Table 2.5.5.1 -- Catalyst performance and short-term durability test conditions**

Inlet temperature ramp-up(light-off temperature) tests		Steady-state tests	
Air flow/SLPM	4210	Air flow/SLPM	4210
Pressure/atm	9.4	Pressure/atm	9.4
Inlet temperature (°C)	300-600	Inlet temperature (°C)	400
Tad/(°C)	1000	Tad/(°C)	1350

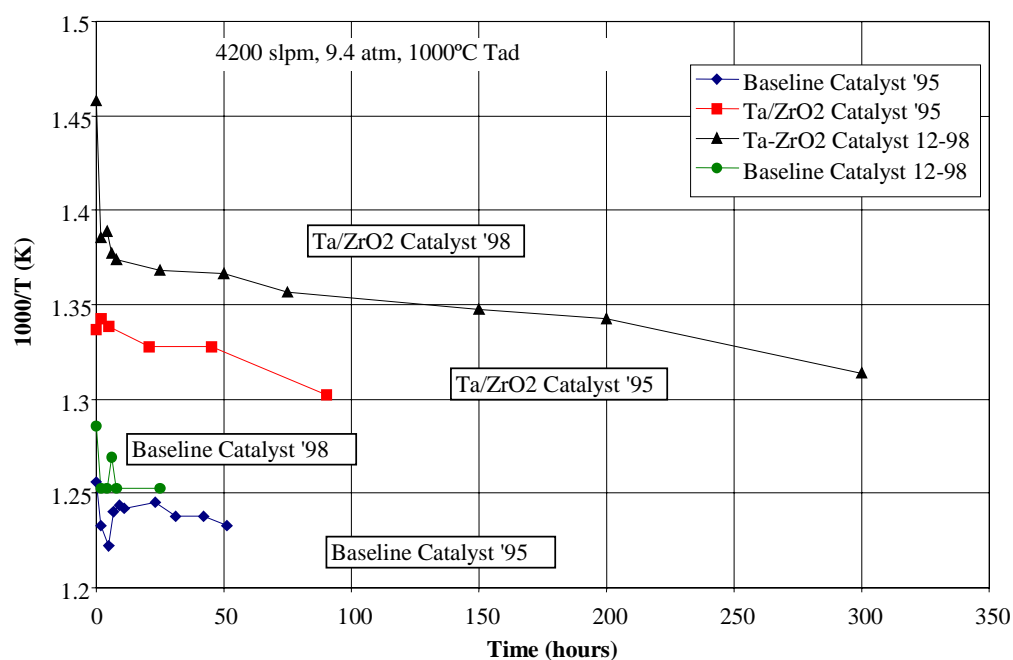


**Figure 2.5.5.2 -- Sub-scale catalyst performance (light-off) test results**

The inlet and outlet gas temperatures and the corresponding fuel conversion data for the durability test with the new Ta-Zr oxide catalyst and the corresponding baseline catalyst (Figure 2.5.5.3) show that the new material is more stable over a few hundred hours operation. This result is perhaps attributable to the greater initial activity of the Ta-Zr oxide supported catalyst.

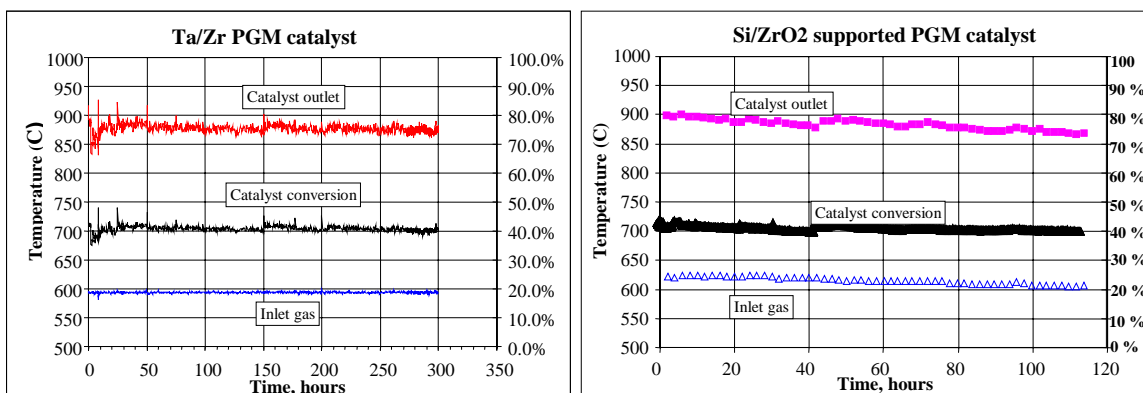


**Figure 2.5.5.3 -- Results of sub-scale short-term durability tests**

Subsequent to the durability tests, a section of the Ta-Zr oxide supported catalytic monolith foil was cut into inlet and outlet halves and scraped to remove the catalyst material. A fresh piece of monolith foil was saved before testing and scraped for comparison with the sample taken after aging. The scraped samples were analyzed for BET total surface area via N<sub>2</sub> physisorption and by titration of reduced metal surface using hydrogen chemisorption (Table 2.5.5.2). Included in Table 2.5.5.2 are results from a baseline monolith catalyst aged in the pressurized aging furnace (HPAR) at 900°C as well as the HPAR results for the new Ta-Zr oxide based catalyst as described in Section III.

**Table 2.5.5.2 --Characterization of fresh and aged catalysts**

Catalyst sample & reference number	BET total surface area (m <sup>2</sup> /g)	H <sub>2</sub> Chemisorption reference number (μmol surface PGM/g)
Ta-Zr oxide (no metal), 1000°C/10-hrs 886-149-1	26.4	-
Ta-Zr oxide catalyst fresh 1020-021-B	16.3	15
Ta-Zr oxide catalyst aged inlet half 1020-021-IB300	13.6	12.8
Ta-Zr oxide catalyst aged outlet half 1020-021-OB300	12.5	13.9
Baseline catalyst fresh 886-141-D	17.4	18.5
Baseline catalyst HPAR aged 300-hrs 886-141-D300	10.2	11.5

The physical conditions of the HPAR aging test mimic the conditions used during the sub-scale durability tests with the exception of a much lower flow rate and the absence of heat release by oxidation of the fuel. The specific surface areas of the Ta-Zr oxide supported catalyst both total and reduced metal (the active component) initially were moderately lower (~10 percent) than the baseline catalyst, but showed moderately superior (~10 percent) values after 300-h aging in sub-scale tests and in the HPAR reactor. This confirms the greater short-term stability of catalysts prepared with the new supporting oxide seen in the sub-scale tests.

#### **2.5.6. Production of Engine Catalyst**

The data from the sub-scale testing allowed us to assess the level of improved performance from the new catalyst materials. The sub-scale tests through 300-h showed the superior initial performance and the superior short-term stability of the new materials. The 8000-h stability of the total surface area in the presence of the metal and under commercially relevant conditions was also encouraging. These promising results were encouraging, but not sufficient to show a milestone improvement. The long-term performance of the catalyst, based on the stability of the active metal surface dispersed by new supporting oxide, was found not to be superior to that of the commercial baseline catalyst after 8000 hours at 900°C and 4000 hours at 950°C. The stability of the supporting oxide apparently is not sufficient to prevent the loss of surface area of the active metal. Based on the long-term performance a full engine catalyst was not warranted. This catalyst system was not incorporated into the RAMD testing program.

#### **2.5.7. Conclusions**

The key findings for this task include:

- After a preliminary evaluation of co-precipitation processing, the most important steps in the preparation of mixed Ta-Zr oxide powders were identified as mixing and drying.
- Precipitation of the Ta-Zr mixed oxide was found to be a viable and more commercially attractive process than sol gel methods. The use of a dual chamber sonic jet mixer combined with commercial batch CO<sub>2</sub> supercritical drying of centrifuged precipitates produced materials equivalent to those prepared using sol-gel approaches.
- Catalytic monolith tests using the precipitated powders verified earlier results which showed that catalytic monoliths prepared using Ta-Zr mixed oxide as a support exhibit superior light-off performance even after 300 hours of sub-scale testing under conditions simulating turbine combustion under full load conditions.
- Catalysts prepared with the new Ta-Zr oxide showed greater short-term (300-h) stability for the active metal surface area than the current formulation. The activity of the catalysts prepared with the new oxide was about twice that of those prepared current baseline supporting oxide when normalized by reduced metal surface area measurements. An investigation into the enhancement of specific combustion activity by the Ta-Zr oxide supported catalyst is an interesting finding, but it was not investigated further.
- Unfortunately the stability of the active metal surface area was not sustained for 8000-hours at 900°C and 4000-hours at 950°C. Therefore, full-scale testing with the new more expensive supporting oxide material was not justified.

- Since the completion of this task, subsequent investigations of the long-term aging of supported metal catalyst have also shown that the stability of the ceramic dispersing oxide is not sufficient to insure stability of the active metal component.

## **2.6. Fuel Variability Study**

A more extensive description of this study is in Appendix VI: Variability in Natural Gas Fuel Composition and Its Effects on the Performance of Catalytic Combustion Systems.

### **2.6.1. Introduction**

Natural gas is composed primarily of methane with small amounts of higher hydrocarbons and diluents, which vary by region and over time. Compositions of natural gas from domestic and worldwide sources were surveyed with respect to content of higher hydrocarbons and diluents. The survey showed slight compositional variability between most of the gases, with a small fraction of them containing significantly larger contents of higher hydrocarbons than the mean. As gas-fired turbines will be used for power generation all over the world, they will need to tolerate operation with fuels with a wide variety of compositions, particularly with respect to the concentration of higher hydrocarbons and diluents. Subscale catalytic combustion modules typical of those used in gas turbine power generation with ultra low emissions of pollutants were tested in a subscale test system with natural gas alone and with added known levels of hydrocarbon compounds and diluents. The range of compositions tested contained the range observed in the survey. Test results were used to calculate the effect of composition on catalyst performance. The compositional variability is of little consequence to the catalyst for most of the gases in the survey, including nearly all of the gases delivered in the U.S. To accommodate the remaining gases, the catalyst inlet temperature must be lowered to maintain combustor durability. These results support commercial acceptance of catalytic combustion systems for use in gas natural gas fired turbines in distributed power generation with ultra low NO<sub>x</sub> emissions.

### **2.6.2. Approach**

The approach to this project involved two primary tasks: 1) Surveying the range of natural gas compositions that are encountered in the United States and worldwide. 2) Taking a catalyst system with proven performance with domestic pipeline natural gas and testing it over the composition range obtained in the survey to observe the effects of varying natural gas composition, specifically higher hydrocarbons and diluents, on the performance of the system. The information obtained in this program has been used to adapt catalytic combustion systems to accommodate the observed range of compositions.

### **2.6.3. Modification of CESI test facilities**

The current high-pressure test facility takes natural gas from the Pacific Gas and Electric distribution pipeline and compresses this gas to pressures as high as 500 psig for metering to the catalyst test system. At the start of the project, no provision was available to feed hydrocarbon mixtures or to inject low concentrations of liquid fuels. The goal of this effort was the design and installation of a fuel feed and mixing system to permit the doping of the current natural gas fuel with low levels of higher hydrocarbons. It was necessary to feed propane and higher hydrocarbons up to dodecane (C<sub>12</sub> - kerosene used as a surrogate) and mix these with the

natural gas fuel. Concentration levels were up to 8 vol percent for propane. Typical concentrations of the minor fuel constituents for natural gas sources in the United States are also shown in Table 2.6.3.1, and include values for regions that mix in propane during periods of high demand, or peakshaving. C3 refers to additional propane injected by supplier typical of propane peak shaving processes

**Table 2.6.3.1 -- Composition Variability of Natural Gases in the United States**

<b>Concentration mole percent</b>	<b>Methane</b>	<b>Ethane</b>	<b>Propane</b>	<b>Propane +C3 *</b>	<b>Hexanes</b>
<b>Mean</b>	93.9	3.2	0.7	0.7	0.1
<b>Minimum</b>	74.5	0.5	0	0	0
<b>Maximum</b>	98.1	13.3	2.6	23.7	0.4

#### **2.6.4. Natural Gas Variability Parametric Tests**

The testing approach was to use pipeline natural gas and dope this relatively clean natural gas as needed for the parametric tests. In addition, this pipeline natural gas can be “cleaned-up” using activated carbon adsorption beds to produce a relatively pure methane for selected tests and for tests at relatively low levels of additive species. To minimize the complexity of the doping system, multiple species could be procured in a single bottle using either methane as the carrier or some large concentration dopant such as carbon dioxide. In this manner, a group of higher hydrocarbon compounds can be added at one time. The work reported here, however, tested dopants one at a time. The parametric tests studied the composition variations with the following dopants:

- Natural Gas & Higher Hydrocarbon Mixtures
  - Propane up to eight percent
  - Hexanes up to four percent
  - Dodecane (kerosene as surrogate) up to 1 percent
- Diluent Components
  - CO<sub>2</sub>, N<sub>2</sub>
- Trace Liquids
  - Vaporized kerosene

Natural gas composition data was obtained from several reports and from sampling data in Tulsa, OK and Milpitas, CA.<sup>9,10,11,12,13,14</sup> The listings contained the concentrations of methane, ethane, propane, butanes, pentanes, hexanes+, CO<sub>2</sub> and nitrogen in the gas. Heating values and specific gravities were calculated from the gas composition. Figure 2.6.4.1 summarizes the overall data in a plot of cumulative distribution functions of maximum and mean higher heating values (HHV) of natural gas delivered to U.S. cities, in U.S. pipelines, and in pipelines outside the U.S. Each point represents the fraction of cities/pipelines that have gas with a lower HHV.



- Most of the available gas has an HHV between 1010 and 1060 Btu/scf, consisting of primarily methane with small amounts of higher hydrocarbons (mostly ethane and propane) and diluents. Gas with HHV lower than 1010 Btu/scf generally has higher diluent content, and gas with HHV higher than 1060 Btu/scf has larger amounts of higher hydrocarbons. From the figure, it is evident that natural gas delivered to U.S. cities is more uniform than the gas flowing in pipelines. Foreign pipeline gas generally tends toward higher HHV than U.S. pipeline gas.

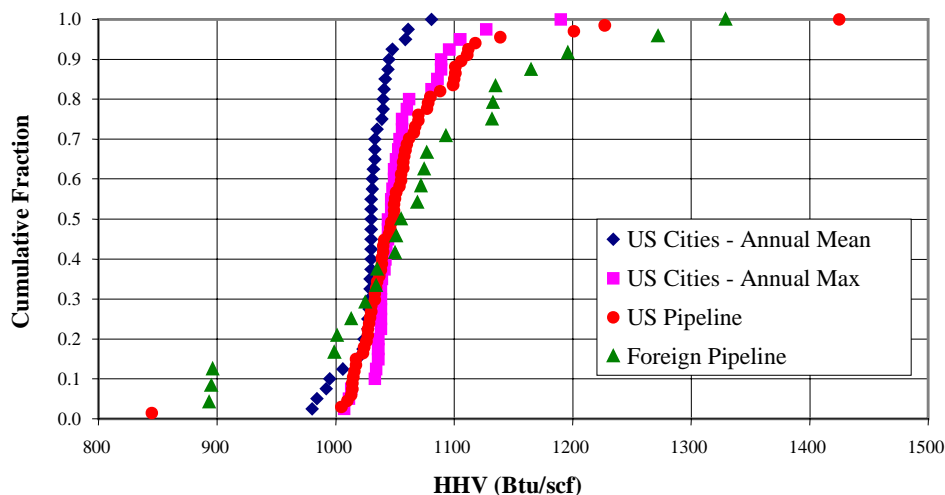


Figure 2.6.4.1 -- Heating Value Distributions

#### 2.6.4.1. Testing Procedures

Ambient air and pipeline natural gas are compressed separately to 500 psig. Flow of each stream and the reactor pressure are automatically controlled. The catalyst inlet temperature is controlled with an electric resistance heater. In line static mixers are used to provide uniform temperature and fuel concentration profiles at the catalyst inlet. The feed stream is sampled and analyzed to confirm the fuel concentration. Catalyst wall, interstage, and downstream temperatures are monitored with S-type thermocouples. The effluent is sampled 25 ms downstream of the catalyst exit face and analyzed for CO, unburned hydrocarbons, oxygen, and NO<sub>x</sub>.

Tests were run at constant adiabatic temperature. When the catalyst inlet temperature was changed, the fuel flow was adjusted to keep the temperature in the postcatalytic zone constant. Other tests were run at constant catalyst inlet temperature, while varying the adiabatic temperature by adjusting the fuel flow. Typically, inlet temperature or fuel flow was increased until the durability limit was reached, then decreased until the emissions limit was reached.

Propane, hexane, and kerosene were delivered with a syringe pump. Carbon dioxide was delivered from cylinders via the alternate gas delivery system. Dopant flows were adjusted in each run to maintain a constant percentage in the fuel.

Each series of runs with a particular dopant included a baseline with natural gas alone. Runs were performed with increasing amounts of dopant until the operating window shifted by

more than 20 °C. Runs were performed at 10 and 20 atm pressure, typical of the pressures in gas turbines that are targeted for the distributed power generation market. Catalyst inlet temperatures were varied between 350 °C and 550 °C, within the range of temperatures that can be achieved with a low-NO<sub>x</sub> generating preburner upstream of a catalyst in a gas turbine combustor. The catalyst inlet face velocity (13 m/s at 450 °C) reflects current practice.

#### 2.6.4.2. Test Results

Operating windows were measured at 10 and 20 atm pressure. The pressures were chosen to cover the expected range of compression ratios of turbines that will serve the distributed generation market. The airflow rate was chosen to deliver 13 m/s velocity calculated at a catalyst inlet face temperature of 450°C. This velocity was chosen to be typical of Xonon® applications. Windows were measured at two adiabatic combustion temperatures ( $T_{ad}$ ), 1200°C and 1300°C, varying the inlet temperature to find the emissions and durability limits. A window measurement was also done at a fixed inlet temperature, varying  $T_{ad}$  by adjusting the fuel/air ratio. These measurements were done for natural gas alone, for each concentration of dopant, and for 99.97 percent pure methane.

An example of a natural gas-only operating window is shown in Fig. 2.6.4.2.1, showing the emissions (lower) limit and durability (upper) limit of the catalyst operating window. The plot shows the catalyst inlet temperature vs. burnout or adiabatic combustion temperature ( $T_{ad}$ ). With any combination of catalyst inlet and burnout temperature at the emissions design limit, the catalyst converts just enough gas to achieve homogeneous combustion downstream of the catalyst such that the emissions targets on CO and unburned hydrocarbons are met at the turbine exhaust. Similarly, at the durability limit, the catalyst is stressed such that its expected life is reduced below the required target. Some factors associated with combustor durability are oxidation of metal parts and catalyst life.

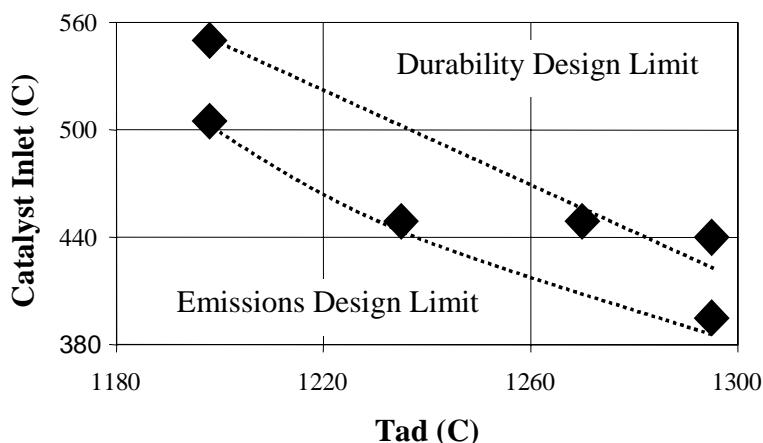


**Figure 2.6.4.2.1 -- Baseline Operating Window**

When hydrocarbon dopants are added, the reactivity downstream of the catalyst increases such that the emissions design limit is reached at a lower catalyst inlet temperature than in the undoped case. The reactivity within the catalyst also increases such that the durability design limit is also reached at a lower catalyst inlet temperature than in the undoped case. These effects

are shown schematically in Figures G1 and G2 in Appendix G. Figure G3 shows the decrease in catalyst inlet temperature at the durability and emissions design limits with increasing hexane content for 10 atm pressure and 1300 °C T<sub>ad</sub>.

The base composition of the natural gas was presumed to be that of the 1991/92 annual average from PG&E (Table 2.6.4.2.1). The gas used in tests did not vary significantly in composition from this base.

**Table 2.6.4.2.1 -- Milpitas Mixer Annual Average Gas Composition (1991-1992)**

<b>Component</b>	<b>Volume percent</b>
Methane	95.9
Ethane	2.05
Propane	0.1
i-Butane	0.01
n-Butane	0.02
i-Pentane	0.01
n-Pentane	0
C6+	0.01
HHV (Btu/scf), dry	1013
Specific Gravity	0.57

For higher hydrocarbon (C<sub>2</sub>+) contents in excess of that in the base gas, the catalyst inlet temperature at the durability limit was observed to shift downward. The higher the carbon number in the component, the larger the shift. Using this correlation, shifts in the durability limit were calculated for the gases shown in Figure 2.6.4.2.2. The cumulative distribution functions of these shifts are shown in Figure 2.6.4.2.2. Natural gas compositions to the left of the limit line would operate without difficulty. Natural gas compositions on the right side of the limit line would require a lower catalyst inlet temperature.

Negative (upward) shifts relative to the base gas are calculated for the gases that are essentially pure methane, but the shift is less than 5 degrees. The methane-only rig test also showed such a minor upward shift. The majority of the gases surveyed, particularly in the U.S. (97 percent of the annual averages sampled), had higher hydrocarbon contents low enough to yield shifts that were within the 20 °C limit. However, a number of gases in the survey had sufficient content of higher hydrocarbons to yield shifts greater than 20 °C. For these gases, the catalyst can and does convert the gas without driving the catalyst outside of its preferred operating window. Provisions must be made, however, for lowering the catalyst inlet temperature with increasing

content of higher hydrocarbons, thus maintaining the durability of the catalytic combustor without sacrificing emissions performance.

Testing with CO<sub>2</sub> showed no appreciable shift in operating window at concentrations up to 25 vol percent in the fuel (Wobbe number of 750). This shows that the catalyst itself is insensitive to the presence of inerts at these concentrations in the fuel.

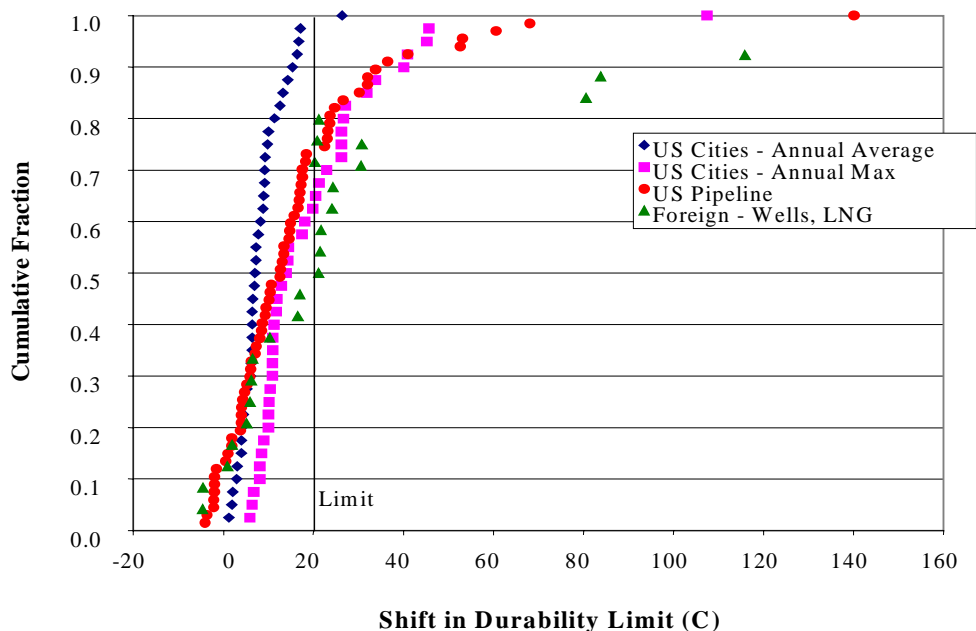


**Figure 2.6.4.2.2 -- Durability Limit Shift Distribution of Surveyed Gases**

The addition of higher hydrocarbons increases the gas phase reactivity of the fuel mixture, bringing the homogeneous combustion front closer to the catalyst outlet face for a given outlet gas temperature and  $T_{ad}$  (see Figure G4). Therefore, the emissions limit is reached at lower catalyst inlet temperature, and the operating window bottom is lowered. At a fixed catalyst inlet temperature, addition of higher hydrocarbons to the fuel increases the reactivity on the catalyst, increasing the outlet stage wall temperature (see Figure G5). Therefore, the durability limit is also reached at lower catalyst inlet temperature, lowering the operating window top. An example of the operating window shift is shown in Figure G6 for 2 vol percent hexane doping.

The effect of 8 vol percent propane doping was similar to 2 vol percent hexane doping (Figure G7), but represents twice the heat content, so propane has less of an effect on both a volume percent and heat content basis. The shift with 1 vol percent dodecane doping (kerosene as surrogate) had a greater effect than 2 vol percent hexane doping (Figure G8), even though the heating content was the same, so kerosene has a greater effect than hexane on both a volume percent and heating value basis.

CO<sub>2</sub> had no effect on burnout, and practically no effect on catalyst reactivity, so there was less than a 20 °C shift in operating window at all percentages tested, up to 25 vol percent (Figure G9).

Table 2.6.4.2.2 summarizes the limits at which the 20 °C shift was observed in all of the experiments, and the average of three experiments for each pressure and dopant. When the 20 °C shift limit is not obtained, the highest tested value is listed (designated by a + symbol). It is evident that the limits are tighter with increasing carbon number and at higher pressures.

**Table 2.6.4.2.2 -- Maximum Allowable Dopant Levels**

<b>Pressure</b>	<b>Type</b>	<b>1300C Tad</b>	<b>1200C Tad</b>	<b>450C Tph</b>	<b>Average</b>
<b>10 atm</b>	Hexane	1.7	1	1.3	1.3 v percent C6
	Kerosene	0.6	0.5	0.5	0.5 v percent C12
	Propane	8.0+	8	5.4	7.1 v percent C3
	CO <sub>2</sub>	25+	25+	25+	25+ v percent CO <sub>2</sub>
<b>20 atm</b>	Hexane	1.2	1.4	0.6	1.1 v percent C6
	Kerosene	0.2	0.5	0.2	0.3 v percent C12
	Propane	6	8.0+	5.3	6.4 v percent C3
	CO <sub>2</sub>	15+	15+	15+	15+ v percent CO <sub>2</sub>

### **2.6.5. Conclusions**

When hydrocarbon dopants are added, the key findings for this task include:

- The reactivity of the gas-phase mixture downstream of the catalyst increases such that the emissions design limit is reached at a lower catalyst inlet temperature than in the undoped case.
- The durability design limit is also reached at a lower catalyst inlet temperature than in the undoped case.
- Since the addition of hydrocarbon dopants increases reactivity, the homogeneous combustion front moves closer to the catalyst outlet face for a given outlet gas temperature.

### 3.0 Project Outcomes

#### 3.1. Technical Outcomes

CESI has successfully completed the development efforts to improve the performance and reliability of selected catalytic combustion technologies and the Xonon® combustion system. The extent to which the project technical objectives were met will be discussed, in detail, in the Technical Discussion section (Section III) of this report. This section includes brief summaries of specific technical results.

***1) Demonstrate the catalytic combustion technology and the Xonon® combustor to a reliability of 98 percent and availability of 96 percent***

The performance of the Xonon® system averaged over 8,128 operating hours is summarized in Table 3.1.1. The program exceeded the goal for reliability (goal – 98 percent) and fell short on availability (goal – 96 percent). The lower availability value is primarily due to a higher than anticipated accumulation of reserve shutdown hours (RSH). The program plan, depicted graphically in Figure 1.1.2.1, was to achieve 8,000+ hours of continuous operation while inserting design improvements “on the fly” along the way. In some instances the RAMD operation was interrupted in order to conduct engine tests of potential hardware or software improvements (e.g., controls algorithms), so the 8,128 RAMD operating hours were accumulated over the course of two years and four combustor builds. Additionally, some key components were replaced to improve durability and performance. Based on the data collected that validate our model projections, the final combustor configuration can achieve the 8,000 hour life goal.

**Table 3.1.1 – RAMD values after 8128 hours of operation**

RAMD Values (8128 hours)	
<b>Reliability</b>	99.2 percent
<b>Availability</b>	91.2 percent
<b>Maintainability</b>	NA
<b>Durability</b>	NA

***2) Demonstrate RAMD emissions below 3 ppm NO<sub>x</sub>, and 5 ppm CO and UHC***

The Xonon® equipped KHI M1A-13X engine accumulated 8,128 hours of on-grid RAMD operation. Emissions were continuously monitored and recorded at one-second intervals and then summarized in 30 minute, 1-hour rolling and 3-hour rolling averages. Table 3.1.2 below shows the 30-minute averaged data for the entire 8,128-hour duration of the RAMD test program. The data clearly shows that the Xonon® combustion system emits uniformly low levels of NO<sub>x</sub>, CO and UHC that fall well below the program targets (NO<sub>x</sub> < 3 ppm, CO < 5 ppm, UHC < 5 ppm) during base-load operation. Refer to Section 3.1 for more details relating to the RAMD test program.

**Table 3.1.2 -- RAMD emissions for 8128 hours of operation (30 minute averages corrected to 15 percent O<sub>2</sub>)**

	<b>Min</b>	<b>Avg</b>	<b>Max</b>
<b>NO<sub>x</sub> (ppm)</b>	0.5	1.3	2.9
<b>CO (ppm)</b>	0.0	0.9	94.5
<b>UHC (ppm)</b>	0.0	1.3	9.1

**3) *Develop a control strategy able to meet the load following and load step performance required by the power generation industry***

CESI completed a task to develop a fuel control system capable of accepting complete load loss without exceeding the turbine over-speed or surge limits. The control logic developed as a result of this activity improved the operational characteristics of the system in the following areas:

- **Load following** – the control system is now able to react to step changes in load without losing stability. Load steps of 300 kW and 600 kW were successfully demonstrated without the loss of system stability.
- **Load rejection** – in the event of the complete loss of load, the engine remains stable at full speed no load conditions without reaching over-speed limits. The control system demonstrated suitable system stability when rejecting loads from 300 kW, 600 kW, 900 kW, and 1050 kW.
- **Breaker Auto-Resynchronization** – the control system was modified to allow for automatic resynchronization to the power grid following a load rejection. In order for a generator to synchronize with the grid the rotational frequency of the shaft must match the frequency of the grid within +/- 0.5 Hz.

A more detailed discussion of the control system development can be found in Section 2.2 of this report.

**4) *Develop a robust mechanical support system for the catalyst that will exceed 8,000 operating hours***

A detailed study was conducted using a combination of structural analysis and material testing to determine the durability of the axial catalyst mechanical support (designated the Bonded Metal Monolith or BMM). The material test portion of the activity, although limited in scope, provided valuable data on the mechanical behavior of thin H214 structures. These data combined with detailed finite element and thermal analyses were used to determine the fatigue and creep life of the BMM component.

The analysis showed that the average calculated fatigue life is 650 cycles (50 cycles initiation and 600 cycles of propagation) which is well within the design life (8,000 hours or approximately 100 cycles) of the BMM. These analytical results agree favorably with the actual hardware which showed signs of crack initiation after 50 cycles (4,128 hours)

The analytical creep deformation results, in contrast to the fatigue results, did not agree well with actual hardware observations. In fact, the analysis predicted creep deformation 2.7 times lower than that measured on the actual hardware at the end of 4,128 hours. The lack of accurate material creep data is believed to be the reason for this discrepancy. This discrepancy notwithstanding, the observed creep deformation is a clear indicator that the creep life of the BMM does not meet the design goal of 8,000 hours.

Due to the low creep life of the BMM design, CESI initiated a redesign activity under a company sponsored program. The resulting axial support design is currently undergoing engine testing at the Silicon Valley Power test facility. A more detailed discussion of the axial support activity can be found in Section 3.3 of this report.

#### ***5) Design and test an axial fuel/air premixer design for the Xonon® combustion system***

A detailed study was conducted using a combination of computational fluid dynamic (CFD) analysis and cold flow rig testing to determine the feasibility of incorporating an axial fuel/air premixer into the Xonon® catalytic combustion system. The results indicated that the lobed axial mixer configurations studied would not perform better than the current Xonon® radial mixer design. While the original proposal included an engine-testing subtask, it was decided (with CEC concurrence) that the early results did not support further expenditure of program resources on this task. Even though the predicted performance of the axial fuel/air premixer was lower than the current radial design, several important findings were determined as the result of this study:

- A greater number of mixing lobes results in a modest improvement in mixing effectiveness.
- With fuel gas velocities below 100 fps, the NACA0030 airfoil is the best choice for the fuel gas shape. For gas velocities above 100 fps, the NACA0033 is preferred.
- The cold flow mixer effectiveness testing shows poor mixing directly downstream of fuel gas locations.

A second aspect of this task was to study the effects of temperature, pressure, gas velocity and geometry on flameholding and to determine those parameters that will reduce the possibility of flameholding in future CESI premixer designs. Specific flameholding findings include:

- The mechanism for flameholding appears to exhibit a sharp transition that occurs somewhere between a 0.0375" and a 0.125" step expansion. Perturbations less than 0.0375" are much less favorable to flameholding.
- Temperature variations had little effect on flameholding; however, variation in velocity and pressure were found to have a significant influence.

A more detailed discussion of the fuel/air premixer activity can be found in Section 3.4 of this report.

#### ***6) Develop catalyst materials that will exceed 8000 operating hours***

The primary objective of this task was to prepare and test the short- and long-term performance of thermally stable catalysts using commercially scaleable processing and commercially relevant test conditions. Sub-scale reactor tests showed that the new catalyst formulations demonstrated



superior initial performance and short-term stability when compared to the current baseline catalyst. Encouraging results were also seen during the 8000-hour total surface area testing which showed improvement over the current catalyst system formulation. However, the long-term stability of the active metal surface dispersed on the new supporting oxide was found to be inferior to that of the commercial baseline catalyst after 8000 hours at 900°C and 4000 hours at 950°C. It appears that the stability of the supporting oxide is not sufficient to prevent the loss of surface area of the active metal.

Based on the long-term performance test results, it was determined that the new catalyst formulations were not superior to the current baseline catalyst system. As a result, the new catalyst systems were not incorporated into the RAMD testing program. A more detailed discussion of the catalyst development activity can be found in Section 3.5 of this report

### ***7) Determine the effect of variability in natural gas fuel composition on the performance of catalytic combustion systems***

This task involved two primary objectives: 1) Survey the range of natural gas compositions found in the United States and worldwide and 2) Test a catalyst system over the composition range found in the survey to observe the effects of varying natural gas composition, specifically higher hydrocarbons and diluents, on the performance of the system. The results of this task show the following:

- The catalyst is insensitive to inerts (nitrogen and/or carbon dioxide) in the fuel at concentrations up to 25 vol percent; and
- The inclusion of higher hydrocarbon constituents increases the reactivity of the catalyst, causing a shift of the operating window resulting in:
  - The emissions design limit being reached at a lower catalyst inlet temperature and
  - The catalyst durability design limit being reached at a lower catalyst inlet temperature.

Relatively large amounts of higher hydrocarbons do not damage the catalyst in the short term, and can actually increase long-term durability by operating at lower catalyst inlet temperatures

The increase in reactivity moves the homogeneous combustion front closer to the catalyst outlet face for a given outlet gas temperature and  $T_{ad}$  (Combustor exit temperature)

## **3.2. Project Economic Outcomes**

Since the Xonon® technology is in the pre-production phase of development, actual economic results are not available. However, CESI has developed economic models based on industry trends, production readiness assessments and OEM production orders. These models project that Xonon® technology can produce net power costs that are only 7-9 percent greater than an uncontrolled high-emission turbine. In areas where less than 3 ppm NO<sub>x</sub> emissions are required, Xonon® achieves the same NO<sub>x</sub> emissions levels as the DLN plus SCR option at costs that are 7-21 percent lower. See Section 3.2.1 for more details on the projected cost benefits of Xonon®.

### **3.2.1. Commercialization Potential**

A more detailed discussion of this topic is contained in Appendix I: Market Requirements Development.

#### **3.2.1.1. Market Background**

There has been remarkable growth in worldwide prime mover (combustion turbines and reciprocating engines) demand during the past decade. This is driven by several factors, including growth in developing nations and a demonstrable market shift away from conventional large-scale thermal power plants toward the use of prime movers for power generation—especially larger (over 30 MW) gas turbines in simple- and combined-cycle configurations.

The application of gas turbines for stationary power generation has grown considerably over the past decade and is projected to continue to grow in the future. Strong gas turbine demand is based on several key product attributes associated with combustion turbines—high efficiency in combined-cycle configurations; low capital, operating, and maintenance costs; high reliability and availability; shortened lead time for permitting and construction; and low emissions.

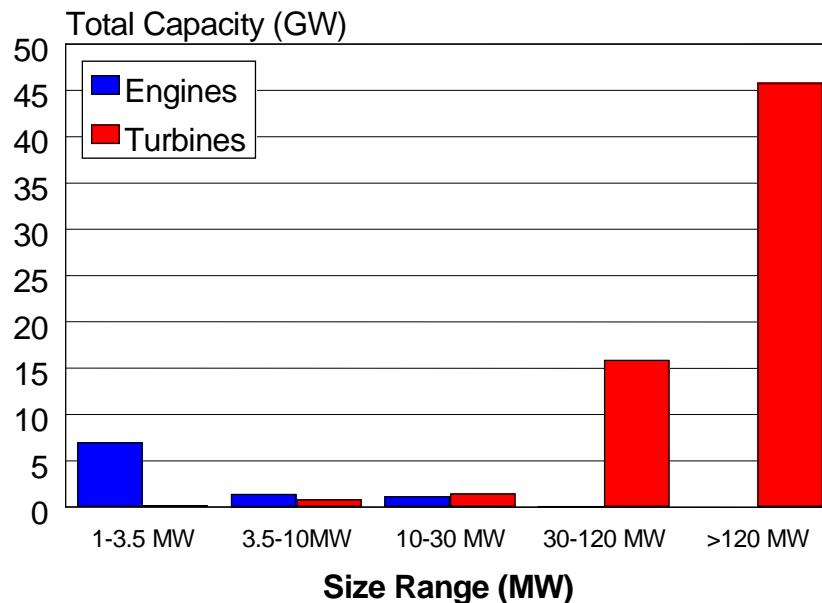
While exhaust emissions from natural gas-fueled and distillate-fueled combustion turbines (CT) are low, continued environmental pressure is resulting in permitted emission limits in some areas being below what is commonly achievable even with advanced dry low NO<sub>x</sub> (DLN) combustors. An alternative combustion approach, catalytic combustion, offers the potential to achieve ultra-low NO<sub>x</sub> emission levels without the complications and cost of post-combustion emission controls.

#### **3.2.1.2. Current Gas Turbine Market**

Continued market growth is expected for natural gas-fueled prime movers, primarily turbines and reciprocating engines. Gas turbines in both simple- and combined-cycle systems have accounted for the vast majority of power generation capacity added in the last five years in both international and U.S. markets. These are predominantly central station power plants greater than 50 MW. Large gas turbines have become the power generation technology of choice for many power providers. This trend is expected to continue over the foreseeable future. Several factors contribute to the strong position of gas turbine-based power generation and the likely role turbines will play in the future:

- An optimistic outlook for the supply and price of natural gas;
- Technology advances that produced substantial improvements in efficiency and emissions;
- Emissions regulations that could favor gas turbine projects over traditional fossil-fueled steam turbines; and
- Attractive initial capital costs and reduced time and cost for power plant permitting and installation, compared to traditional power plants.

Figure 3.2.1.2.1 shows the total 1999 worldwide orders for engines and turbines in sizes over 1 MW (based on data reported by Diesel and Gas Turbine Worldwide). The figure clearly shows a substantial increase in demand for large turbines over 30 MW in size.



Source: Diesel & Gas Turbine Worldwide

**Figure 3.2.1.2.1 -- Worldwide prime mover orders (over 1 MW)**

Total gas turbine orders amounted to over 64 GW of capacity during this one-year period. This represents a significant level of acceleration in gas turbine orders compared to 1997-1998, when just over 32 GW of orders were reported. Using a nominal price of \$400 kW for gensets, new gas turbine annual sales fall in the range of \$12 to \$25 billion. This is consistent with market information reported by Forecast International (Figure 3.2.1.2.2).

### 1999 Gas Turbine Market

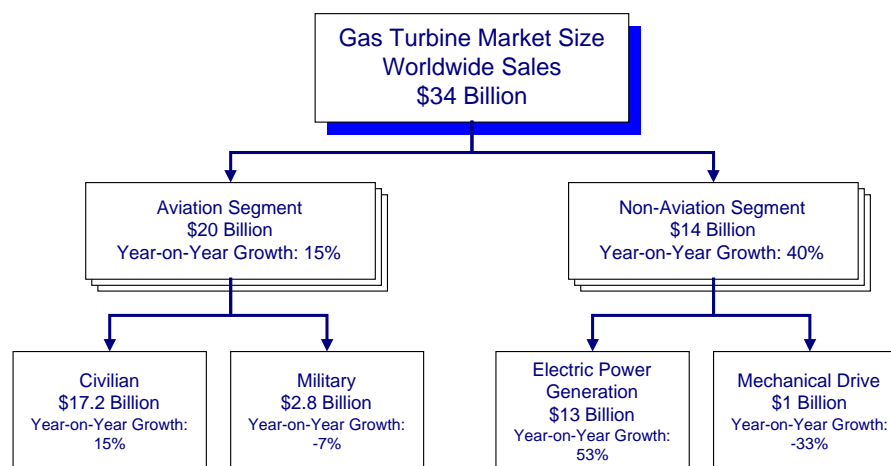


**Figure 3.2.1.2.2 -- Estimated gas turbine market (Forecast International, 1999)**

Gas turbines cover a broad spectrum of sizes, from 10's of kW for microturbines up to nearly 200 MW for large frame turbine platforms. However, most of the order volume -- on a capacity basis -- resides above 60 MW (89.8 percent) and nearly 96 percent lies above 30 MW (Table 3.2.1.2.1). On a unit basis, there were a total of 875 gas turbines ordered during this one-year period.

**Table 3.2.1.2.1 -- Gas turbine orders by size range (1999)<sup>15</sup>**

<b>Year</b>	<b>Orders (GW)</b>	<b>Share ( percent of Capacity)</b>	<b># Units</b>	<b>Share</b>
1-10 MW	1.07	1.70 percent	313	35.80 percent
10-30 MW	1.46	2.30 percent	75	8.50 percent
30-60 MW	3.99	6.20 percent	103	11.80 percent
Over 60 MW	57.73	89.80 percent	384	43.90 percent
<b>Totals:</b>	<b>64.25</b>		<b>875</b>	

The 1999 turbine order level represents a significant increase from historical levels. Table 3.2.1.2.2 shows gas turbine orders as reported by Diesel and Gas Turbine Worldwide over the recent past. Turbine orders have grown by a factor of 5 to 10 in the past fifteen years. The long-term trend indicates an increase in the “average” turbine unit size. In actuality, the gas turbine market is bi-modal, with a large number of units sold between 1-10 MW and over 60 MW. The interest in over 60 MW size units has continually expanded over the past decade and is the main driver in increased total GW of demand.

**Table 3.2.1.2.2 -- Gas turbine order trend (1984-1999)<sup>16</sup>**

<b>Year</b>	<b>Total Orders (GW)</b>	<b>Total Orders (Units)</b>
<b>1984</b>	6.5	435
<b>1988</b>	17	466
<b>1994</b>	27.43	796
<b>1998</b>	33.2	754
<b>1999</b>	64.25	875

The overall market situation supports a conclusion that gas turbine demand has dramatically changed over the past ten to fifteen years. Annual growth in new orders is about 13 percent per year on a compounded basis (excluding 1999, where orders exploded by over 90 percent in one year). New gas turbine orders will likely remain strong into the future and continue at levels well above historical levels.

Increased turbine demand is primarily due to a distinct market shift away from large, coal-fired central-station thermal power plants toward 100-500 MW combustion turbine power plants (simple- or combined-cycle, fueled by natural gas or liquid fuels). Gas turbines have gained favor in the inter-industry competition with thermal power plant producers, in part by increasing their upper generating capacity limits. The dominance of combustion turbines over conventional thermal power plants will continue until fuel price differentials (natural gas to coal or distillate to coal) change significantly.

While the market and business climate is quite favorable for large gas turbines, gas turbines in the distributed generation market (1-10 MW) face greater challenges. Fundamental market drivers favor large gas turbine power plants because of lower capital costs and shorter construction and permitting lead times than traditional fossil-fueled steam turbines. Large combined-cycle systems have efficiencies in the 50-58 percent range, based on the fuel's lower heating value (LHV). The environmentally clean nature of these plants is evidenced by their ability achieve 9 ppm of nitrogen oxides (NO<sub>x</sub>) emissions without exhaust treatment and lower than 3 ppm with post-combustion control technologies.

A natural facet of the combustion turbine market evolution is an increase in the number of market participants and expansion of the value of gas turbine products sold. All this has occurred while unit prices (\$/kW) have trended downward and efficiency values have increased. The market has shifted more to an intra-industry competition for sales and market share between different gas turbine producers and project developers. Under these circumstances, unique product features and benefits—that is, differentiators—will become increasingly important in providing an edge during the sales process. Advanced technology such as catalytic combustion can play a role in a company's strategic product planning.

On the smaller end of the spectrum—below 30 MW—gas turbines face strong inter-industry competition from reciprocating engines. This competition accelerates at unit sizes below 10 MW and becomes exponential with decreasing size (Table 3.2.1.2.3). For example, in the 1 to 2 MW size range, reciprocating engines outsell gas turbines by nearly a 33:1 margin.

**Table 3.2.1.2.3 -- Gas turbine and reciprocating engine orders (1999, 1-30 MW)<sup>17</sup>**

<b>Year</b>	<b>Turbine Orders (MW)</b>	<b>Engine Orders (MW)</b>
1-10 MW	1,070	8,350
10-30 MW	1,046	1,157

Below 1 MW, nearly all of the demand for stationary prime movers has been satisfied by liquid-fueled and gaseous-fueled reciprocating engines. The total demand for power generation engines below 1 MW is estimated to be about 23,000 MW. Figure 3.2.1.2.3 shows data from Parkinson Associates on their estimation of worldwide demand for stationary power generation engines. This figure demonstrates a significant growth market for smaller (under 10 MW) gas turbines if they can become more competitive or preferred power generation options. The

interest in microturbines is directed at the nearly quarter million reciprocating engines sold in the 75 kW and less size range (as well as in new market growth opportunities).

#### Worldwide Engine Generator Sets

Total Units Sold - 1998 Data

Total Capacity: 32.7 GW

Source: Parkinson (EGSA 8/99)

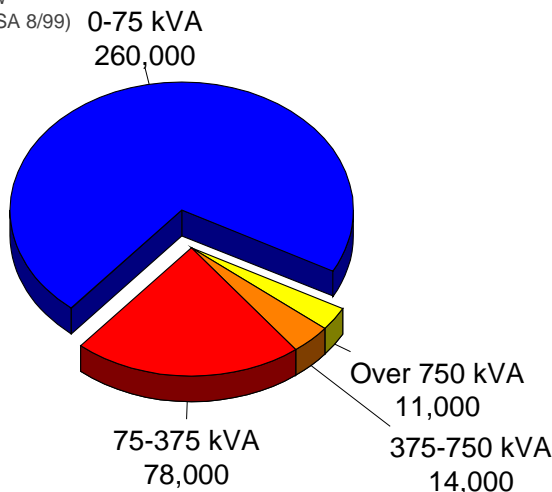


**Figure 3.2.1.2.3 -- Worldwide reciprocating engine sales**

For smaller gas turbines to gain market share, they need a combination of product improvements, improved competitive pricing, and possibly external market factors such as environmental drivers working to their benefit. Gas turbines with advanced technologies such as catalytic combustion would seemingly offer substantial emission/environmental impact differentiation relative to the majority of reciprocating engine products in the market.

#### 3.2.1.3. Emissions as a Market Driver

The environmental permitting process is a relatively complex process—particularly in the U.S. This regulatory process begins with the Clean Air Act (CAA and its amendments) and flows down through the requirements of the National Ambient Air Quality Standards (NAAQS). From the NAAQS program, the severity of emissions as a driver depends largely on whether or not an area is in attainment or not for various NAAQS species (e.g., ozone, CO), the degree of non-attainment (if applicable), and the size of the unit and its operational characteristics and/or potential to emit.

For new units, customers will likely be required to comply with either state or local guidelines for new sources. In attainment areas, this will likely mean satisfying BACT (Best Available Control Technology). In non-attainment areas, this will likely mean satisfying LAER (Lowest Achievable Emission Rate) limits—which may include the need to obtain emission offsets.

BACT and LAER have been used over the years as a technology forcing mechanism to push for increasingly lower emission levels from new sources in attainment and non-attainment regions. This has resulted in the introduction of many new emission control technologies, including DLN for gas turbines. However, there is growing concern on the equity and effectiveness of this approach since it increasingly penalizes new technologies while encouraging the operation of older, higher polluting systems. There is likely to be an increasing trend toward incentive-based

systems in the future as a means of providing more options for cost-effectively meeting NAAQS limits.

Recent air quality requirements in California and Texas have reflected a movement toward uniform emissions limits from all distributed generation sources. These limits are output-based (e.g., lb/MWh) and make it clear that air regulators would prefer that Distributed Generation (DG) units be as clean as the lowest emitting, highest efficiency central station plants, i.e., new gas turbine combined cycle installations. Brief summaries of the California requirements (SB 1298) and Texas (Texas Natural Resource Conservation Commission (TNRCC) Air Quality Standard Permit for Electric Generating Units) are presented below.

California SB 1298 requires the California Air Resources Board (CARB), on or before January 1, 2003, to adopt a certification program and uniform emissions standards for distributed generation that are currently exempt from district permitting requirements, and would require that those standards reflect best performance achieved in practice by existing electrical generation equipment.

CARB has adopted a two-phased approach with limits for specific applications, i.e., PPO (Power Production Only), CHP (Combined Heat and Power), and CZEP (Power Production combined with Zero Emission Technology such as renewables and fuel cells) in Phase 1 to begin in January 2003 and uniform limits in Phase 2 to begin in January 2007 regardless of technologies. Table 3.2.1.3.1 illustrates the legislated limits. Beginning in 2007, all DG technologies regardless of configuration will be held to 0.07 lb/MWh NO<sub>x</sub>, 0.10 lb/MWh CO, and 0.02 lb/MWh VOC's. There are currently no commercially available technologies that guarantee 0.07 lb/MWh NO<sub>x</sub>.

**Table 3.2.1.3.1 -- SB 1298 Two-Phase Emissions Limits**

<b>2003 Emissions Limits</b>				<b>2007 Emissions Limits</b>
<b>Pollutant</b>	<b>Power Production Only (PPO) [lbs/MWh (ppm)]</b>	<b>Combined Heat and Power (CHP) [lbs/MWh (ppm)]</b>	<b>Integrated with Wind or Solar Technology (IWR) [lbs/MWh (ppm)]</b>	<b>All DG regardless of configuration [lbs/MWh (ppm)]</b>
NO <sub>x</sub>	0.5 (9)	0.7 (15)	1 (21)	0.07 (1.5)
CO	6 (200)	6 (200)	6 (200)	0.1 (3.0)
VOC's	1	1	1	0.02

Note:ppm based on a representative 5 MW gas turbine with 11,300 Btu/kWh heat rate and 8000 hours of operation corrected to 15 percent O<sub>2</sub>

The requirement for the emission levels that Xonon® catalytic combustion system can achieve is geography-specific and currently limited to “environmentally constrained areas”. The environmentally constrained areas include states in the ozone transport region of the Northeast, Northeast States for Coordinated Air Use Management (NESCAUM), Mid-Atlantic Regional Air Management Association (MARAMA) and other counties that have been identified as serious,

severe and extreme non-attainment for ozone. More specifically, the environmentally constrained regions include:

- State segregation in Ozone Transport Region – CT, DE, ME, MD, MA, NH, NJ, NY, PA, RI, VT, parts of VA and District of Columbia
- State segregation in NESCAUM- CT, ME, MA, NH, NJ, RI, VT
- State Segregation in MARAMA – DE, District of Columbia, MD, NJ, NC, PA, VA
- County segregation with serious, severe or extreme non-attainment status – CA, IL, IN, TX, WI, GA, LA, AZ

The competitive options that exist for meeting emission limits will vary depending on the state or local emission requirements. In attainment areas with modest BACT requirements (over 25 ppmv), little may be required from new sources. In severe or extreme non-attainment areas—or regions with “aggressive” environmental regulations—ultra low NO<sub>x</sub> emission levels may be required (below 9 ppmv). Table 3.2.1.3.2 illustrates this on a qualitative basis. Catalytic combustion clearly becomes a competitive consideration in circumstances requiring ultra-low NO<sub>x</sub> levels and may become competitive under baseline (9-25 ppmv) situations if it offers operational or cost advantages over DLN combustors (e.g., improved combustion stability), or, if market incentives such as emissions trading provide a driver for “over complying” with emission limits.

**Table 3.2.1.3.2 -- Qualitative Emission Limits and Options**

<b>Emission Limit</b>	<b>Main Competitive Options</b>
“High” Emission Limits (Over 25 ppmv)	- Conventional diffusion combustors - Steam or water injection
Baseline Emission Limits (9-25 ppmv)	- Dry Low NO <sub>x</sub> combustors (lean premix) - Conventional diffusion combustors with SCR - Catalytic combustion
Ultra-Low Emission Limits (Under 9 ppmv)	- Conventional diffusion combustors with SCR - Dry Low NO <sub>x</sub> combustors with SCR - Catalytic combustion

#### **3.2.1.4. Technology Cost and Performance**

It is expected that for turbine-based generation technologies to meet future certification requirements, they will ultimately need to reduce NO<sub>x</sub> emissions to 2.5 to 3.5 ppm levels. In fact, SB1298 will require emissions levels that are half of this level by 2007. Because of this, 2.5 ppm was selected as the performance target for NO<sub>x</sub> emissions for a technology cost analysis. The analysis shows that there are significant benefits at the 2.5 ppm level in the reduction of emissions from older central station plants and in avoiding customer boiler emissions for DG systems in CHP duty.



To meet the 2.5 ppm values, we compared DLN combustion, DLN with selective catalytic reduction (SCR) of exhaust emissions, and catalytic combustion using Catalytica's Xonon® technology. The analysis was based on three OEM turbine packages with the following capacities:

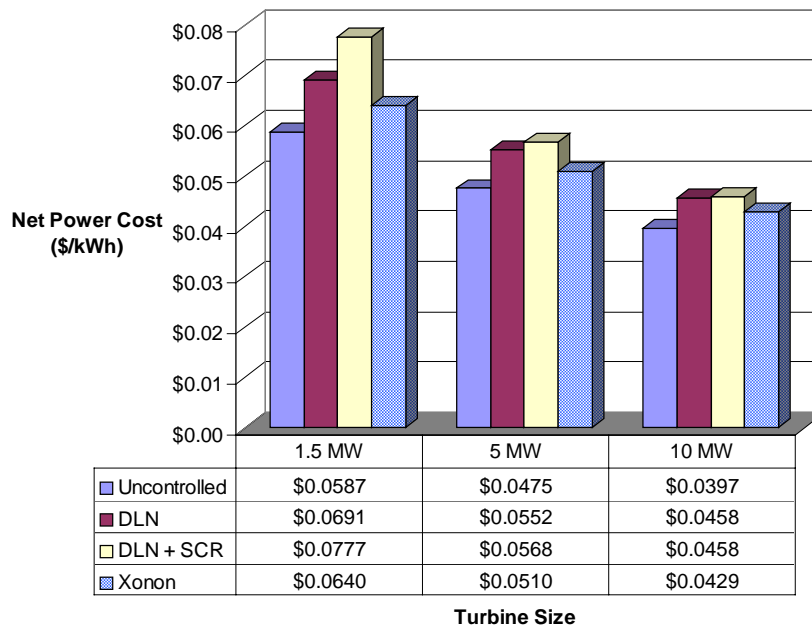
- 1.5 MW
- 5.0 MW
- 15.0 MW

Table 3.2.1.4.1 summarizes the capital and operating cost impacts for these three systems with three environmental control alternatives: DLN, DLN plus SCR, and Xonon® catalytic combustion. The table shows the basic costs for the turbines and the three environmental control technologies. In addition, hidden costs are also identified that act to increase the capital or operating costs of the systems. These costs and parameter definitions are shown in Appendix A.

**Table 3.2.1.4.1 – Capital and operating impacts of pollution control systems**

<b>Size</b>	<b>Costs</b>	<b>DLN</b>	<b>DLN/SCR</b>	<b>Xonon®</b>
1.5 MW Turbine	Capital (\$/kW)	\$179	\$300	<b>\$85</b>
	Operating Cost (mills/kWh)	7.8	14.6	<b>4.9</b>
5.0 MW Turbine	Capital (\$/kW)	\$178	\$185	<b>\$54</b>
	Operating Cost (mills/kWh)	5.2	7	<b>3.8</b>
15.0 MW Turbine	Capital (\$/kW)	\$184	\$157	<b>\$51</b>
	Operating Cost (mills/kWh)	4.6	5.2	<b>3.7</b>

For each of the systems shown in the table, we calculated the net power cost from a CHP system. The net power cost is the fully amortized owning and operating costs on a per kWh basis after the avoided costs of a separately fueled boiler are subtracted from the operating costs. These systems are based on natural gas fuel costs of \$4.50/MMBtu. Figure 3.2.1.4.1 shows the comparison of costs for an uncontrolled system, DLN, DLN plus SCR, and Xonon®. All of the hidden costs are incorporated into these cost estimates except for the uncontrolled case that is included for reference only – not as a realistic alternative for nonattainment areas.



**Figure 3.2.1.4.1 – Comparison of net power costs in CHP duty**

Xonon® technology can produce net power costs that are only 7-9 percent more costly than an uncontrolled turbine. In addition, Xonon® achieves the same NO<sub>x</sub> emissions levels as the DLN plus SCR option at costs that are 7-21 percent lower.

To put these unit numbers in perspective, an individual 5 MW CHP project meeting its emissions requirements with a Xonon® control system can produce power with a net cost that is 10 percent cheaper than a system with DLN/SCR control. However, this 10 percent cost reduction produces a 70 percent increase in the annual savings when compared with an estimated average power cost of \$0.065/kWh. Figure 3.3.4.2 shows the comparison in annual user savings for the SCR/DLN and the Xonon® systems. The 5 MW CHP customer using SCR could save \$341,000 per year compared to purchased power and a separately fueled boiler, whereas a CHP customer using Xonon® would save \$582,000 per year.

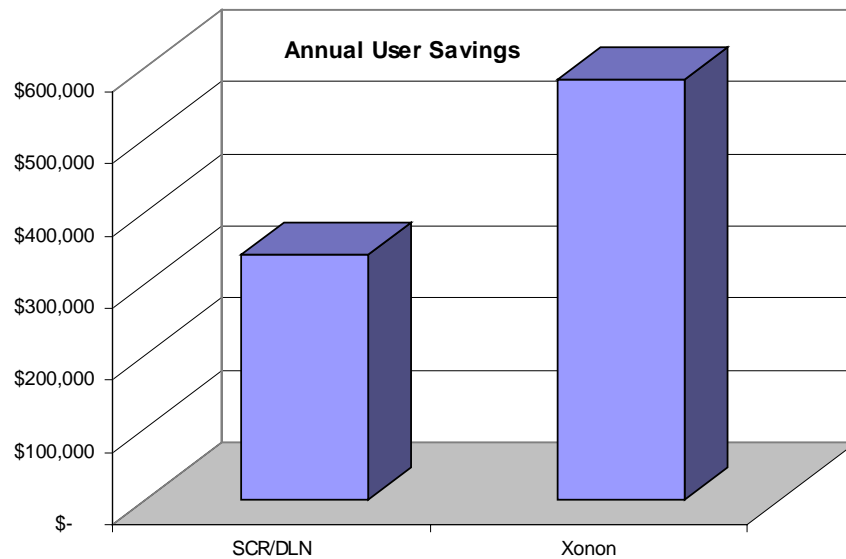


**Figure 3.2.1.4.2 -- Comparison of yearly savings for 5 MW system: purchased fuel and power costs versus fully amortized CHP owning and operating costs**

### 3.2.1.5. Market Penetration

The CHP market model previously developed for the Commission<sup>18</sup> was modified to reflect recent changes in fuel and power outlook and to updated the technology cost and performance values using the data presented in Section 3.3.4. The net result from these changes is that Xonon® equipped gas turbines can achieve an additional 855 MW of market penetration in California between now and 2017, compared to gas turbines using DLN plus SCR to achieve the same level of emissions reduction. These added systems represent an 18.5 percent increase in the CHP market for California.

Market penetration was based on the historical rate of market penetration in California during the 1991-1996 period. The market penetration forecast is based on the relationship between the project internal rate of return (IRR) during the historical period and the IRR figures calculated for each size bin and year. (Some modifications to the prior approach were made to ensure that market penetration rates would not exceed the technical market potential.)

The cumulative market penetration estimates for the revised market model are shown in Table 3.2.1.5.1. In the size range of interest between now and 2017, future cumulative market penetration of CHP based on gas turbines using DLN plus SCR equals 4,587 MW. Using Xonon®, cumulative market penetration increases to 5,443 MW – a net increase of 856 MW. Market penetration of the 1.5 MW product for CHP applications is very low due to the higher cost and poor heat rate that lead to a lack of competitiveness with both purchased power and fuel options and also reciprocating engine based systems.

**Table 3.2.1.5.1 -- Comparison of the Impacts of DLN/SCR and Xonon on CHP Market Penetration**

CHP Size Category	Cumulative Penetration in MW		
	Market Penetration with DLN plus SCR	Market Penetration with Xonon	Added Market Penetration due to Xonon
1-5 MW	10	66	57
5-20 MW	522	757	235
> 20 MW	4,056	4,620	565
<b>Total</b>	<b>4,587</b>	<b>5,443</b>	<b>856</b>

### **3.2.1.6. Market Requirements**

The approach used in the review of commercialization requirements consisted of targeted telephone interviews with what were identified to be a sample of key stakeholders in the development, commercialization and utilization of catalytic combustion systems for industrial gas turbines.

Companies contacted and interviewed included those that manufacture or package industrial size (1-10 MW) gas turbine systems, develop gas turbine based projects, supply emission control equipment, and various other stakeholders including environmental regulatory agencies, permitting consultants and energy policy influencers.

#### **Interview Topics**

Each telephone interview included a discussion of target markets and applications, minimum customer requirements, design and integration issues and maintenance issues. The principal topics of discussion included:

- **Company Background** – a brief description of the company’s product offerings and role in the industrial gas turbine market
- **Target Market Segments and Applications** – identify the applications of the company’s product line such as CHP, standby, prime or rental power. Identify primary market segments include health care, schools, commercial, industrial, etc.
- **Current Environmental/Air Quality Issues** – identify current emissions requirements, trends, and recent precedent setting projects/permits. Perception of the options available to customers, costs (capital and operating), ease of implementation, costs of offsets, and any other issues associated of each option.
- **Successful and Unsuccessful Product Strategies** – discuss experience with innovative and early-commercial emissions control technologies. Interviewees were asked to describe a successful experience and an unsuccessful one.
- **Technology Issues that Affected Integration of Technologies** – discuss experience with integrating technologies from a technical/design perspective. For example, footprint requirements, onsite handling and storage of ammonia, etc.

- **Barriers that Affect Commercial Use of Technologies** – discuss the obstacles of integrating technologies into product offerings. For example, cost to reconfigure current products, air emission permitting, installation costs, operating costs, durability, etc.
- **Awareness and Perception of Combustion Technology Options** – discuss the primary differences between combustion (pollution prevention) and exhaust treatment (pollution control) options. Perception of key players and the ability to deliver.
- **Reaction to CESI** – discuss Xonon® specifications and perception of current state of product readiness.
- **Desired Characteristics of a Successful Technology/Partnership** – discuss the criteria for a successful and economically viable emission control system for industrial gas turbines.
- **Future Strategies** – discuss how companies are positioned to address the emissions issues in the small gas turbine market in light of their past experience and new technologies entering the market

### **Companies Interviewed**

Representatives from the following organizations were contacted to participate in the survey effort. Their discussions are compiled later into this section of the report. Their descriptions should not be construed to represent the official views or policies of the company itself, but rather as a compilation of experience and opinions based on an individual's experience in the industry. Companies include:

- **Alliance Power**, Project developer of industrial sized gas turbine power plants. Alliance has an existing relationship with CESI.
- **Alstom (formerly ABB)**, Manufacturer and packager of gas turbine systems. Family of GT's from industrial to large central station.
- **Alzeta**, Developer of low emission combustion technology.
- **Bay Area Air Quality Management District**
- **California Air Resources Board**
- **Cormetech**, Developer and provider of high (>800 F) and conventional temperature (400-800 F) SCR equipment.
- **Engelhard**, Catalyst provider. Developer of high temperature (>800 F) SCR.
- **Enron Energy Services**, Global conglomerate with roots in oil and gas business. It has diversified into all segments of the energy market and beyond to include broadband communications and online trading. Services include management of energy commodities, assets, information, facilities and capital, efficiency improvements and distributed generation.
- **GE/Nuovo Pignone/ Stewart & Stevenson**, Multinational corporation that develops, manufactures, packages, and finances GT power plants.
- **Goal Line Environmental Technologies**, Developer of zero ammonia exhaust treatment technology
- **Kawasaki**, Manufacturer and packager of gas turbine systems.

- **Onsite Energy Corp**, Energy services company (ESCO). Onsite was founded in 1982 primarily as a provider of cogeneration and other power generation/supply side services (inside the fence). In 1988, Onsite expanded to include demand side management services and now is a full-service ESCO with an emphasis on energy efficiency and distributed generation, related consulting services, and direct access planning services for commercial and industrial customers.
- **Precision Combustion Inc.**, Developer of catalytic combustion technologies.
- **Resource Catalyst**, California-based air quality and permitting consultant.
- **Rolls Royce**, Multi-national firm that manufactures aircraft engines and aero-derivative engines among other products. Rolls Royce has acquired the Allison Engine Company in Indianapolis. They developed a business plan for a 50 kW and 250 kW micro-turbine, however, it has not been initiated.
- **Solar Turbines**, Developer, manufacturer, and packager of industrial size gas turbines.
- **South Coast Air Quality Management District**
- **Southern California Gas Company**, Natural gas distribution utility. SoCal Gas serves a territory of 23,000 square miles that ranges from central California to the Mexican border. SoCal Gas has an ambitious R&D program that actively collaborates with the energy industry, manufacturing partners, and government agencies to promote new technologies, improve existing technologies and streamline day-to-day operations.
- **Texas Natural Resources Conservation Commission**

### **Summary of Interviews**

In the completion of this task it was clear that the level of understanding and familiarity with Xonon® ranges from very familiar to limited knowledge of low emission combustion systems. The general sentiment from most interviewees was that there was some degree of uncertainty with regard to both the commercial readiness of Xonon® and the emissions regulations that would require a product like Xonon®.

It was nearly unanimous among interviewees that the potential growth for gas turbines in the 1-10 MW size range was large (the previous market status section verifies the growth in this segment), but that the realization of that potential will not be easy. Technology developments, such as Xonon®, and a regulatory environment that gave small gas turbines an advantage over higher polluting reciprocating engines would go a long way toward realizing some of the already noted potential.

Gas turbine manufacturers made a point to recognize the substantial benefits of pollution prevention approaches like Xonon® in this size range over pollution control technologies such as SCR and SCONOx. However, the manufacturers made it clear that they were examining multiple approaches to pollution control due to the perceived high development costs associated with a Xonon®-based solution. Durability and maintenance levels consistent with their current product offerings were cited as minimum requirements.

Project developers stressed the desire to not add additional technical risk to opportunities they were pursuing and had questions regarding what entity would provide warranties on

performance and maintenance. Impacts on life-cycle costs in cycling and peaking applications were an issue identified.

Selected noteworthy comments and perspectives are listed below:

Those in the gas turbine manufacturer and environmental regulatory communities had the highest understanding of the development and commercialization status of Xonon®. Both manufacturers and environmental regulators were aware of demonstration of Xonon® at Silicon Valley Power and the positive results.

Gas turbine manufacturers acknowledged existing development programs with Catalytica and identified issues such as development costs and an uncertain regulatory environment as potential hurdles for a Xonon® based product.

Environmental regulatory agencies identified emission limit trends that are relevant to the need for products like Xonon® for the DG market (e.g., SB1298 in California and eastern Texas regulations and guidelines that will eventually put the same emissions limits on DG as there currently are on central station plants; NSR being reviewed; and emission limits that may favor CHP).

Project developers, while familiar with low emission combustion approaches, had acknowledged very little experience with Xonon® and were uncertain about its current commercial availability and performance guarantees.

Project developers had also expressed some initial confusion about current emission requirements and the control technologies on which current limits are based.

Project developers supported the development of any technology that would open markets that are currently closed to them due to strict emissions limitations.

- Project developers and gas turbine developers stressed strongly their aversion to risk and perceived uncertainties associated with Xonon® (e.g., not certain of actual commercial rollout date, warranty issues, perceived high financial risk and the desire to limit technical risks).

### **Key Stakeholder Perspectives**

The Commercial Requirements Task identified four key classes of stakeholders that will influence the commercialization of the Xonon® combustion system. In some cases the groups are the combination of two or more stakeholder groups that going in to this task of the project were thought to have held some unique and distinct perspectives and issues. Based on the results of interviews and the emphasis on the DG (<10 MW market) we chose to group some (e.g., developers with end-users) whose concerns and issues were very much aligned.

Those four stakeholder groups are:

- Developers and End-Users
- Gas Turbine Manufacturers (OEM's)
- Environmental Regulators (Air)
- Regulatory/Government/Energy Policy Bodies

The following sections present critical issues and concerns of the stakeholder groups at the time the interviews were conducted.

### **Developers and End-Users**

Fear risk

Can't afford to "wait" for product

Are uncomfortable with product and technology uncertainties – e.g., they aren't certain when Xonon® will finally be ready and aren't sure what the operational warranties will be

Feel they are taking substantial financial risk and seek to limit technology risk

Have historically preferred larger projects as project development costs are approximately equal for small and large projects and payback to developer is larger for big project

Recognize competition with reciprocating engines at low end of range.

See near term market opportunity for capacity needs in certain regions (even outside California)

### **Original Equipment Manufacturers (OEMs)**

- Desire internal ownership of technology;
- Perceive the current emissions regulations environment as unfavorable;
- Prefer the availability of pollution prevention approaches over exhaust clean up
- Active in innovative combustion development efforts with DOE and other outside funding sources;
- Emphasize catalyst life and durability as issues;
- Recognize the engineering difficulties of integrating Xonon® in specific models (e.g., external/can approach as being easier first application and perceive difficulties in annular combustor);
- Question the incentive to invest if emissions regulations will require exhaust cleanup regardless of turbine emission levels;
- Possess uneasiness in reliance on an outside supplier playing a key role in a critical component of their machines (some would like to see other providers of catalytic combustors if they ever do become commercialized fully);
- Are active in evaluating other approaches besides Xonon®;
- Seek to reduce risk by leveraging external funding (DOE, CEC, others) to test, demonstrate, and develop; and
- Are unable to make a firm commitment to commercialize at this point.



### **Environmental Regulators**

- Consider themselves as forcing technology, not prescribing it;
- Desire emissions controls technologies to be proven in practice;
- Track extensively development efforts and demonstrations;
- Project DG emissions becoming an issue, as they typically weren't closely regulated and don't want diesels finding a backdoor;
- Have advocated regulations favorable to clean technologies;
- Support rapid permitting of DG but don't want it any dirtier than typical new plant (i.e., new combined cycle);
- Recognize the value of CHP with its high total efficiency and fuel utilization;
- Initiate CHP outreach programs to facilitate CHP (e.g., US EPA); and
- Monitor EPA Review New Source Review (NSR) and impact on CHP at an existing site still not clear.

### **Regulatory and Government**

- Make energy policy a state and national priority;
- Consider greenhouse gas emission limits a high priority but political issue;
- Feel strongly that CHP and other high efficiency measures should play an important role in energy policy;
- Have subsidized clean technologies (e.g., renewables, fuel cells) in both R&D and support of commercial demonstrations;
- Considering whether CHP should get the same treatment as the referenced clean technologies; and
- Have been lobbied by the CHP community for changes to tax laws and rate issues (primarily utility standby rates).

#### **3.2.2. Conclusions**

To achieve the increasingly strict limits on NO<sub>x</sub> emissions in California, gas turbine distributed generation systems must utilize control technologies such as dry low NO<sub>x</sub> combustion plus selective catalytic reduction or Xonon® catalytic combustion.

DLN is capable of reducing NO<sub>x</sub> emissions to 25 ppm in the size range considered (1.5 to 10 MW). Direct costs range from \$37 to \$56/kW. SCR needs to be added to DLN system to bring emissions down to levels of 2.5 to 3 ppm. These systems are very costly in smaller systems costing \$268/kW in the 1.5 MW size down to \$109/kW in the 10 MW size range. Direct operating costs for DLN in the 10 MW size range add about 0.7 mills/kWh to O&M costs. The corresponding increase in O&M for SCR and Xonon® is about 3 mills/kWh for each technology. In smaller sizes, the direct operating costs for SCR increase at a faster rate than Xonon®. These direct costs understate the true costs of DLN and SCR because there are hidden costs that add the cost of generation. These hidden costs include revenue lost for air permit delays for less effective or more complex control systems, pressure drop and additional parasitic power use (for SCR), increases in unscheduled shutdowns due to additional risk

factors inherent in DLN and SCR systems, and higher emissions offset costs for systems that attempt to certify using DLN alone.

Based on an analysis of CHP applications between 1.5 and 10 MW, Xonon® technology can produce net power costs that are only 7-9 percent more costly than an uncontrolled turbine. In addition, Xonon® achieves the same NO<sub>x</sub> emissions levels as the DLN plus SCR option at costs that are 7-21 percent lower. An individual 5 MW CHP project meeting its emissions requirements with a Xonon® control system would have annual energy cost savings of \$582,000 – over 70 percent higher than the corresponding savings using DLN plus SCR.

Projections indicate that Xonon® equipped gas turbines can achieve an additional 855 MW of market penetration in California between 2001 and 2017, compared to gas turbines using DLN plus SCR to achieve the same level of emissions reduction. These added systems represent an 18.5 percent increase in the CHP market for California.

The total sum of user cost savings is over \$10 billion for the Xonon® based market penetration case. This figure is nearly \$3 billion greater than in the DLN/SCR penetration case. The net present value today of the increased future stream of savings due to Xonon® is over \$1 billion. These savings correspond directly to increased productivity for California's commercial and industrial sectors. The total energy savings from CHP using Xonon® technology over the forecast period equal about 2 quads of energy. The differential energy savings due to Xonon® are on the order of 0.3 quads.

The market penetration scenario based on the use of Xonon technology reduces total NO<sub>x</sub> emissions by 11,443 tpy compared to the existing mix of power generation and commercial and industrial boilers in California. Comparing emissions to new central station and boiler emission factors produces lower savings of 2,932 tpy. The higher market penetration rates for Xonon based CHP systems compared to DLN/SCR systems results in lower emissions attributable to Xonon – even though the Xonon and DLN/SCR technologies have equivalent emissions levels at each site.

The Xonon® technology will help the California economy by increasing the productivity of industrial and commercial facilities, encouraging stability of fuel and power markets by reducing demand pressure, and encouraging an accelerated reduction of air pollution in the state.

### **3.3. Production Readiness**

This section was submitted earlier as a Topical Report: Task 2.5 Xonon® Production Readiness. It is reproduced as Appendix VII.

#### **3.3.1. Introduction**

In managing the PIER Program, the California Energy Commission (the Commission) has a goal of bringing environmentally safe, affordable, and reliable energy services and products to the marketplace. In pursuit of this goal, the Commission requires that Contractors who receive PIER funding deliver a Production Readiness Plan that describes the proposed manufacturing processes, capabilities, constraints, and timing to achieve a commercially viable product. The degree of detail in the Plan should be directly related to the complexity of producing the

proposed product and its state of development. That is, the more complex the process and the closer it is to being market-ready, the more important it is that the Commission has the information to assess its viability for bringing products to the marketplace.

The product manufactured by Catalytica Energy Systems, Inc. (CESI) to achieve ultra-low emissions from gas turbines is the Xonon® catalyst module. For the Xonon module:

- The production process is relatively simple.
- Development and optimization of the process have been ongoing for ten years.
- The equipment configuration and critical steps in the commercial production process were proven more than five years ago.
- The first commercial Xonon® catalyst modules were produced for shipment in August 2001 --- the process works. Modules are manufactured in response to sales of the associated Xonon®-equipped turbines. As of January 2002, Xonon® catalyst modules have been produced for three commercial Kawasaki M1A-13X gas turbines.

Several turbine components besides the catalyst module must be specially designed to assure the effectiveness of the Xonon® combustion system. While CESI typically works in partnership with each turbine manufacturer to design such key components as the preburner, the fuel-air mixer, the air staging system, and the necessary controls system, the manufacturer is responsible for the final design, manufacturing, and performance of those components.

None of the CEC PIER Program funds have been directed at developing or refining the module manufacturing process.

### **3.3.2. Manufacturing Overview**

A Xonon® catalyst module consists of the catalyst itself and the surrounding container. A catalyst “stage” is formed by winding a long strip of corrugated foil, coated with the catalytically active material, around a spindle to form a cylindrical shape. An example is shown schematically in cross-section in Figure 3.3.2.1. Typical catalyst diameters are from 8 inches to more than 20 inches, with thicknesses (heights) ranging from 2 inches to 5 inches. The unit in Figure 3.4.3.1 is a single stage module; but, depending upon the application, the optimal system design can consist of 1, 2 or 3 catalyst stages stacked within a single container.

The container must be designed: 1) to maintain the physical position of the catalyst against the aerodynamic forces of the combustor gas flow, and 2) to seal the catalyst perimeter against gas leakage during the thermal and flow transients of turbine operation. [Note: Design aspects of the Bonded Metal Monolith (BMM) supports for the catalyst stages in the module are the subject of a separate topical report for this PIER 1 project, a copy of which is provided in Appendix III.] Figure 3.3.2.2 is a photograph of a three-stage unit with 20-inch diameter stages, each 2.5-3.5 inches high and each supported by a bonded metal monolith attached to the container wall. The picture shows the downstream (exit) face of the module --- the support for the outlet stage is not shown because it was placed on the module during installation in the combustor. The module shown in Figure 3.3.2.2 was a developmental unit that was used in testing at the General Electric Company.<sup>6</sup>

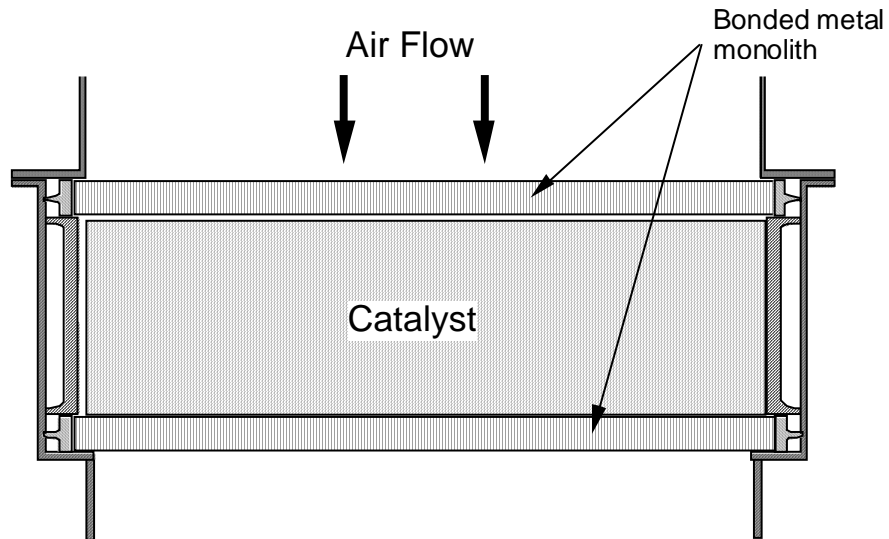


**Figure 3.3.2.1 -- Schematic diagram of the catalyst module with bonded metal monolith (BMM) structures at inlet and outlet**



**Figure 3.3.2.2 – Photograph of catalyst in container. See text for descriptive details.**

CESI has a manufacturing operation in Mountain View, CA that produces the catalyst modules for the commercial Kawasaki 1.4 megawatt M1A-13X gas turbines. The catalyst material is manufactured in-house solely by CESI. The mechanical parts of the container are designed by CESI, fabricated by outside vendors, and assembled at the CESI facility. The manufacturing process for the catalyst itself has been under development and refinement for nearly ten years. The currently proven and available production capacity will be adequate to support the initial commercial demands for Xonon®-equipped turbines. A photograph of the Mountain View manufacturing facility is reproduced in Figure 3.3.2.2.

CESI has attained ISO 9001 registration for its catalyst manufacturing operation and the associated quality assurance procedures. While the projected initial commercial demand for Xonon® modules can be met using the Mountain View manufacturing facility, planning is underway to install additional production capacity at a more spacious site in the Phoenix, AZ area. The new site will be located in Hewson Development Corporation's Fiesta Tech Centre in Gilbert, Arizona at 1388 N. Tech Boulevard. The 43,472 square-foot build-to-suit facility will house various administrative functions as well as the Company's Engineering Center and its commercial manufacturing operations. CESI will begin to occupy this new facility in October 2001, with a dedicated commercial module production operation scheduled to come on-line next year.



**Figure 3.3.2.3 -- Catalytica Energy Systems, Inc. manufacturing facility in Mountain View**

Production of a Xonon® catalyst module involves the following steps: (1) raw material receiving and inspection, (2) foil preparation, (3) catalyst preparation, (4) catalyst installation in the container, and (5) catalyst module testing. The catalytic components are produced entirely on site using proprietary processes and equipment developed at CESI. The raw materials for these components are sourced from US-based suppliers except when a US-based source of supply cannot be identified. Over 90 percent of the raw materials used for these components are sourced from within the US. CESI has already demonstrated success in implementing statistical process control tools and Failure Modes and Effects Analysis (FMEA) to identify and correct production challenges.

### 3.3.3. Production Capacity Constraints

There are no significant capacity constraints in CESI's current production systems. Moreover, the modular design of the CESI catalyst manufacturing operation allows for facile expansion of capacity when the need arises. Larger equipment and the associated issues of equipment redesign and testing are not needed to achieve an increase in Xonon® catalyst production volume. Production capacity is a matter only of throughput rate, not of equipment size. Thus, capacity can be added simply by installing a replicate of the grouping ("cell") of already proven machines. This is reflected in the floor plan shown in Figure 3.3.3.1 for the new CESI manufacturing operation in Gilbert, AZ. In the diagram, CELL 1 will provide the initial supplement to the current production capability in Mountain View, CA (Figure 3.4.2.2). The CELL 1 equipment will match the design of the proven machines now in place in Mountain View. When the business requires further expansion of production, CELL 2 and then CELL 3 can be installed and brought on line at the Gilbert site. Process development activities will continue to be carried out in Mountain View.

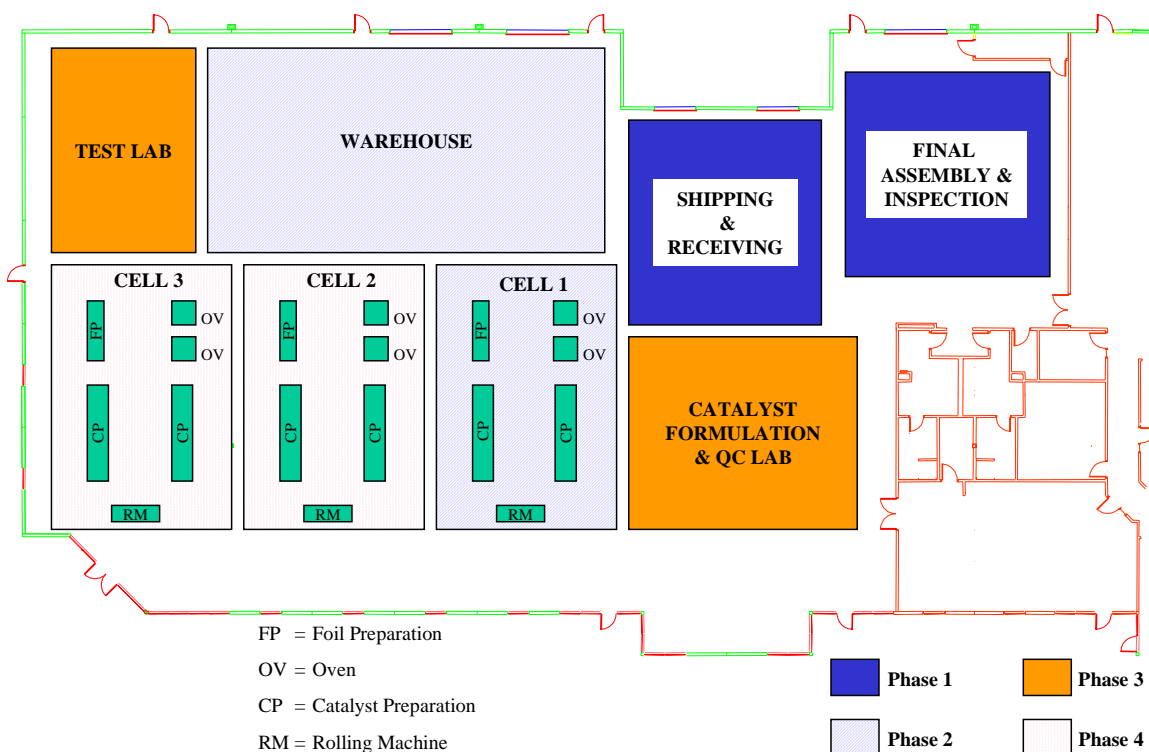


Figure 3.3.3.1 -- Floor plan of Catalytica Energy Systems, Inc. manufacturing facility in Gilbert, AZ

### 3.3.4. Identification of Hazardous or Non-recyclable Materials.

There are currently no hazardous or non-recyclable materials in CESI's Xonon® catalytic combustion systems.

### **3.3.5. Projected Product Cost**

Many factors, some within and some outside of CESI's control, will affect the cost of the Xonon® module and the associated combustion system. Certain of the factors are typical of any manufacturing process:

- Module size
- Raw materials costs
- Unit production volume
- Selling, general, and administrative costs incurred by CESI

For the Xonon® system, the interplay between the module design (and, thus, cost) and the requirements of each individual gas turbine adds an extra dimension of complexity to the estimation of product cost for a given application. Specifically,

- Different combustor configurations (e.g., single combustor, multi-combustor, or annular) can be used to generate the same turbine power output. The design and cost of the catalyst module(s) for the turbine's combustion system will depend heavily upon the configuration chosen.
- Even for a given combustor configuration, each turbine model requires a unique Xonon® module design. Besides the turbine size (commonly expressed as the maximum electrical power output), the individual sets of temperatures, pressures, and air flow rates that define each turbine's operating cycle are critical parameters for designing the catalyst module(s).
- The product that is marketed to the end user is the complete gas turbine, not simply the Xonon® module produced by CESI. Thus the turbine manufacturer, not CESI, dominates the cost and pricing features of installing Xonon® technology.

In spite of the complexities and uncertainties, CESI recognizes the Commission's desire to have a basis for estimating the commercial implications of applying Xonon® technology to the gas turbine market. With the caveats listed above, then, CESI has projected a production "should cost" for three turbine size classes, based upon each Xonon® module being in full-scale production. The cost of the Xonon® modules is expressed as a range due to the reasons outlined above, so the values are rough order of magnitude figures and should be used for informational purposes only.

- Small Turbines (1 - 15 MW) = \$10,000-\$13,000/MW on an average basis.
- Medium Turbines (15 - 60 MW) = \$7,000-\$9,000/MW on an average basis.
- Large Turbines (60 -170 MW) = \$4,000-\$6,000/MW on an average basis

### **3.3.6. Commercialization Investment**

CESI plans to spend \$10M to launch the commercial product, which includes \$6M for new equipment and \$4M for establishing the manufacturing facilities.

### **3.3.7. Production Implementation Plan**

CESI plans to begin high-volume production 1Q 2003. In order to meet this date, we are currently focusing our efforts in the following areas:

- (1) Upgrade of existing manufacturing equipment in Mountain View;
- (2) Development and testing of next-generation catalysts in Mountain View;
- (3) Development of new high-volume production equipment for Gilbert, AZ; and
- (4) Competitive quoting and developing multiple ISO certified sources for all parts.

CESI currently has enough capacity in Mountain View to meet expected demands for at least the next two years and have designed the facility (Figure 3.4.3.1) in a modular manner to facilitate further expansion quickly. Development of the new Gilbert facility will allow CESI to meet all of our sales forecasts for the foreseeable future.

### **3.4. Benefits to California**

Catalytic combustion systems provide ultra-low emissions levels of pollutant species such as NO<sub>x</sub>, CO and UHC. This allows the development of distributed power systems in urban and suburban areas throughout much of California. Today most of these areas have emission regulations sufficiently severe that gas turbines using conventional combustion systems cannot be used without the use of exhaust gas clean-up systems. One such system is selective catalytic reduction or SCR, which catalytically reduces NO<sub>x</sub> with ammonia gas that is injected into the exhaust stream ahead of the SCR catalyst. The economies of scale of SCR systems impede its use on small gas turbines, typical of the size turbine that would be used in distributed power scenarios, as the much larger percentage of added cost (capital and operating) from SCR render power generation with small engines uneconomical. This economic penalty has largely eliminated the use of small gas turbine power generation in areas with severely restrictive emission regulations.

Catalytic combustion systems can break this paradigm by providing NO<sub>x</sub> levels as low as or lower than those provided by SCR at a cost that is significantly lower for all sizes of gas turbine generation units. This breakthrough allows the distributed power concept to become reality in areas of California. The approval for use as an alternative BACT system (in progress), requires demonstration of the practicality (*i.e.*, durability and fuel flexibility) of the catalytic combustion system. The results of this project demonstrate the ability to operate on natural gas with the range of compositions delivered to California cities, allowing gas turbines to penetrate this emerging and very important power generating market segment in California.

Program success will lead to the economic viability of small gas turbines in distributed power generation that locates generating systems at or near the point of end use. Power generation in this manner will provide, by minimizing the costs of transmission and distribution, lower electricity prices to the consumer. Also, locating the generation at the “end-of-line” in industrial or institutional facilities accommodates cogeneration, or the use of the exhaust heat from the turbine to replace heat that would otherwise be obtained from a separate burner. Cogeneration is a much more efficient method of fuel conversion, and not only consumes less fuel, but produces lower emissions. Distributed power generation will also improve the reliability of the power supply network, thus avoiding widespread planned or unplanned interruptions in power delivery.



### 3.4.1. Economic and Energy Benefits<sup>19</sup>

The successful commercialization of catalytic combustion technology will bring significant economic and energy benefits to the California consumer including:

- Xonon®-equipped turbines will meet the regulatory BACT requirements and will create no new environmental or safety issues, so permitting will be simple and straightforward.
- Enhanced air quality as new gas turbines with ultra-low emissions are installed to increase generating capacity and/or to replace older turbines and diesel engines.
- Reduced risk of exposure to the toxic materials associated with exhaust gas cleanup technologies (like SCR).
- Reduced cost of electricity due to the reduced cost of complying with environmental regulations.

Accelerated installation of high-efficiency co-generation facilities due to the environmental friendliness and straightforward permitting of Xonon®-equipped turbines in locations near the end-users. Increased efficiency translates into lower production of greenhouse gases (mostly CO<sub>2</sub>) per unit of turbine output.

Improved reliability of the electric power infrastructure due to expansion of distributed generation capacity, thus discouraging users from installing emergency generators (typically high-polluting diesels) to ensure a stable supply of electricity

This section quantifies the economic, energy, and environmental benefits associated with use of the Xonon® catalytic combustion technology compared with the more costly DLN plus SCR. As discussed in Section 3.2.1.4, a CHP site can generate power more cheaply using the Xonon® technology than with SCR. This cost reduction saves money for each site operating a CHP system using the technology. In addition, applications that are uneconomic or marginal with SCR may become economic using Xonon®. The estimate of annual user and energy savings is shown in Figure 3.4.1.1. The figure shows the annual stream of user benefits from CHP systems using either DLN/SCR or Xonon® for emissions control based on the market penetration estimates shown in the previous section. As market penetration increases, the cumulative number of operating CHP systems also increases providing users with reduced energy costs. By 2017, in the SCR case, users will save \$709 million in meeting their energy needs. In the Xonon® case, this figure increases to \$977 million/year.

The total sum of benefits (the area under the curve) is over \$10 billion for the Xonon® based market penetration case. This figure is nearly \$3 billion greater than in the DLN/SCR penetration case. The net present value today, using a 10 percent discount rate, of the increased future stream of savings due to Xonon® is over \$1 billion. These savings correspond directly to increased productivity for California’s commercial and industrial sectors – money that can go into newer processes, more equipment, more workers, etc., rather than into meeting energy bills.

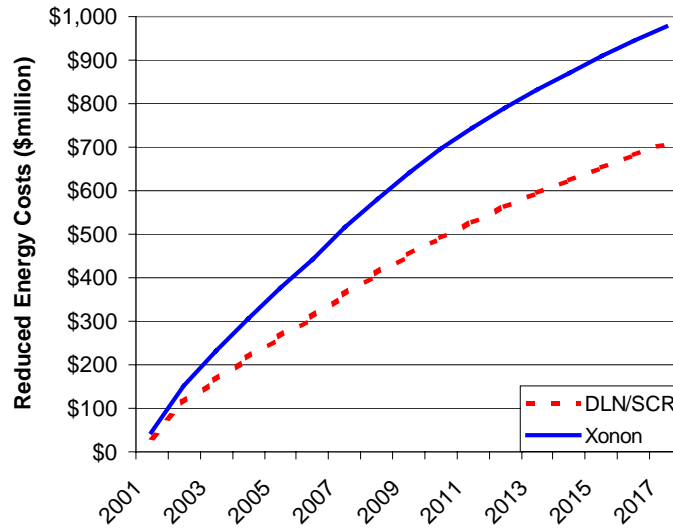


**Figure 3.4.1.1 -- Comparison of Annual User Benefits for CHP Sites based on the SCR and Xonon® Market Penetration Rates**

Figure 3.4.1.2 shows the annual stream of energy savings due to CHP in the two market scenarios. CHP systems use less energy than central station power plants and separate boilers because the exhaust heat is utilized productively in meeting onsite thermal needs rather than being wasted as it is in central power stations. Future market penetration will be greater using the less costly Xonon® technology; therefore, the total market energy savings will be greater. The total energy savings from CHP using Xonon® technology over the forecast period equal about 2 quads of energy. The differential energy savings due to Xonon® are on the order of 0.3 quads.

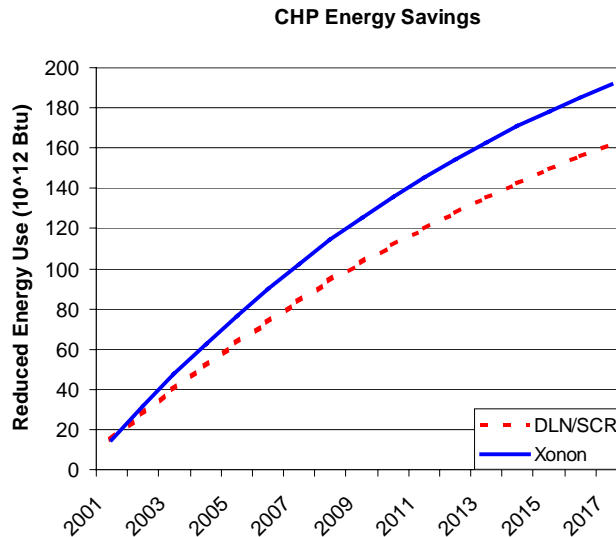


**Figure 3.4.1.2 -- Comparison of Annual Energy Savings for CHP Sites based on the SCR and Xonon® Market Penetration Rates**

Apart from the user savings already quantified, energy savings represent a social benefit in lowering the pressure on fuel and electricity supply and infrastructure, thereby providing lower prices for all consumers. In addition, lowered energy use helps to reduce CO<sub>2</sub> emissions that contribute to global warming. These impacts are difficult to quantify, but represent at least part of the motivation behind social goals, evident in California, to increase the efficiency of energy utilization.

### 3.4.2. Environmental Benefits<sup>20</sup>

The DLN/SCR and Xonon® technologies compared for this analysis were set to provide the same level of NO<sub>x</sub> emissions; therefore, one might expect that there is no change in environmental impact. However, the CHP systems, either with DLN/SCR or Xonon®, provide an environmental benefit compared with the emissions produced by central station power plants and the on-site boiler emissions. To the extent that the Xonon® technology encourages greater CHP market penetration, these environmental benefits are correspondingly increased.

Two cases of environmental benefit were examined. In the first case the values for average California central station emissions and boiler emissions from a previous California Air Resources Board (CARB) study<sup>21</sup> were used in the analysis. The average NO<sub>x</sub> emissions from the California utility industry are 0.13 lbs/MWh. The avoided boiler emissions, as defined in the CARB study are 0.098 lbs/MMBtu. In the second case, we used a NO<sub>x</sub> emissions standard of 0.05 lbs/MWh as a representative measure of the NO<sub>x</sub> emissions from a state-of-the-art combined cycle power plant. (Note: A NO<sub>x</sub> limit of 0.05 lbs/MW-hr was initially proposed for 2007 in the SB 1298 regulation. The final approved value in SB 1298 was 0.07 lbs/MW-hr, as shown in Table 3.2.1.3.1. The cost analysis discussed below was completed before SB 1298 was

released in its final form.) For the avoided boiler emissions, a value of 0.035 lbs/MMBtu representing low NO<sub>x</sub> burners and flue gas recirculation was used.

The net change in NO<sub>x</sub> emissions for each scenario is based on the following:

- $\text{CHP Generation} = \text{Cumulative CHP capacity additions} \times \text{hours of use in each size class (approximately 7000)}$
- $\text{Avoided Utility Generation} = \text{CHP Generation} \times (1 + \text{line loss percent (6 percent)})$
- $\text{Avoided Boiler Fuel} = \text{CHP Generation} \times \text{thermal energy per kWh} / \text{Boiler efficiency (80-85 percent)}$

Table 3.4.2.1 shows the NO<sub>x</sub> emissions impacts of the two emissions control strategy market penetration scenarios using the CARB study values for avoided generation and boiler emissions described above. In this case, the emissions from the CHP systems are cleaner than the corresponding existing generation that is being avoided. In addition, the on-site CHP systems emit only one-sixth of the NO<sub>x</sub> of the boiler systems that they are replacing. In this comparison, overall NO<sub>x</sub> emissions reductions from CHP implementation are expected to reach 9,587 tons/year in the DLN/SCR market penetration scenario. The Xonon® market penetration scenario reduces emissions by 11,443 tons/year – a net decrease of 1,855 tons/year.

**Table 3.4.2.1 -- NO<sub>x</sub> Emission Reductions for the DLN/SCR and Xonon® CHP Market Penetration Scenarios based on Backing out Existing Boiler and Generation Technology**

	<b>CHP Category by Size</b>	<b>Cumulative Penetration in MW</b>	<b>CHP Emissions tpy</b>	<b>Boiler Emissions tpy</b>	<b>Utility Emissions tpy</b>	<b>Net Change tpy</b>
<b>SCR Case</b>	1-5 MW	10	4.4	29.4	4.4	-29.4
	5-20 MW	522	191.7	1,091.60	237.9	-1,137.80
	> 20 MW	4,056	1,396.00	7,969.30	1,847.40	-8,420.70
	Total	4,587	1,592.20	9,090.30	2,089.70	-9,587.80
<b>Xonon® Case</b>	1-5 MW	66	30.5	201.5	30.2	-201.3
	5-20 MW	757	277.9	1,581.80	344.7	-1,648.70
	> 20 MW	4,620	1,590.40	9,078.90	2,104.60	-9,593.10
	Total	5,443	1,898.70	10,862.20	2,479.50	-11,443.00

### **3.4.3. State and Local Economic Impact**

There will likewise be private benefits to the companies and individuals involved in manufacturing, marketing, and using the turbines equipped with catalytic combustors. Specific benefits will include:

- Increased employment opportunities as a result of business growth at manufacturers of small turbines and components for catalytic combustion.
- Increased tax revenues associated with the business activities of manufacturing, installing, and servicing the new Xonon®-equipped turbines.
- Reduced costs for industrial users of electricity and, in co-generation applications, heat .
- Decreased need for backup power provisions and the associated investments.
- Increased revenues for suppliers of turbines, parts, and services.

#### 4.0 Conclusions and Recommendations

CESI has completed a three-year program to develop and test a pre-production catalytic combustion system on gas fired turbine platform. The system performed well and met many of the program goals and objectives. Some additional development work needs to be completed on selected individual components in order to validate durability estimates. Some of the key overall program conclusions are:

- The Xonon® catalytic combustion system demonstrated ultra-low levels of NO<sub>x</sub>, CO and UHC emissions for 8,128 hours of on-grid operation.
- The Xonon® catalytic combustion system demonstrated a reliability of 99.2 percent (goal 98 percent) and an availability of 91.2 percent (goal of 96 percent).
- The Xonon fuel control system is now able to adjust to load loss, large load step increases and grid resynchronization without loss of stability.
- The axial catalyst support did not have the required durability to meet the 8,000-hour life goal. A new support system was designed and is currently being tested in the RAMD engine test bed.
- The new axial fuel/air mixer design did not meet the goal for mixing uniformity. As a result, the current radial swirler was kept as the primary design for the RAMD testing.
- Some new catalyst formulations showed early promise during short-term testing; however, long-term test results showed that the new formulations were inferior to the current catalysts.
- An increase in the concentration of heavy hydrocarbons shifts the catalyst's operating window and moves the homogeneous combustion wave front closer to the catalyst outlet face. These changes in operational characteristics should not adversely affect the catalyst module if the proper control logic is in place.
- The Xonon® combustion technology is positioned to capture a significant portion of new pollution control business for the small to medium size gas turbine market.
- The growth in new gas fired turbine projects is projected to be 13 percent per year on a compounded basis.
- Xonon® offers several competitive advantages over other pollution control technologies. These include:
  - Lower initial capital acquisition costs
  - Lower operational costs
  - Shorter permitting time
  - Ultra-low emissions (NO<sub>x</sub> < 3 ppmv, CO < 5 ppmv, UHC < 5 ppmv)
  - Xonon® is a pollution prevention technology instead of a pollution clean-up technology

- Xonon® modules are recyclable and do not use the environmentally hazardous chemicals (like ammonia) utilized by emission clean up technologies
- CESI is committed to the commercialization of Xonon® and has allocated significant financial resources to improving CESI's manufacturing infrastructure and facilities.

## 5.0 Glossary

<b>40 CFR</b>	US Code of Federal Regulations Title 40 contains all Federal environmental regulations
<b>Activity Test</b>	Regular testing is conducted to assess the condition of the catalyst module. The test procedure involves incrementing the catalyst inlet temperature, and then varying the engine load to establish the envelope for operation within the emissions limits.
<b>BACT</b>	Best Available Control Technology
<b>BMM</b>	Bonded Metallic Monolith – the first-generation, honeycomb-like axial retainer
<b>BOZ</b>	Burn Out Zone – area where the combustion process is completed
<b>CAA</b>	Clean Air Act
<b>CARB</b>	California Air Resources Board
<b>CESI</b>	Catalytica Energy Systems, Inc.
<b>CEMS</b>	Continuous Emissions Monitoring System
<b>CFD</b>	Computational Fluid Dynamics
<b>CGA</b>	Cylinder Gas Audit, as defined by the CEMS QA/QC plan.
<b>Corrected Emissions</b>	Actual stack emission concentrations are corrected to 15 percent O <sub>2</sub> on a dry basis. The procedure for this correction is contained in 40 CFR 60.335.
<b>CO</b>	Carbon Monoxide
<b>Daily Calibration</b>	The CEMS undergoes an automatic calibration check each day at 6:00 AM to assess the zero and span drift. One or two 15 minute averages are lost each day because of the calibration.
<b>DAS</b>	Data Acquisition System



<b>DG</b>	Distributed Generation
<b>DLN</b>	Dry Low NO <sub>x</sub> – a lean pre-mix combustor technology to reduce emissions
<b>DOE</b>	Department of Energy
<b>EPAG</b>	Environmentally Preferred Advanced Generation
<b>EGT</b>	Exhaust Gas Temperature. This is the limiting parameter for gas turbine power. The turbine control system uses measured EGT to adjust the fuel schedule for operation at maximum design capacity under normal operating conditions
<b>Event</b>	Any abnormality in operation that warrants an explanation.
<b>Load Step Test</b>	Regular testing is conducted to assess the condition of the catalyst module. This test involves incrementing the engine load, and collecting data to assess the level of conversion in the catalyst module.
<b>FID</b>	Flame Ionization Detector
<b>FOH</b>	Forced Outage Hours – Hours when the unit is not available due to a condition beyond the control of the operator which requires that the condition be corrected before the end of the next weekend.
<b>FOR</b>	Forced Outage Rate
<b>FSNL</b>	Full Speed No Load - engine operating at 100 percent speed with no load
<b>IR</b>	Infra-Red
<b>KHI</b>	Kawasaki Heavy Industries
<b>LAER</b>	Lowest Achievable Emission Rate
<b>MARAMA</b>	Mid-Atlantic Regional Air Management Association
<b>MTBO</b>	Mean Time Between Overhaul

<b>MTTR</b>	Mean Time To Repair
<b>Maximum Design Capacity</b>	The maximum power that the turbine can produce at the prevailing ambient conditions (primarily temperature)
<b>NAAQS</b>	National Ambient Air Quality Standards
<b>NESCAUM</b>	Northeast States for Coordinated Air Use Management
<b>Normal Operation</b>	Full load (over 98 percent of capacity) and steady state.
<b>NO<sub>x</sub></b>	Nitric Oxides
<b>PH</b>	Period Hours – Hours when the unit is in the configuration necessary to support the test objective, whether actually operating or not.
<b>POH</b>	Planned Outage Hours – Hours when the unit is not available for operation due to a shutdown that has been defined in advance
<b>OD</b>	Outer Diameter
<b>QA/QC Plan</b>	Quality Assurance / Quality Control plan for the emission monitoring system (40 CFR 60 Appendix F)
<b>RAMD</b>	Reliability, Availability, Maintainability, Durability
<b>RATA</b>	Relative Accuracy Test Audit is performed annually as defined by the CEMS QA/QC plan.
<b>Rolling Average</b>	Calculated each 30 minutes using the last 2 (for 1 hour) or 6 (for 3 hour) 30-minute data records. No rolling average is shown unless there is data for the entire averaging period.
<b>RF</b>	Reliability (Factor)
<b>RSH</b>	Reserved Shutdown Hours – Hours when the unit is available for operation according to the test objective, but is currently shutdown by choice

<b>MOH</b>	Maintenance Outage Hours
<b>SCR</b>	Selective Catalytic Reduction – a form of emission clean up technology
<b>SH</b>	Service Hours
<b>SVP</b>	Silicon Valley Power
<b>THC</b>	Total Hydrocarbons
<b>TNRCC</b>	Texas Natural Resource Conservation Commission
<b>UHC</b>	Unburned Hydrocarbons
<b>Xonon®</b>	CESI's flameless combustion system for NOx control

## 6.0 Notes and References

### Notes

- <sup>1</sup> Chuck Simchick, *Technical and Cost Replan of Durability of Catalytic Combustion Systems Project*, California Energy Commission Report, (May 1999).
- <sup>2</sup> Abbott and von Doenhoff, *Theory of Wing Sections*, 1949.
- <sup>3</sup> Computational Dynamics, "STAR\*CD Version 3.05a User's Manuals", (London, England, 1998).
- <sup>4</sup> Norris, L. H. and Reynolds, W. C., "Turbulent Channel Flow with a Moving Wavy Boundary", Report No. FM-10, Dept. of Mechanical Engineering, Stanford University, (1975).
- <sup>5</sup> Chen, Y. S. and Kim, S. W., "Computation of Turbulent Flows Using an Extended k-epsilon Turbulence Closure Model, NASA CR-179204, (1987).
- <sup>6</sup> Armaly et al., "Experimental and Theoretical investigation of backward-facing step flow", J. Fluid Mech. 127, pp. 473-496, (1983).
- <sup>7</sup> Chen, C-J and Jaw, S-Y, *Fundamentals of Turbulence Modeling*, (Taylor & Francis, 1998), 158-159.
- <sup>8</sup> Abott, D. E. and Kline, S.J., "Experimental investigation of subsonic flow over single and double backward facing steps", J. Basic Engineering (1992), 84, 317-325.
- <sup>9</sup> Liss, W. E. *et al.*, *Variability of Natural Gas Composition in Select Major Metropolitan Areas of the United States*, Gas Research Institute Report PB92-224617, (1992).
- <sup>10</sup> U.S. Bureau of Mines, *Analyses of Natural Gases*, (Amarillo, TX.1991), PB92-154863, 1986-1990.
- <sup>11</sup> Palais de la Decouverte, Revue, vol. 4, (4/1976).
- <sup>12</sup> Esselte Forlag, (1982).
- <sup>13</sup> Sample Data – Tulsa, OK 4/97-12/97, Silicon Valley Power data 11/98.
- <sup>14</sup> Energy Nexus Group, interview with Pacific Gas and Electric, (12/1993-7/1994, 6/1999-12/1999).

### References for Section 2.3 --- Commercialization Potential

*Market Assessment of Combined Heat and Power in the State of California*, California Energy Commission, Onsite Energy Corporation, September 2, 1999.

*Air Pollution Emission Impacts Associated with Economic Market Potential of Distributed Generation in California*, California Air Resources Board and the California Environmental Protection Agency, Distributed Utility Associates, June 2000.

*Cost Analysis of NO<sub>x</sub> Control Alternatives for Stationary Gas Turbines*, November 1999, ONSITE SYCOM Energy Corp. report to U.S. Department of Energy, 1999.

---

The Market and Technical Potential for Combined Heat and Power in the Commercial/Institutional Sector, *ONSITE SYCOM Energy Corp. report to U.S. DOE/Energy Information Administration, January 2000*

The Market and Technical Potential for Combined Heat and Power in the Industrial Sector, *ONSITE SYCOM Energy Corp. report to U.S. DOE/Energy Information Administration, January 2000*

Reciprocating Engines for Stationary Power Generation: Technologies, Products, Players, and Business Issues, *SFA Pacific for GRI, Chicago, IL and EPRIGEN, Palo Alto, CA, GRI-99/0271 & EPRI TR-113894, December 1999.*

Major, W., and Davidson, K., *Gas Turbine Power Generation Combined Heat and Power Environmental Analysis and Policy Considerations*, prepared for DOE Office of Industrial Technologies and Gas Research Institute, November 1998.

*Opportunities for Micropower and Fuel Cell Gas Turbine Systems in Industrial Applications*, DOE/ORE 2095, Arthur D. Little, Inc., January 2000.

Energy Information Administration, *Manufacturing Consumption of Energy 1994*, DOE/EIA-0512 (94), Washington, DC, December 1997.

*Commercial Buildings Energy Consumption Survey, 1995*, U.S.DOE, Energy Information Administration, Washington, DC, 1998.

*Independent Power Database*, Hagler-Bailly Consulting Inc, Arlington, VA, 1999.

California Air Resources Board website, [www.arb.ca.gov](http://www.arb.ca.gov).

Texas Natural Resources Conservation Commission website, [www.trncc.state.tx.us](http://www.trncc.state.tx.us).

*Industrial Applications for Micropower: A Market Assessment*, DOE/ORE 2096, Resource Dynamics Corporation, January 2000.

*Collaborative Report and Action Agenda*, California Alliance for Distributed Energy Resources, January 1998.

Liss, W.E., Kincaid, D.E., *Distributed Generation Using High Power Output, High Efficiency Natural Gas Engines*, Gas Research Institute, American Power Conference, 1999.

Solt, C., *The Ultimate NO<sub>x</sub> Solution for Gas Turbines*, ASME 98-GT-287, 1998.

Bautista, P.J., "Rise in Gas-Fired Power Generation Tracks Gains in Turbine Efficiency," *Oil & Gas Journal*, August 12, 1996.

"Annual Survey of Engine Sales," *Diesel & Gas Turbine Worldwide*, October 2000.

2000-2001 Gas Turbine World Handbook, Pequot Publishing, 2000.

*Diesel & Gas Turbine Worldwide Catalog: Product Directory & Buyers Guide*, Brookfield, Wisconsin, 1999.

SOAPP-CT.25 Workstation: Version 1, SEPRIL, 11c, January 1999.

---

<sup>15</sup> “Annual Survey of Engine Sales,” *Diesel & Gas Turbine Worldwide*, (October 2000).

<sup>16</sup> *Ibid.*

<sup>17</sup> *Ibid.*

<sup>18</sup> Onsite Energy Corporation report to the California Energy Commission, *Market Assessment of Combined Heat and Power in the State of California*, California Energy Commission, Onsite Energy Corporation, September 2, 1999. (September 2, 1999).

<sup>19</sup> Appendix I, 54-62.

<sup>20</sup> *Ibid*, 60-62.

<sup>21</sup> Joseph Iannucci, *et al.*, *Air Pollution Emission Impacts Associated with Economic Market Potential of Distributed Generation in California*, California Air Resources Board and the California Environmental Protection Agency, Distributed Utility Associates, (June 2000).

## 1.0 Appendix A – Cost Data for Technology Cost and Performance Data Analysis

Cost Category	DLN	DLN/SCR	Xonon
<b>1.5 MW Turbine</b>			
Turbine Package Cost (\$/kW)	\$600	\$600	\$600
CHP Installed Cost exc. emissions control (\$/kW)	\$1,168	\$1,168	\$1,168
<b>Emissions Control Cost Additions</b>			
Direct Capital Cost Additions (\$/kW)	\$56	\$268	\$85
Direct Operating Cost Additions (mills/kWh)	2.8	12.3	4.1
<b>Hidden Cost Additions</b>			
Revenue Lost for Air Permit Delay (\$/kW)	\$123	\$32	\$0
Pressure Drop and Parasitic Power (mills/kWh)	0	1	0
Unscheduled Shutdown (mills/kWh)	0.7	0.8	0.4
Offset Cost (mills/kWh)	4.3	0.4	0.4
<b>Total Emissions Control Costs</b>			
<b>Capital (\$/kW)</b>	<b>\$179</b>	<b>\$300</b>	<b>\$85</b>
<b>Operating Cost (mills/kWh)</b>	<b>7.8</b>	<b>14.6</b>	<b>4.9</b>
<b>5.0 MW Turbine</b>			
Turbine Package Cost (\$/kW)	\$400	\$400	\$400
CHP Installed Cost exc. emissions control (\$/kW)	\$845	\$845	\$845
<b>Emissions Control Cost Additions</b>			
Direct Capital Cost Additions (\$/kW)	\$41	\$141	\$54
Direct Operating Cost Additions (mills/kWh)	1	4.9	3.1
<b>Hidden Costs Additions</b>			
Revenue Lost for Air Permit Delay (\$/kW)	\$138	\$43	\$0
Pressure Drop and Parasitic Power (mills/kWh)	0	0.9	0

Unscheduled Shutdown (mills/kWh)	0.7	0.8	0.4
Offset Cost (mills/kWh)	3.4	0.3	0.3
<b>Total Emissions Control Costs</b>			
<b>Capital (\$/kW)</b>	<b>\$178</b>	<b>\$185</b>	<b>\$54</b>
<b>Operating Cost (mills/kWh)</b>	<b>5.2</b>	<b>7</b>	<b>3.8</b>
<b>15.0 MW Turbine</b>			
Turbine Package Cost (\$/kW)	\$300	\$300	\$300
CHP Installed Cost exc. emissions control (\$/kW)	\$679	\$679	\$679
<b>Emissions Cost Additions</b>			
Direct Capital Cost Additions (\$/kW)	\$37	\$109	\$51
Direct Operating Cost Additions (mills/kWh)	0.7	3.1	3
<b>Hidden Costs</b>			
Revenue Lost for Air Permit Delay (\$/kW)	\$146	\$48	\$0
Pressure Drop and Parasitic Power (mills/kWh)	0	0.9	0
Unscheduled Shutdown (mills/kWh)	0.7	0.8	0.4
Offset Cost (mills/kWh)	3.2	0.3	0.3
<b>Total Emissions Control Costs</b>			
<b>Capital (\$/kW)</b>	<b>\$184</b>	<b>\$157</b>	<b>\$51</b>
<b>Operating Cost (mills/kWh)</b>	<b>4.6</b>	<b>5.2</b>	<b>3.7</b>

### Direct Costs

- Basic turbine package cost

Installed cost of a CHP system, exclusive of environmental control costs

- Added capital costs for the environmental control package selected – DLN, SCR, or Xonon®

Added direct operating costs – labor, contract maintenance, catalysts, parts, materials, added taxes

### Hidden Costs



- *Revenue Lost for Air Permit Delays* – Permitting turbine systems in highly controlled areas such as California and the Northeast using DLN control technology only will become increasingly difficult if not impossible. There will be delays or denial of certification. For DLN plus SCR systems there will likely be delays related to demonstrating the safety of the ammonia handling system. For this comparison, we assumed 9 months was required to certify a DLN system, 5 months for DLN plus SCR system, and 3 months for a Xonon® system.
- *Pressure Drop and Parasitic Power* – The SCR system adds to turbine back pressure and requires additional parasitic power consumption. These losses amount to about a 1.1% reduction in system capacity, and about 0.4% increase in fuel use per unit of output.
- *Unscheduled Shutdown* – DLN systems have had some history of failures due to vibration and flame instability. SCR systems based on DLN will have these same tendencies plus additional risk factors related to the SCR system. It was assumed that the Xonon® system would face fewer unscheduled shutdowns than the DLN or SCR system – only a quarter of one percent of operating hours or about 22 hours/year.
- *Offset Cost* -- Systems in California and in some other markets must provide offsets for added emissions. It was assumed that these offsets would cost \$6,000/ton. Both the SCR and Xonon® systems are designed to control NO<sub>x</sub> down to 2.5 ppm so they have the same offset cost. DLN at 25 ppm will have offset costs that are 10 times higher.

### **Market Penetration Analysis Assumptions**

The Commission CHP market assessment had the following components:

Gas and electric price forecasts through 2017 (updated for this analysis)

Cost and performance estimates for CHP systems in 5 sizes (modified here based on technology estimates developed in Section 2.3.4.)

Prototype customer economic models in these size categories that combine the customer load characteristics, technology cost and performance, and future fuel and power prices to define year-by-year internal rate of return (IRR) estimates (unchanged.)

Remaining technical market potential was determined using a detailed database analysis (unchanged.)

Market penetration was based on the historical rate of market penetration in California during the 1991-1996 period. The market penetration forecast is based on the relationship between the project IRR during the historical period and the IRR figures calculated for each size bin and year. (Some modifications to the prior CEC approach were made to ensure that market penetration rates would not exceed the technical market potential.)

According to the Commission electric price forecast used for the 1999 analysis, average retail commercial costs were expected to drop from 9.2 to 6.2 ¢/kWh and industrial

costs were expected to drop from 6.7 to 4.8 ¢/kWh. Given the price increases that have taken place since this forecast, we assumed that the real price of electricity would be 8.5 ¢/kWh in the commercial sector and 6.5 ¢/kWh in the industrial sector.

The gas price forecast used in the 1999 analysis showed commercial gas prices ranging from \$2.80 to \$3.40/MMBtu and industrial gas prices ranging from \$2.30 to \$3.00/MMBtu over the forecast period. For this analysis we assumed that commercial gas prices would stabilize at \$5.50/MMBtu and industrial gas prices at \$4.50/MMBtu.

The technology/customer performance models were rerun using the new price forecasts and the new technology specifications. The technology specifications were only changed in the sizes appropriate for gas turbines, i.e., 1-5 MW, 5-20 MW, and greater than 20 MW. In these sizes, the industrial power and fuel rates apply.

## **2.0 Appendix B – RAMD Basic Definitions**

### **Deactivated Shutdown**

The unit is not "active", and not intended to be available to support the stated test objective. For purposes here, deactivated shutdown corresponds to those periods of time when the engine is not assembled in the "RAMD configuration"

### **Reserve Shutdown**

The unit is available for operation according to the test objective, but is currently shutdown by choice. A shutdown for customer demo, for example, would be considered a reserve shutdown.

### **In Service**

The unit is operating in the configuration necessary to support the test objective.

### **Planned Outage**

The unit is not available for operation due to a shutdown that has been defined in advance. A specific time duration for advance planning is not defined in the literature, but the intent of the activity should be consistent with the test objectives in order for it to be considered planned. Examples of planned outages would include.

- Site maintenance activities requiring a shutdown
- Inspection of the catalyst axial support structure
- Inspection of key combustor components per recommendation of structural engineer
- Modification of the transition piece to change bypass air
- Installation of upgraded components/control system

Note that the timing is not necessarily defined in advance, but is based on the analysis of data using appropriate guidelines as determined by the team.

### **Basic / Extended Planned Outages**

The predetermined time estimate to execute a planned outage represents the basic planned outage time. If during this planned outage, the actual work takes longer than expected, the remainder of the outage period becomes an extended planned outage. (The distinction is not important for our current purposes, and would primarily come into play when considering maintainability.)

### **Unplanned Outage**

The unit is not available to support the test objectives due to circumstances for which down time could not be, or was not, planned in advance. Unplanned outages are further categorized as either forced or maintenance outages, depending on the urgency

of need for the shutdown. The distinction comes into play if we use the forced outage rate (FOR) to characterize unit reliability.

### **Forced Outage**

The unit is not available due to a condition, beyond the control of the operator, which requires that the condition be corrected before the end of the next weekend. There are various classes defined based on specific time frames, but the distinctions are not currently important for this application. As an example, a high CO condition, which would lead to a permit violation, might force a decision to shutdown immediately.

### **Maintenance Outage**

The unit is not available due to a condition which requires a shutdown prior to the next planned outage, but which can be deferred until after the next weekend. Note that we could choose to shutdown sooner (even immediately), but if the unit could operate satisfactorily in a way consistent with the test objectives beyond the next weekend, it is considered a planned outage.

### **Period Hours**

This is the total time span of interest, during which the unit configuration can support the intended test objective. It consists of available and unavailable time. The remainder of the calendar time would be considered deactivated shutdown hours.

Period Hours (PH) = Service Hours (SH)

- + Reserve Shutdown Hours (RSH)
- + Planned Outage Hours (POH)
- + Forced Outage Hours (FOH)
- + Maintenance Outage Hours (MOH)

### 3.0 Appendix C – RAMD Emission Results

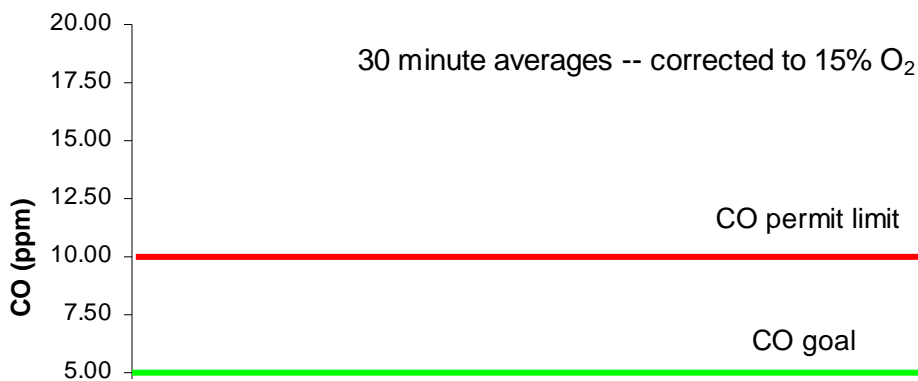
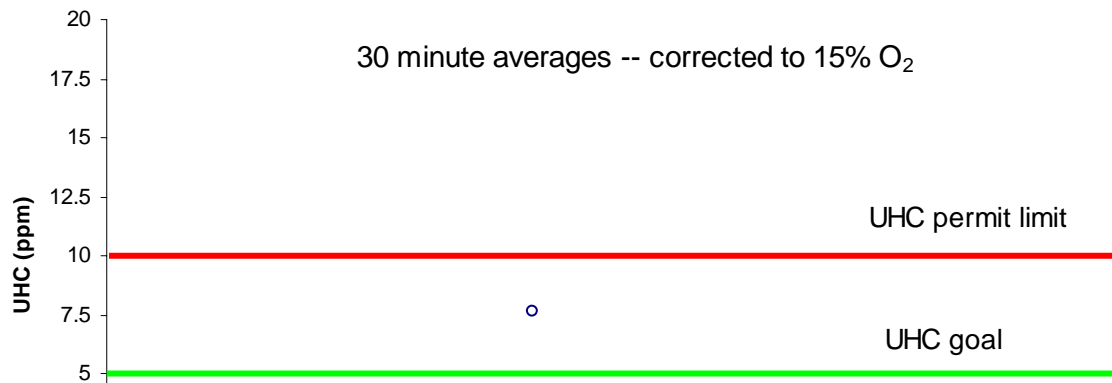
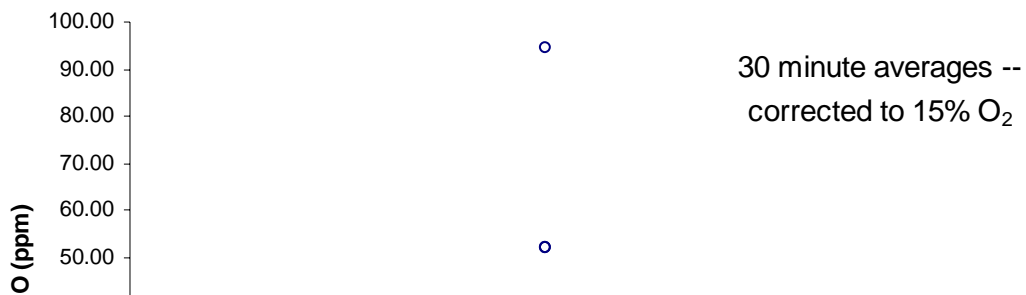
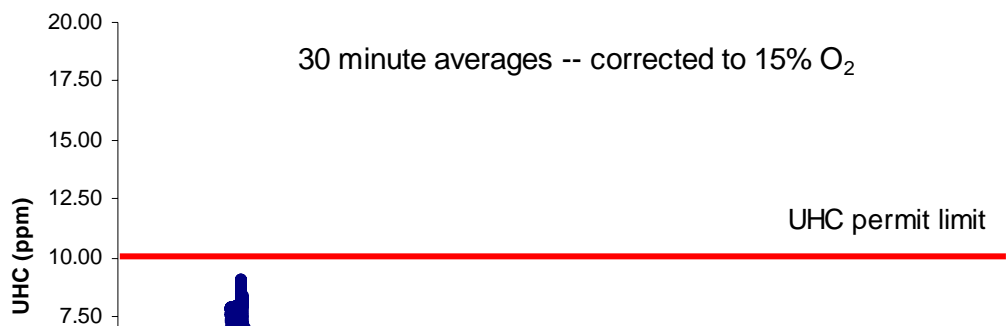
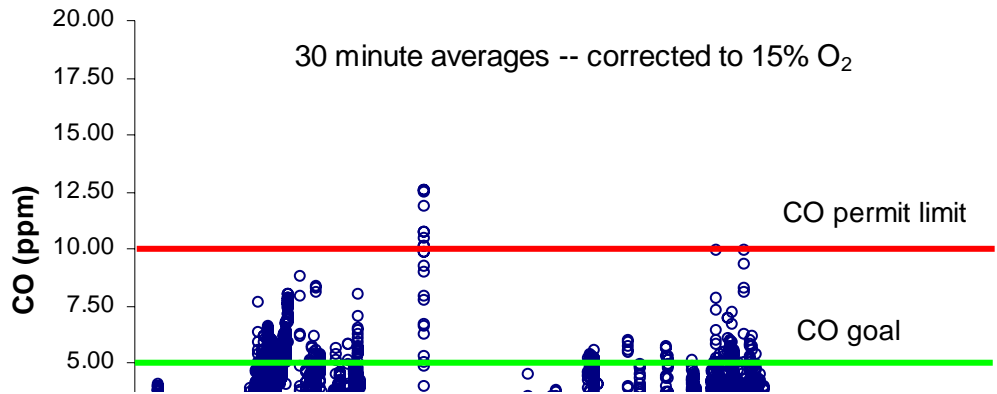
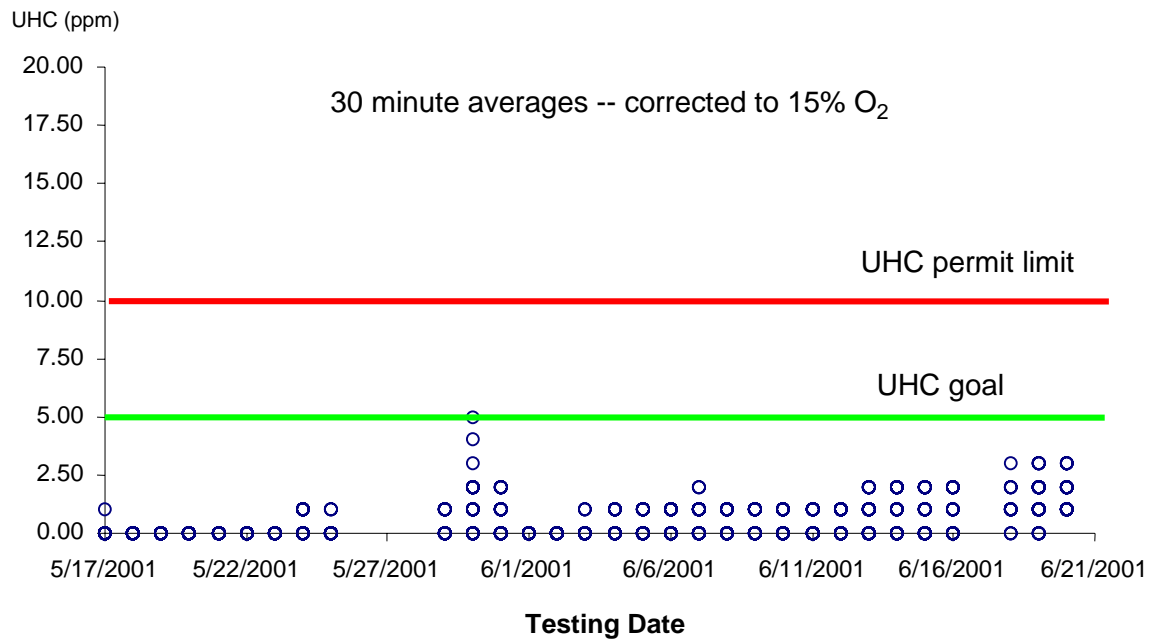


Figure C5 -- Phase III CO emissions results (30 minute averages)



## 4.0 Appendix D – Axial Retainer Material Test Results

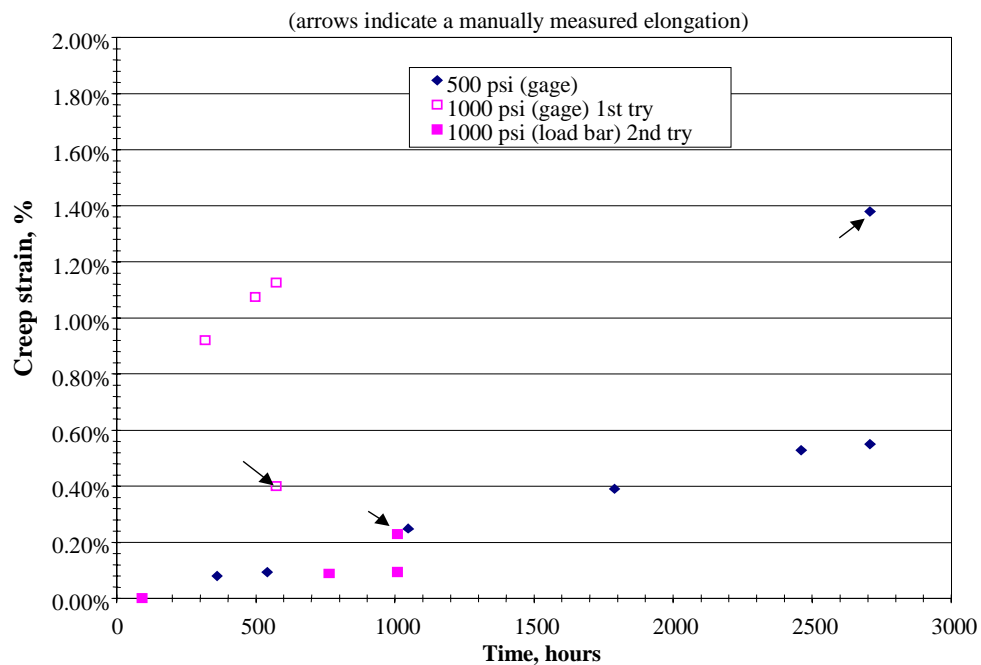


Figure D1 -- Creep results of H214 foils done at 1562 F (850C)

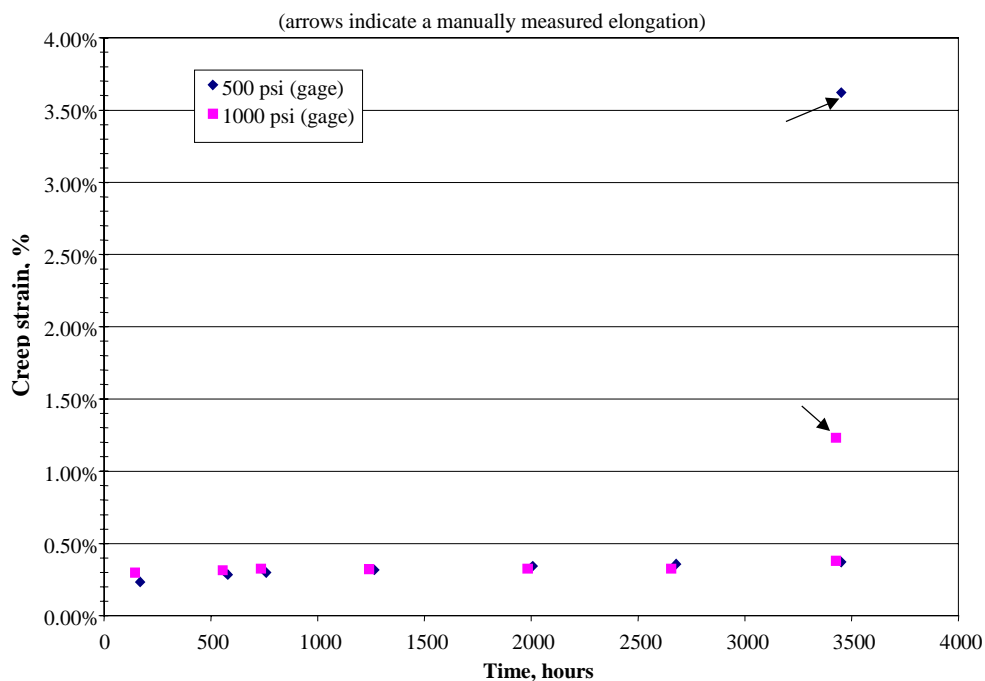


Figure D2 -- Creep results of H214 foils done at 1652 F (900C)

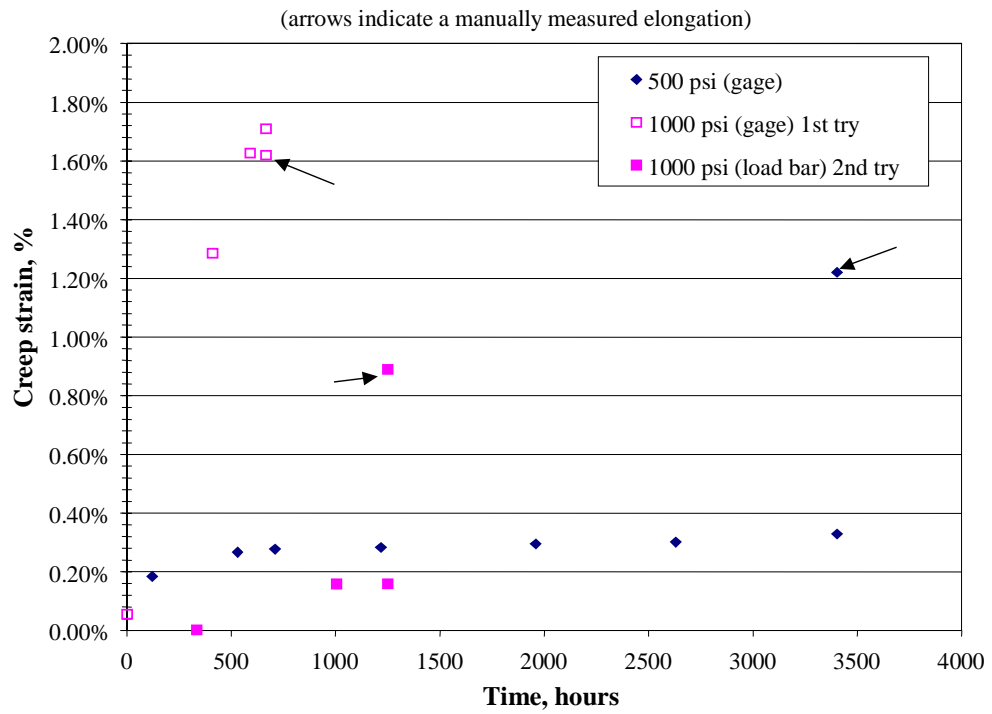


Figure D3 -- Creep results of H214 foils done at 1742 F (950C)



## 5.0 Appendix E – Fuel/Air Premixer Figures

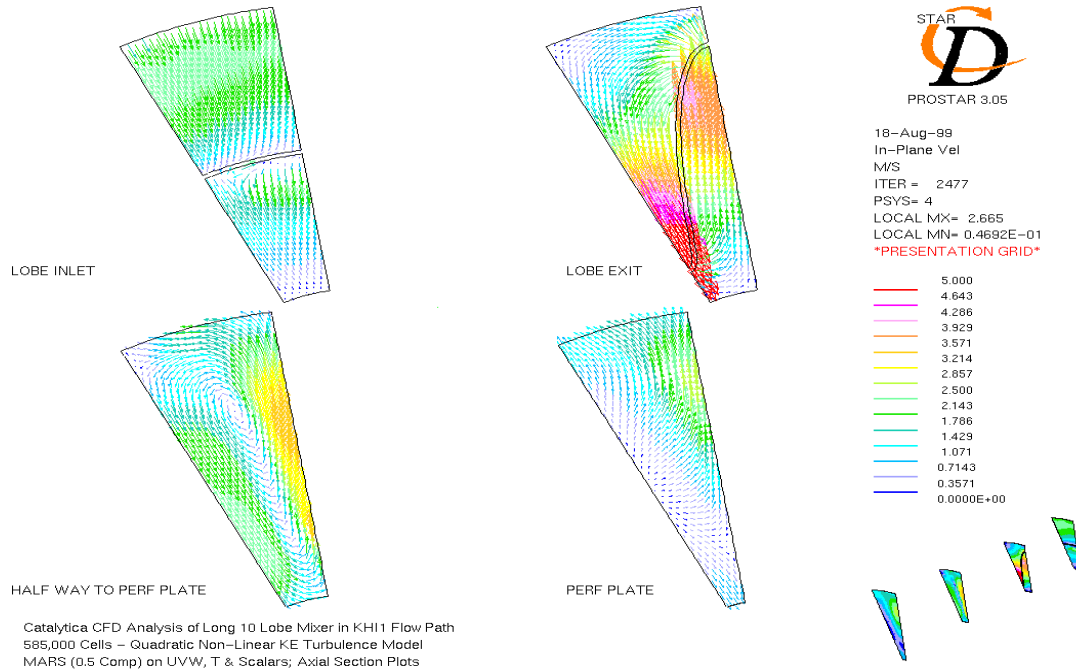


Figure E1 -- Ten Lobe Mixer In-Plane Velocities

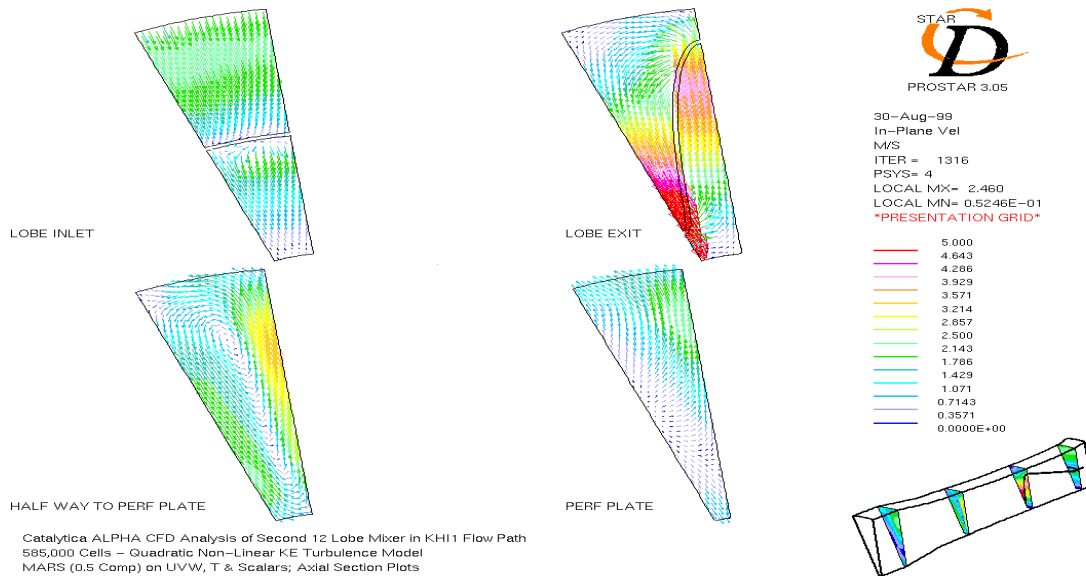
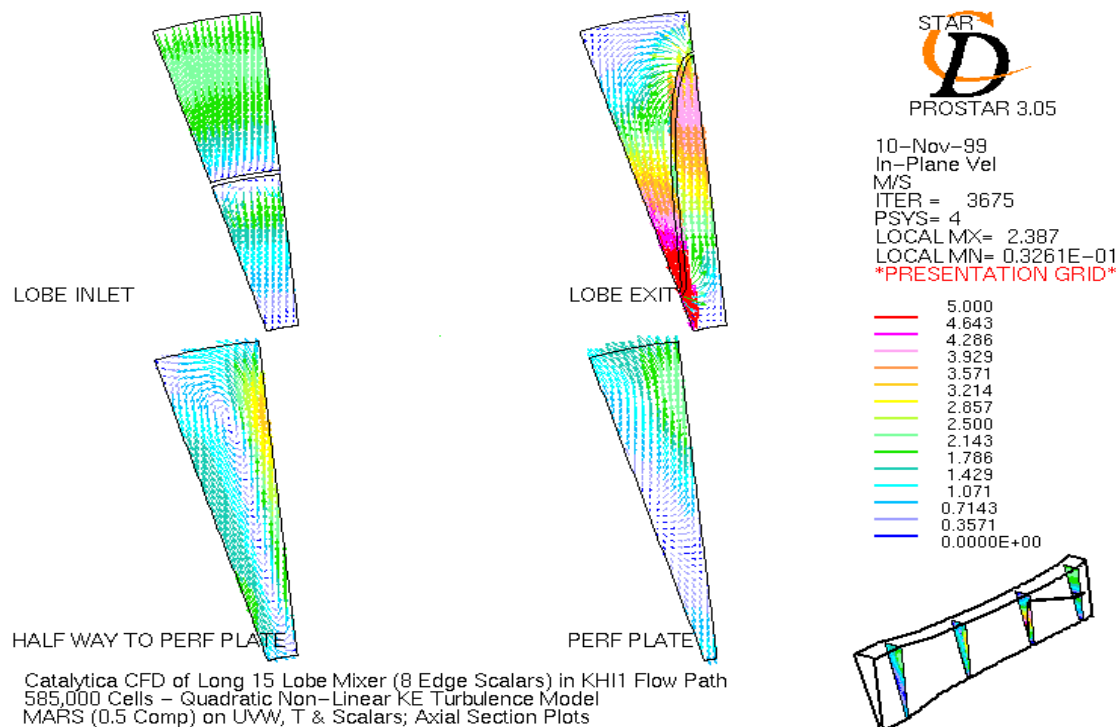
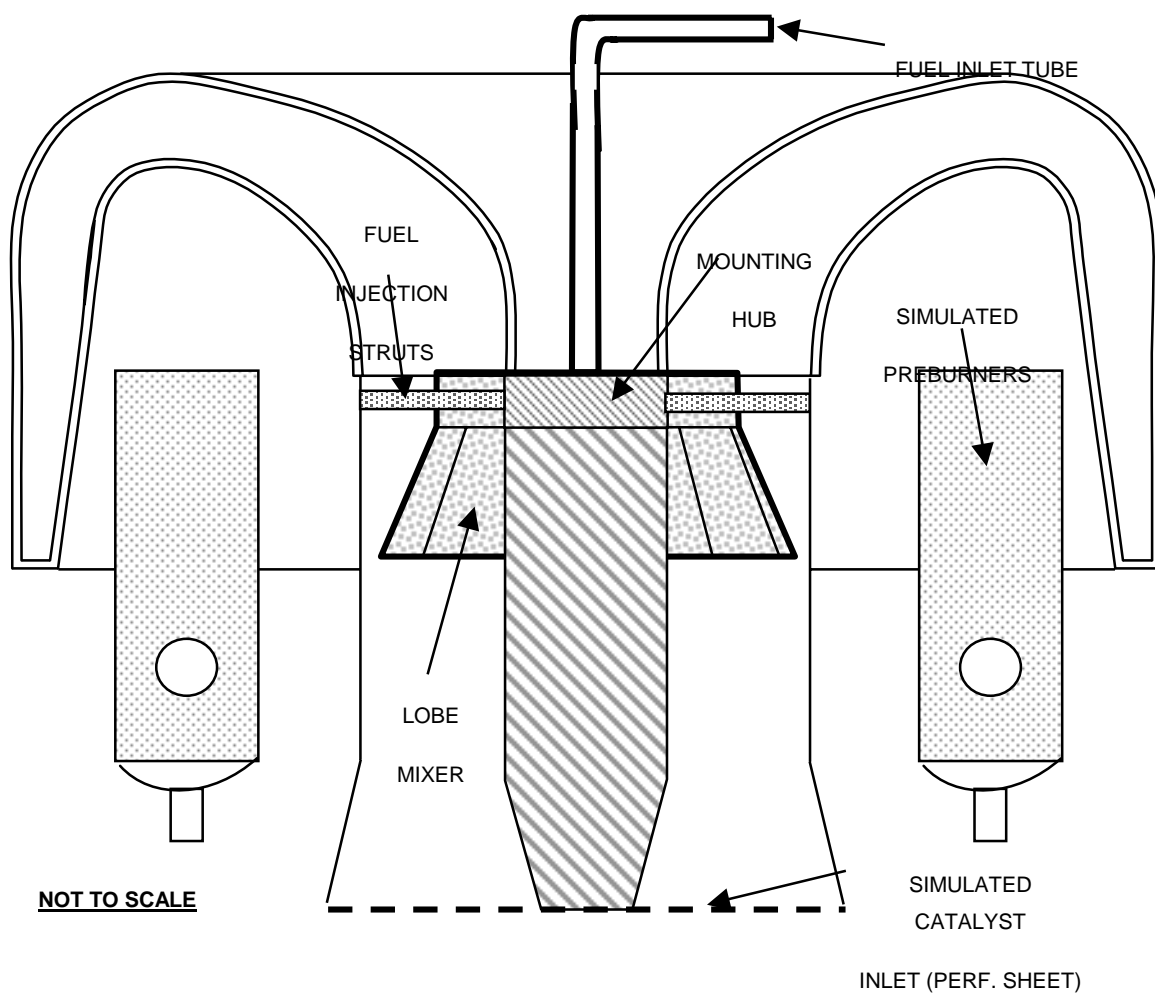


Figure E2 -- Twelve Lobe Mixer In-Plane Velocities



*Figure E3 -- Fifteen Lobe Mixer In-Plane Velocities*

Figure E4 - CS view of lobe mixer installed in cold flow rig



Block	Temp (F)	Pressure (atm)	Velocity (ft/s)	Predicted WE Limit*	Measured WE Limit	Repeated Points	Corrected Measured WE Limit	Corrected Repeated Points
.25"	600	2	100	0.494	0.690	0.730	0.483	0.511
	600	2	200	0.550	N/A		N/A	
	600	7	100	0.470	0.580		0.406	
	600	7	200	0.523	0.780		0.546	
	750	2	150	0.471	0.670		0.469	
	750	4.5	100	0.429	0.600		0.420	
	750	4.5	150	0.456	0.520		0.364	
	900	2	100	0.398	0.620		0.434	
	900	2	200	0.443	0.660		0.462	
	900	7	100	0.379	0.430		0.301	
	900	7	200	0.421	N/A		N/A	
	600	2	100	0.494	0.730	repeat	0.511	
.125"	600	2	100	0.552	0.680	0.670	0.476	0.469
	600	2	200	0.614	0.660		0.462	
	600	7	100	0.525	0.590		0.413	
	600	7	190	0.580	0.790		0.553	
	750	2	150	0.526	0.650		0.455	
	750	4.5	100	0.479	0.680		0.476	
	750	4.5	150	0.510	0.680		0.476	
	825	4.5	150	0.483	0.660		0.462	
	900	2	100	0.444	0.630	0.640	0.441	0.448
	900	2	200	0.494	0.620		0.434	
	900	7	100	0.422	0.450		0.315	
	900	7	200	0.470	0.870		0.609	

	600	2	100	0.552	0.67	repeat	0.469	
	900	2	100	0.444	0.64	repeat	0.448	
.0375"	600	2	100	0.693	N/A	0.730		0.511
	600	2	200	0.772	N/A			
	600	7	100	0.660	N/A			
	600	7	165	0.713	N/A			
	750	2	150	0.661	N/A			
	750	4.5	100	0.601	0.670		0.469	
	750	4.5	150	0.640	0.690		0.483	
	900	2	100	0.558	N/A			
	900	2	200	0.621	N/A			
	900	7	100	0.531	N/A			
	900	7	200	0.591	N/A			

*Table E1 -- Results of test matrix for sudden expansion wall*

## 6.0 Appendix F – Catalyst Materials Development Figures

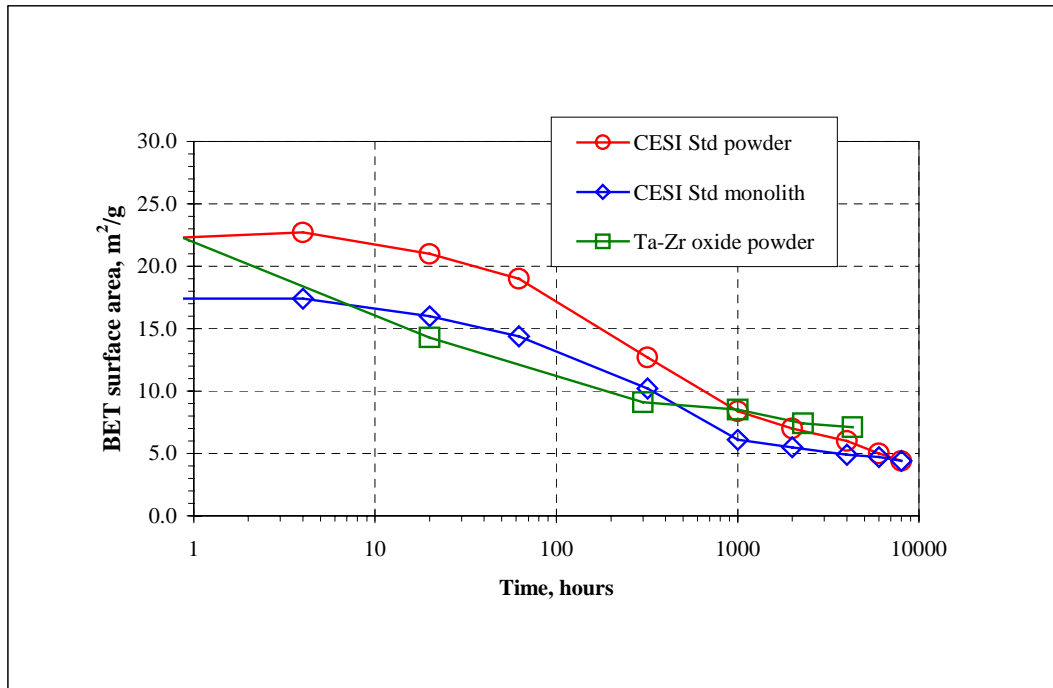


Figure F1 – Total (BET) surface area analysis

results for catalysts aged at 900°C

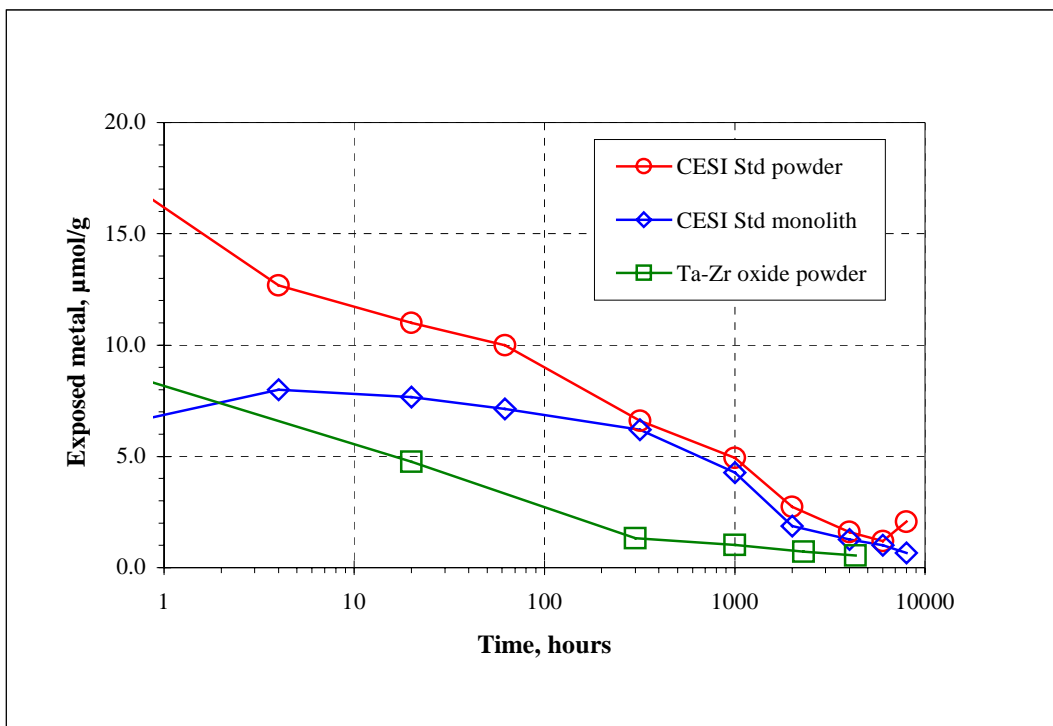


Figure F2 – Normalized active component surface area for catalysts aged at 900°C

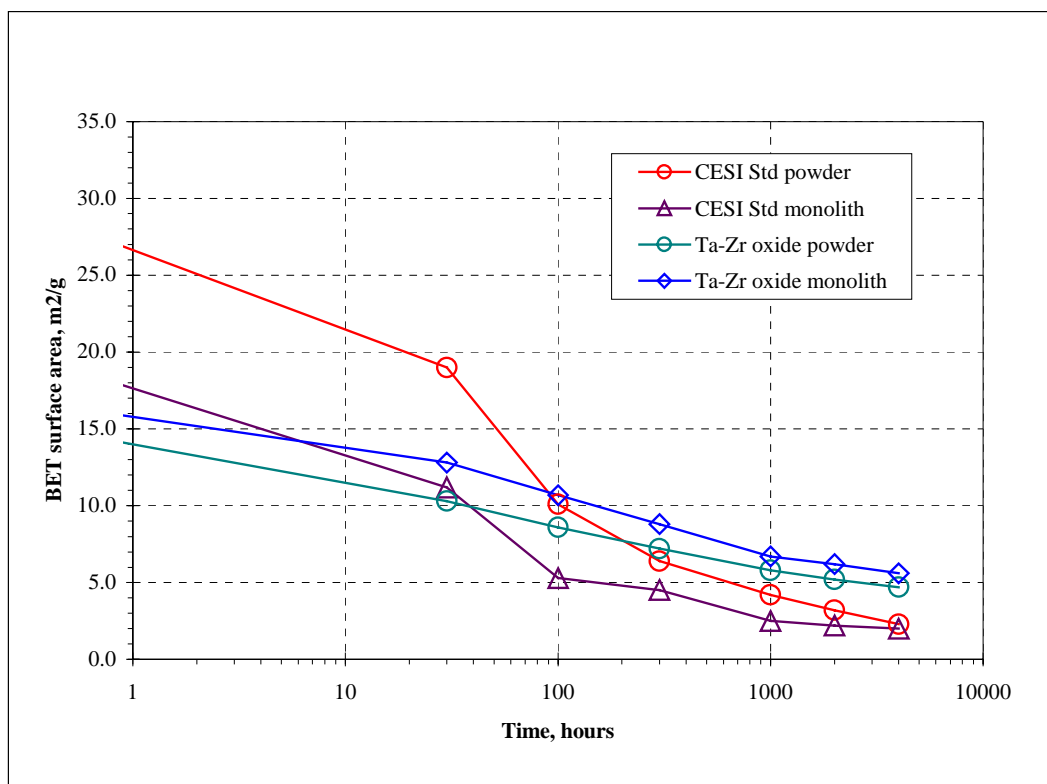


Figure F3 -- Total (BET) surface area analysis results for catalysts aged at 975°C

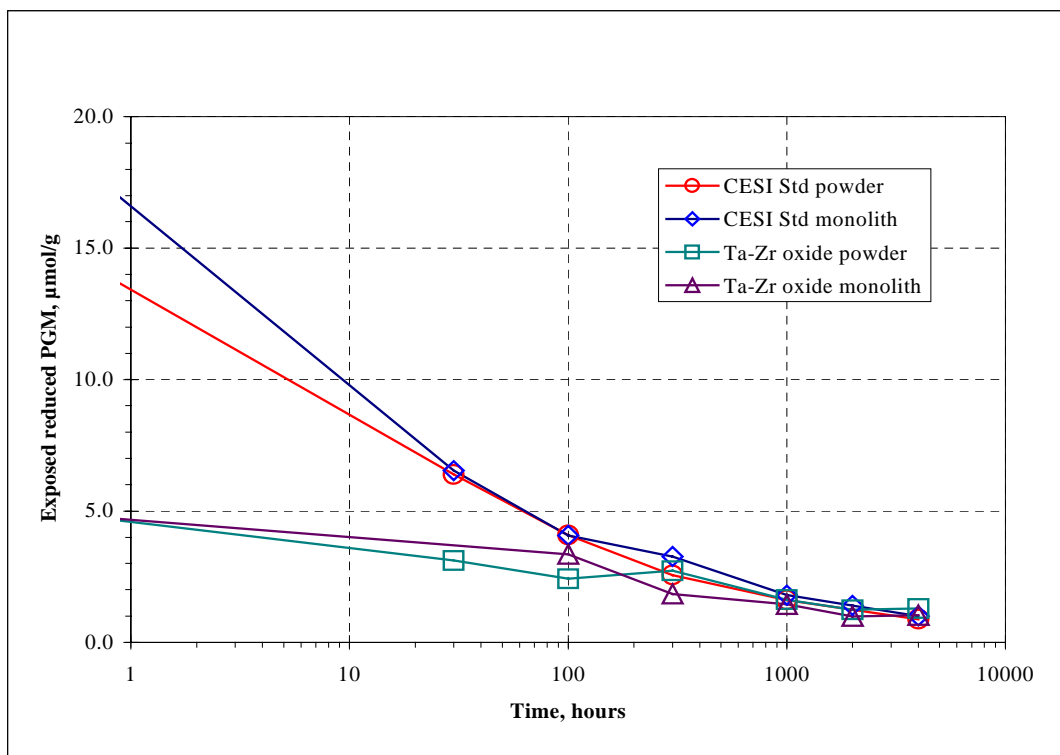


Figure F4 -- Active component surface area for catalysts aged at 975°C

## 7.0 Appendix G – Fuel Variability Figures

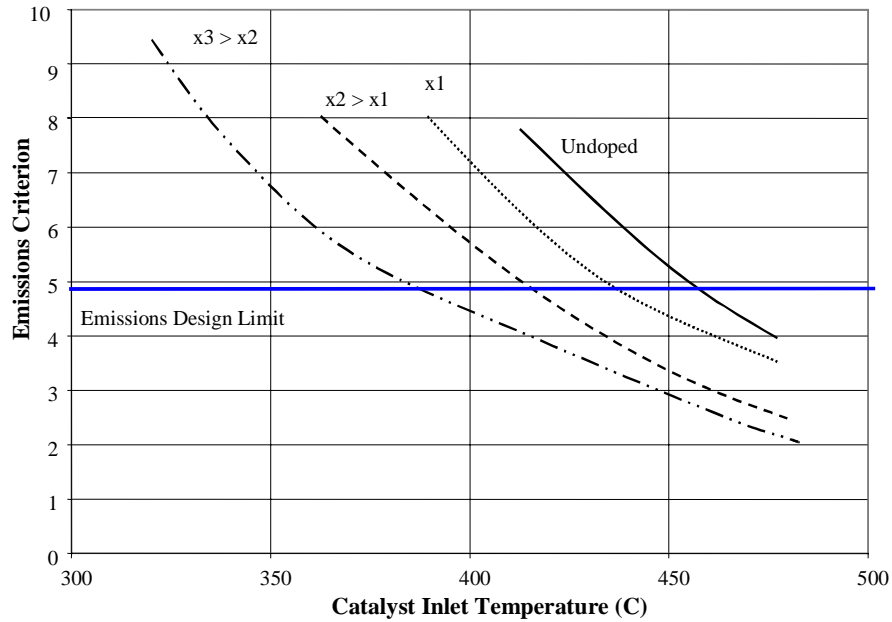


Figure G1 -- Effect of Hydrocarbon Dopants on Emissions Limit

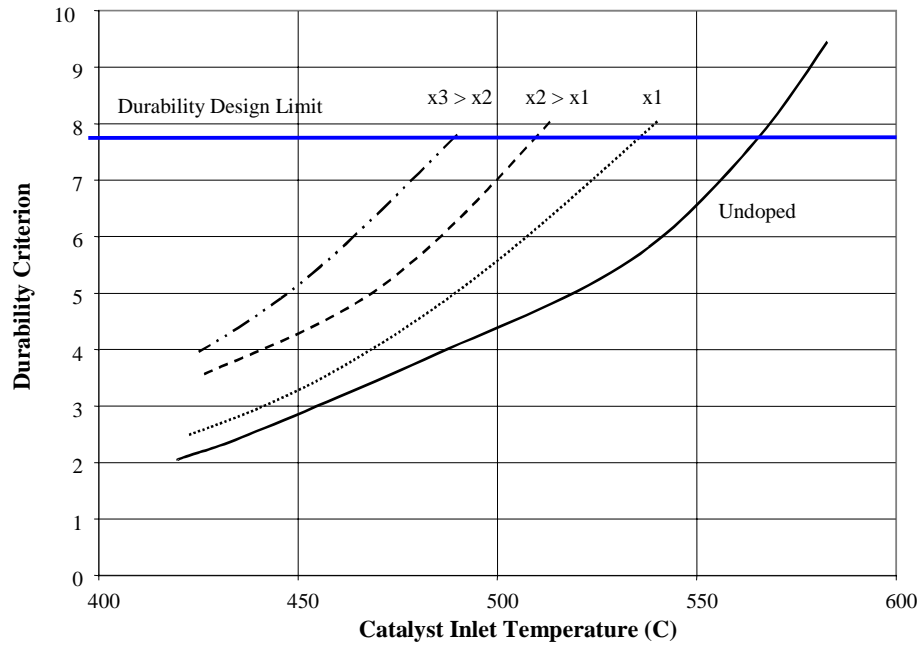


Figure G2 -- Effect of Hydrocarbon Dopants on Durability Limit



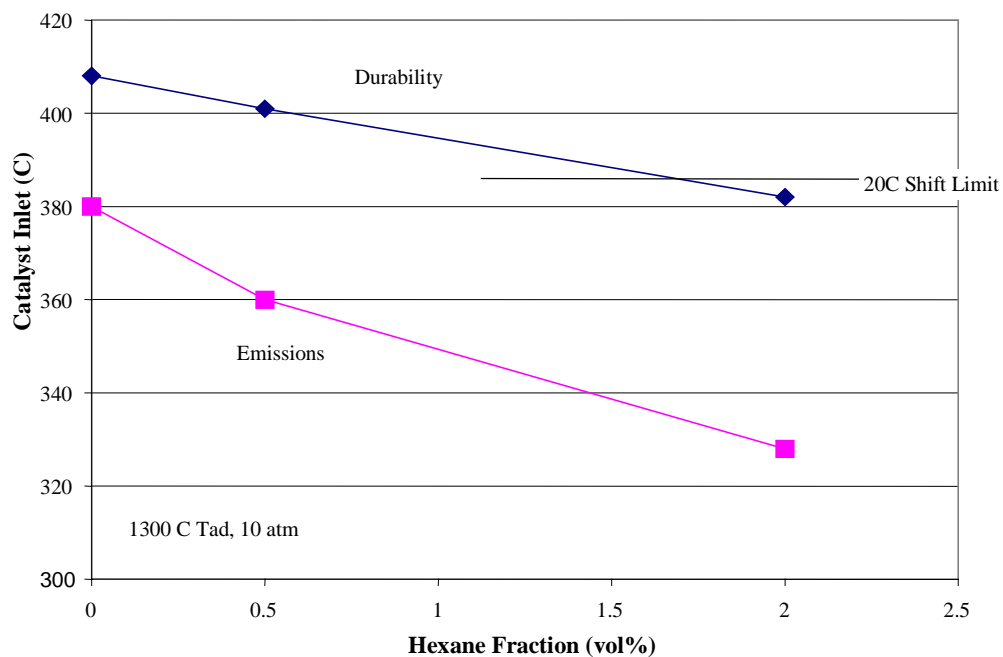


Figure G3 -- Operating Window Limits - Hexane Addition

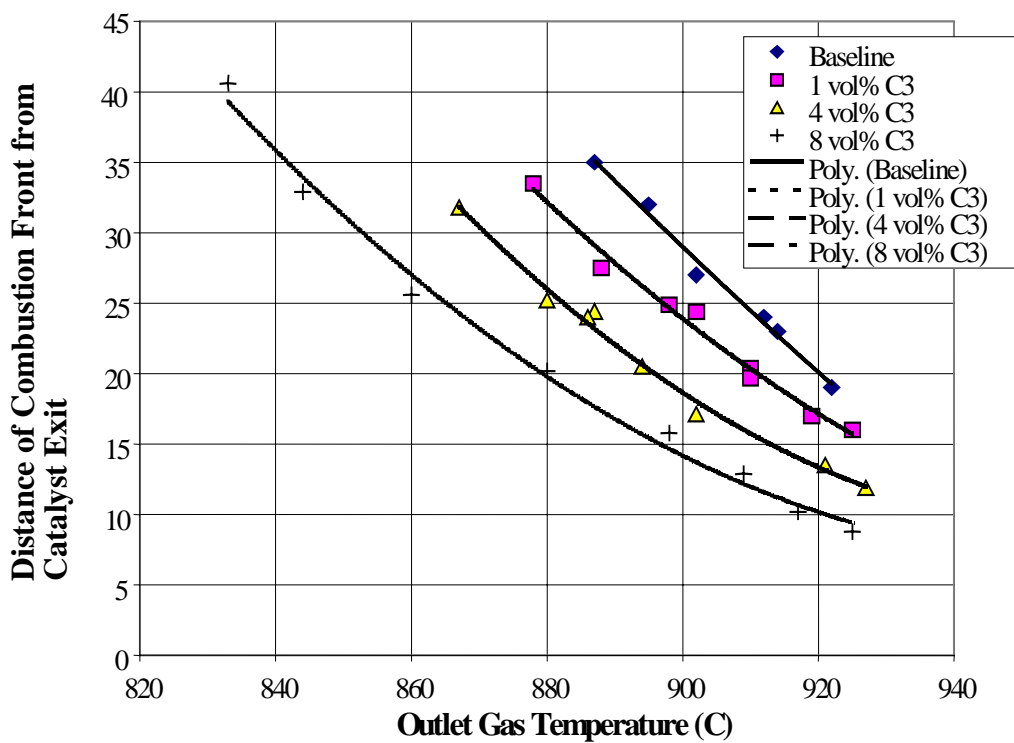
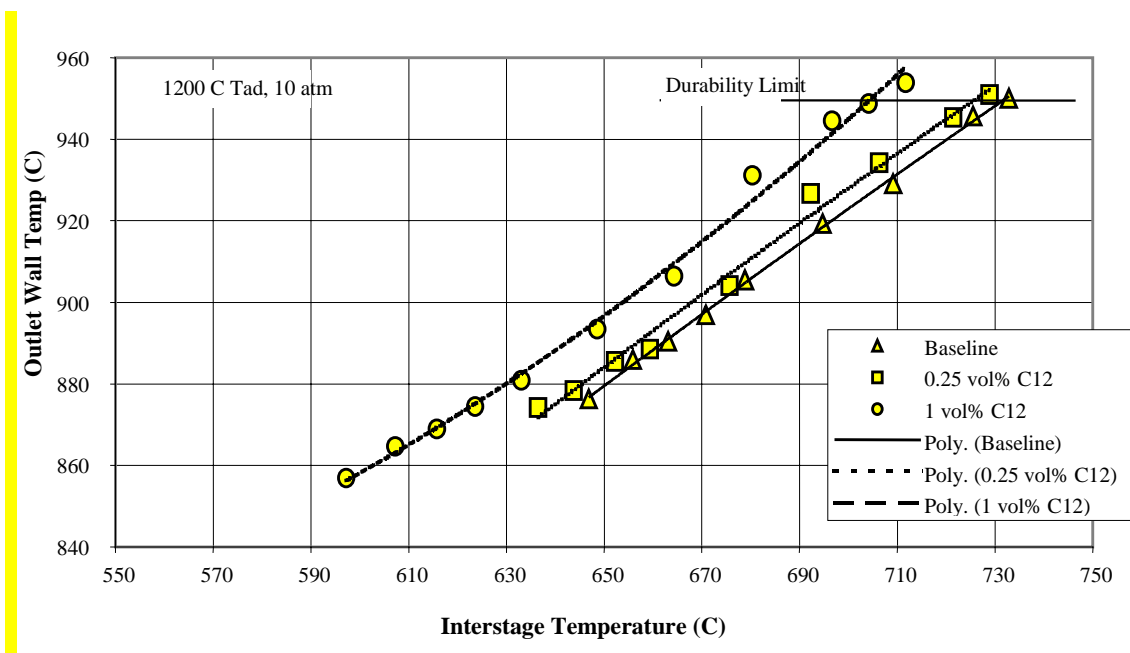


Figure G4 -- Combustion Front Locations - Propane Addition



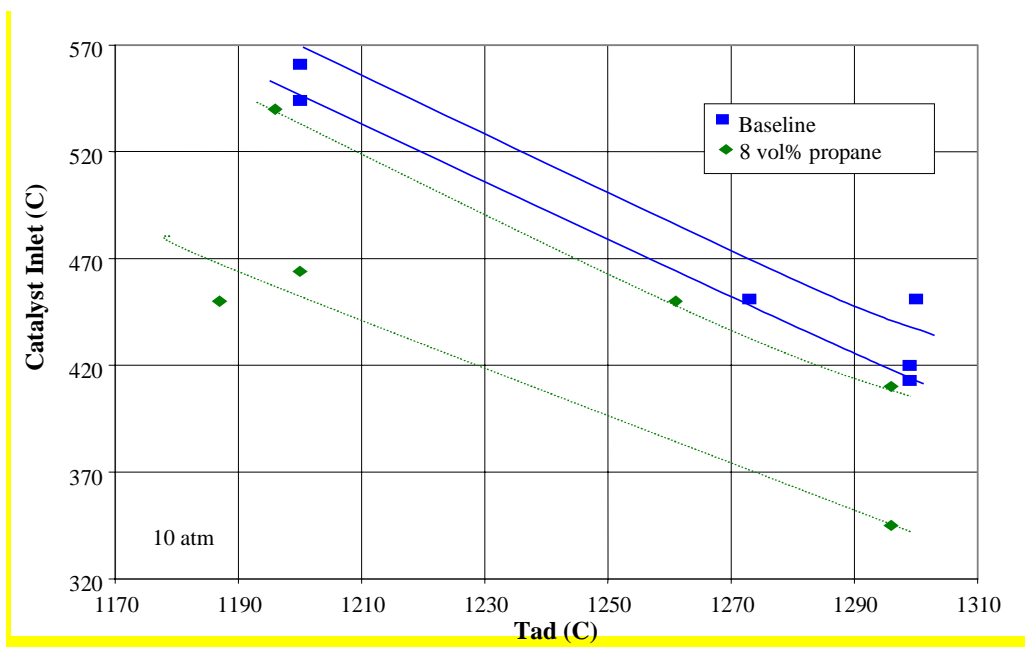


Figure G7 -- Operating Window Shift - Propane Addition

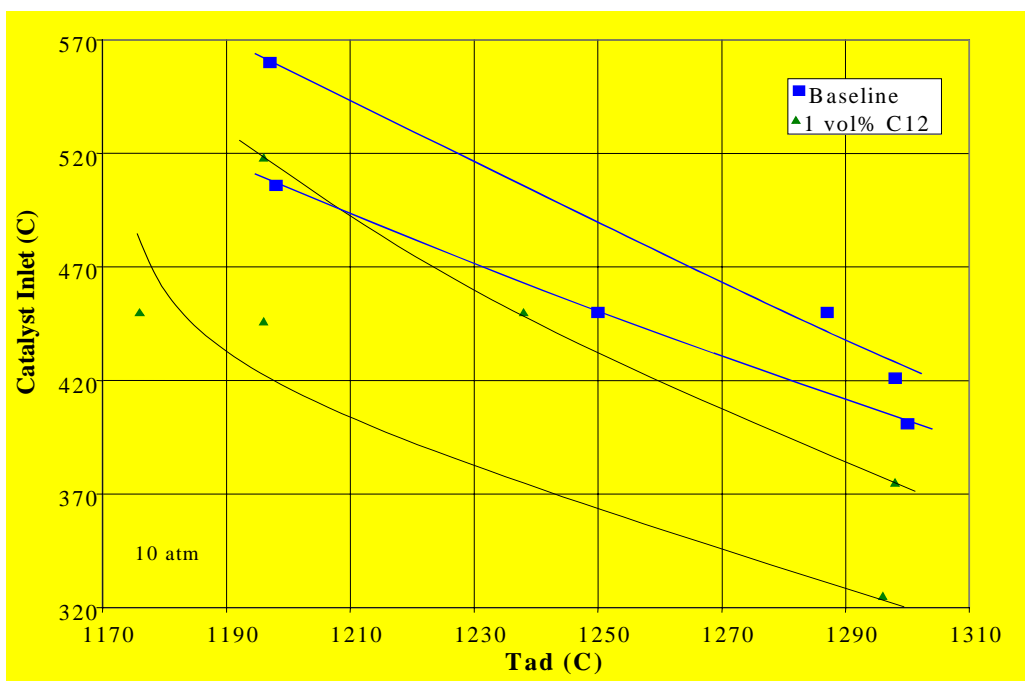


Figure G8 -- Operating Window Shift - Kerosene (C12) Addition

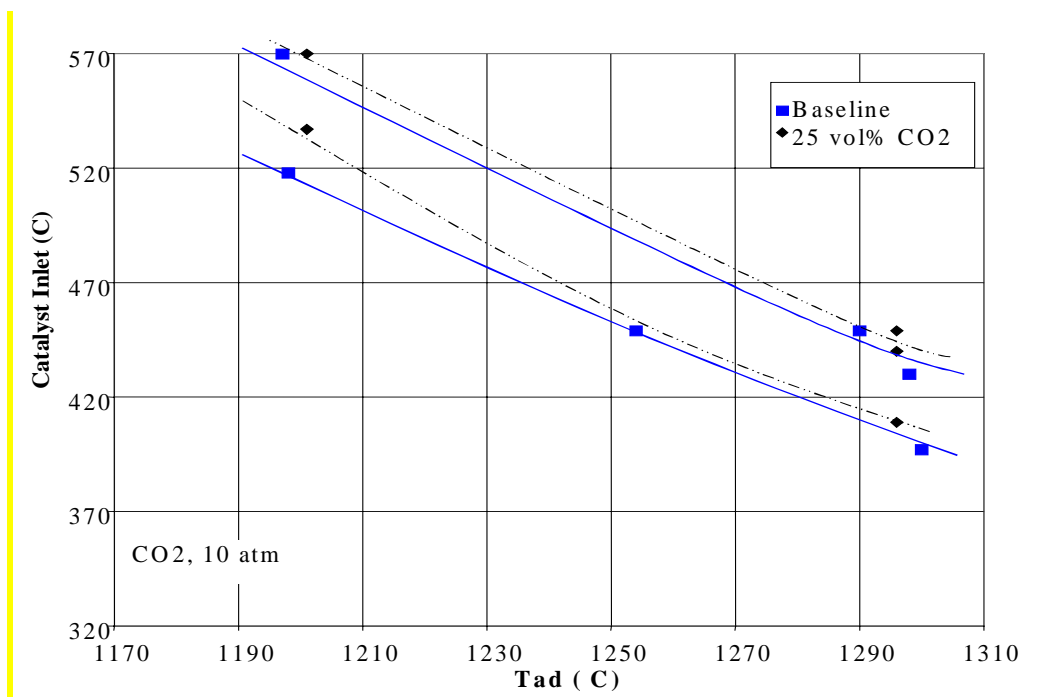


Figure G9 -- Operating Windows - CO2 Addition

## **Appendix I – Market Requirements Development**

## **Appendix II – RAMD Testing and Control System Development**

## **Appendix III – Combustion Catalyst Axial Support Mechanical Durability**

## **Appendix IV – Fuel/Air Premixer Development**



## **Appendix V – Catalyst Materials Development**

## **Appendix VI – Variability in Natural Gas Fuel Composition and Its Effects on the Performance of Catalytic Combustion Systems**

## **Appendix VII – Xonon Production Readiness**